2012

Annual Report

Department of Microelectronics

Institute of Advanced Materials, Physicochemical Processes, Nanotechnology and Microsystems

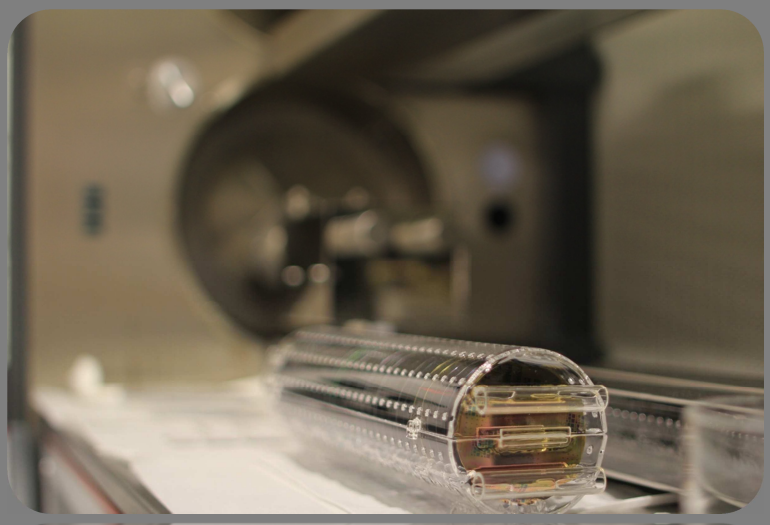

National Center for Scientific Research "NCSR "Demokritos"

Aghia Paraskevi, Athens GREECE
www.imel.demokritos.gr

TABLE OF CONTENTS

		Page
Table of contents		1
Preface		2
Objectives and Activities		3
Organizational structure		6
MAIN RESEARCH RESULTS		
Project I.1:	Materials for Lithography and Organic/Hybrid Electronics	9
Project I.2:	Plasma Enabled Nanofabrication: Processing, Simulation, Metrology and Applications	20
Project I.3:	Thin Films by Chemical Vapor and Atomic Layer Deposition (CVD-ALD)	45
Project II.1	Nanostructures for Nanoelectronics, Photonics and Sensors	54
Project II.2:	Materials and Devices for Memory and Emerging Electronics	64
Project II.3:	Molecular Materials as Components of Electronic Devices	73
Project II.4:	Computational Nanotechnology	79
Project III.1A:	Mechanical and Chemical Sensors	84
Project III.1B:	Energy Harvesting Materials and Devices	91
Project III.2:	Bio-Microsystems	97
Project III.3:	Thin Film Devices for Large Area Electronics	102
Project III.4:	Circuits & Devices for Sensor Networks & Systems	107
Project III.5:	Photonic Crystals, Metamorphic Materials and Novel RF Systems	109
ANNEXES		
ANNEX I :	**Personnel**	113
ANNEX II :	**Infrastructure**	114
ANNEX III:	**Research and Education Output**	116
ANNEX IV:	**Funded projects in 2012**	125

PREFACE

The Department of Microelectronics (former Institute of Microelectronics – IMEL) is one of the three departments of the Institute of Advanced Materials, Physicochemical Processes, Microsystems and Nanotechnology (IAMPPMN) of NCSR Demokritos that resulted after a governmental decision for merging in March of 2012.

IMEL was established in 1986 as one of the eight Research Institutes of NCSR Demokritos, a medium size, multidisciplinary Research Center under the General Secretarial for Research and Technology of the Ministry of Development. The Institute's mission was to promote research related with Microelectronics in Greece fostering at the same time the involvement and contribution of the country to European R&D in the field. Since then, IMEL has been able to acquire cutting-edge research equipment in micro-nanofabrication and material/device characterization, has successfully participated in numerous National and European research projects and has been producing high quality research focused mostly on silicon technology and associated microsystems.

The know-how and expertise developed within more than 25 years of operation cover the physicochemical and technological understanding of silicon processing steps, the mastering of novel micro and nanofabrication routes compatible with silicon technology, the development of new organic and inorganic materials for alternative electronics and optoelectronics, as well as innovative device design and realization, extending from sensors and portable microsystems to electronic memories and photonic devices.

On the national level the expertise and infrastructure of the Department of Microelectronics are unique in Greece, which it leader in the development of novel technologies, in technology and know-how transfer to the industry and in the development of high-quality human potential through Master and Ph.D. concrete programs that has staffed high-tech companies and University departments. In addition the research output has been exploited either in commercial products or in spin-off companies. Furthermore, the Department has developed mechanisms to promote the field at the national level through the establishment and coordination of thematic networks and scientific societies (MMN Network, Micro & Nano scientific society). IMEL is a member of the European Academic and Scientific Association for Nanoelectronics (AENEAS-technology platform ENIAC) and a founding member of SINANO, the European Institute of Nanoelectronics and member of the Hellenic Semiconductor Industry Association.

During the year 2012, the research activity of the Department of Microelectronics resulted in 179 scientific papers (96 in refereed journals and 83 in conference proceedings). The Educational activities resulted in 8 Master Theses while 20 PhD Theses were in progress. The Department hosted 20 running projects (9 of them started this year) which include the EU-SP2/Ideas project of N.Chronis (external collaborator). Furthermore, in the context of the Micro and Nanosystems Center of Excellence REGPOT project, a new Electron Beam Lithography System EBPG5000 was installed in the clean room of the Department. This unique tool with resolution capability down to 8 nm is expected to create new research opportunities at national and international level.

Despite the economic difficulties and the problems that came up from the merging procedure, 2012 was a successful year. This is due to the dedication of all the personnel to the common effort, their adaptation to the new administration, and their ability to exploit all available resources in order to advance forward.

The Department Coordinator

Dr N.Glezos

OBLECTIVES AND ACTIVITIES

Main objectives

- To conduct medium- to long-term multidisciplinary research and foster innovation in Micro-Nanofabrication, Nanoelectronics, Photonics, Sensors and Microsystems including BioMEMS.
- To promote the transfer of R&D results into specific knowledge-intensive products with applications in prioritized KET-driven industry sectors (Information and Communication Technologies, Medicine & Healthcare, Energy & Environment, Agriculture & Food safety).
- To provide expertise and efficient access to cutting-edge facilities in micro-nanofabrication and material/device characterization for academic, industrial and government bodies in Greece and abroad.
- To strengthen innovative thinking & multidisciplinary collaborative approaches for increasing creative capacity as well as to promote R&D&I transnational cooperation and networking.
- To encourage patent application for IP protection as well as to promote efficient transfer of research results to industry and stimulate the creation of spin-off companies.
- To provide scientific and technical training for companies and individuals including active involvement in post-graduate education.
- To produce high-level scientific knowledge, increase visibility and attract substantial R&D funding including structural funds.

Fields of Research

Research Activities at the Department of Microlectronics are spread across three programs, each of them being composed of smaller projects. A scientist is in charge of each research project, while a program representative is assigned for the management of each program. The research programs and corresponding projects are:

Program I: MICRO AND NANOFABRICATION

- Project I.1 Materials for Lithography and Organic/Hybrid Electronics
- Project I.2 Plasma Enabled Nanofabrication
- Project I.3 Thin Films by Chemical Vapor Deposition and Atomic Layer Deposition

Program II: NANOSTRUCTURES AND NANOELECTRONIC DEVICES

- Project II.1 Nanostructures for Nanoelectronics ,Photonics and Sensors
- Project II.2 Materials and Devices for Memory and Emerging Electronics
- Project II.3 Molecular Materials as Components of Electronic Devices
- Project II.4 Computational Nanotechnology

Program III: SILICON SENSORS AND MICROSYSTEMS

- Project III.1a Mechanical & Chemical Sensors
- Project III.1b Energy Harvesting Materials and Devices
- Project III.2 Bio-Microsystems
- Project III.3 Thin Film Devices for Large Areal Electronics
- Project III.4 Circuits and Devices for Sensor Networks and Systems
- Project III.5 Photonic Crystals, Metamorphic Materials and Novel RF Systems

Infrastructure

By providing access to centrally managed micro/nanofabrication and material/device characterization facilities with state-of-the-art equipment, the Department offers scientists and engineers unique resources for the creation of new materials, processes, devices, and systems. Such facilities include (1) a ISO/9001:2008 “Nanotechnology & MEMS Laboratory” with a fully operational silicon processing line serving as National and European Research Infrastructure, (2) a plasma lab with 2 ICP reactors, (3) a ISO/17025:2005 electrical characterization lab reinforced since 2006 with a Cascade RF manual probe station and a VNA DC-40 GHz Anritsu, and since 2007, with a low-temperature wafer prober (4K-400K), as well as (4) MEMS and sensor characterization labs equipped in 2005-2012 with various equipment such as a micro-CNC system (2008) and a 3-D printer (2012), (5) material characterization facilities including FEG-SEM (2008), AFM (2006), STM (2006), FTIR, UV-Vis spectroscopy, Stylus profilometer, UV spectrophotometer (2009) etc.

New E-Beam Writer

In mid-2012, a new electron beam lithography system was installed at IMEL. The EBPG5000plusES tool from Vistec Lithography is a state-of-the-art E-beam writer operating at 100keV and is capable of producing sub-8nm features. The machine was purchased as part of the project MiNaSys-CoE (Micro and Nanosystems – Centre of Excellence) funded from the FP7-REGPOT programme. The tool was paired with the software BEAMER from GeniSys to facilitate data preparation and proximity effect correction.

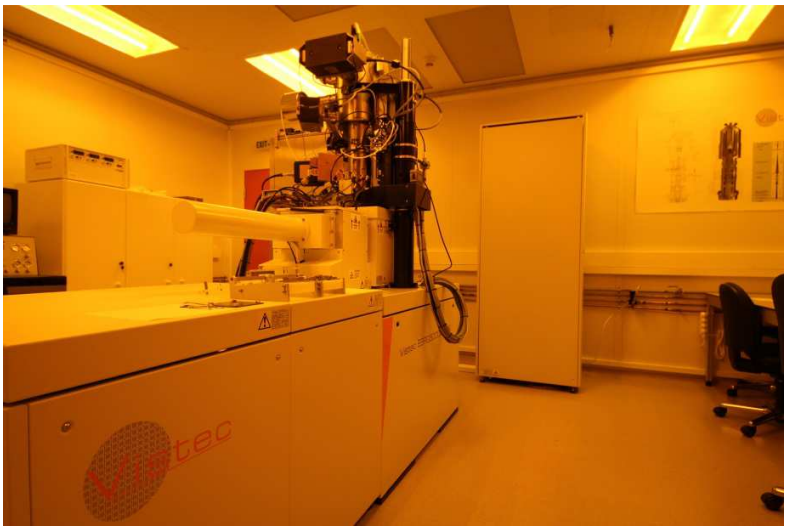

E-beam machine installed in the clean room of IMEL. June 2012

Several processes have started being developed for supporting and reinforcing the research activities of the Department of Microelectronics in the areas of sensors, nanoelectronics, and photonics . The efforts were concentrated on the fabrication of nanowire transistors, photonic elements, electrodes, and templates for material growth or novel etching studies.

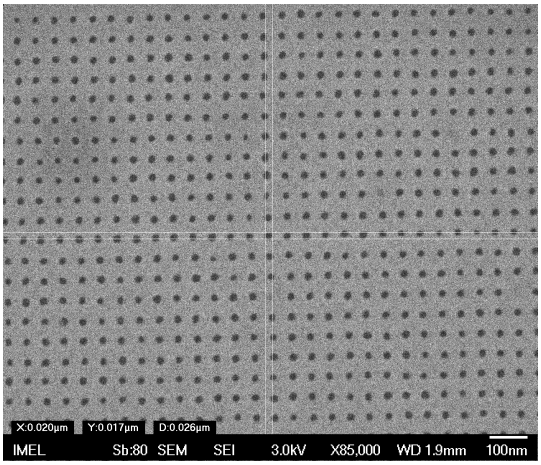

Sub-20nm holes in SiO_2 for selective nanowire growth

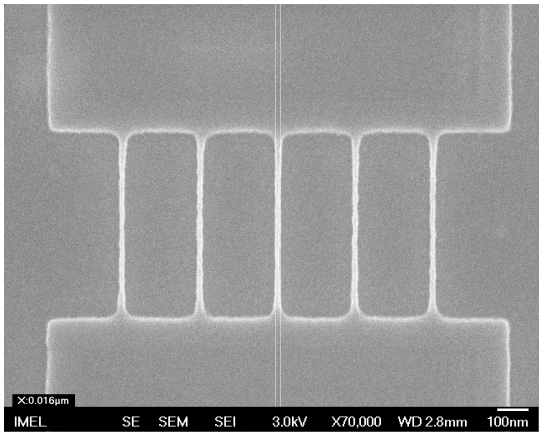

16nm nanowire structure on SOI

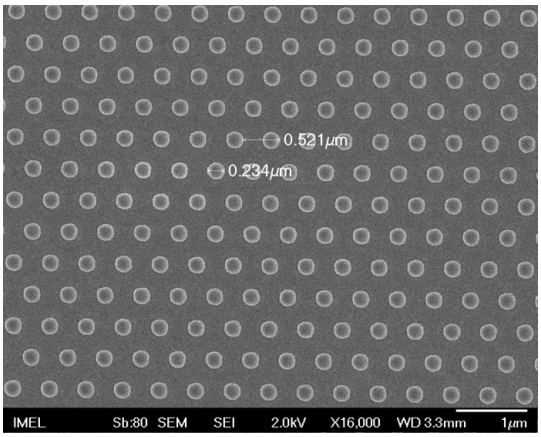

250nm posts in hexagonal configuration

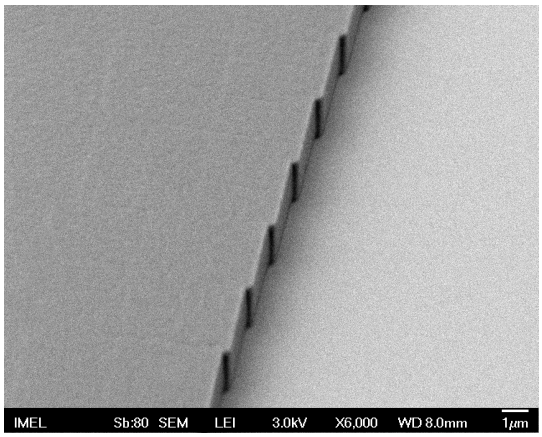

Echelle grating with a groove facet of 170nm

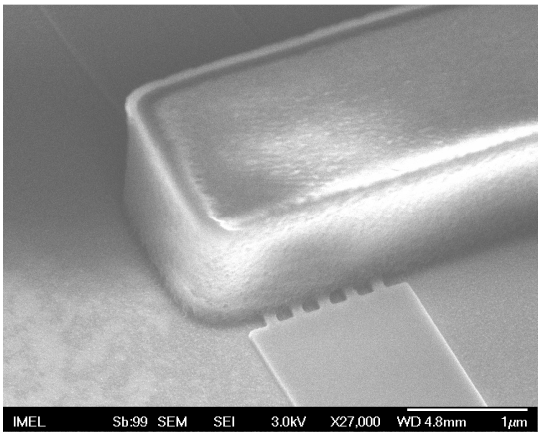

Gate electrode lithography on top of nanowire transistor structures

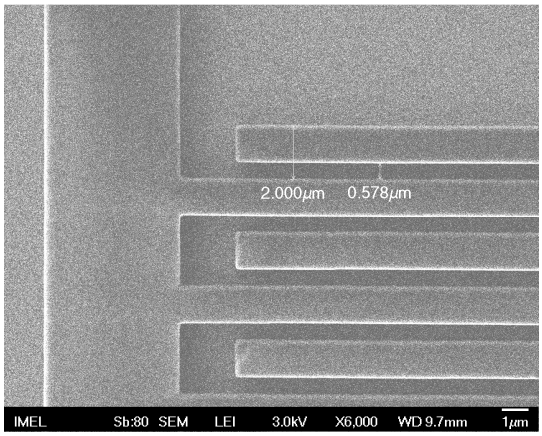

Interdigitated electrodes for chemocapacitive sensor

ORGANIZATIONAL STRUCTURE

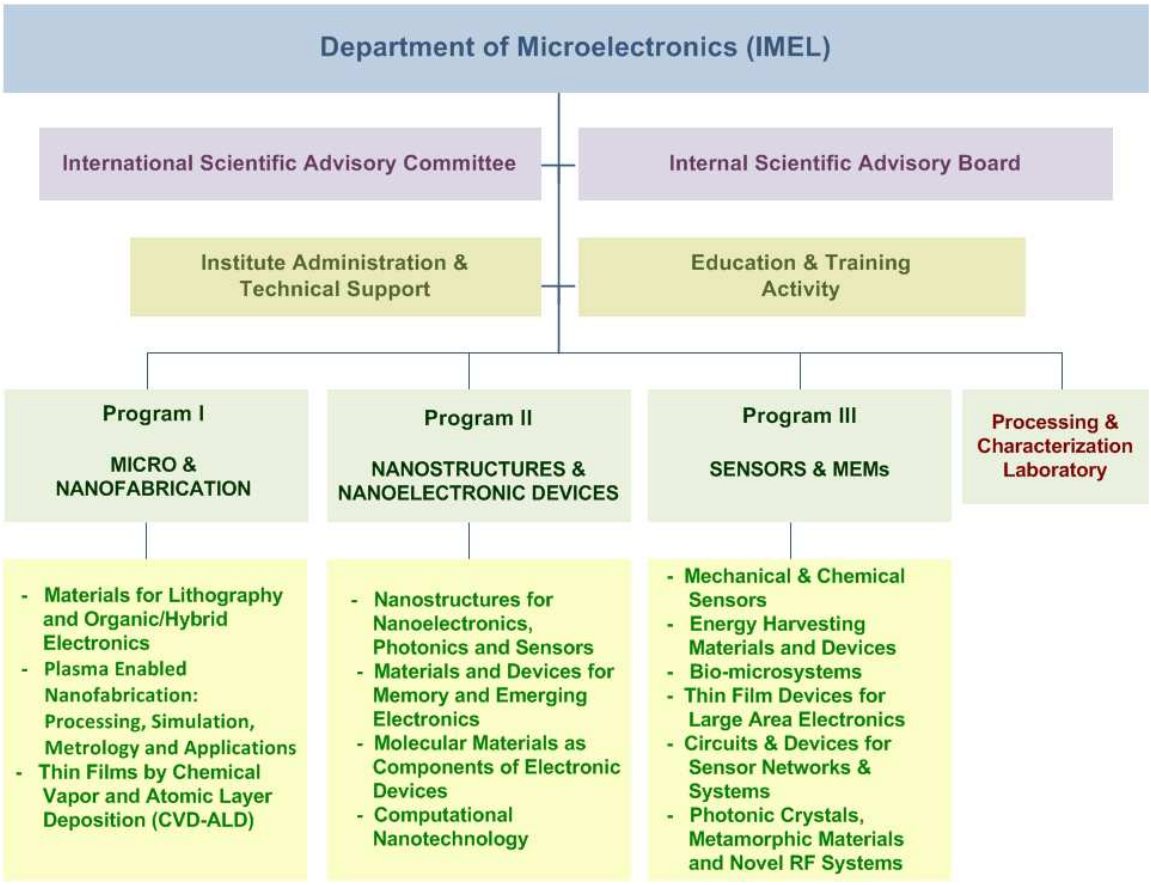

MAIN RESEARCH RESULTS

PROGRAM I

MICRO and NANOFABRICATION

PROGRAM I

MICRO and NANOFABRICATION

PROJECTS

- **MATERIALS FOR LITHOGRAPHY AND ORGANIC/HYBRID ELECTRONICS**
- **PLASMA ENABLED NANOFABRICATION: PROCESSING, SIMULATION, METROLOGY AND APPLICATIONS**
- **THIN FILMS BY CHEMICAL VAPOR AND ATOMIC LAYER DEPOSITION (CVD-ALD)**

PERSONNEL

RESEARCHERS

P. Argitis, E. Gogolides, A. Tserepi, D. Davazoglou

COLLABORATING RESEARCHERS

P. Normand, N. Glezos, P. Dimitrakis, I. Raptis, G. Pistolis, S. Chatzandroulis, K. Misiakos

PERMANENT SCIENTIFIC STAFF

M. Vasilopoulou, A.M. Douvas, V. Constantoudis

POST DOCTORAL SCIENTISTS

G. Kokkoris, D. Moschou, N. Vourdas, K. Tsougeni, G. Papadakis, G. Papadimitropoulos, A. Olziersky

PhD STUDENTS

D.G. Georgiadou, T. Manouras, P. Pavli, C. Katsogridakis, A. Soultati, M.-E.Vlachopoulou, A. Malainou, D. Kontziampasis, K. Ellinas, A. Smyrnakis, N. Skoro, V.K. Murugesan Kuppuswamy, I. Kostis

MSc STUDENTS

S. Tzani, S. Kazazis, N. Vitsaras, E. Polydorou, A. Zeniou, E. Kouris, N. Karasmani, S. Mouchtouris, Th. Christoforidis, K. Tsevas, N. Panousis, N. Pasipoularidis

STUDENTS

D. Simatos, V. Poulakis

PROJECT I.1
MATERIALS FOR LITHOGRAPHY AND ORGANIC/HYBRID ELECTRONICS

Project Leader: P. Argitis

Permanent Scientific Staff: M. Vasilopoulou, A.M. Douvas

PhD Students: D.G. Georgiadou, T. Manouras, P. Pavli, C. Katsogridakis, A. Soultati

MSc Students: S. Tzani, S. Kazazis, N. Vitsaras, E. Polydorou

Collaborating researchers from other IAMNMPP groups: D. Davazoglou, P. Normand, N. Glezos, P. Dimitrakis, E. Gogolides, I. Raptis, G. Pistolis

External Collaborators: M. Chatzichristidi (Univ of Athens), L. Palilis, S. Kennou, N. Vainos, S. Kouris, D. Alaxandropoulos (Univ of Patras), E. Kapetanakis (TEI Kritis), S. Kakabakos, P.S. Petrou (IRRP-NCSR-D), N. Stathopoulos, S. Savaidis (TEI Piraeus), S. Boyatzis (TEI of Athens), D. Dimotikali (Nat. Tech. Univ. Athens), A.G. Coutsolelos, M. Vamvakaki (Univ. of Crete/FORTH), I. Petsalakis, I. Theodorakopoulos (Nat. Hel. Res. Foundation)

OBJECTIVES

A. Materials research for organic/hybrid electronic devices
Research topics

- Electron/hole transporting interfacial layers of organic optoelectronic devices
- Material options for improving charge separation and transport in organic/hybrid photovoltaics (OPVs)
- New optoelectronic devices based on organic semiconductors
- Emission colour tuning in Organic Light Emitting Diodes (OLEDs)

The current research priorities include investigation of a) different material options as charge transporting layers in OLEDs and OPVs, including metal oxides, related solution processable materials and organic molecular layers, and b) new device architectures and manufacturing processes enabled by the versatility of organic material properties.

B. Research on organic thin films and molecular layers chemistry for development of new lithographic materials, micro- nanopatterning processes and coatings related technologies
Research topics

- Investigation of new resist chemistries and photochemical imaging processes
- Lithographic materials for nanopatterning and alternative patterning schemes aiming at MEMs, bio-MEMs and related fields
- Characterization technology for organic protecting coatings

The current research priorities include new lithographic materials based on imaging through polymer back-bone breaking including laser writing processes, patterning processes for biosystems fabrication and characterization of organic coatings used in restoration applications.

FUNDING

a) Thalis "Polymeric photonic systems for application in information technologies, Photopolys" (2012-2015)
b) Archimides III "Novel and highly efficient Hybrid organic photovoltaic, NHyOPV" (2012-2014)
c) Archimides III "Novel low power consumption Hybrid OLEDs with improved operational characteristics, NHyOLED" (2012-2014)
d) Archimides III "Organic Electronic Devices for Radiation Detection" (2012-2015)
e) GSRT "Blu-Ray" Development of Optical Discs Technology (2011-2014)
f) IKYDA, IKY DAAD Collaborative Project with LM University of Munich (2012)

MAIN RESULTS in 2012

1. Approaches for performance improvement in OLEDs

a) Under-stoichiometric transition metal oxides as charge transport interlayers in OLEDs

i) Sub stoichiometric tungsten oxide as efficient hole injection layers

We demonstrated the unique hole injection and transport properties of a substoichiometric tungsten oxide with precise stoichiometry, in particular $WO_{2.5}$, obtained after the controlled hydrogen reduction during growth of tungsten oxide, using a simple hot-wire vapour deposition technique. We presented clear evidence that tungsten suboxide exhibits metallic character and that an almost zero hole injection barrier exists at the anode/polymer interface due to the formation/occupation of electronic gap states near the Fermi level after oxide's reduction. These states greatly facilitate hole injection and charge generation/electron extraction enabling the demonstration of extremely efficient OLED devices based on poly[(9,9-dioctylfluorenyl-2,7-diyl)-co-(1,4-benzo-{2,1',3}-thiadiazole)] (F8BT) as the emissive layer (Figure 1). Moreover, electroluminescent devices using $WO_{2.5}$ as both, hole and electron injection layer, and exhibited high efficiencies up to 7 cd/A and 4.5 lm/W, while, stability studies revealed that these devices were extremely stable, since they were operating without encapsulation in air for more than 700 hours (Figure 2).

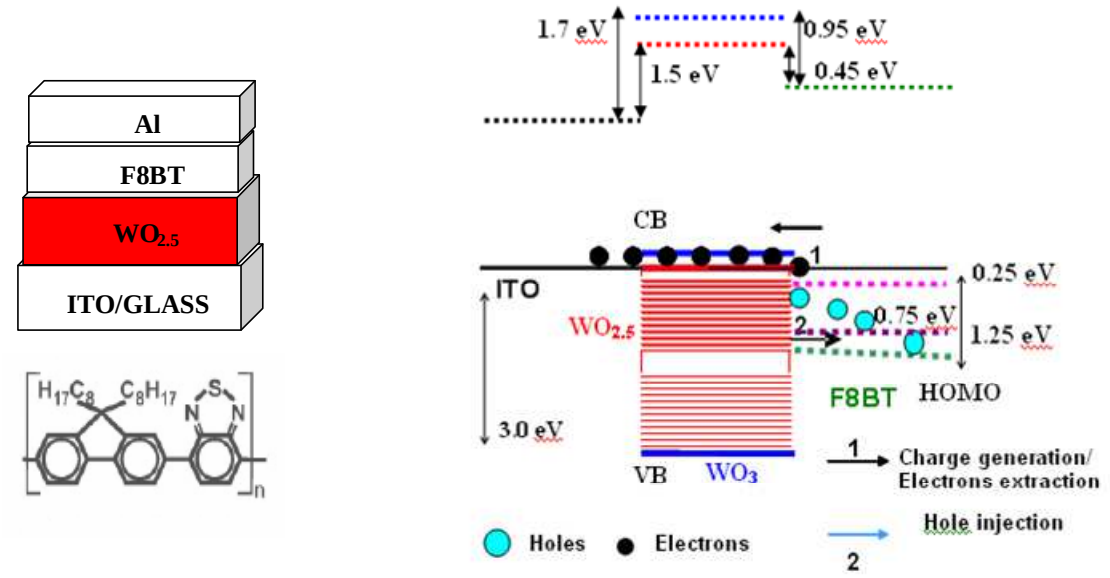

Fig. 1. *(left) F8BT based OLED architecture using tungsten oxides as anode interfacial layers and the chemical structure of F8BT. (right) The corresponding energy level diagram and illustration of the possible hole injection mechanism.*

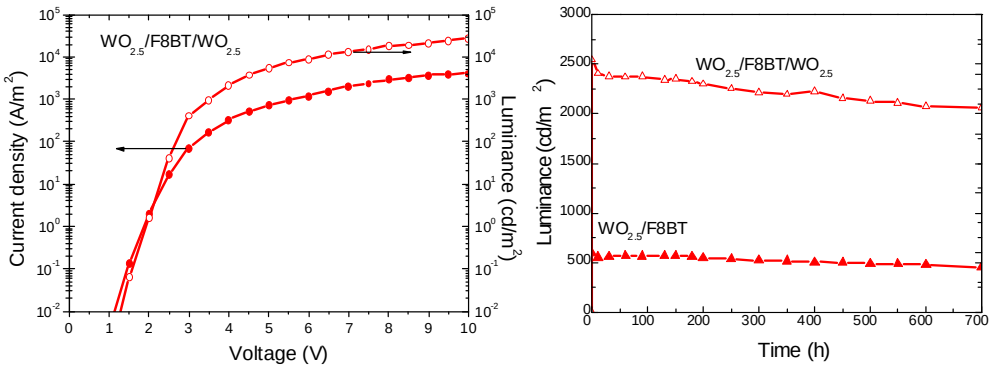

Fig. 2. *(left) Current density (solid cycles)-luminance (open cycles)-voltage characteristics of symmetric F8BT based OLEDs with $WO_{2.5}$ as both hole and electron injection layers in F8BT based OLEDs. (right) Stability data for non-encapsulated OLEDs based on tungsten suboxide $WO_{2.5}$ as HIL: Luminance and operational voltage versus time of operation in air at room temperature with a constant driving current density of 200A/m^2.*

ii) Hydrogenated and oxygen-deficient molybdenum oxides as hole injection layers

Molybdenum oxides were used as low resistance anode interfacial layer in applications such as organic light emitting diodes (OLEDs). In particular, we investigated the beneficial role of hydrogenation (the incorporation of hydrogen within the oxide lattice) versus oxygen vacancy formation in tuning the electronic structure of molybdenum oxides while maintaining their high work function. A large improvement in the operational characteristics of polymer light emitting devices based on the green-emitting copolymer poly[(9,9-dioctylfluorenyl-2,7-diyl)-co-(1,4-benzo-{2,1',3}-thiadiazole)] (F8BT) incorporating hydrogenated Mo oxides as hole injection layers was achieved (Figure 1, left) as a result of favourable energy level alignment at the metal oxide/organic interface, as revealed from the ultraviolet photoelectron spectroscopy measurements (Figure 3, right), and also enhanced charge transport through the formation of a large density of gap states at the Fermi level (Figure 4).

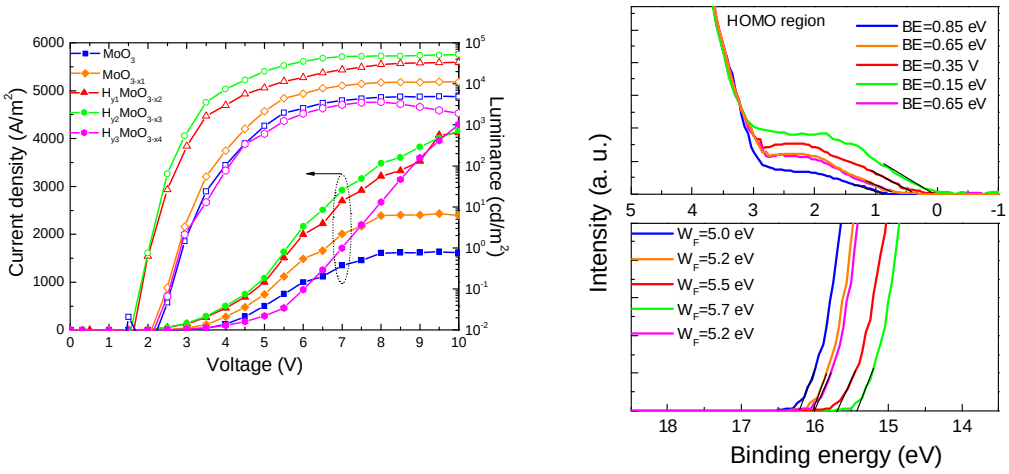

Fig. 3. *(left) Current density-voltage (solid symbols) and luminance-voltage (open symbols) characteristic curves of OLEDs with the structure ITO/Mo oxides (5 nm)/F8BT/POM (2 nm)/Al devices. (right) UPS spectra of thin (less than 10 nm) F8BT layers deposited on top of the different Mo oxides: the expanded valence region (up) and the high BE cut-off region (down).*

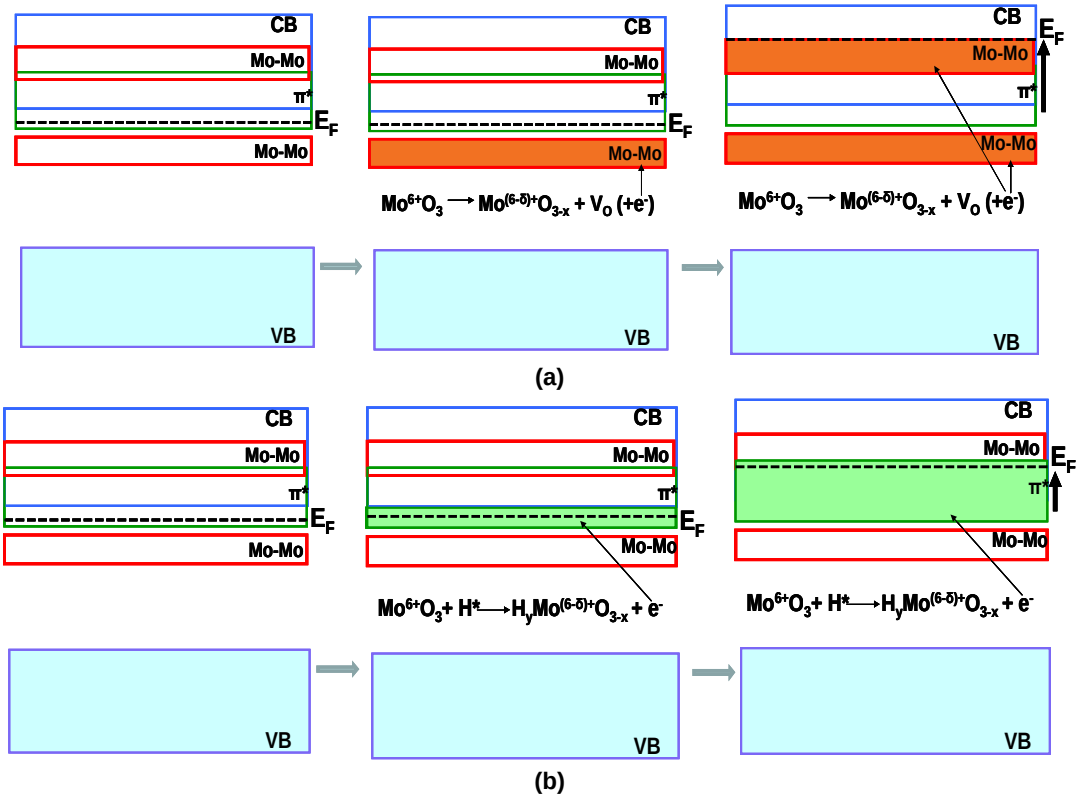

Fig. 4. *Schematic illustration of the evolution of gap states occupation and Fermi level movement towards higher binding energies in Mo oxides (a) with the progress of oxygen vacancy formation in the oxygen deficient film and (b) with the evolution of hydrogen intercalation in the hydrogenated one.*

b) Improved injection and transport in Polymer Light Emitting Diodes (PLEDs) upon organic salts addition in the emissive layer

Triphenyl sulfonium (TPS) salts have been shown to improve PLEDs characteristics when blended with the yellow-emitting F8BT copolymer in the active layer of PLEDs with structure glass/ITO/PEDOT:PSS/active layer/Al. This is attributed to the accumulation of salt anions - upon application of a bias- at the anode interface and the formation of a space charge that reduces substantially the energetic barrier for hole injection. The investigation of a similar system based on the blue-emitting wide band-gap poly(*para*-phenylene) derivative, i.e. CN-PPP, reveals that the intermixing of triphenyl sulfonium triflate molecules in the active layer influences not only injection of holes but also injection and transport of electrons. This is substantiated by the strong salt concentration dependence of the PLED characteristics (see Figure 5).

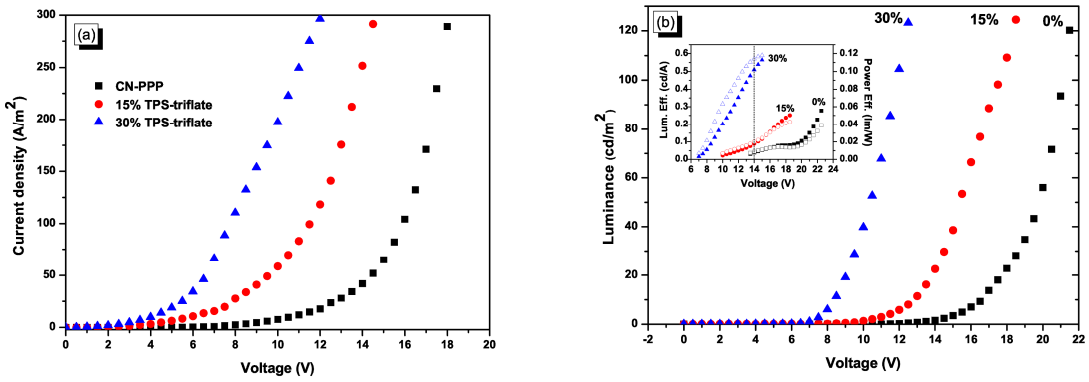

Figure 5: (a) *Current density - voltage (J-V) and (b) luminance - voltage (L-V) characteristics of PLED devices based on CN-PPP, where TPS-triflate has been added in the emissive layer in order to*

demonstrate the effect of the salt concentration on the performance of the devices. Inset: Efficiencies vs voltage characteristics depicting the improvement in device performance upon TPS-triflate addition.

In particular, higher luminance and overall efficiencies are obtained, while both current density and luminance turn-on voltages decrease with increasing salt concentration. This indicates that, apart from the effect exerted by the anions at the polymer/anode interface, the triphenyl sulfonium cations -due to their conjugated nature- act also as electron transport sites, effectively aiding the transport of electrons from the cathode to the polymer lowest unoccupied molecular orbital (LUMO). The latter is schematically represented in the energy level diagram depicted in Figure 2a (published in RSC Advances in 2012, D.G. Georgiadou et al., see publication list).

Additional evidence to the above proposed mechanism is given by studying the electroluminescence profile of these PLEDs (Figure 2b). Interestingly, the addition of the triphenyl sulfonium salts modifies the emission spectrum of CN-PPP polymer in the sense that a totally new red-shifted emission peak appears in the electroluminescence (EL) spectrum (i.e. upon electrical excitation of the active layer) of the TPS-salt containing PLEDs, which is not present in the photoluminescence (PL) spectrum (i.e. upon optical excitation). This new peak is attributed to a bimolecular charge transfer excited state complex, a so-called *electroplex*, which is being formed from holes residing in the polymer HOMO and electrons residing in the polymer LUMO (see also Figure 6a).

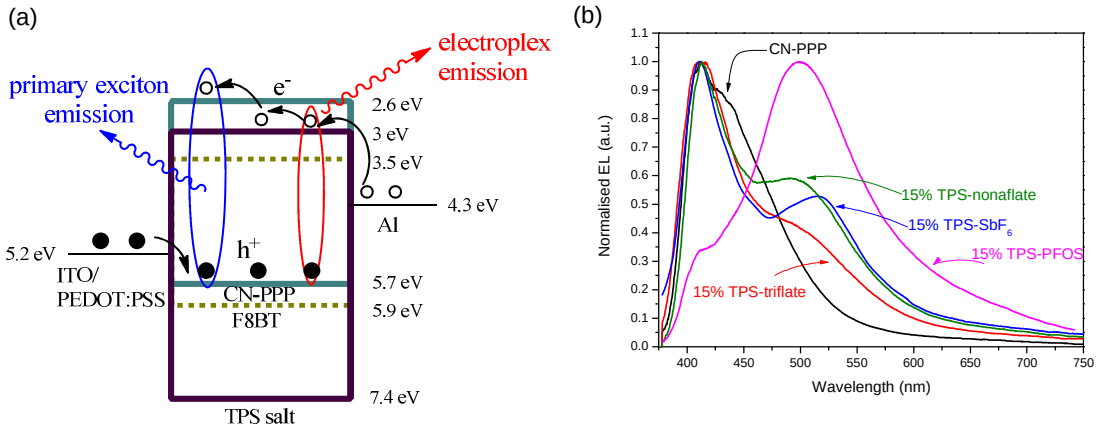

Fig. 6. *(a) Energy level diagram showing also the proposed mechanism and electroplex formation: ITO/PEDOT:PSS (anode) and Al (cathode) work function levels, CN-PPP, F8BT and TPS-salt HOMO-LUMO energy levels. Modification of the polymer/anode interface facilitates hole injection to the polymer HOMO via anion accumulation there. Electron injection is directed towards the polymer's LUMO in the F8BT case (green dotted line), whereas TPS-salts act as intermediate steps in the case of CN-PPP (see arrows from Al). Holes residing in the CN-PPP HOMO may recombine with electrons residing either at the polymer LUMO (primary excitonic emission) or at the TPS LUMO (electroplex emission). (b) Electroluminescence spectra of PLEDs with an active layer based on TPS-salts with different anions blended with CN-PPP polymer. The effect of the counteranions on the deviation from a polymer-dominated to electroplex dominated emission profile is obvious.*

Furthermore, the type of the counter-anion of the TPS-salts plays a significant role in the optoelectronic characteristics of the TPS-salt modified CN-PPP PLEDs, since it influences not only the dispersion properties of the salt in the polymer matrix and consequently the film morphology, but also its size determines the lowest turn-on voltage (Figure 7) and its chemical nature influences the emission profile (see Figure 6b). Consequently, the smallest size anions, which do not contain heavy metals that may be responsible for exciton quenching (e.g. SbF_6^-), such as triflate and nonaflate, resulted in the highest device performance, namely high luminance, low turn-on voltage and high efficiency (published in Synthetic Metals in 2013, D.G. Georgiadou et al.,).

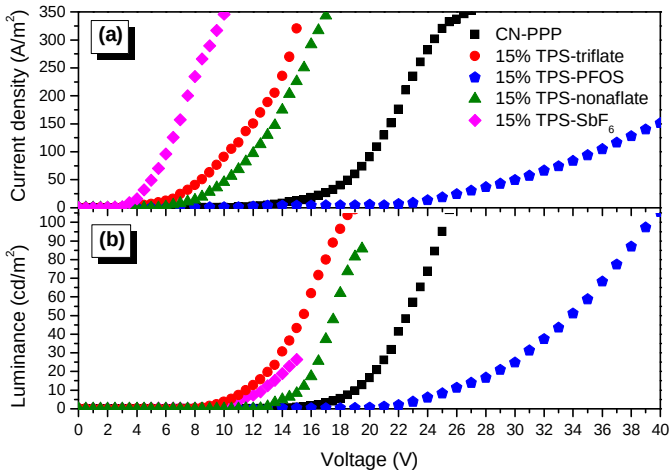

Fig. 7. *(a) Current density - voltage (J-V) and (b) luminance - voltage (L-V) characteristics of PLED devices based on CN-PPP, where different TPS-salts have been added in the emissive layer in order to demonstrate the effect of the anion on the performance of the devices.*

2. Interfacial layers for high performance OPVs

a) Vacuum deposited transition metal oxides as hole extraction layers in OPVs

Hydrogenated and substoichiometric Mo oxides described previously were incorporated as hole extraction/transport (HEL/HTL) layers in P3HT:$PC_{71}BM$ (1:0.8 wt/%) bulk heterojunction solar cells. A significant improvement in the short circuit current (Jsc), the open circuit voltage (Voc), the fill factor (FF), and the cell power conversion efficiency (PCE) was achieved for substoichiometric Mo oxides, compared to the stoichiometric MoO_3 HEL. In particular, Voc increases from 0.53 for MoO_3 to 0.69 when a hydrogenated Mo oxide is used as the HEL. This represents a 30% improvement for the device incorporating the substoichiometric Mo oxide with the highest amount of hydrogen, approaching the theoretical limit of ~0.7 V for a P3HT:PCBM solar cell with ohmic contacts. Similarly, the Jsc increases by a factor of 2 (from 5.68 to 11.64 mA/cm^2) and the FF increases from 0.32 to 0.54 (almost a 70% improvement). The large enhancement of both the Jsc and the FF are reflected in the considerable reduction of the series resistance (from 50 to 7.5 Ω cm^2) and the moderate increase of the shunt resistance (from 202 to 300 Ω cm^2) of the substoichiometric Mo oxide modified cell, clearly suggesting a reduced contact resistance, improved hole transport through gap states, and reduced leakage currents, respectively. The significant improvement of all the solar cell parameters results in a dramatic increase of the PCE to 4.34 %, compared to only 0.96% for the MoO_3 based cell (a more than a factor of 4 enhancement). Current-density-voltage (J-V) characteristics under simulated 1.5G solar irradiation are shown in Figure 5 (left) while the variation of Jsc and Voc values are plotted versus the degree of reduction of Mo atoms and the hydrogen content are also presented in this Figure (right panel).

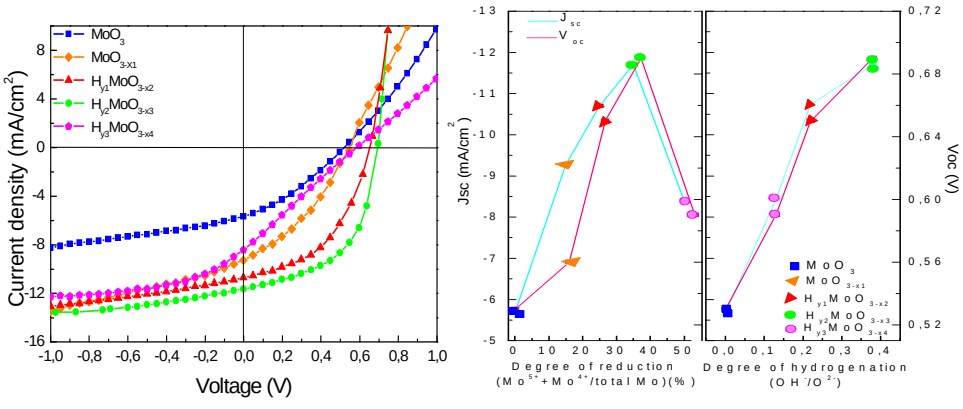

Fig. 8. *(left) Current density versus voltage characteristics for P3HT:$PC_{71}BM$ BHJ devices embedding 5 nm Mo oxide hole extracting layers. (right) Variation of J_{sc} and V_{oc} with the degree of reduction (the portion of Mo atoms with oxidation states 5+ and 4+ relative to the total Mo cations, as derived from 3d Mo XPS measurements) and the hydrogen content (the amount of Mo-OH relative to Mo-O bonds, as derived from O 1s XPS results), respectively.*

b) Solution-processed polyoxometalates as electron injection layers in OPVs

Interface engineering by using solution processed compounds with the desired charge transport properties is of great importance and may offer and efficient method to simplify OPV device manufacturing using functional materials processed from environmental-friendly solvents.The use of a water-soluble, tungsten polyoxometalate (PW12-POM) as an efficient cathode interlayer incorporated into poly(3-hexylthiophene):[6,6]-phenyl-C_{61}-butyric acid methyl ester (P3HT:PCBM-61) bulk heterojunction solar cells was demonstrated (Figure 6, top). The short circuit photocurrent density of the PW12-POM modified device is enhanced by ~40% and the Voc increases from 0.61 V to 0.65 V, resulting to corresponding power conversion efficiency enhancement by ~70% (from 1.57 for the reference to 2.7% for the PW12-POM modified device) (Figure 6, down-left). The improvement was attributed to enhanced electron transfer/extraction at the PW12-POM/Al interface as a result of the favourable interfacial energy level alignment and possible enhancement of the local electric field due to the nanoscale morphology of the PW12-POM layer, as evidenced by AFM measurements. Reduced degradation rate was measured for PW12-POM modified devices stored in dark and measured in ambient conditions. Taking into account the advantageous solution processability of PW12-POM, the large increase in the efficiency of the devices and the improvement of their time stability, we manifest that PW12-POM has highly desirable properties in order to be embedded as cathode interlayer in OPV devices (Figure 6, down-right).

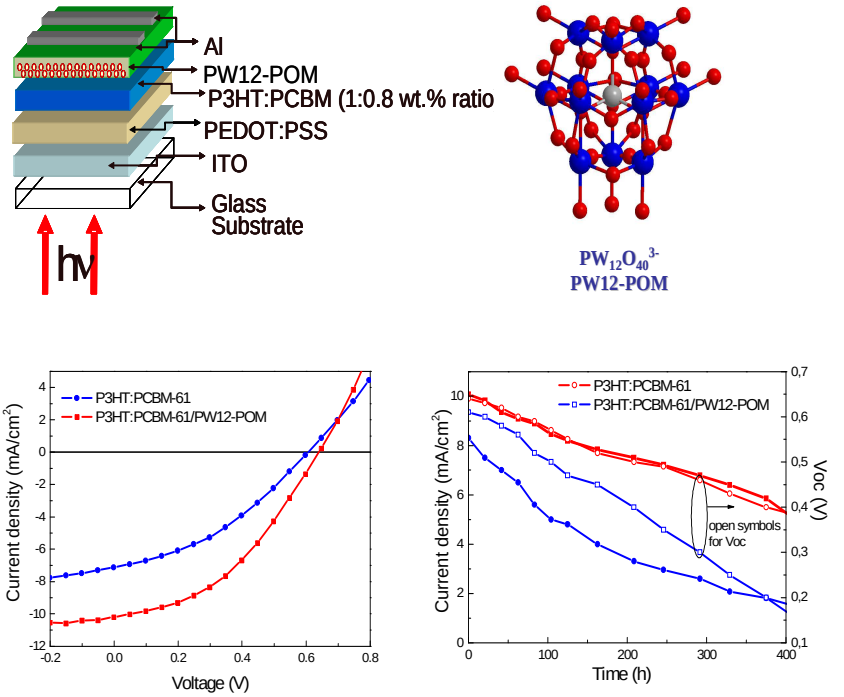

Fig. 9. *(Up) Schematic architecture of the fabricated OPVs (left) and the Keggin structure of the $(PW_{12}O_{40})^{3-}$ tungsten polyoxometalate (PW12-POM) (right). (Down) Photocurrent density-voltage (J-V) characteristics of reference and HyOPVs for an optimized 20 nm PW12-POM EEL/ETL (left), Representative stability data depicting Jsc (solid symbols) and Voc (open symbols) of the above devices measured under ambient conditions (right).*

3. Alternative Patterning Processes

a) Patternable polymeric materials with ultra low dielectric constants

Polyhedral oligomeric silsesquioxane (POSS) based materials hold great promise for developing a photopatternable low-*k* material which eliminates the need for sacrificial layers when patterning low-*k* dielectric films. In this work we demonstrate that organic materials based on partially fluorinated, polyhedral oligomeric silsesquioxane (POSS)-functionalized (meth)acrylates (POSS-F) containing appropriate amounts of the photoacid generator (PAG), triphenylsulfonium perfluorooctylsulfonate (TPS-PFOS), in order to achieve positive tone imaging, present ultra low k- values (lower than 2.0) which are further decreased when the amount of the photoacid generator is increased due to the large percentage of C-F bonds in the selected PAG. An optimum concentration of about 5 % w/w of the acid generator was calculated in order to obtain both acceptable photolithographic behaviour and ultra low-k properties.

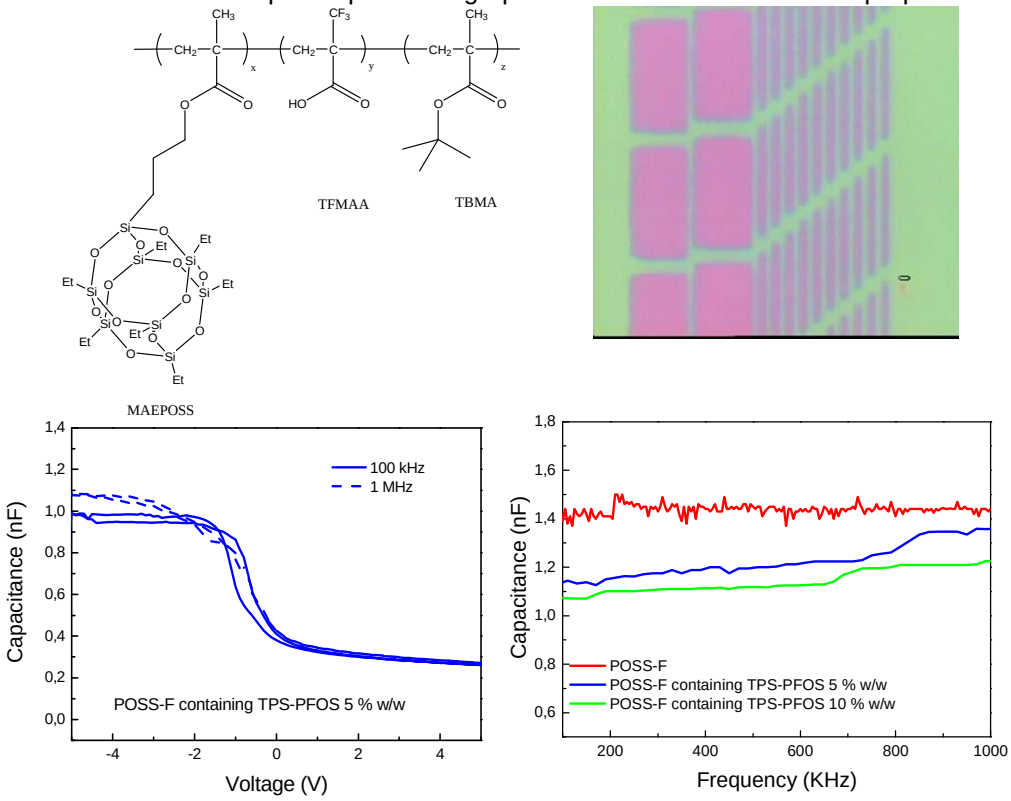

Fig. 10. *(Up) The chemical structure of a partially fluorinated, POSS-based methacrylate terpolymer (POSS-F) (left). Photolithographic patterns of POSS-F thin films containing TPS-PFOS at concentrations 5 % w/w (right). (Down) Capacitance–voltage curves of POSS-F containing 5 % w/w TPS-PFOS thin films measured at 100 KHz and 1 MHz (left). Capacitance-frequency curves of POSS-F thin films containing TPS-PFOS in concentrations 0, 5 and 10 % w/w (down).*

4. Spectroscopic characterization of protective coatings in conservation of antiquities and works of art

The experience of our team in spectroscopic characterization of thin organic films was successfully applied in the assessment of protective polymeric coatings of metal substrates (bronze and iron coupons) used in art conservation. In particular, an ethylene-methacrylic acid copolymer, formulated by BASF as a water-borne suspension of its alkylammonium salt and used in art conservation as a temporary protective coating, was characterized mainly with FT-IR spectroscopy. It was proved that in the freshly applied state of the copolymer film both carboxylic acid and carboxylate ion functional groups coexist, whereas in the working state of the film only acidic groups exist (Fig. 11). Also, the working state showed a 1:12 ratio of methacrylic acid towards ethylene units. Finally, in the case of bronze coupons interaction of carboxylate ions with the copper substrate was detected.

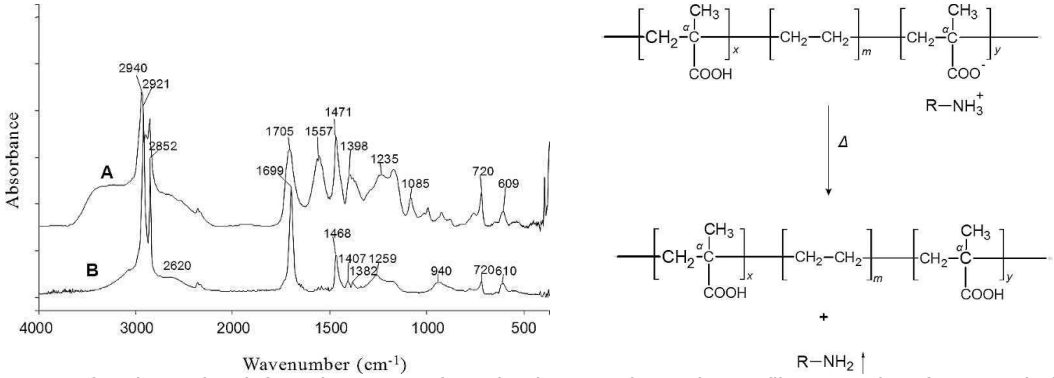

Fig. 11. *Left: Absorption infrared spectra of randomly coated copolymer films on Si wafer recorded (A) immediately after coating; and (B) 8 months after coating. Right: Transformation between the two states of the film material.*

PROJECT OUTPUT in 2012

Publications in International Refereed Journals

1. *The influence of hydrogenation and oxygen vacancies on molybdenum oxides work function and gap states for application in organic optoelectronics,*
   M. Vasilopoulou, A.M. Douvas, D.G. Georgiadou, L.C. Palilis, S. Kennou, L. Sygellou, A. Soultati, I. Kostis, G. Papadimitropoulos, D. Davazoglou and P. Argitis
   J. Am. Chem. Soc. 134, 16178-16187, 2012
2. *Photodegradable polymers for biotechnological applications,*
   G. Pasparakis, T. Manouras, P. Argitis, M. Vamvakaki
   Macromol. Rapid Commun., 33 (3) , pp. 183-198, 2012
3. *Barrierless hole injection through sub-bandgap occupied states in OLEDs using substoichiomeric MoOx anode interfacial layer*,
   M. Vasilopoulou, L.C. Palilis, D. G. Georgiadou, S. Kennou, I. Kostis, D. Davazoglou, P. Argitis
   Appl. Phys. Letters, 100, 013311, 2012
4. *Reduced Transition Metal Oxides as Electron Injection Layers in Hybrid-PLEDs,*
   M. Vasilopoulou, D.G. Georgiadou, L.C. Palilis, P. Argitis, S. Kennou, L. Sygellou, N. Konofaos, A. Iliadis, I. Kostis, G. Papadimitropoulos, D. Davazoglou
   Microelectron. Eng., 90, 59-61, 2012
5. *High performance organic light emitting diodes using substoichiometric tungsten oxide as efficient hole injection layer,*
   M. Vasilopoulou, G. Papadimitropoulos, L.C. Palilis, D. G. Georgiadou, P. Argitis, S. Kennou, I. Kostis, N. Vourdas, N.A. Stathopoulos, D. Davazoglou
   Organic Electronics, 13, 796-806, 2012
6. *Patternable Fluorinate Polyhedral Oligomeric Silsequioxane-Functionalized polymer materials with ultra low dielectric constants,*
   M. Vasilopoulou, A.M. Douvas, P. Argitis,
   Materials Chemistry and Physics, 135, 880-83, 2012
7. *Conduction mechanisms in tungsten-polyoxometalate self-assembled molecular junctions,*
   D. Velessiotis, A.M. Douvas, P. Dimitrakis, P. Argitis, N. Glezos
   Microelectronic Engineering, 97, 150-53, 2012
8. *Effect of triphenylsulfonium triflate addition in wide band-gap polymer light-emitting diodes: improved charge injection, transport and electroplex-induced emission tuning,*
   D. G. Georgiadou, L. C. Palilis , M. Vasilopoulou , G. Pistolis , D. Dimotikali and P. Argitis
   RSC Adv., 2 (31), 11786-11792, 2012
9. *Substoichiometric hot-wire WO_x films deposited in reducing environment,*
   Vourdas N.' Papadimitropoulos G., Kostis I., Vasilopoulou M., Davazoglou, D., Thin Solid Films, 520, 3614, 2012.
10. *Omnidirectional antireflective properties of porous tungsten oxide films with in-depth variation of void fraction and stoichiometry*,
    Vourdas N. , Dalamagkidis K., Kostis I., Vasilopoulou M., Davazoglou, D.
    Optics Communications, 285, 5229-5234, 2012
11. *Characterization of a water-dispersible metal protective coating with fourier transform infrared spectroscopy, modulated scanning calorimetry, and ellipsometry,*
    S. C. Boyatzis, A. M. Douvas, V. Argyropoulos, A. Siatou, M. Vlachopoulou
    Applied Spectroscopy 66(5), 580-590, 2012

Published Conference Proceedings

1. *Selective adhesion and directed growth of fibroplasts on micropatterned substrates for tissue engineering,*
   A. Bourkoula, P. Pavli. E. Mavrogonatou, D. Kletsas, P. Petrou, P. Argitis, S. E. Kakabakos
   Wound Repair and Regeneration, Vol. 20, A86, Sep-Oct 2012

Conference Presentations

1. *Water-soluble porphyrin thin films as nanostructured electron extraction layers in organic photovoltaic cells*,
   M. Vasilopoulou, A. M. Douvas, L. C. Palilis, L. Sigellou S. Kennou, D. G. Georgiadou, V. Constandoudis, S. Gardelis, T. Lazarides, A. G. Coutsolelos and P. Argitis,
   E-MRS, Spring Meeting 2012, Strasbourg
2. *Interface Engineering in Organic Photovoltaic Devices Using Transition Metal Oxides with Tunable Properties as Charge Extraction/Collection Layers,*
   M. Vasilopoulou, L. C. Palilis, A. Douvas, D. G. Georgiadou, A. Soultati, St. Kennou, L. Sygellou, I. Kostis, G. Papadimitropoulos, D. Davazoglou and P. Argiti
   E-MRS, Spring Meeting 2012, Strasbourg
3. *Substoichiometric tungsten oxide hole injection/extraction layers for improved performance organic optoelectronic devices,*
   A. Soultati, M. Vasilopoulou, L. C. Palilis, A. Douvas, D. G. Georgiadou, St. Kennou, L. Sygellou, ., G. Papadimitropoulos, D. Davazoglou and P. Argitis
   International Conference on Organic Electronics (ICOE 2012), 25-27 June 2012, Tarragona, Spain
4. *The mechanism of tuning the electronic structure of transition metal oxides through hydrogen incorporation for high performance organic optoelectronic devices,*
   M. Vasilopoulou, I. Kostis, L. C. Palilis, D. G. Georgiadou, S. Kennou, A. M Douvas, A. Soultati, G. Papadimitropoulos, D. Davazoglou and P. Argitis
   International Conference on Organic Electronics (ICOE 2012), 25-27 June 2012, Tarragona, Spain
5. *Triphenylsulfonium salts as electron transporting organic ionic compounds for enhancing charge injection and transport in polymer light emitting devices,*
   D. G. Georgiadou, L. C. Palilis, M. Vasilopoulou, S. Kazazis, P. Dimitrakis, V. Constantoudis, D. Dimotikali, P. Argitis
   International Conference on Organic Electronics (ICOE 2012), 25-27 June 2012, Tarragona, Spain
6. *Hydrogen doped transition metal oxides for advanced interface engineering in efficient organic light emitting devices*,
   M. Vasilopoulou, A.Soultati, D. G. Georgiadou, L.C.Palilis, A. M. Douvas, I. Kostis, S. Kennou, N. A. Stathopoulos, N. Konofaos, A. Iliadis, D. Davazoglou, P. Argitis
   5th International Symposium on Flexible Organic Electronics (IS-FOE), Thessaloniki, Greece
7. *Substoichiometric tungsten oxide hole injection layers for improved performance organic optoelectronic devices,*
   A.Soultati, D. G. Georgiadou, L.C.Palilis, A. M. Douvas, I. Kostis, G. Papadimitropoulos, D. Davazoglou, S. Kennou, P. Argitis, M. Vasilopoulou
   5th International Symposium on Flexible Organic Electronics (IS-FOE), Thessaloniki, Greece
8. *Current-transport studies of metal/organic/metal diodes based on triphenylsulfonium salts addition in a semi-conducting polymer matrix,*
   St. Kazazis, D. G. Georgiadou, P. Dimitrakis, P. Normand and P. Argitis
   5th International Conference "Micro&Nano2012" on Micro - Nanoelectronics, Nanotechnologies and MEMS, Crete, October 2012
9. *Photoresist based on backbone breakable polyacetal with bound PAGs,*
   T. Manouras, M. Chatzichristidi and P. Argitis
   5th International Conference "Micro&Nano2012", Crete, October 2012
10. *Patterning photodegradable polyacetals grafted to epoxy modified silicon substrates,*
    S. Tzani, T. Manouras, M. Chatzichristidi, P. Argitis
    5th International Conference "Micro&Nano 2012", Crete, October 2012
11. *Polyacetals grafted to silicon substrates for photopatterning*,
    S. Tzani, T. Manouras, M. Chatzichristidi, P. Argitis
    Hellenic Polymer Society Conference, Thessaloniki 2012

Invited Talks

1. *Control of Charge Injection/Extraction Barriers in Organic Optoelectronic Devices,*
   P. Argitis, M. Vasilopoulou, A.M. Douvas, D.G. Georgiadou, A. Soultati, I. Kostis, G. Papadimitropoulos, D. Davazoglou, S. Kennou, L. Sygellou, L.C. Palilis
   28th Panhellenic Conference on Solid State Physics & Materials Science, September 2012, Patras,

Greece
2. *Electron/Hole Extraction Layers in Organic Photovoltaics,*
   P. Argitis
   Workshop on Biomimetic Utilization of Solar Energy, University of Crete, Department of Chemistry, October 2012, Iraklion, Crete, Greece
3. *RTD Activities in the field of Organic Electronics at NCSR Demokritos,*
   P. Argitis
   Organic Electronics Meeting, 19 November 2012, Thessaloniki, Greece
4. *Approaches for improved charge injection/extraction in organic optoelectronic devices,*
   P. Argitis
   Workshop on Molecular/Organic Electronics, Technical University of Cyprus, December 2012, Limassol, Cyprus

Awards

Water-soluble porphyrin thin films as nanostructured electron extraction layers in organic photovoltaic cells,
M. Vasilopoulou, A. M. Douvas, L. C. Palilis, L. Sigellou S. Kennou, D. G. Georgiadou, V. Constandoudis, S. Gardelis, T. Lazarides, A. G. Coutsolelos and P. Argitis
Best Poster Award in E-MRS, May 2012, Strasbourg

Doctoral Dissertations completed in 2012

1. *Lithographic Materials Based on Photoinduced Cleavage of Polyacetals Backbone,*
   Theodoros Manouras
   University of Athens, Department of Chemistry, June 2012
2. *Photochemical Modifications of Thin Polymeric Films for Nanobiotechnology Applications,*
   Pagona Pavli
   National Technical University of Athens, Department of Chemical Engineering, October 2012
3. *Modification of Optoelectronic Characteristics in Organic Light Emitting Devices by Using Sulfonium Salts,*
   Dimitra G. Georgiadou
   National Technical University of Athens, Department of Chemical Engineering, December 2012

Masters Dissertations completed in 2012

1. *High performance organic photovoltaic devices using transition metal oxides as hole injection/extraction layers,*
   Anastasia Soultati
   University of Athens, Department of Informatics and Telecomunications, February 2012 Supervisors: M. Vasilopoulou, P. Argitis
2. *Binding of photodegradable polymers on surfaces,*
   Sofia Tzanni
   University of Athens, Department of Chemistry, October 2012
   Supervisors: M. Chatzichristidi, P. Argitis

PROJECT I.2

PLASMA ENABLED NANOFABRICATION: PROCESSING, SIMULATION, METROLOGY AND APPLICATIONS

Key Researchers: E. Gogolides, A. Tserepi

Permanent Scientific Staff: V. Constantoudis

Post Doctoral Scientists: G. Kokkoris, D. Moschou, N. Vourdas, K. Tsougeni, G. Papadakis

Collaborating Researchers:

- For activity A-Plasma Nanofabrication: I. Raptis (optical characterization), A. Olziersky (e-beam lithography)
- For activity D2-Microfluidics-Lab on Chip for Life Sciences: S. Chatzandroulis, K. Misiakos
- For activity D3-Nanodevices for Energy: P. Argitis, P. Normand, P. Dimitrakis, M. Vasilopoulou

PhD Students: M.-E.Vlachopoulou, A. Malainou, D. Kontziampasis, K. Ellinas, A. Smyrnakis, N. Skoro, V.K. Murugesan Kuppuswamy

MSc Students: A. Zeniou, E. Kouris, N. Karasmani, S. Mouchtouris, Th. Christoforidis

External collaborators:

- For activity A-Plasma Nanofabrication: C. Cardinaud (Univ. of Nantes, France), W. Coene, M. Riepen, M. Van Kampen (ASML, Netherlands), D. Ehm (Zeiss, Germany), U. Cvelbar (Josef Stefan Inst., Slovenia), N. Puač, S. Lazovic (Inst. of Physics, Belgrade, Serbia)
- For activity B-Nanometrology: W. Coene (ASML, Netherlands), G. Gallatin (NIST, USA), R. Gronheid, A.P. Vaglio (IMEC, Belgium), E. Pargon (CEA/LETI, France)
- For activity C-Modeling and Simulation: A. Boudouvis, N. Cheimarios, G. Pashos, (NTUA, Greece), C. Vahlas (U.de Toulouse, France), P. Brault, A.L. Thomann (Univ. d'Orléans, France), G. Gallatin (NIST, USA)
- For activity D1-Smart Nanostructured Surfaces: A. Boudouvis, A. Papathanasiou, D.P. Papageorgiou, C. Charitides, E. Pavlatou (NTUA, Greece), K. Beltsios, I. Panagiotopoulos (Univ. of Ioannina, Greece), E. Amanatides, D. Mataras (Univ. of Patras, Greece), H. Zuilhof, S. Pujari (Wageningen Univ., Netherlands)
- For activity D2-Microfluidics-Lab on Chip for Life Sciences: S. Kakabakos, P. Petrou (IRRP, NCSR-D, Greece), A. Vlahou, S. Pagakis (IIBEAA, Greece), G. Kaltsas (TEI of Athens, Greece), D.S. Mathioulakis (NTUA, Greece), E. Sarantopoulou (NHRF, Greece), E. Gizeli (FORTH, Greece), A. Speliotis (IMS, NCSR-D, Greece), T. Rudin, S.E. Pratsinis (ETH Zurich, Switzerland), J.L. Viovy, S. Descroix (Inst. Curie, France), B. Depuis (Inst. Pasteur, Paris, France), G. Jobst (Jobst Technologies, Germany)
- For activity D3-Nanodevices for Energy: S. Christiensen (IMPP, Germany)

OBJECTIVES

The activities of project I.2 can be seen schematically below:

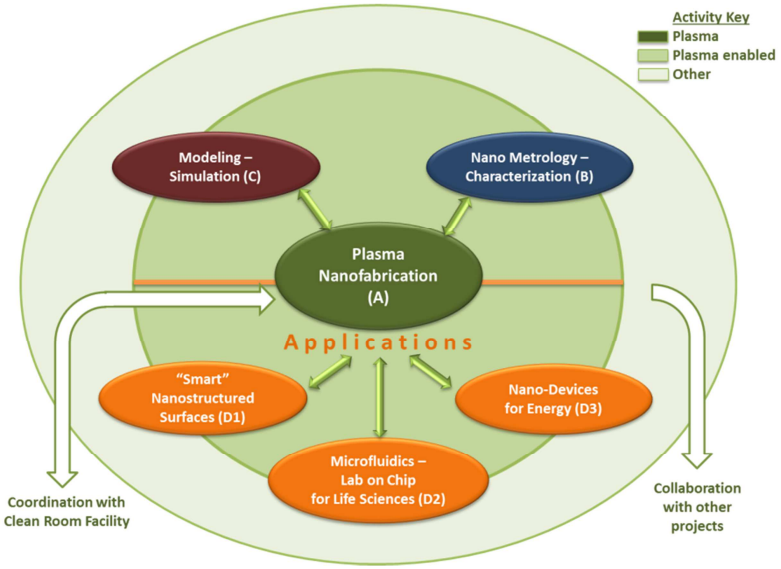

Fig. 1. *Schematic of project I.2 activities for Plasma Enabled Nanofabrication*

The heart of our activities and our first objective is to advance and promote plasma nanofabrication, nanopatterning and plasma nanotechnology enabling various applications. This is seen as the central circle in Fig.1 and described in section A below.
Around plasma nanotechnology a series of activities for nanometrology-characterization (B), modeling-simulation (C) and applications (D) are clustered depicted visually in the second circle around A. A third outer circle includes other activities not directly enabled by plasma nanotechnology but linked to the activities of the second circle (B, C, D), as well as to other projects.
Indeed, after fabrication of micro and nanostructures and devices using plasma processing, **our second objective is to develop nanometrology and characterization methodologies for nanostructure description** (see section B). **Our third objective is to understand and improve plasma and other processes using modeling and simulation** (see section C). Finally, **our fourth objective is to exploit our plasma nanotechnology** toolbox to enable **a variety of applications including Surface Engineering** ("smart surfaces" see section D1), **Microfluidics and Lab on Chip for Life Sciences** (see section D2), **and NanoDevices for Energy** (see section D3). For all these objectives, we work in coordination with the clean room facility, often transferring samples to and from it, and in collaboration with several other projects such as the Biomicrosystems project, and the Lithography project.

For 2012 our main achievements are:
Plasma Nanonofabrication: We improved our new planar technology to fabricate nanotexture (nanoroughen) and surface-modify polymeric microfluidics and bioMEMS (cf. A.1). We established our recent plasma-directed assembly process for nanodot formation on plasma etched polymers (cf. A.2). We characterized Hydrogen Plasmas for plasma cleaning of sensitive optical surfaces (cf. A.3). We developed two novel plasma processes for ultra high aspect ratio fabrication of Silicon Nanowires and nanopillars and measured their optical properties (cf. A.4).
Nanometrology: We developed a methodology to measure the thickness of thin protein and other films on nanostructured surfaces using AFM data (cf. B.1). We developed software for the extraction of noise from SEM images and measurement of Line-Edge-Roughness (cf. B.2). We initiated the use of complex network theory for the description of rough surfaces (cf. B.3).
Modeling and Simulation: We proposed a simple model and rules of thumb for Line-Edge-Roughness Transfer during Plasma Etching (cf. C.1). We modeled Hydrogen Plasmas for Surface Cleaning (cf. C.2). We modeled the lithography process effects on Contact-Edge-Roughness (cf. C.3). We performed Multiscale and molecular Dynamics Simulations for Chemical Vapour Deposition of Si and Al (cf. C.4, C.5). We developed a computational framework for calculation of Cassie-Wenzel transition of drops sitting on microstructured surfaces (cf. C.6).
"Smart" Nanostructured Surfaces: We developed hierarchical superoleophobic surfaces on organic polymers (PMMA, PEEK, PS, PET etc.) and on silicones (PDMS) using Oxygen and SF_6 plasma nanotexturing, respectively. New self-assembled fluorinated monolayers were used

for their surface energy reduction. Low hysteresis and high contact angle were obtained for several oils (cf. D1.1, D1.2, D1.3).
Microfluidics and Lab on Chip for Life Sciences: We compared the flow in rough hydrophilic and superhydrophobic microchannels using pressure drop and Particle Image Velocimetry experiments, and showed the reduced pressure drop and large slip velocities in the second case (cf. D2.1, D2.2). We fabricated TiO_2 affinity microcolumns and demonstrated phosphopeptide enrichment (cf. D2.3). We fabricated a DNA amplification Lab on Chip (μPCR) on a polymeric substrate with accurate temperature control (cf. D2.4). We developed new nanoscale arrays of proteins using colloidal lithography followed by plasma etching and selective protein immobilization (cf. D2.5).
Nanodevices for Energy: We established our first Silicon Nanowire p-n junction devices and demonstrated good photovoltaic performance (cf. D3.1).

FUNDING

- SPAM, Marie Curie-ITN,Contract No 215723
- "DNA on waves: an integrated diagnostic system" GSRT Contract No. LS7(276)
- CORSED, Contract No. PE8(844)
- Love Food, Contract No. 317742
- Plasma Nanofactory, Contract No. 695
- DesireDrop, Contract No. MIS 380835
- Project III41011 of MESTD of Serbia and Post Doctoral Fellowship from Serbian Government for Dr Nevena Puac

MAIN RESULTS in 2012

A. Plasma Nanofabrication

A.1 A planar technology for polymeric chip micro-patterning, applicable to microfluidics and labs on chip

K. Tsougeni, E. Gogolides

We propose a new technology for polymeric microchip fabrication based on lithography directly on the polymeric substrate followed by plasma etching of the substrate. We developed lithographic processes for thick and easily strippable photoresist patterning, (where stripping is performed without attacking the polymeric substrate) and plasma etching processes to transfer the pattern and chemically modify the polymeric substrates providing microfluidic channels with desired geometrical and wetting characteristics. We ensured that the photoresist has high resolution for photoresist heights of 5-20 microns (for example resolution down to 1 - 4 μm). In case the photoresist is used to transfer the pattern on the substrate we selected photoresists with high etch resistance and high selectivity with respect to the polymeric substrate. We evaluated single layer, bilayer silicon containing resists, and hard metallic masks. We tested different kinds of photoresists: (a) strippable thick resists such as AZ 15nXT (negative), AZ 9260 (positive), and maP-1275 (positive). However, we noticed deformation of posts after the plasma processing. This process is therefore not suitable for deep polymer etching. (b) Bilayer Si containing strippable photoresist, such as Ormocomp (negative) in combination with a bottom release layer (LOR=Lift-Off-Resist). Lithography is done on the stack LOR layer / Ormocomp. Removal of the LOR can be easily done using weak alkaline solutions, thus the technology is applicable even to extremely sensitive polymeric substrates. Fig.2 shows SEM images of a bilayer of LOR / Ormocomp after O_2 plasma etching before and after removal of the stack. High selectivity (Selectivity 30:1) was obtained after plasma etching because of ORMOCER oxidation to SiO_2. After removing the LOR / ORMOCER stack, clean polymeric surfaces are obtained allowing thermal bonding of the microfluidic lid. We concluded that this resist is a good candidate for patterning and deep etching of polymeric substrates, followed by thermal bonding.

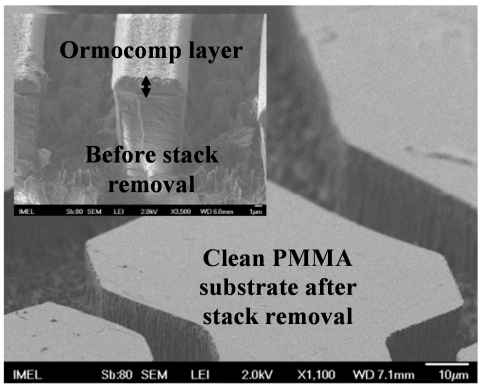

Fig. 2. *SEM images of a bilayer of LOR / Ormocomp after O_2 plasma etching before and after removal of the stack.*

A.2 Plasma Directed Organization of Nanodots on Polymers: A statistical analysis as a study on the reproducibility of the phenomenon.

D. Kontziampasis, E. Gogolides

In the previous years, we demonstrated a plasma directed, organized, nanodot formation on organic polymers. This year, we expand our work on plasma directed organization and perform statistics to see how reproducible the phenomenon is, i.e. if it produces the same results using the same reactor, the same plasma etching conditions and the same polymeric material. Also we study whether in the same sample all the areas that are measured have the same statistical characteristics (order, height, width, period etc.) under the same plasma etching conditions, since plasma is considered to be uniform in this area.
The statistical analysis was performed measuring the parameters of samples etched since 2007 and up to 2012. The etching conditions used are; 1 min etching, O_2 plasma, pressure 0.75 Pa, temperature (electrode) 65^{o}C, bias Voltage 0V (Bias generator closed), gas flow 100 sccm and power 1800 W. The statistical parameters measured in this study were the root mean square (rms), correlation length, period and order parameter of the surfaces. The analysis was performed after measuring the samples with AFM (CP-II from Veeco) and analyzing the x-y-z topography of each surface with the home-made software SURFANALYSIS.

Table I. Statistical analysis of 50 different samples, etched under the same conditions for a period of 5 years.

Parameter / Statistics	RMS (nm)	Period λ (nm)	Correlation Length (ξ) (nm)	Order Parameter ω
Mean Value	5.86	62.3	13.9	1.6
Standard Deviation	0.43	7.2	3.2	0.4

Table I shows the size and order parameters after analyzing AFM measurements of surfaces that were etched from 2008 to 2012. A total of 50 different samples were analyzed. In it, we observe a significant deviation in the statistics of the surfaces. Nevertheless, we know that the plasma reactor has undergone through several changes due to maintenance and repairs. The most important one was the maintenance in the cooling system, which can bring significant change in the temperature of the sample during etching. In order to be certain that the deviations are not affected by the changes in the reactor, we perform a series of experiments in which the samples are etched at the same day. Table I shows the analysis of the etched surfaces that were etched the same day (7 samples measured), after AFM measurements. As in the previous series, we calculate rms, correlation length, period and order parameter for each surface.

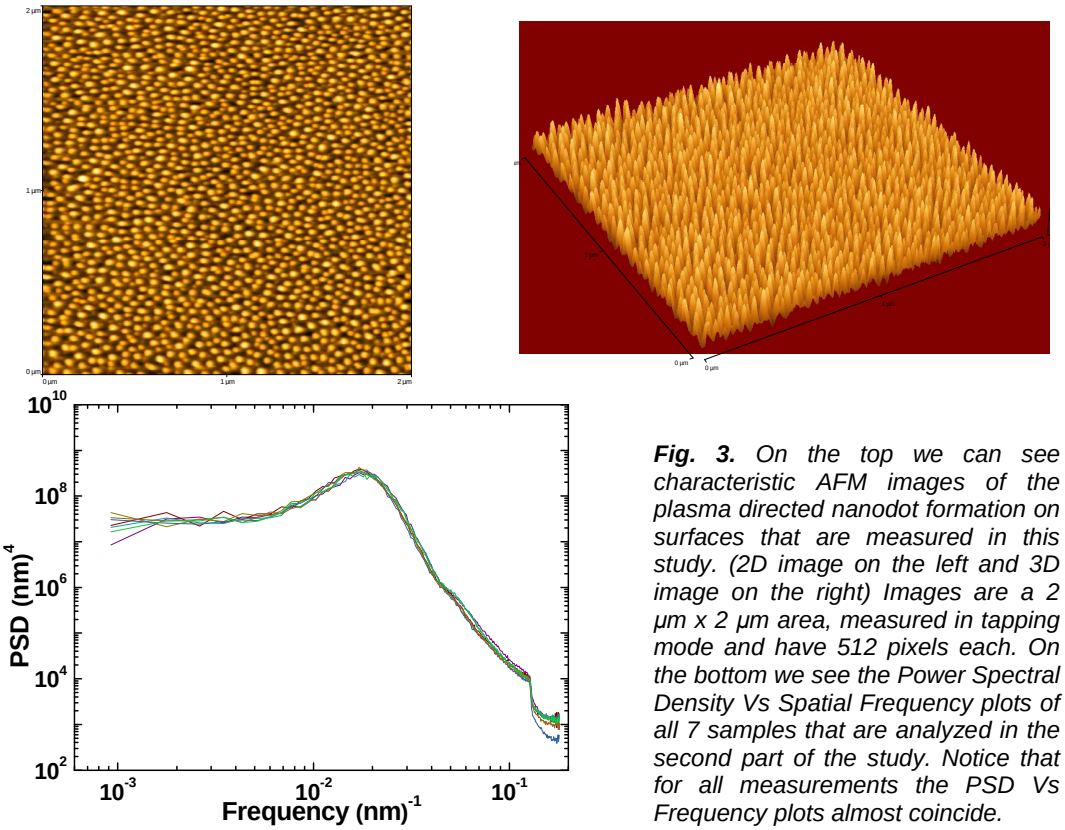

Fig. 3. *On the top we can see characteristic AFM images of the plasma directed nanodot formation on surfaces that are measured in this study. (2D image on the left and 3D image on the right) Images are a 2 μm x 2 μm area, measured in tapping mode and have 512 pixels each. On the bottom we see the Power Spectral Density Vs Spatial Frequency plots of all 7 samples that are analyzed in the second part of the study. Notice that for all measurements the PSD Vs Frequency plots almost coincide.*

Table II. Statistical analysis of 7 different samples, etched under the same conditions at the same day.

Parameter / Statistics	RMS (nm)	Period λ (nm)	Correlation Length (ξ) (nm)	Order Parameter ω
Mean Value	**6.16**	**57.9**	**10.6**	**1.8**
Standard Deviation	**0.10**	**1.9**	**1.9**	**0.2**

By observing the values of Table II we can clearly see that the standard deviation is below 10% and lies in the limits of statistical error of each measurement with the AFM.
From the above we can conclude that as long as the reactor's condition is unchanged this method can produce well defined, uniform, nanostructures of the same average height, width, distance and order on the surface of polymeric films.

A.3 Characterization and global modeling of low-pressure Hydrogen-based RF plasmas suitable for surface cleaning processes

N. Škoro, N. Puač, G. Kokkoris, E. Gogolides and external collaborators

We performed measurements and global modeling of low-pressure inductively coupled H_2 plasma which is suitable for surface cleaning applications aiming at understanding mirror cleaning in an Extreme Ultraviolet Lithography (EUVL) Tool. The plasma was ignited at 1 Pa in our helicon-type reactor and is characterized using optical emission measurements (optical actinometry) and electrical measurements, namely Langmuir and catalytic probe. By comparing catalytic probe data obtained at the center of the chamber with optical actinometry results, an approximate calibration of the actinometry method as a semi-quantitative measure of H density was achieved. Coefficients for conversion of actinometric ratios to H densities were tabulated and provided in the table below. Best agreement with catalytic probe results was obtained for (Hβ, Ar750) and (Hβ, Ar811) actinometric line pairs. Additionally, concentrations of electrons and ions as well as plasma potential, electron temperature and ion fluxes were measured in the

chamber center at different plasma powers using a Langmuir probe. Moreover, a global model of inductively-coupled plasma was formulated using a compiled reaction set for H_2/Ar gas mixture. The model results compared reasonably well with the results on H atom and charge particle densities and a sensitivity analysis of important input parameters was conducted. After characterization of the reactor, Si wafers with PMMA and carbon layers were processed in low-pressure H2 plasma. Measurements showed that etching rates of PMMA film were much higher than amorphous carbon layers. This work was partially supported from the SPAM (Surface Cleaning for Advanced Manufacturing) Marie Curie project, and by a post-doctoral Fellowship program of the Serbian government supporting Nevena Puac.

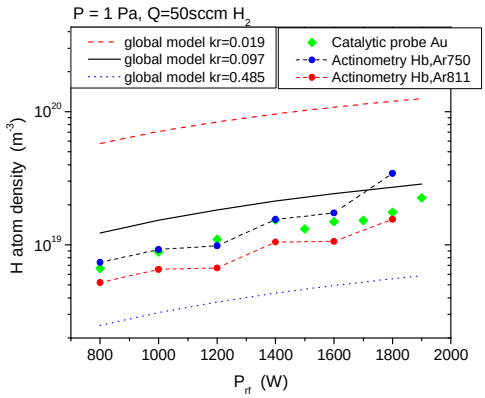

Fig. 4. *Comparison of H density obtained from the global model for three different values of surface recombination coefficient and the catalytic probe and actinometry data.*

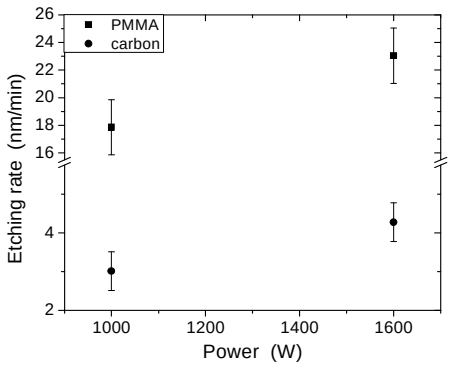

Fig. 5. *PMMA (squares) and carbon (circles) layer etching rates dependence on power in H2 plasmas. Different samples used and processed for 5 min.*

Table III. Coefficients used for conversion of actinometric ratios to H densities.

Actinometry ratio used	λ-involved (nm)	Detector response ratio in our system	Ratio of A coefficients	γ	Actinometric conversion coefficient γ * k_{Ar}^{dir}/k_H^{dir} to convert intensity to concentration ratio of N_H/N_{Ar}.					
					2eV	2.5	3eV	3.5	4eV	4.5
Hα/Ar750	656/750	0.7	2.2	1.4	0.25	0.31	0.36	0.41	0.44	0.48
Hα/Ar811	656/811	0.4	2.3	0.8	0.19	0.20	0.22	0.22	0.23	0.23
Hβ/Ar750	486/750	1.7	3.6	3.9	3.55	4.16	4.70	5.19	5.60	5.99
Hβ/Ar811	486/811	1.1	3.6	2.2	2.62	2.71	2.78	2.83	2.85	2.87

A.4 Nanoscale silicon etching: High aspect ratio silicon nanowire fabrication using colloidal self-assembly as a masking layer

A. Smyrnakis, A. Zeniou, E. Gogolides, A. Tserepi

High aspect ratio perpendicular to the substrate silicon nanowires (SiNWs) as well as micro- or nanopillars with controlled sizes and period are of extreme interest due to their structural, electrical and optical properties and their possible application in photovoltaics, sensors and energy harvesting devices. For the fabrication of such features, we developed a cryogenic silicon etching process that uses a SF_6/O_2 gas mixture at cryogenic temperature (T<−100 °C) and a time multiplexed deep reactive ion enhanced (DRIE) etching process at room temperature using one cycle of SF_6 followed by a C_4F_8 cycle. For the patterning, we use either the cost effective process of colloidal particle self-assembly (polystyrene micro particles serving as etch mask), optical lithography or e-beam lithography. We further optimize and improve our silicon etching process to reach as high aspect ratio as possible. Fabrication process offers full versatility in wire/pillar pitch, diameter and height, showing high anisotropy and etch rate, clean, smooth and controllable sidewall profile. Sub-200 nm diameter SiNWs with high aspect ratio up to 100:1 are demonstrated.

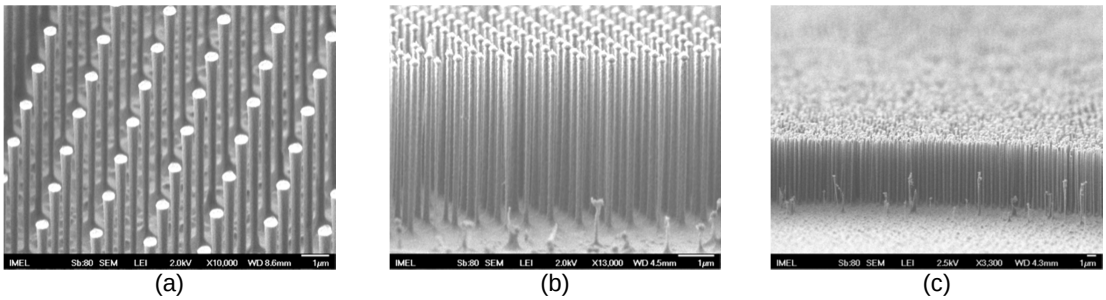

(a) (b) (c)

Fig. 6. *(a) SEM image of ordered SiNWs fabricated by optical lithography followed by cryogenic plasma etching process. The diameter of the wires is ~450 nm with an aspect ratio of 17:1. (b)-(c) SEM image of SiNWs fabricated by colloidal lithography followed by cryogenic plasma etching process. The diameter of the wires is ~200 nm with an aspect ratio of 26:1 and 37:1 respectively.*

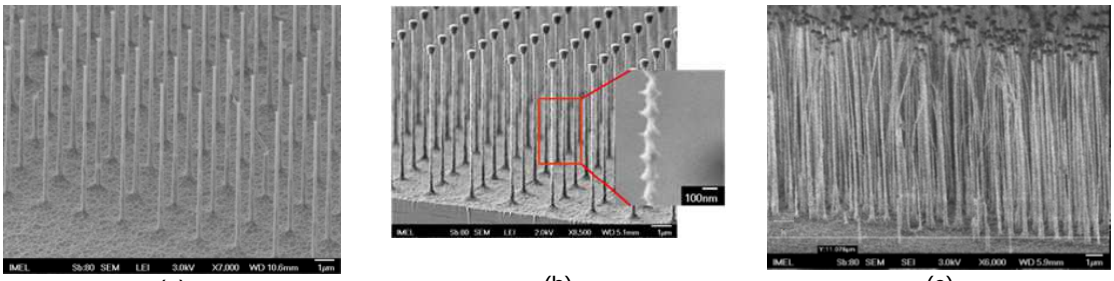

(a) (b) (c)

Fig. 7. *(a) SEM image of ordered SiNWs fabricated by e-beam lithography followed by time multiplexed DRIE plasma etching process. The diameter of the wires is ~200 nm with an aspect ratio of 40:1. (b)SEM image of SiNWs fabricated by optical lithography followed by time multiplexed DRIE plasma etching process. The diameter of the wires is ~100 nm with an aspect ratio of 46:1. (c)SEM image of SiNWs fabricated by colloidal lithography followed by time multiplexed DRIE plasma etching process. The diameter of the wires is ~100 nm with an aspect ratio >100:1.*

Reduction of optical reflection is important for many technologies including solar energy, photodetectors, and high-contrast, antiglare and stealth surfaces. In order to examine the optical properties of our silicon nanowires and evaluate their possible use in photovoltaic devices, we performed reflectance and FTIR measurements. Using a reflection probe we measure the Specular Reflectance as a percentage (%R) relative to the reflection from a standard reference substance. Fig.6 presents, the specular reflectance of silicon surface with high aspect ratio perpendicular SiNWs of different diameter (d), height (h), period (a), where low reflectance is identified. The characteristics of the SiNWs are mentioned in the text box embedded. We note that those samples were fabricated by the colloidal lithography that gives hexagonally packed wire arrays, and the cryogenic process was used for the silicon etching. Fig.7 shows the transmittance in the near/mid infrared regime of Si pillars of the same diameter and height but of different period (2 um and 3 um) of a square lattice. The pillars show characteristics minima in NIR Transmittance showing interest in the NIR regime for applications such as sensors.

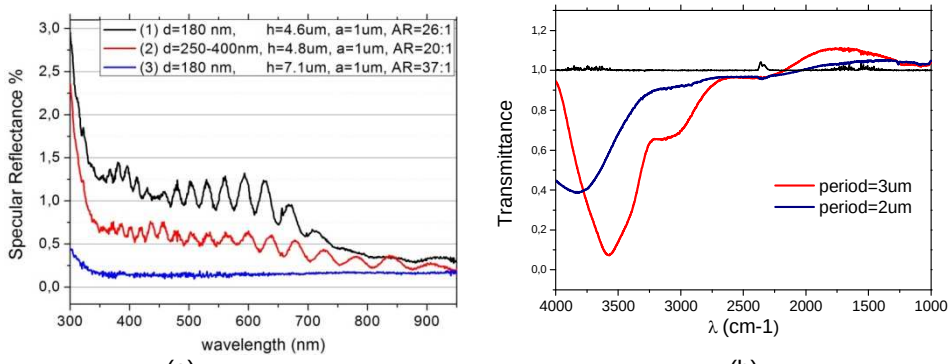

(a) (b)

Fig. 8. *(a) Specular reflectance of silicon surface with perpendicular silicon nanowires (SiNWs) of different diameter, d, height, h, period, a. (b) Transmittance in the near/mid infrared regime of Si pillars.*

B. Nano Metrology – Characterization

B.1 Measurement of thickness of very thin films on plasma patterned spots by means of Atomic Force Microscopy

V. Constantoudis, A. Malainou, A. Tserepi and external collaborators

In many applications, plasma etching is used for the fabrication of closely packed spots with various geometries on a substrate and the selective chemical modification of their top surfaces. The measurement of the height of these spots may be critical since it may reveal the selective deposition of some material on these (for example proteins as is the case of the work reported in D.2.5 “Nanoscale protein patterning on Si substrates using colloidal lithography and plasma processing). A method which has been proposed for this measurement is to obtain the Atomic Force Microscopy topography of the pattern and the histograms of its heights. Ideally, the histogram would have two peaks, difference of which would give the average spot height. However, when the spots are densely patterned the AFM tip cannot follow the topography elevations and give reliable measurements of the substrate height (“flying tip effect”). To remedy this shortcoming, we proposed a method to control the flying tip effects by changing the relative orientation of tip scanning direction and spot arrangement. We have observed that when the scanning direction coincides with the post orientation then the flying tip effect is enhanced and the substrate peak in the histogram is broken down to the artifact peak and the real one (see Fig.9b). We have applied this technique with success in the measurement of the thickness of a protein monolayer (~2nm) deposited selectively on the top surfaces of SiO_2 spots developed on a Si substrate (see D.2.5 “Nanoscale protein patterning on Si substrates using colloidal lithography and plasma processing).

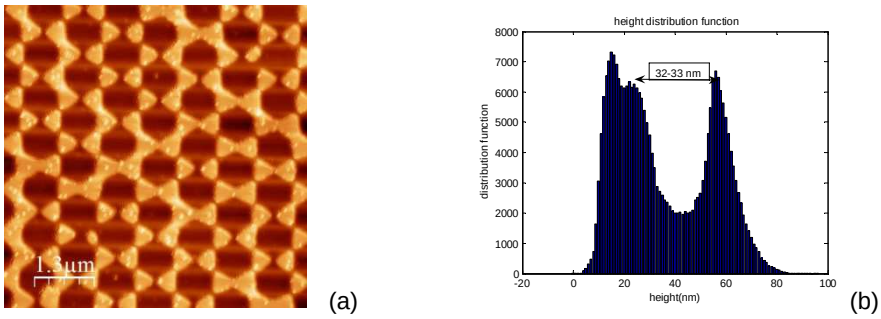

Fig. 9. *AFM image (a) and height histogram (b) of SiO_2 spots on Si substrate. Notice that due to the coincidence of the scanning direction with the post orientation the first peak of the histogram which corresponds to the Si surface is composed of two sub-peaks (Fig. 9b). The first sub-peak is an artefact due to the “flying tip effect”, whereas the second peak corresponds to the actual Si background. Therefore, the height of the SiO_2 nanoislands is measured approximately 32-33 nm in agreement with SEM measurement of the SiO_2 nanoisland height.*

B.2 Evaluation of methods for noise-free measurement of edge roughness of lithographic line/space patterns using synthesized CD-SEM images

V. Constantoudis and external collaborators

The dimensions and edge morphology of the nanoscale patterns are usually measured from top-down Scanning Electron Images. This technique is widely applied in the measurement of the critical dimension and edge roughness of lithographic linear and circular features (Line Edge Roughness (LER) AND Contact Edge Roughness (CER)). The accuracy of the measurements is degraded due to the noise of the SEM measurement process. Since the measured quantities are at nanoscale regime, the evaluation of the noise effect is of paramount importance in nanometrology. The aim of the work reported here is to contribute to the understanding of the effects of noise on LER parameters when they are measured through the analysis of top-down CD-SEM images. To this end, first we have developed a methodology for the generation of synthesized CD-SEM images including resist lines with predetermined CD/pitch and LER parameters in which the noise level can be tuned at will (see Fig.10). The sources of noise can

be the shot noise of SEM electron beam (Poisson-type) and the microscope electronics (Gaussian-type). Then we have used the generated CD-SEM images to evaluate three methods devised and proposed for the reduction of noise effects and the extraction of noise-free LER/LWR parameters. The first method (called fractal method) is presented for first time, while the next two (model filtering and Power Spectral Density) have been already proposed and applied in literature. We found that the all methods are able to reproduce the true RMS value except for the cases with high signal to noise ratio and small input RMS (0.5nm) or correlation length (10nm). The reduction of the noise effects on ξ, α and the prediction of their true values seems to be more difficult, although at low noise levels successful predictions are achieved by both methods (fractal and PSD) especially for the correlation length ξ.

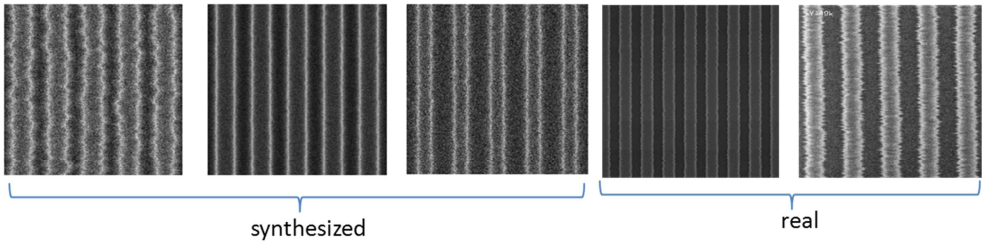

Fig. 10. *Three examples of synthesized images generated by the algorithm described in the text for different choices of input parameters. Notice their apparent similarity with real top-down SEM images of line/space patterns (typical examples are also shown in the Figure)*

B.3 Alternative methods for the characterization of the morphology of nanostructures: Rough surfaces as complex networks

N. Karasmani, V. Constantoudis

The measurement and characterization of the degree of periodicity and order in a surface is critical especially in self-assembled nanostructures. Conventional tools for periodicity detection and evaluation suffer from their own limitations. For example, Fourier transform due to the kernel of harmonic waves it implies is not only sensitive to the degree of periodicity but also to the shape of the repeated structure. The above limitations motivate us to seek alternative methods for the characterization of surface roughness. To this end, we employed the recent advances in complex network theory and critically examined the benefits of their application in roughness characterization. The key idea here is to transform a surface to a network by considering the measured grid points of the surface as the nodes of the network and the link between two nodes inversely proportional to the difference of their heights (Height-Similarity Method, see Fig. 11a). After the application of this method to totally random and self-affine surfaces, we proceeded this year to examine its sensitivity to the detection of the different kinds of deviations from periodicity. We considered surfaces consisting of identical Gaussian bumps in full periodic arrangements. The deviations from periodicity can be modeled either by changing randomly the position of the bumps (position-based deviation) or the bump shape (shape-based deviation). Fig. 11b and Fig. 11c shows the node-degree distribution of the networks generated by surfaces with position and shape-based deviation from full periodicity respectively. The graphs demonstrate the sensitivity of the degree distribution to the kind of the deviation from periodicity and motivate us for further investigation of the prospects of the network approach to morphology characterization.

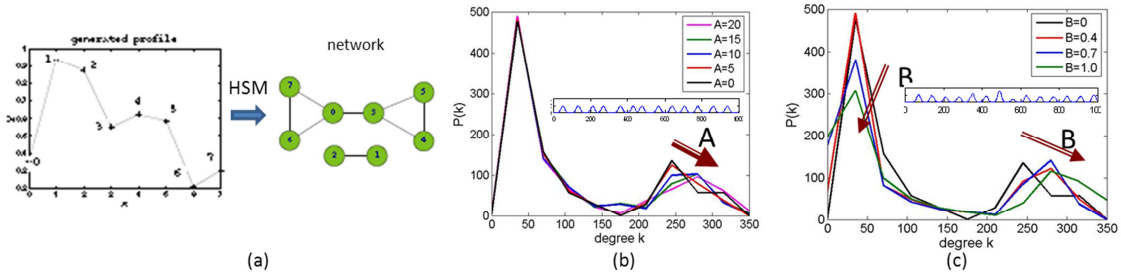

Fig. 11. *(a) Schematic of the Height Similarity method for the generation of a network from a rough profile, (b) and (c) the degree distribution of the network nodes for surfaces with increased position and height-based deviation from periodicity respectively.*

C. Modeling – Simulation

C.1 Modeling of Line Edge Roughness transfer during plasma etching: Comparison with experiments and rules of thumb

V. Constantoudis, G. Kokkoris, E. Gogolides

The main application of plasma technology in microelectronics is the transfer of the resist patterns formed with some kind of lithography (optical, electron, nanoimprint, colloidal, etc.) to the substrate(s). When the dimensions of the transferred pattern are in the nanoscale regime then any kind of deviation from the ideal shape in the final pattern (Line Edge Roughness, sidewall slope and shape) becomes critical and should be under control. The contributions to these deviations mainly come from the resist sidewall roughness and profile shape and the plasma etching transfer process. In order to evaluate these contributions and help their control, our group has proposed some years ago a geometrical model of pattern transfer process which takes into account a detailed representation of resist sidewall roughness and profile shape while considers a simple anisotropic ion-driven etching process for pattern transfer. The first results and predictions of this model and its 3D extension have been presented in the reports of the previous years.
During this year, we have proceeded to a systematic comparison of model predictions with the available in literature experimental results. The comparison was mainly focused on the LER rms value (3σ) and power spectrum. As we can see in Fig.12 for rms, modeling results reproduce the experimental trends and behavior with high fidelity. Similar agreement has been observed in the transfer of the power spectra of sidewall roughness.

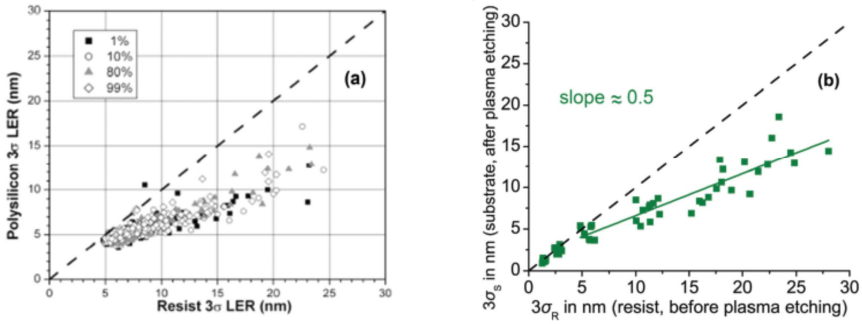

Fig. 12. *Experimental (a) and modeling (b) results for the substrate LER after pattern transfer (3σS) versus the resist LER before pattern transfer (3σR). The modeling results are taken for resist thickness 150nm, correlation length 30nm, roughness exponent 0.6, etching depth150nm and resist profile slope 86.2o. Notice the almost quantitative agreement of the model predictions and experimental measurements.*

Furthermore, inspired by the model we have devised some rules of thumb governing the pattern transfer etch process. The most important regards the necessary condition for getting LER reduction after pattern transfer. According to this the resist roughness and shape parameters σ_R *(rms value),* ξ_R (correlation length) and $\tan\theta_R$ (sidewall slope) should obey the condition: $(\sigma_R/\xi_R)\tan\theta_R > 1/c$ where c=2.5-3.

C.2 Global modeling of plasma reactors: Application in Hydrogen cleaning plasmas

N. Skoro, S. Mouchtouris, G. Kokkoris, E. Gogolides

A global (0d) model for H_2/Ar plasma was formulated including both gas phase and surface reactions (c.f. Table IV). The model results were compared (cf. section A.3) with measurements for H density coming from catalytic probe and actinometry and for electron density and temperature coming from Langmuir probe. Good agreement between experimental and modeling results was found. The important model parameters were extracted and a sensitivity analysis was performed. Using realistically calculated surface recombination coefficient, the

model results were compared well with the measured H density. The sensitivity analysis showed that H density strongly depended on the surface recombination coefficient. Additionally, there was an agreement of model results with the measured electron temperature. The potential sources of the difference between the model results with the measured electron density were investigated by the sensitivity analysis: electron density was found to be sensitive to the rate coefficients of electronic excitation leading to H_2 dissociation and ionization of H_2. In addition to the latter coefficients, the surface recombination coefficient of H, and the cross section for ion – neutral collisions in the plasma, which is important for the losses of ions at the wall surfaces, were found to be the most important model parameters.

Table IV. Gas phase (G) and surface (S) reactions for the global model of H_2/Ar plasma.

G1	$H_2(X^1\Sigma_g^+) + e \rightarrow H_2(b^3\Sigma_u^+) + e \rightarrow 2H + e$	G12	$H_2^+ + e \rightarrow H^+ + H + e$	G23	$ArH^+ + e \rightarrow Ar + H$
G2	$H_2 + e \rightarrow H_2(B^1\Sigma_u^+) + e$	G13	$H_2^+ + e \rightarrow 2H^+ + 2e$	G24	$H_2^+ + H_2 \rightarrow H_3^+ + H$
G3	$H_2 + e \rightarrow H_2(C^1\Pi_u) + e$	G14	$H_2^+ + e \rightarrow 2H$	G25	$Ar(met) + H_2 \rightarrow Ar + 2H$
G4	$H_2 + e \rightarrow H_2(c^3\Pi_u) + e \rightarrow 2H + e$	G15	$H_3^+ + e \rightarrow H^+ + 2H + e$	G26	$Ar(met) + Ar \rightarrow 2Ar$
G5	$H_2(X^1\Sigma_g^+, v=0) + e \rightarrow H_2(X^1\Sigma_g^+, v=1) + e$	G16	$H_3^+ + e \rightarrow H_2 + H$	G27	$Ar^+ + H_2 \rightarrow Ar + H_2^+$
G6	$H_2 + e \rightarrow H_2(v=2) + e$	G17	$H + e \rightarrow H^+ + 2e$	G28	$Ar^+ + H_2 \rightarrow ArH^+ + H$
G7	$H_2 + e \rightarrow H_2(v=3) + e$	G18	$Ar + e \rightarrow Ar + e$	G29	$ArH^+ + H_2 \rightarrow H_3^+ + Ar$
G8	$H_2 + e \rightarrow H(n=3) + H + e$	G19	$Ar + e \rightarrow Ar(met) + e$	G30	$H_3^+ + H_2 \rightarrow H_3^+ + H_2$
G9	$H_2 + e \rightarrow H_2^+ + 2e$	G20	$Ar + e \rightarrow Ar^+ + 2e$	S1	$H \rightarrow \frac{1}{2} H_2$
G10	$H_2 + e \rightarrow H + H^+ + 2e$	G21	$Ar + e \rightarrow Ar + e$		
G11	$H_2 + e \rightarrow H_2 + e$	G22	$Ar(met) + e \rightarrow Ar + e$		

C.3 Modeling of the stochastic and topology effects on Contact Edge Roughness dependencies

V. M. Kuppuswamy, V. Constantoudis, E. Gogolides

In nanofabrication, stochastic effects coming from the discrete nature of materials (molecular structure) and of the fabrication means (photons, electrons, ions) induce roughness on the sidewalls of patterned features and variability of their sizes. At the same time, nanofeatures are usually closely packed and proximity inter-feature effects on their morphology should be taken into account (proximity effect). To evaluate the combination of these effects on the sidewall nanoroughness, we developed a modeling framework taking into account both stochastic and proximity effects. The motivation for this model was experimental results described in the Report of 2011 for the dependence of the sidewall roughness of contacts (Contact Edge Roughness) opened by Extreme Ultraviolet Lithography on the exposure dose. Analysis of these results revealed an increase of RMS with exposure dose and contact diameter (CD) (see Fig. 13a) contrary to the expectations according to which the RMS value of the sidewall roughness of resist features should go down with the square root of the exposure dose i.e. the number of incident photons (shot-noise effect). The modeling showed that the proximity effects play a significant role in CER dependence on dose due to the specific 2D topology of contacts; for dense contacts (small pitch) the growth of contact diameter with dose bring these closer especially along the lattice directions. This selective proximity increases the low frequency contact fluctuations and explains the CER increase with dose (see Fig. 13b).

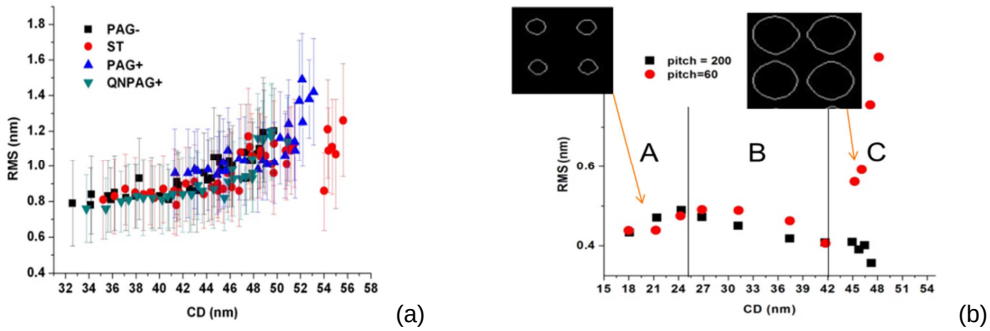

Fig. 13. *Experimental (a) and modelling results for the dependence of the RMS value of CER on the contact diameter (CD). The modelling results are for sparse (pitch=200nm) and dense (pitch=60nm) contact patterns. Notice that the experimental increase at high CD is reproduced only for the dense contacts revealing the critical role of the proximity effects between nearby contacts.*

C.4 Multiscale Computational Analysis of the Interaction between the Wafer Micro-Topography and the Film Growth Regimes in Chemical Vapor Deposition Processes

G. Kokkoris and external collaborators

The limiting step during the chemical vapor deposition (CVD) process of a film can be identified by the Arrhenius plot, which shows the effect of the wafer temperature on the deposition rate. The deposition limiting step, and as a consequence the Arrhenius plot, are affected by the operating conditions of the CVD reactor. By using a multiscale computational framework, it is shown that they are also affected by the existence of a micro-topography (e.g. micro-trenches) on the wafer. The origin of this effect is the loading phenomenon and the multiscale computations are used to quantify it: The deposition rate decreases in the diffusion limited regime; the latter and the transition regime are shifted at lower temperatures compared to the flat wafer case. The evolution of the deposited film profile in the micro-trenches is calculated at all deposition regimes. The film conformality starts to decrease when the wafer temperature exceeds the maximum temperature of the reaction limited regime. Finally, it is shown that the effect of the micro-topography on the species concentrations in the reactor bulk is important only in the transition regime (c.f. Fig.14). The case studies are CVD of a) tungsten from tungsten hexafluoride and b) silicon from silane.

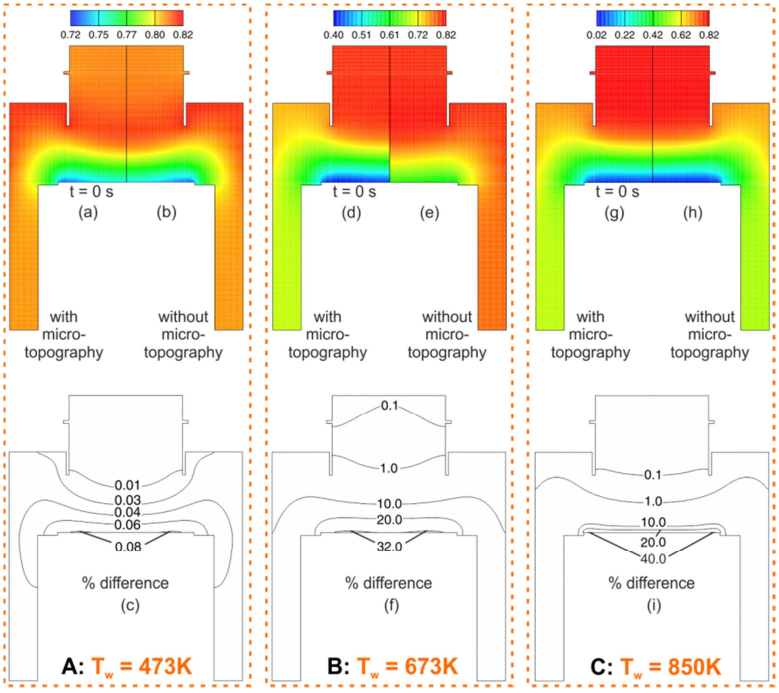

Fig. 14. *CVD of W - mass fraction (of WF_6, which is the precursor) and % difference of the mass fraction inside the reactor. Column A (Tw = 473 K) corresponds to reaction limited regime, B (Tw = 673 K) to transition regime, and C (Tw = 850 K) to diffusion limited regime. (a), (d), and (g) show mass fraction with micro-topography at t=0 s. (b), (e), and (h) show the mass fraction without micro-topography. (c), (f), and (i) show the % difference between the cases with and without micro-topography.*

C.5 Ballistic and molecular dynamics simulations of aluminum deposition in micro-trenches

G. Kokkoris and external collaborators

Two different feature scale modeling frameworks are utilized for the study of aluminum (Al) deposition profiles inside micro-trenches. The first framework, which is applied in metal-organic chemical vapor deposition (MOCVD) of Al, couples a ballistic model for the local flux calculation, a surface chemistry model, and a profile evolution algorithm. The calculated conformity of the deposited film is compared with experimental results corresponding to Al MOCVD from dimethylethylaminealane (DMEAA). The outcome of the comparison is that the effective sticking coefficient of DMEAA is in the range of 0.1 – 1. There is also a strong indication that surface reaction kinetics follows Langmuir – Hinshelwood or Eley – Rideal mechanism. The second framework, which is applied in physical vapor deposition of Al, implements 2D molecular dynamics (MD) simulations. The simulations are performed in a “miniaturized” domain of some hundreds of Angstroms and are used to explore micro-trench filling during magnetron sputtering (MS) deposition of Al on a rotated substrate. Most of the experimental results are qualitatively

reproduced by the MD simulations; the rotation, aspect ratio, and kinetic energy effects are correctly described despite the completely different length scales of simulation and experiment. The sticking probability of Al is calculated 0.6 for the conditions of the experiments.

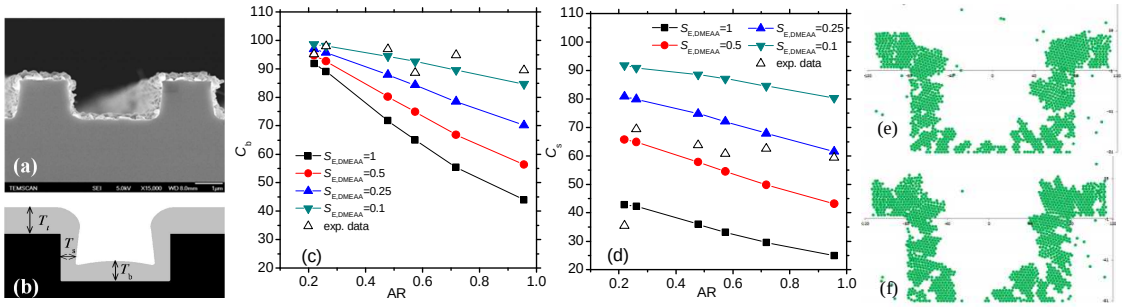

Fig. 15. *(a) SEM image from a film profile in a trench with width equal to 3 μm. (b) Parameters used for the calculation of bottom (C_b) and sidewall (C_s) conformity: $C_x = T_x/T_t$ 100% (x=b, s). (c) C_b and (d) $C_s$vs trench AR. 2D MD simulations of Al MS deposition on Si trenches with AR=0.5. 3200 atoms are launched: (e) Ts= 300 K (surface temperature) and Ek = 0.026 eV (energy of depositing atoms) and (f) Ts= 300 K and Ek = 1 eV.*

C.6 Numerical calculation of the energy barrier for the transition from the Cassie-Baxter to Wenzel state on hydro(oleo)phobic surfaces

G. Kokkoris and external collaborators

The aim is to find the surface morphology (geometric pattern) which favors heterogeneous wetting (Cassie-Baxter, CB) state and exhibits increased resistance to fully wetting (Wenzel, W) state under the effect of disturbances induced by pressure, temperature, or electrical field. The resistance of a surface morphology to fully wetting state comes from the energy barrier that we have to overcome to get from the CB to the W state. In this work, a methodology for the calculation of the energy barrier for a simple system consisting of one droplet lying on one pillar is described. The effect of the shape of the pillar on the energy barrier is sought. The core of the methodology is the numerical solution (by the Galerkin/finite element method) of the Young Laplace equation which gives us the shape of the droplet on the pillar. The first step of the methodology is the continuation of the solution branch (Fig.16a) which shows that multiple equilibrium states exist for the same contact angle (θ_Y). The energy barrier comes from the energy difference between the unstable equilibrium state (U) and the CB state. For droplets with small volume (<10μl), the energy barrier is $\gamma_{LV}(A_{LV,U} - A_{LV,CB}) - \gamma_{LV}(A_{SL,U} - A_{SL,CB})\cos\theta_Y$ (γ is the interfacial tension and A is the interfacial area, L,V,S stand for liquid, vapor, solid). Thus, if we know the shape of the droplet at the different equilibrium states for a specific contact angle, we can calculate the energy barrier for this contact angle. The calculations show that the energy barrier increases with the aspect ratio (AR) and the sidewall slope of the pillar (Fig.16b) and decreases with the droplet to pillar volume ratio (V_d/V_p). The energy barrier is greater for pillars with negative slope compared to pillars with positive slope (Fig.16c).

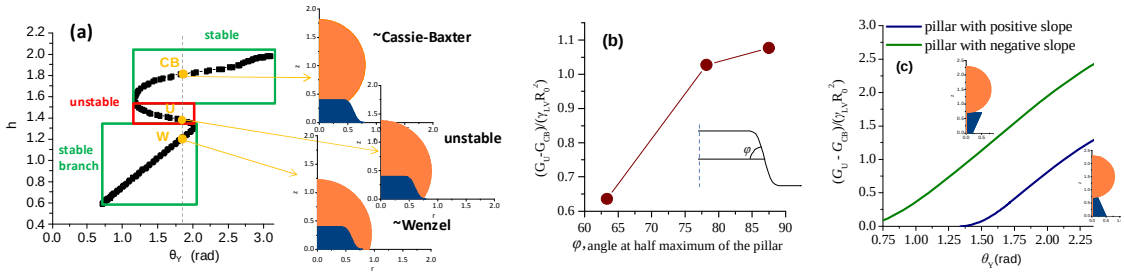

Fig. 16. *(a) Continuation of the solution branch: The maximum height (z coordinate) of the droplet vs. the Young contact angle. 2 stable and 1 unstable braches of the solution are shown. (b) Energy barrier from CB to W state for a specific contact angle as a function of slope of a pillar with positive slope (V_d/V_p=5, AR=0.5). (c) The energy barrier for pillars with positive and negative slope vs. θ_Y (V_d/V_p=7, AR=1). G_U, G_{CB} are the energies of the unstable and CB states. R_0 is a length constant to make the energy barrier unitless.*

D. Applications

D1. "Smart" Nanostructured Surfaces

D1.1 Hydrophobic coatings and monolayers on flat plasma oxidized polymeric surfaces

K. Ellinas, G. Boulousis, E. Gogolides, A. Tserepi and external collaborators

Here, we compared different techniques for polymeric surface hydrophobization following a mild plasma oxidation. We established the use of fluorinated SAMs (PFOTS-perfluorinated octyl trichloro silane self assembled monolayers) by two different coating processes (wet & dry) and compared their wetting properties versus aplasma deposited fluorocarbon coating. In the following Table V, we present the static contact angle of different test liquids on three different coatings. As clearly see the PFOTS monlayers have improved performance compared to plasma deposited teflon-like fluorocarbon coatings, at least as far as contact angle increase is concerned.

Table V. Contact angles of PFOTS and plasma deposited fluorocarbon layers

Flat PMMA substrate		Wet deposited PFOTS	Dry deposited PFOTS	Plasma deposited C_4F_8
After grafting	Water	125 (15° hysteresis)	119	110
	Soya oil	90	88	62
	Hexadecane	75	72	41

D1.2 Hierarchical, oxygen plasma nanotextured, superoleophobic polymeric surfaces with random or ordered nanostructures

K. Ellinas, G. Boulousis, E. Gogolides, A. Tserepi and external collaborators

We fabricated two types of superoleophobic surfaces. Random, plasma nanotextured surfaces were simply etched in oxygen plasma. Ordered, plasma nanotextured surfaces were first coated with polysterene microspheres and then etched and nanotextured in oxygen plasma (see Fig. 17). Hydrophobization of both surfaces followed using the PFOTS wet deposited monolayers (see D1.1 above). Dynamic contact angle measurements on micro - nano textured PMMA and PEEK after 20 min O_2 plasma treatment and subsequent FDTS grafting are provided in Table VI. Superolephobicity is observed for all liquids tested, and a significant improvement compared to fluorocarbon plasma deposited coatings (using C_4F_8 plasma). These findings of the current study are consistent and slightly improved (PMMA 20min surface) from those superoleophobic surfaces reported in the literature for similar techniques.

Table VI. The static, advancing, receding contact angles and hysteresis are shown for water, soya oil and hexadecane on silane modified hierarchical randomly rough plasma nanotexturedsurfaces of PMMA.

Liquid	Contact angle	**PMMA 20 min O_2plasma**
Water	Static	167
	Adv/Rec(Hyster)	168/166 (2°)
SoyaOil	Static	157
	Adv/Rec(Hyster)	157/153 (4°)
Hexadecane	Static	142
	Adv/Rec(Hyster)	145/135 (10°)

* 5 μL liquid, error in Static ±2° advancing and receding ±5° (hysteresis is shown in parenthesis)

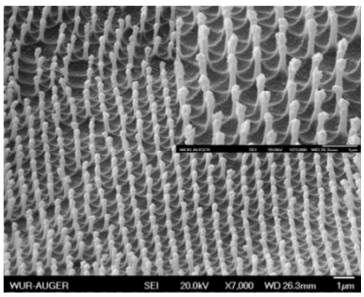

(a)

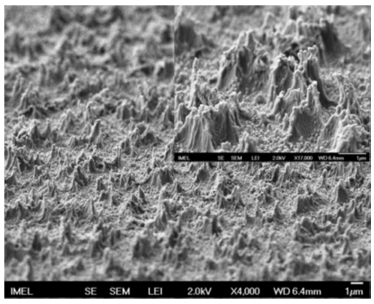

(b)

(c)

Fig. 17. *(a) 60 degrees tilted SEM images of the hierarchical, ordered hexagonical packed pillar-like structured surfaces using 1 μm PS particles followed by plasma etching (b) 10 min plasma nanotextured PMMA surface after the silanization process (c) Various liquid drops (water, diiodomethane, soya oil) on superoleophobic PMMA surfaces*

D1.3 Hierarchical, SF_6 plasma nanotextured, superhydrophobic PDMS surfaces with random nanostructures: Effect of PDMS thickness

M.-E. Vlachopoulou, E. Gogolides, A. Tserepi

The effect of PDMS substrate thickness on the SF_6-plasma induced nanoroughness and consequently on superhydrophobicity was investigated. In Fig. 18, the evolution with plasma etching time of PDMS nanoroughness height is presented for different PDMS film thicknesses, revealing the roughness decrease for increasing film thicknesses. Measurements of water contact angle on nanoroughened PDMS surfaces after the deposition of ~20nm fluorocarbon (FC) film reveals that superhydrophobic (SH) surfaces are obtained only in the case of very thin PDMS films, while thicker PDMS substrates present larger values of CA hysteresis (see Table VII). However, if the same surfaces are immersed in deionized water and dried, the CA hysteresis is drastically reduced, rendering all substrates superhydrophobic. This can be attributed to the induced modification of the surface topography as a result of wetting and drying and constitutes an interesting approach of making PDMS substrates superhydrophobic, independently from their thickness.

Table VII.

15 min SF_6	Without immersion			With immersion		
Thickness	Static (°)	Advancing (°)	Hysteresis (°)	Static (°)	Advancing (°)	Hysteresis (°)
20 μm	145	153	8	145	151	1
0.5 mm	145	146	11	147	154	4
2 mm	137	152	28	147	152	6

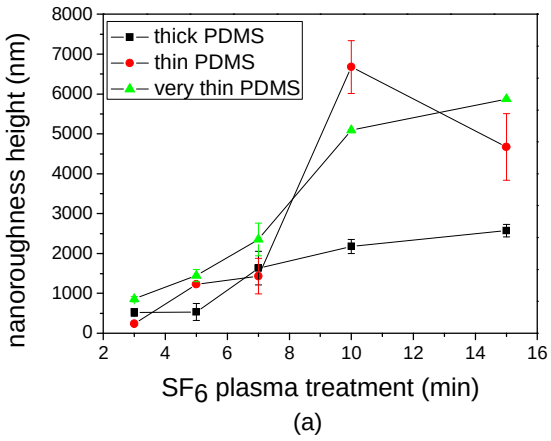

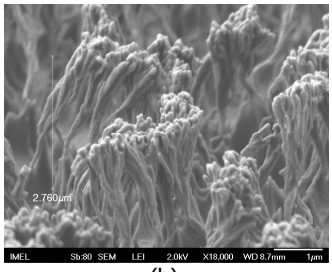

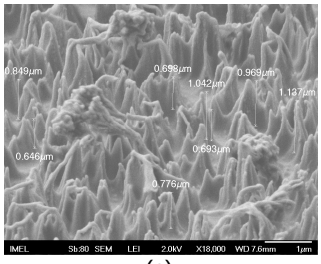

Fig. 18. *(a) PDMS roughness height evolution with etching time for different PDMS film thicknesses: ~2 mm (thick PDMS), ~0.5 mm (thin PDMS) and ~ 20 μm (very thin PDMS) and SEM images of 15 min SF_6 treated thin PDMS before (b) and after (c) immersion in DI water*

D2. Microfluidics – Lab on Chip for Life Sciences (see also project III.2)

D2.1 Comparison of pressure drop in Superhydrophobic and superhydrophilic, hierarchical, plasma-nanotextured polymeric microchannels sustaining high-pressure flows

D. P. Papageorgiou, K. Tsougeni, A. Tserepi, E. Gogolides

We fabricated superhydrophilic and superhydrophobic polymeric microfluidic devices with controlled hierarchical, random roughness, using plasma processing. We implemented a dye staining technique to visually demonstrate the persistence of the superhydrophobic state under flow for pressures in excess of 2.5 bar inside the microchannel. We further confirmed the stability of superhydrophobicity by pressure drop measurements, friction factor and slip length calculations under laminar flow conditions. We also compared identical rough superhydrophilic and superhydrophobic microchannels showing reduced pressure drop in the latter by as much as 22 %. Plasma etching and simultaneous nanotexturing (followed by optional fluorocarbon plasma deposition) were thus shown as an easy-to-implement method for attaining robust Cassie-state against high-pressure microchannel flows.

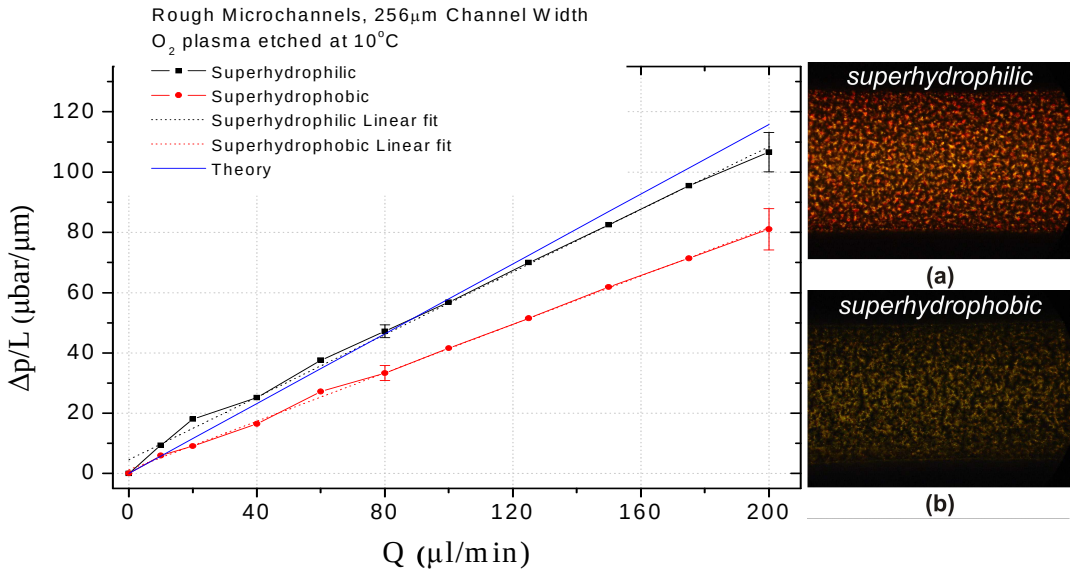

Fig. 19. *Comparison of flow properties in rough superhydrophilic and superhydrophobic microchannels.(a) Pressure drop (μbar/μm) versus flow rate Q (μl/min). Mean values of three independent runs are shown for each curve. Diagrams correspond to 256μm wide, 25μm deep and 38.3mm long channels etched at 10 °C and stabilized with wetting. Data for other microchannels are shown in supporting information. Black lines correspond to superhydrophilic channels, and red lines to superhydrophobic ones. Dimensions of hierarchical micro-hills are: ~2-3 μm high, 1.5-4 μm wide, spaced 2-4 μm apart. Optical microscope dark-field images on stained superhydrophilic and superhydrophobic microchannels. (a) Superhydrophilic microchannel is stained after red-dye flow. (b) Superhydrophobic microchannel is not stained after red-dye flow.*

D2.2 Comparison of flow field in superhydrophobic and superhydrophilic, hierarchical, plasma-nanotextured polymeric microchannels using micro PIV

K. Tsougeni, K. Ellinas, Th. Christoforidis, A. Tserepi, E. Gogolides and external collaborators

Plasma processing was used to roughen (texture) and control the wetting properties of polymeric Poly(methyl methacrylate) (PMMA) microchannels from superhydrophilic to superhydrophobic. A trapezoidal microchannel was used to provide three nanotextured walls (superhydrophilic or superhydrophobic). Particle Image Velocimetry (PIV) was then employed to monitor the velocity field, and observe the different flow behavior in the two wetting states during water flow. Using the ensemble PIV processing tool of the available software, several hundreds of images were analyzed in order to obtain the velocity field at various depths of each channel. Significant velocity was measured on the superhydrophobic walls.

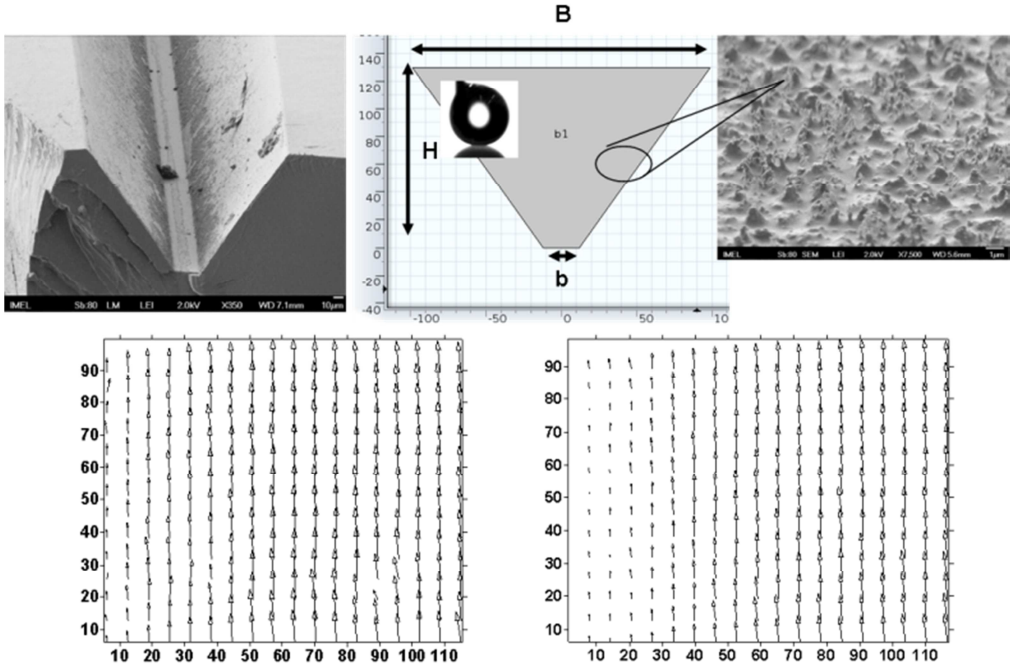

Fig. 20. *Cross-section of an open microchannel with three superhydrophobic walls. Schematic of the cross-section and a zoom up of the rough walls. Velocity field comparison (dimensions in microns) of superhydrophobic (left) and superhydrophilic (right) microchannels showing higher liquid velocity on the superhydrophobic wall.*

D2.3 Phosphopeptide Enrichment and Separation in an Affinity Microcolumn on a Silicon Microchip: Comparison of Sputtered and Wet-Deposited TiO_2 Stationary-Phase

K. Ellinas, K. Tsougeni, G. Boulousis, A. Tserepi, E. Gogolides

We microfabricated a TiO_2 Affinity Chromatography microcolumn on silicon, comprising a deposited TiO_2 stationary phase, and demonstrated enrichment and separation of a standard mono-phosphopeptide with high capacity in this microcolumn. The TiO_2 stationary-phase is formed either with wet deposition or sputtering, and was found to be either amorphous (after sputtering), or crystalline (after sputtering and annealing or after wet deposition). All three methods of deposition (sputtering, sputtering and annealing, liquid deposition) provide enough capacity despite the non-porous nature of the deposited TiO_2. The chip design allows an expansion of its capacity (currently 1μg) by means of increasing the number of parallel microchannels at a constant sample volume. Our approach provides an alternative to off-line extraction tips (with typical capacities of 1 – 2 μg and sample volumes of 1 - 10 μL), and to on-chip efforts based on packed bed and frit formats using a standard material for MEMs and standard microfabrication techniques.

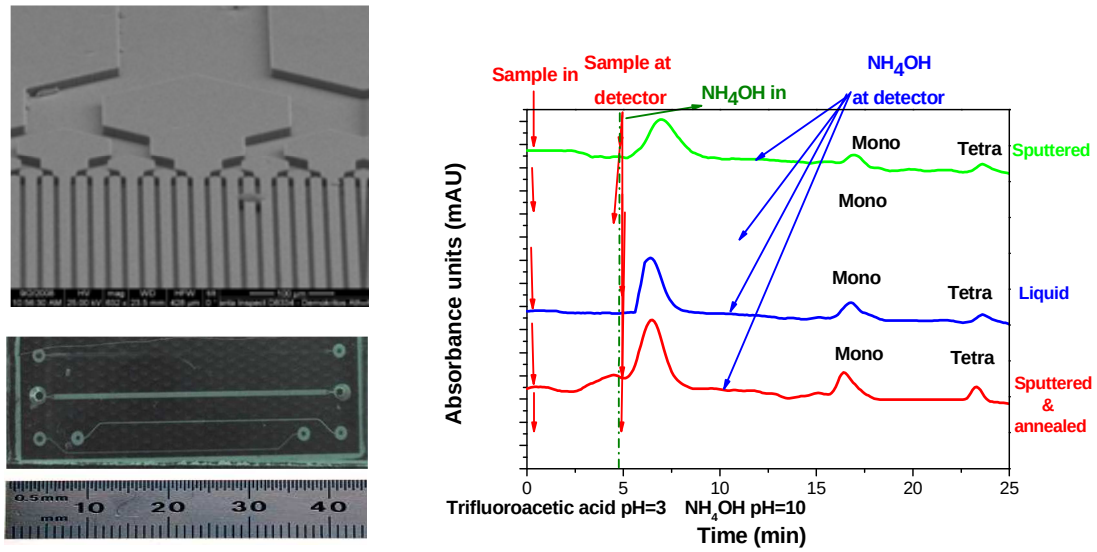

Fig. 21. *(Left) Silicon microcolumn consisting of 32 parallel microchannels. (Right) Affinity chromatography on chip is shown, with retention, elution and separation of the peptide mixtures using the three different microcolumns. Some baseline shifts are due to shifting of the intensity of the Deuterium lamp. The sample quantity is 0.1nmol for each peptide (~0.2 μg for the mono-phosphopeptide, ~0.3 μg for the tetra-phosphopeptide and ~0.17 μg for the non-phosphorylated peptide).*

D2.4 Continuous-flow microfluidic device for DNA amplification (μPCR) on flexible polyimide substrate and integration in a Lab-On-Chip platform

D. Moschou, N. Vourdas, G. Kokkoris, G. Papadakis, S. Chatzandroulis, A. Tserepi

The development of a continuous flow μPCR device integrated with microresistors on a flexible polyimide (PI) substrate was continued this year further improving the device design and the fabrication process, while evaluating the robustness of the device and its performance for DNA amplification. A slightly modified device was proposed (microchannel of two different widths, depending on the desired sample residence time at each zone), and its behavior in respect to temperature uniformity was evaluated by means of numerical calculations. In addition, the fabrication process time and complexity were reduced, with the employment of photopatternable polyimide layers for the formation of microchannels by means of lithography. These improvements allowed us to evaluate the performance of our fabricated chips (Fig.22a) in respect to their DNA amplification efficiency (Fig.22b). Our devices achieved DNA amplification much faster (within a few minutes, depending on the sample flow rate) than conventional thermocyclers (a few hours). Building on the successful fabrication of microfluidics with photopatternable polyimide, we proceeded in developing a Lab-On-a-Chip platform on PCB substrates (Fig.23), integrating both a μPCR module and Si-based biosensors (placed in a cavity of the PCB, see image and inset), to allow DNA amplification and detection on the same chip.

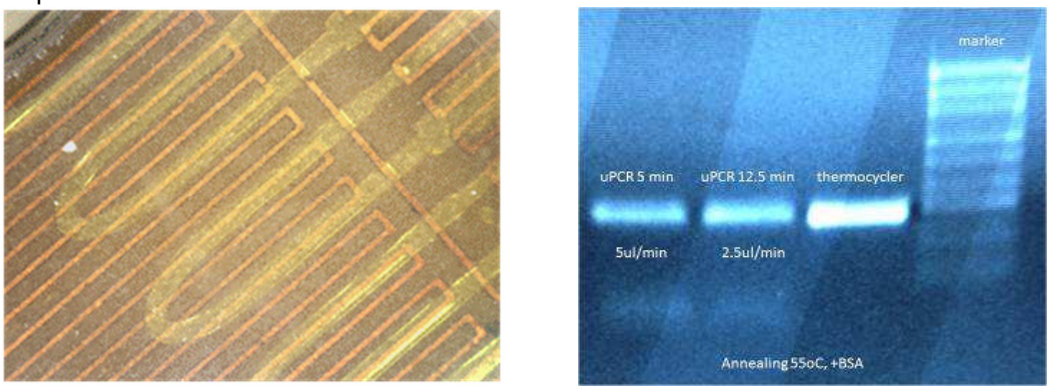

Fig.22. *(a) Fabricated μPCR chip with integrated microheaters (b) Demonstration of DNA amplification performed on our device and comparison with a commercial thermocycler (amplified DNA products on agarose gel).*

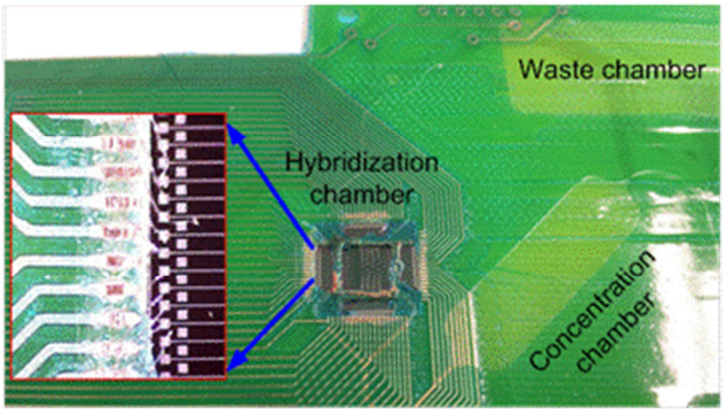

Fig.23. *Fabricated prototype of a Lab-On-a-Chip on PCB integrating a μPCR device and an array of Si-based biosensors*

D2.5 Nanoscale protein patterning on Si substrates using colloidal lithography and plasma processing

A. Malainou, K. Ellinas, V. Constantoudis, E. Gogolides, A. Tserepi and external collaborators

The potential of proteins to be integrated into micro or nanofabricated devices is steadily gaining importance for applications such as biosensors, bioMEMS, tissue engineering, and protein arrays. To create protein patterns, photolithography-based methods have been extensively used. However for features smaller than 1 μm, photolithography is reaching its limits, and becomes non cost-efficient. Moreover, dip-pen and e-beam lithography are serial processes and, as such, lack scalability. We propose a method for low-cost, large scale and high throughput, selective immobilization of proteins on nanopatterned Si, based on colloidal lithography and plasma processing in order to define the areas (< 300 nm) where proteins are *selectively* immobilized. A close-packed monolayer of PS microparticles is deposited on oxidized Si and, either after microparticle size reduction or alternatively after metal deposition through the PS close-packed monolayer, is used as etching mask to define SiO_2nanoislands (on Si, Fig.24). *Selective* protein immobilization on the SiO_2nanoislands occurs after plasma-induced chemical modification of the substrate. The thickness of the immobilized protein monolayer is estimated by means of detailed AFM image (Fig.25) statistical analysis. The method reported herein constitutes a cost-efficient route toward rapid, large surface, and high density patterning of biomolecules on solid supports that can be easily applied in BioMEMS or microanalytical systems.

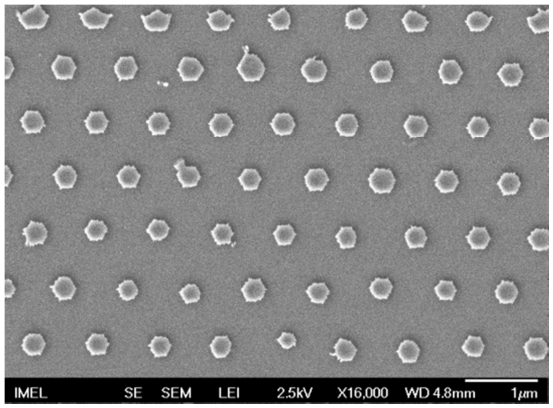

Fig.24. *SEM image of 300 nm SiO_2 nanoislands patterned on Si using colloidal lithography and plasma processing.*

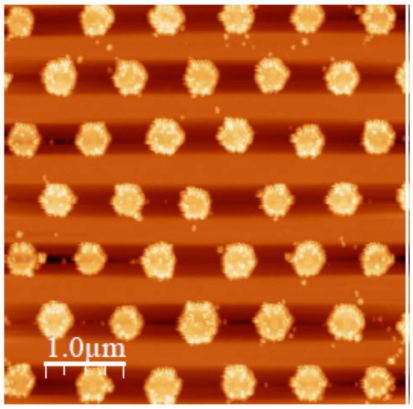

Fig.25. *Atomic Force Microscopy image of SiO_2 nanoislands on Si after selective immobilization of BSA on SiO_2 and not on Si surface.*

D3. Nano-Devices for Energy

D3.1 Devices for energy: Photovoltaic device based on Silicon Nanowires and Nanopillars

A. Smyrnakis, P. Dimitrakis, P. Normand, E. Gogolides

Recently, the potential application of high aspect ratio silicon nanowires (SiNWs) and nanopillars in solar cells was presented. The use of nanowires instead of bulk material or thin films provides opportunities to minimize losses of light absorption, in electron-hole generation and separation as well as in collection efficiency, and combine lower cost. We started our work on energy conversion devices by the fabrication of ordered silicon nanopillar arrays of different diameter and period with p-n junctions along the axial direction of each wire by colloidal lithography and plasma etching starting from a n-type Si wafer which was boron implanted to form a p-type surface layer. Electrical characterization of individual as well as bundle of nanopillars was performed in terms of I-V under light illumination, where promising first results were obtained in terms of short circuit current (I_{sc}) increase and filling factor (FF). The work will continue to the fabrication and characterization of the complete photovoltaic device and it will be extended to the fabrication of SiNWs solar cells with radial p-n junctions.

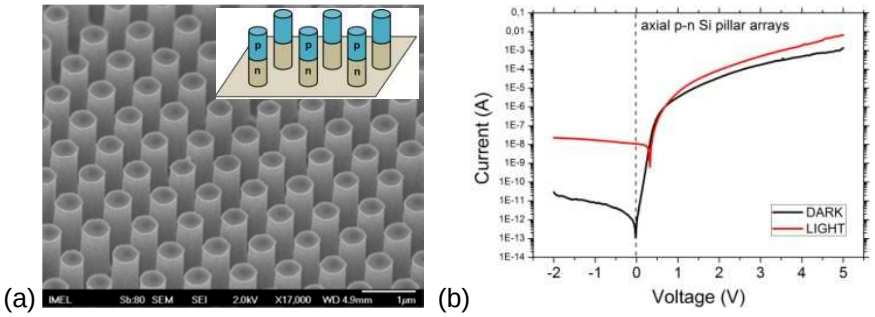

Fig.26. *SEM image of axially modulated p-n junction Si pillar arrays. Inset: the I-V response curve of the axial p-n Si pillar in dark and under illumination.*

PROJECT OUTPUT in 2012

Publications in International Refereed Journals

A. Plasma Nanofabrication

1. *Plasma directed organization of nanodots on polymers: Effects of polymer type and etching time on morphology and order,*
   Kontziampasis, D., Constantoudis, V., Gogolides, E.
   (2012) Plasma Processes and Polymers, 9 (9), pp. 866-872.

B. Nanometrology-Characterization

2. *Contact edge roughness metrology in nanostructures: Frequency analysis and variations,*
   Vijaya-Kumar, M.K., Constantoudis, V., Gogolides, E., Pret, A.V., Gronheid, R., (2012) Microelectronic Engineering, 90, pp. 126-130.
3. *Fractals and device performance variability: The key role of roughness in micro and nanofabrication,*
   Constantoudis, V., Patsis, G.P., Gogolides, E., (2012) Microelectronic Engineering, 90, pp. 121-125.

C. Modeling-Simulation

4. *The potential of ion-driven etching with simultaneous deposition of impurities for inducing periodic dots on surfaces,*
   Kokkoris, G., Gogolides, E.
   (2012) Journal of Physics D: Applied Physics, 45 (16), art.no. 165204
5. *Multiscale computational analysis of the interaction between the wafer micro-topography and the film growth regimes in chemical vapor deposition processes,*
   N. Cheimarios, G. Kokkoris and A. G. Boudouvis,
   (2012) ECS Journal of Solid State Science and Technology 1 P197-P203
6. *A consistent approach for the treatment of Fermi acceleration in time-dependent billiards,*
   Karlis, A.K., Diakonos, F.K., Constantoudis, V.,
   (2012) Chaos, 22 (2), art.no. 026120
7. *Quantum versus classical dynamics in a driven barrier: The role of kinematic effects,*
   Papachristou, P.K., Katifori, E., Diakonos, F.K., Constantoudis, V., Mavrommatis, E.,

(2012) Physical Review E - Statistical, Nonlinear, and Soft Matter Physics, 86 (3), art. no. 036213

8. *Entropy analysis of word-length series of natural language texts: Effects of text language and genre,* Kalimeri, M., Constantoudis, V., Papadimitriou, C., Karamanos, K., Diakonos, F.K., Papageorgiou, H. (2012) International Journal of Bifurcation and Chaos, 22 (9), art. no. 1250223.

D1. "Smart" Nanostructured Surfaces

9. *Nanomechanical and nanotribological properties of plasma nanotexturedsuperhydrophilic and superhydrophobic polymeric surfaces,*
Skarmoutsou, A., Charitidis, C.A., Gnanappa, A.K., Tserepi, A., Gogolides, E.
(2012) Nanotechnology, 23 (50), art. no. 505711
10. *Hierarchical, plasma nanotextured, robust superamphiphobic polymeric surfaces structurally stabilized through a wetting-drying cycle,*
Gnanappa, A.K., Papageorgiou, D.P., Gogolides, E., Tserepi, A., Papathanasiou, A.G., Boudouvis, A.G.
(2012) Plasma Processes and Polymers, 9 (3), pp. 304-315
11. *Superior performance of multilayered fluoropolymer films in low voltage electrowetting,*
Papageorgiou, D.P., Tserepi, A., Boudouvis, A.G., Papathanasiou, A.G.
(2012) Journal of Colloid and Interface Science, 368 (1), pp. 592-598

D2. Microfluidics – Lab on Chip for Life Sciences

12. *Flame aerosol deposition of TiO2 nanoparticle films on polymers and polymeric microfluidic devices for on-chip phosphopeptide enrichment*,
Rudin, T., Tsougeni, K., Gogolides, E., Pratsinis, S.E.
(2012) Microelectronic Engineering, 97, pp. 341-344.
13. *High-capacity and high-intensity DNA microarray spots using oxygen-plasma nanotextured polystyrene slides*,
Tsougeni, K., Koukouvinos, G., Petrou, P.S., Tserepi, A., Kakabakos, S.E., Gogolides, E., (2012) Analytical and Bioanalytical Chemistry, 403 (9), pp. 2757-2764.
14. *Creating highly dense and uniform protein and DNA microarrays through photolithography and plasma modification of glass substrates,*
Malainou, A., Petrou, P.S., Kakabakos, S.E., Gogolides, E., Tserepi, A.
(2012) Biosensors and Bioelectronics, 34 (1), pp. 273-281
15. *Controlled protein adsorption on microfluidic channels with engineered roughness and wettability*,
Tsougeni, K., Petrou, P.S., Papageorgiou, D.P., Kakabakos, S.E., Tserepi, A., Gogolides, E.
(2012) Sensors and Actuators, B: Chemical, 161 (1), pp. 216-222

Published Conference Proceedings

A. Plasma Nanofabrication

1. *Characterization of hydrogen based RF plasmas suitable for removal of carbon layers*,
Škoro, N., Gogolides, E.
(2012) Proceedings of 26thSPIG, August 27-31, 2012, Zrenjanin, Serbia, pp. 231

B. Nano Metrology – Characterization

2. *3d modeling of LER transfer from the resist to the underlying substrate: The effect of the resist roughness,*
Kokkoris, G., Constantoudis, V., Gogolides, E.
(2012) Proceedings of SPIE - The International Society for Optical Engineering, 8328, 83280V

C. Modeling – Simulation

3. *Contact edge roughness and CD uniformity in EUV: Effect of photo acid generator and sensitizer,*
Kuppuswamy, V.-K.M., Constantoudis, V., Gogolides, E., VaglioPret, A., Gronhei, R.
(2012) Proceedings of SPIE - The International Society for Optical Engineering, 8322, art. no. 832207
4. *Noise effects on contact edge roughness and CD uniformity measurement*,
Constantoudis, V., MurugesanKuppuswamy, V.K., Gogolides, E.,
(2012) Proceedings of SPIE - The International Society for Optical Engineering, 8324, art. no. 83240K.

D1."Smart" Nanostructured Surfaces

5. *Hierarchical, Plasma Nanotextured, Superamphiphobic Polymeric Surfaces*,
K. Ellinas, K. Tsougeni, M. Vlachopoulou A. Tserepi, E. Gogolides
(2012) Proceedings of 13th International Conference on Plasma Surface Engineering
6. *Development and characterisation of superhydrophobic α-alumina ceramic membranes with plasma surface nanotexturing*,
Stathopoulos, V., Papandreou, A., Vourdas, N., Tserepi, A., Gogolides, E.
Proceedings of Spring EMRS 2012 Meeting, May 14-18, 2012, Strasbourg, France

D2. Microfluidics – Lab on Chip for Life Sciences

7. *Fabrication of a label-free micromechanical capacitive biosensor and integration with μPCR towards a LoC for disease diagnosis,*
   D. Moschou, N. Vourdas, G. Kokkoris, G. Tsekenis, V. Tsouti, I. Zergioti, A. Tserepi, S. Chatzandroulis
   (2012) Proceedings of the 16th Int. Conference on Miniaturized Systems for Chemistry and Life Sciences (μTAS)
8. *Development of a continuous-flow μPCR device with microheatingelementsintegrated with biosensors towards a LoC system for disease diagnosis,*
   N. Vourdas, D. Moschou, G. Kokkoris, G. Papadakis, S. Chatzandroulis, A. Tserepi
   (2012) Proceedings of 3rd European Microfluidics Conference, paper no. 128
9. *Flow study in randomly-rough superhydrophilic and superhydrophobic plasma nanotexturedmicrochannels using micro-PIV*,
   K. Tsougeni, K. Ellinas, A. Glynou, T. Christoforidis, D.S. Mathioulakis, A. Tserepi, E. Gogolides
   (2012) Proceedings of 3rd European Microfluidics Conference, paper no. 132
10. *Control of flow and protein adsorption on plasma nanotextured microfluidics*,
    K. Ellinas, K. Tsougeni, P.S. Petrou, D.P. Papageorgiou, S.E. Kakabakos, A. Tserepi, E. Gogolides
    (2012) Proceedings of 3rd European Microfluidics Conference, paper no. 133

Conference Presentations

A. Plasma Nanofabrication

1. *High-aspect-ratio Si nanowire fabrication using Colloidal Self-assembly and fluorine-based plasma etching* (poster),
   A. Zeniou, A. Smyrnakis, E. Gogolides
   Plasma Etch and Strip in Microelectronics (PESM) March 15-16, 2012, Grenoble, France
2. *Characterization of Hydrogen-based Plasmas for Cleaning of Organic Contamination from EUV Optics* (poster),
   N. Škoro, E. Gogolides
   Plasma Etch and Strip in Microelectronics (PESM) March 15-16, 2012, Grenoble, France
3. *Plasma directed assembly: A new technology for polymer surface nanotexturing and applications* (oral),
   D. Kontziampasis, A. Bourkoula, A. Smyrnakis, P. S. Petrou, S. E. Kakabakos, E. Gogolides
   XI International Conference on Nanostructured Materials (NANO 2012) August 26-31, 2012, Rhodes, Greece
4. *Cleaning of Organic Contamination from EUV Optics Surfaces Using Hydrogen-based Plasmas* (poster),
   N. Skoro, E. Gogolides
   13th International Conference on Plasma Surface Engineering (PSE), September 10 - 14, 2012, Garmisch-Partenkirchen, Germany
5. *Plasma Directed Assembly: Process Issues, Materials and Applications* (poster),
   D. Kontziampasis, A. Smyrnakis, V. Constantoudis, E. Gogolides
   13th International Conference on Plasma Surface Engineering (PSE), September 10 - 14, 2012, Garmisch-Partenkirchen, Germany
6. *High aspect ratio, plasma etched silicon nanowires: Fabrication and optical property characterization* (oral),
   A. Smyrnakis, A. Zeniou, E. Almpanis, N. Papanikolaou, E. Gogolides
   38th International Micro & Nano Engineering Conference (MNE), September 16-20, 2012, Toulouse, France

B. Nano Metrology – Characterization

7. *Cyclo olefin polymer (COP) liquid chromatography microcolumns for reversed phase anf affinity separations* (poster),
   K. Tsougeni, A. Tserepi, E. Gogolides
   38th International Micro & Nano Engineering Conference (MNE), September 16-20, 2012, Toulouse, France

C. Modeling – Simulation

8. *Contact versus Line Edge Roughness in extreme ultra-violet lithography resists: Effects of exposure dose* (poster),
   V.K. Murugesan Kuppuswamy, V. Constantoudis, E. Gogolides
   38th International Micro & Nano Engineering Conference (MNE), September 16-20, 2012, Toulouse, France
9. *3D modeling of Line Edge Roughness transfer from the resist to the underlying substrate: The effect of resist roughness* (oral),
   G. Kokkoris, V. Constantoudis, E. Gogolides

Plasma Etch and Strip in Microelectronics (PESM) March 15-16, 2012, Grenoble, France

10. *A crossbred multi-parallelmethod for accelerating multiscale computations in a chemical reactor analysis*,
    N. Cheimarios, I. Aviziotis, G. Kokkoris and A.G. Boudouvis
    6th European Congress on computational methods in applied science and engineering, ECCOMAS, Vienna, Austria, September 10-14, 2012
11. *Designing a non-uniform wafer micro-topography for uniform films in chemical vapor deposition processes,*
    N. Cheimarios, S. Garnelis, I. Aviziotis, G. Kokkoris and A. G. Boudouvis
    38th International Micro & Nano Engineering Conference (MNE 2012), Toulouse, France, September 16-20, 2012

D2. Microfluidics – Lab on Chip for Life Sciences

12. *Cell Attachment on Plasma Nanotextured PMMA Substrates* (poster),
    D. Kontziampasis, A. Bourkoula, P. Petrou, A. Tserepi, S. Kakabakos, E. Gogolides
    5th International Conference on Micro-Nanoelectronics, Nanotechnologies and MEMS, 7-10 October 2012, Kokkini Hani, Heraklion, Greece
13. *Integration of a label-free micromechanical capacitive biosensor in a LoC for disease diagnosis* (poster),
    D. Moschou, N. Vourdas, V. Tsouti, G. Kokkoris, G. Tsekenis, I. Zergioti, A. Tserepi, S. Chatzandroulis
    5th International Conference on Micro-Nanoelectronics, Nanotechnologies and MEMS, 7-10 October 2012, Kokkini Hani, Heraklion, Greece
14. *Autonomous, plasma-nanotextured, smart microfluidics, and Lab-on-Chip systems for chemical and biological analysis* (oral),
    Evangelos Gogolides, Katerina Tsougeni, Kosmas Ellinas, Angeliki Tserepi, Panagiota Petrou, and Sotirios Kakabakos
    Micro and Nano 2012

D3. Nano-Devices for Energy

15. *High aspect ratio, plasma etched silicon nanowires for photovoltaic application: Fabrication and characterization* (Invited talk),
    A. Smyrnakis, A. Zeniou, E. Almpanis, N. Papanikolaou, P. Dimitrakis, E. Gogolides,
    XI International Conference on Nanostructured Materials (NANO 2012) August 26-31, 2012, Rhodes, Greece

Seminars – Invited talks

1. *Morphological characterization of nanostructures through the analysis of SEM images* (invited talk),
   V. Constantoudis, V.K. Murugesan Kuppuswamy, N. Karasmani, G. Giannakopoulos, E. Gogolides
   9th International Conference on Nanosciences & Nanotechnologies (NN) July 3-6, 2012, Thessaloniki, Greece
2. *High aspect ratio, plasma etched silicon nanowires for photovoltaic application: Fabrication and characterization* (Invited talk),
   A. Smyrnakis, A. Zeniou, E. Almpanis, N. Papanikolaou, P. Dimitrakis, E. Gogolides, XI International Conference on Nanostructured Materials (NANO 2012) August 26-31, 2012, Rhodes, Greece
3. *Morphological characterization of nanostructures through the analysis of SEM and AFM images* (invited talk),
   V. Constantoudis, V.K. Murugesan Kuppuswamy, N. Karasmani, G. Giannakopoulos, E. Gogolides
   38th International Micro & Nano Engineering Conference (MNE), September 16-20, 2012, Toulouse, France
4. *Autonomous, plasma Nanotextured smart microfluidics, and Lab on a Chip systems for chemical and biological analysis* (invited talk),
   E. Gogolides, K. Tsougeni, K. Ellinas, A. Tserepi, P. Petrou, S. Kakabakos
   5th International Conference on Micro-Nanoelectronics, Nanotechnologies and MEMS, 7-10 October 2012, Kokkini Hani, Heraklion, Greece
5. *Micro & Nanofluidics: Technology and Applications,*
   A.Tserepi
   Summer School “Nanomaterials and Devices”, University of Patras, July 12, 2012, Patras

Conference Participation

- 26th SPIG 2012
- SPIE 2012 - The International Society for Optical Engineering
- 13th International Conference on Plasma Surface Engineering (PSE 2012)

- EMRS 2012 Meeting
- 16th Int. Conference on Miniaturized Systems for Chemistry and Life Sciences (μTAS)
- 3rd European Microfluidics Conference
- Plasma Etch and Strip in Microelectronics (PESM 2012)
- XI International Conference on Nanostructured Materials (NANO 2012)
- 38th International Micro & Nano Engineering Conference (MNE 2012)
- European Congress on computational methods in applied science and engineering (ECCOMAS 2012)
- 5th International Conference on Micro-Nanoelectronics, Nanotechnologies and MEMS
- Micro and Nano 2012
- XI International Conference on Nanostructured Materials (NANO 2012)
- 9th International Conference on Nanosciences & Nanotechnologies (NN)

Masters Dissertations completed in 2012

1. *Mathematical modeling of a continuous flow microfluidic device for DNA amplification by Polymerase Chain Reaction,*
   Elias Kouris
   MSc Thesis held at IMEL/NCSR Demokritos (Supervisors: G. Kokkoris, A. Tserepi),
   Defended at the National and Kapodistrian University of Athens, Physics Department 2012
2. *Nanopillars and vertical silicon nanowires fabrication using silicon plasma etching processes in room temperature,*
   Angelos Zeniou
   MSc Thesis held at IMEL/NCSR Demokritos (Supervisor: E. Gogolides)
   Defended at the National and Kapodistrian University of Athens, Dept. of Informatics and Telecommunications 2012
3. *Analysis of Rough Surfaces with Network Theory,*
   Nikoletta Karasmani, MSc Thesis held at IMEL/NCSR Demokritos (Supervisor: V. Constantoudis), Defended at National Technical University of Athens, School of Applied Mathematical and Physical Sciences 2012

Doctoral Dissertations completed in 2012

Contact edge roughness in EUV lithography: Metrology and process evaluation,
Vijayakumar Murugesan Kuppuswamy
National Technical University of Athens, School of Chemical Engineering, Athens, Thesis Research Supervisor at NCSR Demokritos: Dr. E. Gogolides, Dr V. Constantoudis, Thesis Supervisor at NTUA: Prof. A. Boudouvis

Teaching and Training Activities

1. E. Gogolides, D. Davazoglou, A. Nassiopoulou
   Microelectronics and Microsystems fabrication processes
   Postgraduate Programs on Microsystems and Nanodevices of the National Technical University of Athens and Micro and Nano Electronics of the National and Kapodistrian Univ. of Athens
2. E. Gogolides, G. Kokkoris, V. Constantoudis, A. Tserepi
   Plasma Processing for Micro and Nano Fabrication
   Postgraduate Program on Microelectronics of the National and Kapodistrian Univ. of Athens
3. D. Mathioulakis, I. Anagnostopoulos, A. Tserepi, G. Kokkoris
   Microfluidic systems
   Postgraduate Program on Microsystems and Nanodevices of the National Technical University of Athens
4. *E. Gogolides, G. Kokkoris, V. Constantoudis, A. Tserepi*
   SimulationofMicroandNano-Patterning
   Postgraduate Program on Mathematical Modelling in Modern Technologies and Financial Engineering of the NationalTechnical University of Athens
5. V. Constantoudis
   Measurement and characterization of nanostructure morphology: Fractal and stochastic aspects
   Demokritos Summer School, 09-20 July 2012
6. G. Kokkoris
   Process and device simulation
   Postgraduate Program on Microelectronics of the National and Kapodistrian University of Athens
7. A. Tserepi
   Microfluidic devices: technology and applications
   Demokritos Summer School, 09-20 July 2012

PROJECT I. 3

THIN FILMS BY CHEMICAL VAPOR AND ATOMIC LAYER DEPOSITION (CVD-ALD)

Project Leader: D. Davazoglou

Post Doctoral Scientists: G. Papadimitropoulos, N. Vourdas

PhD Students: I. Kostis

MSc Students: K. Tsevas, N. Panousis, N. Pasipoularidis

Collaborating scientists from other IAMNMPP groups: M. Vasilopoulou, A. Douvas, P. Argitis, P. Dimitrakis

External Collaborators: L. Palilis, S. Kennou, N. Vainos, D. Alaxandropoulos (Univ of Patras), D. Tsoukalas, I. Sterioti, Y. Raptis (NTUA), N. Stathopoulos, S. Savaidis (TEI Piraeus), S. Boyatzis, (TEI of Athens), E. Koudoumas, D. Vernadrou, D. Louloudakis (TEI Heraklion)

OBJECTIVES

The objectives of this group include research and development in the following:

a) Process and material development

b) Characterization of CVD-ALD films

c) Fabrication and characterization of various devices: Si Solar Cells, Hybrid Organic-Inorganic Solar Cells and Gas Sensors

FUNDING

1. Thalis "Polymeric photonic systems for application in information technologies, Photopolys" (2012-2015)
2. Archimides III "Novel and highly efficient Hybrid organic photovoltaic, NHyOPV" (2012-2014)
3. Archimides III "Novel low power consumption Hybrid OLEDs with improved operational characteristics, NHyOLED" (2012-2014)
4. Archimides III "Advanced Low Cost Electrochromic Windows" (2012-2015)
5. SYNERGASIA "TFT Solar" (2009-2012)

MAIN RESULTS in 2012

A. Intermediate Band (IB) Metal-Oxide Films Deposited by Hot-Wire ALD

I. Kostis – G. Papadimitropoulos – N. Vourdas – I. Panousis

An atomic layer deposition (ALD) system was designed and developed equipped with a hot wire (HW-ALD) permitting the separate heating of the gas phase.

Fig. 1. *Photo of the HWALD system that was developed. The reactor and various electronic sub-systems are shown left while on the right a part of the gas line.*

Except of "classical" thermal ALD depositions, heating of the wire only at a pressure of the order of 0.1-1 Torr, in oxidizing (O_2), inert (N_2) or reducing (H_2) environments and/or by pulsed injection of H_2 during deposition, deposits composed of stoichiometric or sub-stoichiometric and/or hydrogen doped oxides of the metallic wire were obtained. By this method a plethora of compounds described by the general formula H_y:MO_x (where M is the metal) were obtained. The degree of oxygen stoichiometry (x) and hydrogenation (y) of these deposits was found to depend on the deposition conditions (deposition environment, rhythm of H_2 injection, time, base pressure, peak pressure, etc.). Oxides of W, Mo and Ta have been deposited with various oxygen stoichiometries and hydrogen doping. In Fig. 2 (left) x-ray photoemission spectroscopy (XPS) results are shown for Mo compounds.

The above oxides are semiconductors with high band gap (above 3 eV), so they are transparent and insulating but the oxygen sub-stoichiometry and/or the H_2 doping cause the creation of electronic states within their gap which, above a certain level may become bands (intermediate bands, IBs), as seen in Fig. 3b for Mo oxide. Moreover, the work function of the material shifts according the sub-stoichiometry and doping (see Fig. 3c). In spite of the formation of IBs, the transparency of these materials is preserved and they now exhibit electronic conductivity. The exact energetic positioning of the intermediate bands, their electrical conductivity and work function may be controlled by choosing the appropriate deposition conditions. Materials exhibiting IBs have attracted much attention during the last decades because theoretical studies have shown that solar cells with high efficiency (of the order of 60%) may be formed on them. Another possible application is to use them as intermediate layers in metal/semiconductor contacts so as to modify the Schottky barrier and with it the turning-on and off voltages and the current through the contact.

Since these oxides are transparent, we have used them to modify electrodes so as to facilitate the injection/extraction of carriers in organic light emitting diodes (OLEDs) and solar cells (OSCs) through the states at the IBs with excellent results. Below a brief account of these activities are given. More details are reported in the Organic Electronics Section of this report Project I 1, Functional molecular materials for lithography and organic-molecular electronics.

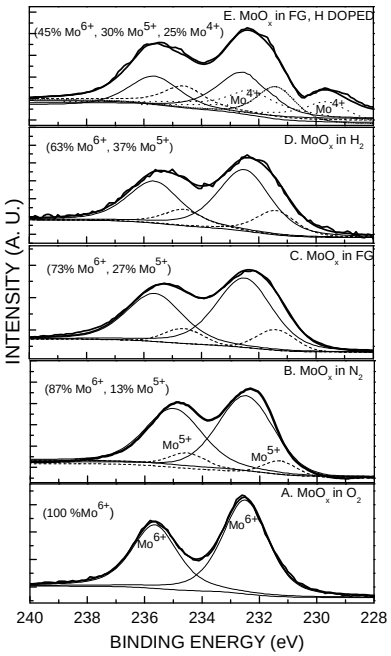

Fig. 2. *XPS results for H_yMoO_{3-x} showing the dependence of the oxidation states of the Mo ion on the deposition and hydrogen doping conditions.*

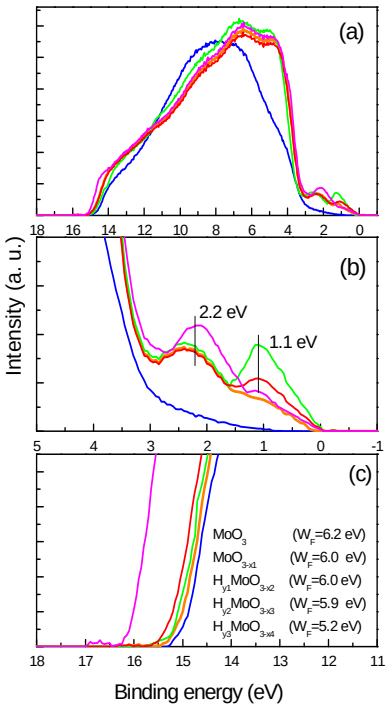

Fig. 3. *UPS result for various H_yMoO_{3-x} compounds. The spectra of the corresponding valence bands are shown in panel a. In panel b the IBs formed within the forbidden gap are shown at energies and intensities dependent on oxygen sub-stoichiometry and hydrogen doping. In panel c the dependence of the work function on the above factors is shown.*

Intermediate band transition metal oxides as charge transport interlayers in OLEDs/OPVs

M. Vasilopoulou – G. Papadimitropoulos – I. Kostis

Organic light emitting diodes (OLEDs) and organic photovoltaics (OPVs) based on organic semiconductors (OSCs) hold the promise for large-area and low-cost electronic devices. This requires the availability of devices offering at the same time high quantum efficiency, low noise and long lifetimes. Although OLEDs and OPVs offer high external quantum efficiencies (EQEs) they still suffer from short lifetimes of only a few hundred hours as well as large dark currents. We demonstrated the simultaneous enhancement of efficiency and of lifetime of OLEDs/OPVs based on the poly[(9,9-dioctylfluorenyl-2,7-diyl)-co-(1,4-benzo-{2,1',3}-thiadiazole)] (F8BT) emissive copolymer and the poly(3-hexylthiophene) (P3HT):[6,6]-phenyl-C71 butyric acid methyl ester ($PC_{71}BM$) blended bulk heterojunction (BHJ) (Figures 4(a) and (b)) respectively, by omitting the widely used poly(3,4-ethylenedioxythiophene): poly(styrenesulfonic acid) (PEDOT:PSS) anode layer and using molybdenum and tungsten oxide layers instead. The OLEDs consist of indium-tin-oxide (ITO) coated glass substrates, a metal oxide like molybdenum oxide (MoO_x) as the hole-transporting layer, the emissive layer, the electron injection layer consisting of under-stoichiometric tungsten oxide (WO_{3-x}) nanoparticles and an aluminum cathode. The devices with the oxide nanoparticles exhibited one order of magnitude higher luminance than the reference ones at 10 V, while their overall performance was highly optimized (Figure 4(a)).

High efficiencies were also obtained in OPV devices based on P3HT as donor and $PC_{71}BM$ as acceptor modified with the metal oxides with an optimized thickness of 10 nm as compared to the devices incorporating the PEDOT-PSS layer. We have attributed these enhanced efficiencies to more efficient absorption of the active layer due to the higher degree of crystallization obtained when it is deposited on top of the metal oxides. These findings

demonstrate the tremendous potential of the incorporation of transition metal oxides in organic electronics.

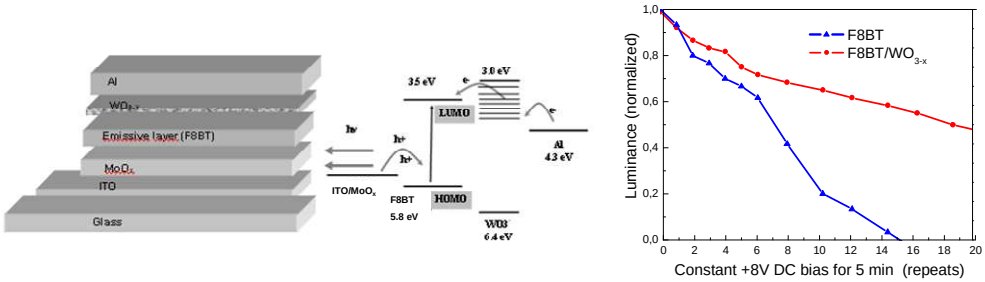

Fig. 4. *(a) (Left) Device architecture of the Hy-PLED investigated and corresponding energy level diagram (Centre). (Right) Time evolution of the performance of OLEDs. Device performance was estimated by measuring the luminance after the application of a DC bias of 8V for 5 min.*

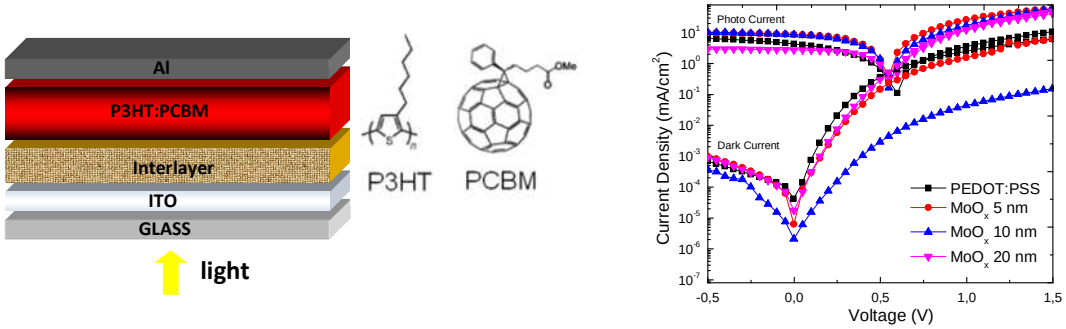

Fig. 4. *(b) OPD device architecture and the chemical structures of P3HT and $PC_{71}BM$ (left). Photocurrent and dark current J-V curves of the OPV cells based on P3HT:$PC_{71}BM$ photoactive layer and with either a PEDOT-PSS or a molybdenum oxide layer of different thicknesses (right).*

Intermediate band transition metal oxides as charge transport interlayers in Al/Si and Cu/Si contacts

Various metallic oxides were also used to modify the Si/metal contact. To this end we fabricated Al-Si-Al and Cu-Si-Al contacts and the corresponding I-V characteristics were recorded at various temperatures. Within the limited time of a Master Thesis (N. Panousis), only stoichiometric oxides were tested.

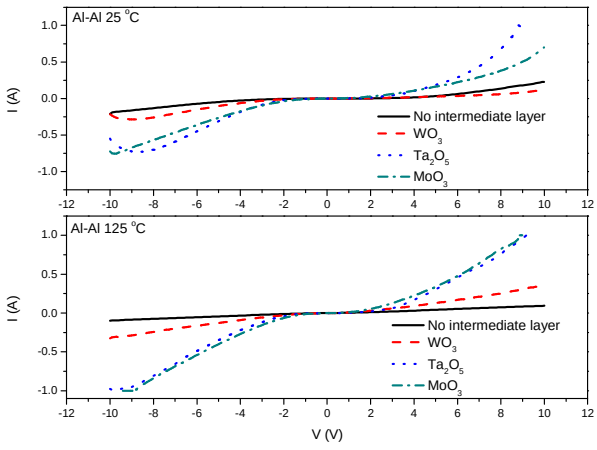

Fig. 5. *I-V characteristics recorded on Al/Metal Oxide/Si/Metal Oxide/Al contacts at 25 and 125 °C, for WO_3, MoO_3 and Ta_2O_5.*

Some indicative results are shown in Fig. 5. As seen in figure, at 25 ^{o}C the turn-on voltage and the forward current of the contact could be shifted towards either lower or higher values relatively to the control sample (Al/Si) by the proper choice of oxide. Similarly, the forward current could be enhanced significantly at 125 ^{o}C. The work continues for sub-stoichiometric and hydrogen doped oxides.

B. Fabrication of partially transparent concentration solar panels based on miniature silicon PV cells

K. Tsevas

Miniature PV cells, with area of 0.15 cm^2 (see Fig. 6) were fabricated on CZ Si wafers using standard methods aiming at keeping the fabrication cost as low as possible.

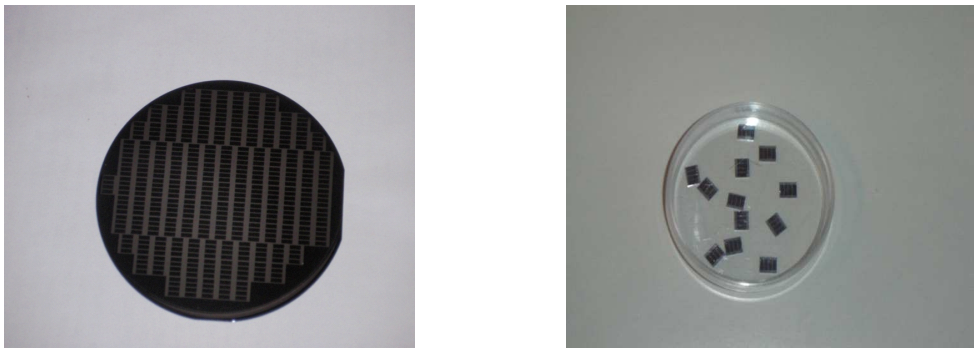

Fig. 6. *Miniature PV Silicon cells with dimensions of 0.15 (0.5X0.3) cm^2 before (left) and after cutting (right).*

These cells were interconnected as shown in Fig. 7a on a transparent carrier (a sheet of PET) using Cu ribbons as current leads. An array of semi-spherical lenses used for the concentration of light on these cells is also shown in Fig. 7.

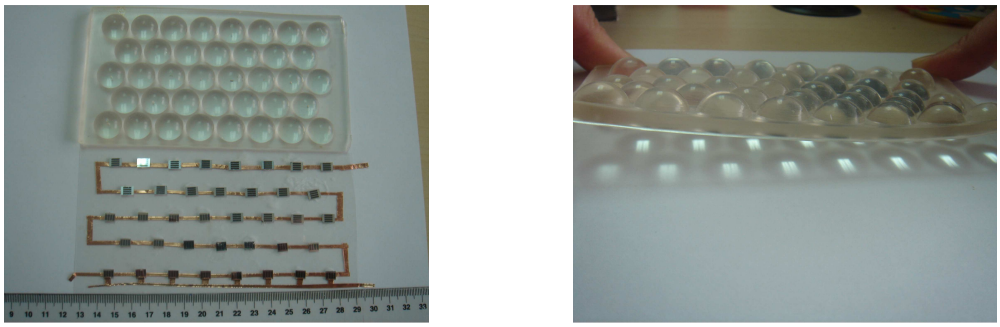

Fig. 7. *(Left, a) Miniature Si PV cells placed on a pierced PET sheet and interconnected from the back side with a Cu ribbon. The front sides (emitters) of the cells of lower array are also interconnected. An array of semi-spherical lenses is shown on top of Fig. 7a and on the right (Fig. 7b).*

After encapsulation of the interconnected cells and of the array of lenses solar panels, as seen in Fig. 8, were obtained. Miniature cells were placed before the focal point of lenses in order to obtain partial transparency of panels. Due to the minimal quantities of Si used and the use of standard technologies for the fabrication of miniature cells the cost of panels is maintained at low levels.

Possible applications of these panels include standard glazing obtaining lighting and generation of electricity. Also, by replacing the front glass of usual solar-thermal collectors with such panels, one may obtain co-generation of electricity and heat using the same collector.

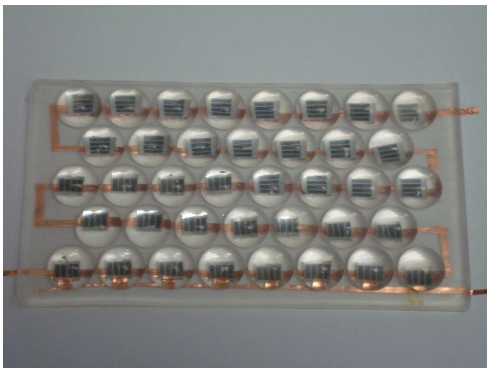

Fig. 8. *A partially transparent concentration solar panel based on miniature silicon PV cells.*

Gas Sensors

G. Papadimitropoulos, N. Pasipoularidis

Resistive gas sensing elements were fabricated using as catalytic (sensing) materials thin films of WO_3, MoO_3 and Ta_2O_5, which were tested using H_2 and CO as target gases. All the above films were highly porous as seen in Fig. 9.

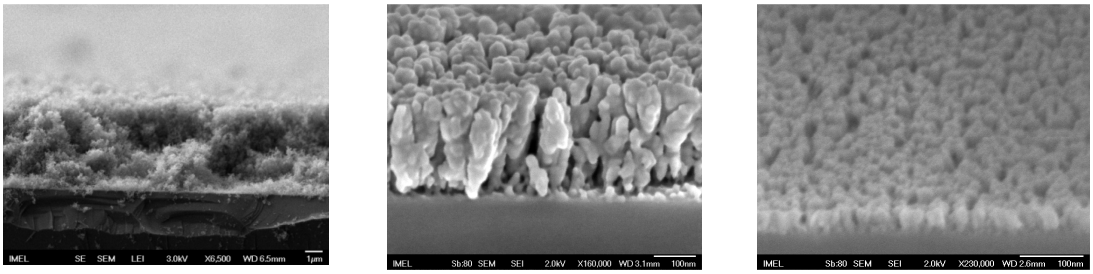

Fig. 9. *SEM micrographs taken on highly porous tungsten (left), molybdenum (center) and tantalum (right) oxide films.*

The resistance variations of these configurations caused by changes in their environment were monitored. As seen in Fig.s 10(a) and 10(b) reversible changes of resistance were observed in these metal oxides films caused by the presence or upon removal of gases (H_2 and CO). The magnitude of these changes, related to the sensitivity, was found to depend on hydrogen and carbon monoxide concentration and temperature of measurement (150 ^oC - 450 ^oC). The time needed (response time) for the resistance to drop or to rise after gas exposure was found comparable to that needed to recover to its initial value after gas removal. Response times of the order of a few seconds were measured on TaO_x films, much shorter than those measured on metal oxides samples deposited by other methods, like chemical vapor deposition (Fig. 11).

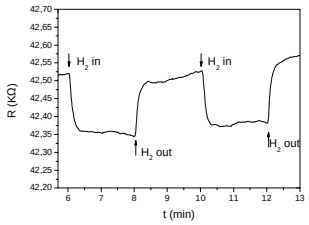

Fig. 10(a). *Time variation of porous tantalum oxide resistance at 200 ^oC for H_2 sensing.*

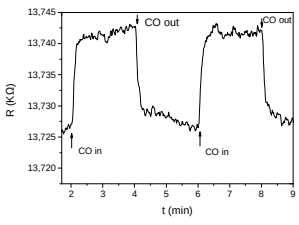

Fig. 10(b). *Time variation of porous tantalum oxide resistance at 350 ^oC for CO sensing.*

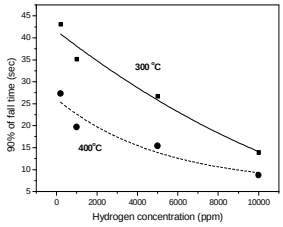

Fig. 11. *Variation of the 90% of fall time with hydrogen concentration for a tantalum oxide sensing element at 300 and 400 ^oC.*

PROJECT OUTPUT in 2012

Publications in International Refereed Journals

1. *On the optical properties of SLS ELA polycrystalline silicon films,*
   Moschou, D.C., Vourdas, N., Davazoglou, D., Kouvatsos, D.N., Vamvakas, V. Emm., Voutsas, A.T.,
   Microelectr. Eng. 90, 69 (2012)
2. *Reduced transition metal oxides as electron injection layers in hybrid-PLEDs,*
   Vasilopoulou, M., Georgiadou, D.G., Palilis, L.C., Argitis, P., Kennou, S., Sygellou, L., Konofaos, N., Iliadis, A. , Kostis, I., Papadimitropoulos, G., Davazoglou, D.,
   Microelectr. Eng. 90, 59 (2012)
3. *Investigation of porous hot-wire WO_3 thin films for gas sensing application,*
   Papadimitropoulos G., Kostis I., Triantafyllopoulou R., Tsouti V., Vasilopoulou M., Davazoglou, D.'
   Microelectr. Eng. 90, 51 (2012)
4. *Substoichiometric hot-wire WO_x films deposited in reducing environment,*
   Vourdas N.' Papadimitropoulos G., Kostis I., Vasilopoulou M., Davazoglou, D.
   Thin Solid Films, 520, 3614 (2012)
5. *Barrierless hole injection through sub-bandgap occupied states in organic light emitting diodes using substoichiometric MoO_x anode interfacial layer,*
   Vasilopoulou M., Palilis L. C., Georgiadou, D. G., Kennou S., Kostis I., Davazoglou D., Argitis P., Applied Physics Letters Vol. 100, (2012), Article number 013311
6. *High performance organic light emitting diodes using substoichiometric tungsten oxide as efficient hole injection layer,*
   Vasilopoulou, M., Papadimitropoulos, G., Palilis, L.C., Georgiadou, D.G., Argitis, P., Kennou, S., Kostis, I., Vourdas, N., Stathopoulos, N.A., Davazoglou, D.
   Organic Electronics Volume 13, (2012), Pages 796-806
7. *Omnidirectional antireflective properties of porous tungsten oxide films with in-depth variation of void fraction and stoichiometry,*
   Vourdas N. , Dalamagkidis K., Kostis I., Vasilopoulou M., Davazoglou, D.
   Optics Communications, Vol. 285, Pages 5229-5234 (2012)
8. *The influence of hydrogenation and oxygen vacancies on molybdenum oxides work function and gap states for application in organic optoelectronics,*
   Vasilopoulou, M., Douvas A.M., Georgiadou D.G., Palilis L.C., Kennou S., Sygellou L., Soultati A., Kostis I., Papadimitropoulos G., Davazoglou_D., Argitis P.
   J. Am. Chem. Soc. Vol. 134, (2012), pp 16178-16187
9. *Hot-wire substoichiometric tungsten oxide films deposited in hydrogen environment with n-type conductivity,*
   Kostis I., Michalas L., Vasilopoulou M., Konofaos N., Papaioannou G., Iliadis A. A., Kennou S., Giannakopoulos K., Papadimitropoulos G., Davazoglou D.
   Journal of Physics D: Applied Physics Vol. 45, (2012), Article No 445101

PROGRAM II

NANOSTRUCTURES and NANOELECTRONIC DEVICES

PROGRAM II

NANOSTRUCTURES and NANOELECTRONIC DEVICES

PROJECTS

- NANOSTRUCTURES FOR NANOELECTRONICS, PHOTONICS AND SENSORS
- MATERIALS AND DEVICES FOR MEMORY AND EMERGING ELECTRONICS
- MOLECULAR MATERIALS AS COMPONENTS OF ELECTRONIC DEVICES
- COMPUTATIONAL NANOTECHNOLOGY

PERSONNEL

RESEARCHERS

A. G. Nassiopoulou, P. Normand, N.Glezos, N. Papanikolaou, S. Gardelis, V. Ioannou-Sougleridis, P.Argitis

COLLABORATING RESEARCHERS

E. Gogolides

PERMANENT SCIENTIFIC STAFF

P. Dimitrakis, A. Douvas

POST DOCTORAL SCIENTISTS

E. Hourdakis, V. Gianneta, A. Sotiropoulos, D.Velessiotis, K. Giannakopoulos

PhD STUDENTS

P. Manoussiadis, P. Sarafis, I. Leontis, K. Valalaki, P. Goupidenis, N. Nikolaou, A.Balliou, E. Almpanis

PROJECT II.1
NANOSTRUCTURES FOR NANOELECTRONICS, PHOTONICS AND SENSORS

Project Leader: A. G. Nassiopoulou

Permanent Researcher: S. Gardelis

Post Doctoral Scientists: E. Hourdakis, V. Gianneta, A. Sotiropoulos

PhD Students: P. Manoussiadis, P. Sarafis, I. Leontis, K. Valalaki

OBJECTIVES

The activities of the group focus in the following:

a) Si nanowires and nanocrystals

Historically the activity on semiconductor nanostructures started within this research group at the early nineties and is conducted within different EU projects. Worldwide pioneering results of the group in this field include the following: The group was the first to report on the fabrication and light emitting properties of Si nanowires (APL 66(9), 1114 (1995)), and on an electroluminescent device based on vertical Si nanowires (APL 69(15), 2267 (1996)). The growth of single and multilayered two-dimensional arrays of Si nanocrystals (NCs) with controllable size embedded in SiO_2 was also reported in the nineties, Si NC memories with good characteristics using LPCVD Si nanocrystal were also developed.

In 2012 the group focused on the following:

- Synthesis, characterization and applications of SiNWs by metal-assisted chemical etching:
- Fabrication and properties of two-dimensional arrays of Si nanocrystals embedded in SiO_2 for solar cell applications

b) *Porous Si*

The group has important expertise and know-how in porous Si formation, properties and applications. Highly porous Si is a nanostructured material composed of interconnected nanowires and nanocrystals. Due to its structure and morphology, porous Si has interesting properties, including its very low thermal conductivity and its tunable dielectric permittivity. Based on the above properties, it finds important applications in thermal isolation and in RF shielding on the Si wafer. Pioneering results of the group over the years using porous Si include the development of efficient porous Si micro-hotplate technology on the Si wafer, a low power Si flow sensor, a flow meter for the car engine and a system for respiration control using the low power flow sensor. Developed processes include the local formation of porous Si thick films formed locally on the Si wafer, porous Si free standing close-type membranes over cavity fabricated in a single electrochemical process and porous Si cantilevers and suspended membranes fabricated by electrochemistry.

In 2012 the group focused on the development of porous Si as an RF substrate material and as a substrate material for cooling and heating devices. Its dielectric permittivity was investigated as a function of material porosity, structure and morphology for the frequency range 0-210 GHz. Its thermal properties were also investigated at both room and low temperatures down to 20K for cryogenic applications. Finally, the growth of metal nanoparticles and nanowires within the pores of the porous Si material is being studied.

c) Porous anodic alumina thin films on Si

The formation, properties and applications of porous anodic alumina thin films on Si are investigated. Highly ordered hexagonal pore arrangement is achieved by electrochemical oxidation of Al films on Si. The applications developed include the formation of nanowires within and the use

of porous alumina films on Si as a masking material for Si nano-patterning. Porous anodic alumina has been also investigated as a high-k dielectric material in memory devices and in metal-oxide-metal (MIM) capacitors.

Key results in 2012

- ⇨ Porous Si thermal conductivity was determined in a wide temperature range of 20–350K. Porous Si shows a much lower thermal conductivity than bulk crystalline Si, this difference exceeding four orders of magnitude at temperatures below 50K.
- ⇨ The dielectric properties of porous Si for its use as a local RF substrate on the Si wafer were investigated in detail. Co-planar waveguides and inductors were fabricated on local porous Si areas on the Si wafer and tested at radiofrequencies.
- ⇨ A detailed comparison was made between porous Si as a local RF substrate and the state-of-the-art RF substrate trap-rich high resistivity (HR) Si. The comparison revealed the important advantages of porous Si for this application, compared to the trap-rich HR Si.
- ⇨ The kinetics of growth of Ni nanoparticles and nanowires into porous Si layers were investigated. The porous Si layers had vertical branched pores of average diameter in the range of 30-45nm. The porous Si layer thickness was in the range of 0.5 to 4 μm. The growth of the Ni nanoparticles and nanowires was achieved using pulsed electrodeposition from a Ni salt solution.
- ⇨ Si nanopatterning through an on-chip self-assembled porous anodic alumina (PAA) masking layer using reactive ion etching based on fluorine chemistry was investigated. The pattern of the hexagonally arranged pores of the alumina film was perfectly transferred to the Si surface.

Infrastructure Development

The electrochemistry laboratory was fully upgraded in 2012
The sputtering system in the laboratory was upgraded. The following materials are deposited: amorphous Si, SiO_2, Al, Cu and Pt.
The optics laboratory for PL, photocurrent and solar cell characterization was also upgraded.

FUNDING

- EU FP7 ENIAC JU Project SE2A, 1/1/2009-31/03/2012- Contract No 120009
- EU FP7 Network of Excellence NANOFUNCTION, 1/9/2010-31/8/2013 - Contract No 257375
- EU FP7 Coordination and Support Action NANO-TEC, 1/9/2010-28/2/2013 - Contract No 257964

MAIN RESULTS in 2012

A. Porous Si as an RF substrate material. Investigation of its dielectric properties

P. Sarafis, M. Hourdakis and A. G. Nassiopoulou

The dielectric properties of porous Si for its use as a substrate material in Si-integrated RF passive devices were investigated and its advantages for this application were demonstrated. The greatest advantage is that porous Si can be combined with CMOS processing and local areas on the Si wafer can be formed, providing an efficient local RF shielding platform on the lossy Si substrate. High performance RF passive devices can be integrated on the local porous Si areas. Co-planar waveguide transmission lines were integrated on porous Si and their performance at RF was assessed [A1].

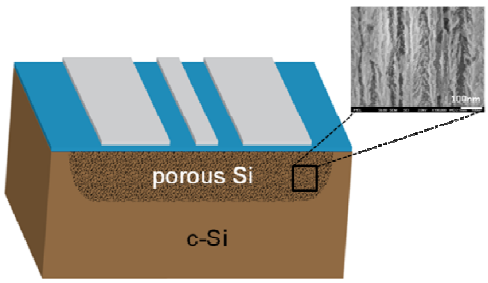

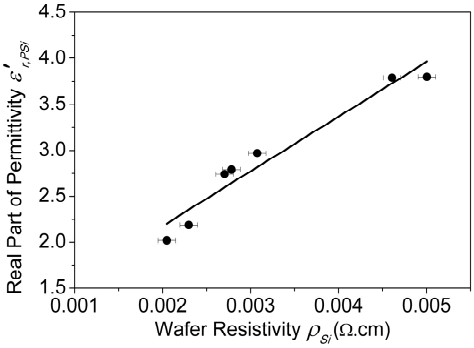

The dielectric permittivity of porous Si layers formed on a low resistivity p-type Si (0.001-0.005 Ω·cm) has been thoroughly investigated in the frequency range 1-40 GHz using analytical expressions within the framework of the broadband transmission line characterization method [A1]. It has been demonstrated that the value of Si resistivity is critical for the resulting porous Si layer permittivity even within the above limited resistivity range. Indeed, the real part of porous Si dielectric permittivity changes monotonically between 1.8 and 4 by changing the Si resistivity between 0.001 and 0.005 Ω·cm (see the graph on the right). The above study was made for porosities between 70 and 84%. The quality factor and attenuation loss of the investigated co-planar waveguide transmission lines were found to be equal to Q=26 and a=0.19dB/mm respectively at 40GHz. These values are competitive to those obtained on quartz, which is one of the off-chip RF substrates with the lowest losses.

[A1] P. Sarafis, E. Hourdakis, and A. G. Nassiopoulou, “Dielectric Permittivity of Porous Si for use as Substrate Material in Si-Integrated RF Devices,” IEEE Transactions on Electron Devices, vol. 60, no. 4, pp. 1436–1443, Apr. 2013 (accepted in 2012).

B. Comparison between Si-based RF substrates for passive devices

P. Sarafis[1], M. Hourdakis[1], A. G. Nassiopoulou[1], C. Roda Neuve[2], K. Ben Ali[2] and J.-P. Raskin[2]
1. NCSR Demokritos, Greece, 2. UCL Belgium

Two novel RF substrate technologies have been compared, namely local porous Si RF substrate technology and high resistivity Si with a trap-rich layer on top (trap-rich HR-Si) [fig. B1]. Using standard Si processing, identical co-planar waveguide transmission lines, crosstalk structures and test inductors were fabricated on the above two substrates, as well as on quartz and on standard p-type Si (fig. B1).

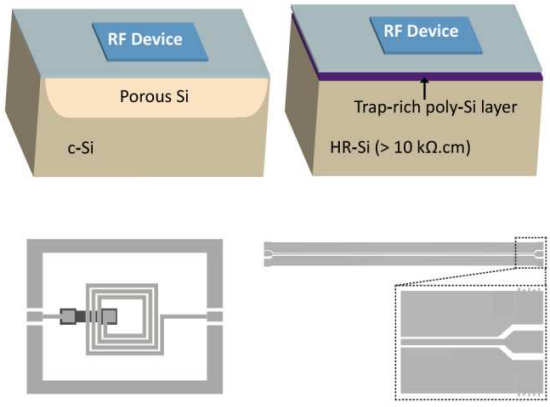

***Fig. B1**. Up-left: Cross-sectional illustration of the local porous Si areas on the Si wafer: Up right: HR-Si with the trap-rich layer on top. Down left: Layout of the square inductors. Down right: Layout of the CPW transmission lines integrated on the two above substrates under comparison.*

Broadband electrical characterization in the frequency range from 40 MHz to 40 GHz revealed that porous Si substrate provides much higher effective resistivity and lower dielectric constant than trap-rich HR-Si, that is comparable with values of a quartz substrate values (see Table I).

TABLE I.

	Electrical Characteristics	Substrates: Quartz	Porous Si	Trap-rich HR-Si	p-type Si (1-10 Ω.cm)
CPW TLine characteristics	Zc (Ω)	78	100	51	34
	$\varepsilon_{r,eff}$	2.5	2.2	5.7	7.2
	α [@ 40 GHz] (dB/mm)	0.23	0.24	0.37	11.4
	Q [@ 40 GHz]	24.9	22.4	23.3	1.0
	P_{out} in 2nd Harm. Distortion [@ P_{out} = 15 dBm] (dBm)	< -110	< -110	-90	> -40
	Crosstalk [@ 25 GHz] (dB)	-22	-25	-15	-15

COMPARISON OF THE DIFFERENT SUBSTRATES

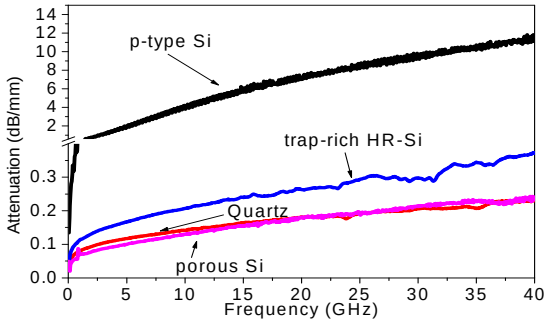

***Fig. B2.** Attenuation constant of the CPW transmission line as a function of frequency for the following devices on porous S, trap-rich HR-Si, quartz and p-type Si (1-10 Ω.cm). The CPW TLine on porous Si shows an attenuation constant as low as that on quartz.*

The higher effective substrate resistivity leads to lower attenuation losses (Fig. B2) and reduced non-linearities, as well as better quality factor for both transmission lines and inductors. In addition, the lower dielectric permittivity of porous Si leads to drastic reduction of crosstalk, to higher operating frequencies for inductors and provides design options for higher characteristic impedance devices.
Conclusively it can be said that porous Si, which is CMOS-compatible and cost-efficient, demonstrates state-of-the-art RF performances even comparable with the off-chip quartz substrate.

C. Thermal conductivity of porous Si at cryogenic temperatures

K. Valalaki and A. G. Nassiopoulou

Porous Si thermal conductivity was determined in a wide temperature range from 20–350K using the steady state dc method and a subsequent Finite Element Method (FEM). The method was applied to a 40 μm thick porous Si layer of ~60% porosity, formed on p-type Si (fig.C1). Our results on PSi were also compared with theoretical ones and were in good agreement with them. The main conclusions of this work are as follows: Porous Si shows much lower thermal conductivity than bulk crystalline Si, this difference exceeding four orders of magnitude at temperatures below 50K, as it is shown in fig.C2. The variation of porous Si thermal conductivity with temperature is monotonic and does not show any maximum for the measured temperature range, as in the case of bulk crystalline Si and other dielectric materials.

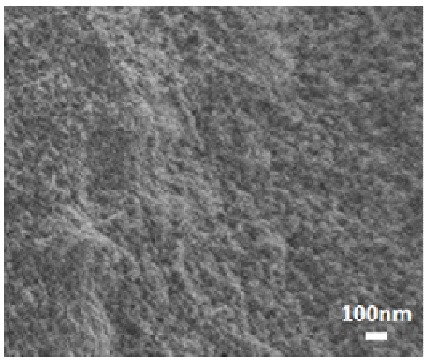

Fig. C1. *Cross sectional SEM image of the studied porous Si layer*

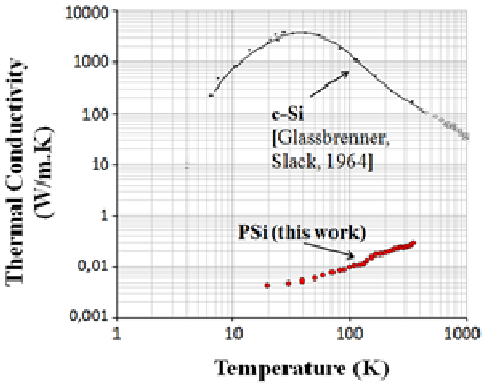

Fig. C2. *Comparison between thermal conductivity of porous Si (this work) and bulk crystalline Si (results from literature) as a function of temperature.*

Phonon confinement in Si nanostructures composing porous Si and phonon-wall scattering, are the basic mechanisms involved, and are at the origin of the above temperature dependence. The effectiveness of local thermal isolation from the Si substrate by a thick highly porous Si layer in a wide temperature range was demonstrated, showing that this material is challenging for use in Si micro-cooling devices.

Part of this work was presented in the 5th International Conference Micro & Nano 2012 on Micro - Nanoelectronics, Nanotechnologies and MEMS which held in Heraklion of Crete on 7-12 October 2012 as oral presentation.

Funding for this work was received from the European Union's 7th Framework Programme (FP7/2007-2013) through the ICT NoE project ‘Nanofunction’ (grant agreement number 257375).

D. Mesoscopic Ni particles and nanowires into porous Si by pulsed electrodeposition

E. Michelakaki, K. Valalaki and A. G. Nassiopoulou

The kinetics of growth of Ni nanoparticles and nanowires into porous Si layers with vertical branched pores of average diameter in the range of 30-45nm and layer thickness in the range of 0.5 to 4 μm, using pulsed electrodeposition from a Ni salt solution were investigated. The effect of pulse duration, number of pulses and total process time on pore filling was investigated for porous Si with different porosities and porous Si layer thicknesses. SEM and TEM were used to characterize the samples. It was demonstrated that at the beginning of electrodeposition, nucleation of Ni nanoparticles on the pore walls takes place, following the Volmer-Weber growth mode. These nanoparticles are dispersed in the whole pore length. By increasing the number of pulses of a given duration, the size of Ni nanoparticles increases by diffusion-controlled growth and neighboring nanoparticles coalesce into larger ones, until a continuous Ni nanowire is formed within the pores. By increasing the layer porosity, the obtained Ni nanoparticles were larger, resulting in all cases in a continuous Ni nanowire, fully filling the pore. By changing the porous Si layer thickness, the final result was qualitatively the same, but the intermediate result was different. Under similar total electrodeposition duration, in the thinner porous Si layer the size of Ni nanoparticles was larger than in the thicker one. However, by increasing the deposition time the pores were also fully filled with Ni in the case of the thicker porous Si layers. From the beginning of the process a metal film starts to form on the porous Si surface and its thickness increases with process time. However, the presence of this film does not impede further pore filling and nanowire formation into the pores. This supports further the diffusion controlled growth mechanism. Finally, it was demonstrated that full pore filling and continuous Ni nanowire formation is also achieved under direct current electrodeposition and the results are quite similar with those obtained with pulsed electrodeposition when the same total deposition time is used in both cases.

The research leading to these results has received funding from the European Community's Seventh Framework Programme (FP7/2007-2013) under grant agreement NANOFUNCTION n°257375.

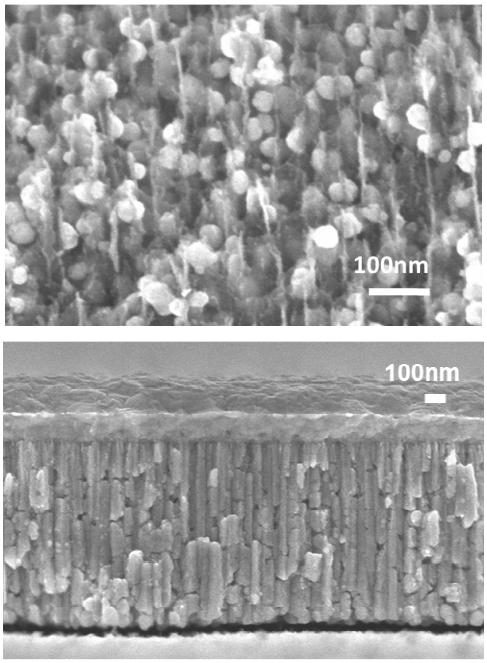

Cross section SEM images of Ni-filled porous Si layers

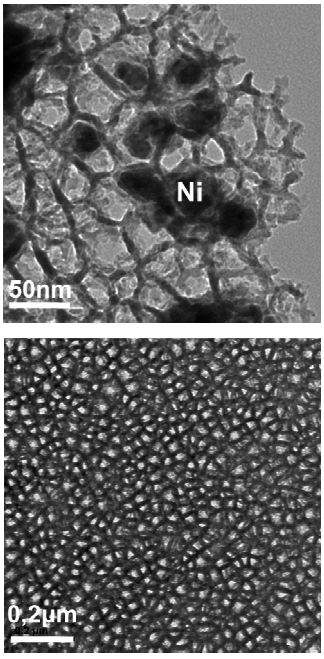

TEM images from a surface area of Ni filled porous Si sample

[D1]: E. Michelakaki, K. Valalaki and A. G. Nassiopoulou, "Mesoscopic Ni particles and nanowires by pulsed electrodeposition into porous Si", Journal of Nanoparticle Research, Volume 15, Issue 4, 2013 (accepted 2012)

E. Si nanopatterning through porous anodic alumina mask

G. Violetta, A. Olziersky and A. G. Nassiopoulou

Si nanopatterning through an on-chip self-assembled porous anodic alumina (PAA) masking layer using reactive ion etching based on fluorine chemistry was investigated. Three different gases/gas mixtures were investigated: pure SF_6, SF_6/O_2, and SF_6/CHF_3. For the first time, a systematic investigation of the etch rate and process anisotropy was performed. It was found that in all cases, the etch rate through the PAA mask was 2 to 3 times lower than that on non-masked areas. With SF_6, the etching process is, as expected, isotropic. By the addition of O_2, the etch rate does not significantly change, while anisotropy is slightly improved. The lowest etch rate and the best anisotropy were obtained with the SF_6/CHF_3 gas mixture. The pattern of the hexagonally arranged pores of the alumina film is, in this case, perfectly transferred to the Si surface. This is possible both on large areas and on restricted pre-defined areas on the Si wafer.

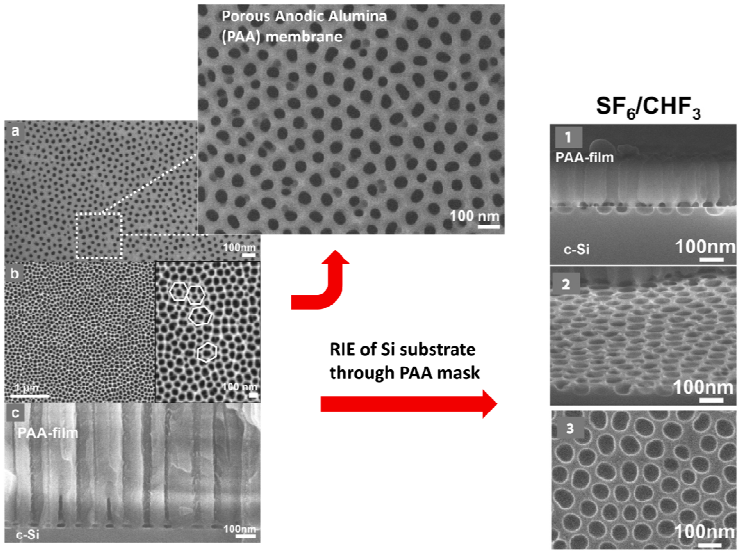

[E1] V. Gianneta, A. Olziersky and A. G. Nassiopoulou, "Si nanopatterning by reactive ion etching through an on-chip self-assembled porous anodic alumina mask", Nanoscale Research Letters, Volume 8, Issue 71, 2013 (accepted 2012)

F. Photo-electrical investigation of Si nanocrystals for photovoltaic cells

P. Manousiadis, S. Gardelis, and A.G. Nassiopoulou

Motivated by the potential use of Si nanocrystals (SiNCs) as absorber material in Si-based photovoltaic designs, we have grown single and multilayered nanocrystalline Si (nc-Si) films containing SiNCs of controlled sizes on quartz by low pressure chemical vapour deposition (LPCVD) of Si and subsequent oxidation at high temperature. The thickness of the nc-Si layers ranged from less than 2 nm up to 25 nm, by choosing suitable growth conditions. The multilayered films consisted of five nc-Si/SiO_2 bilayers. The structure of the films was investigated by high resolution transmission electron microscopy (HRTEM). From optical transmission and reflection measurements, energy band gaps of the SiNCs within the films were estimated and the results were correlated with the sizes of the SiNCs, as observed by HRTEM. Also the light emission properties of the films were investigated by photoluminescence measurements. Finally,

photocurrent was measured. Electron microscopy showed that the films had columnar structure, i.e., they consisted of SiNCs with the z-dimension equal to the film thickness and with lateral sizes with narrow size distribution (Fig. F1(a)).

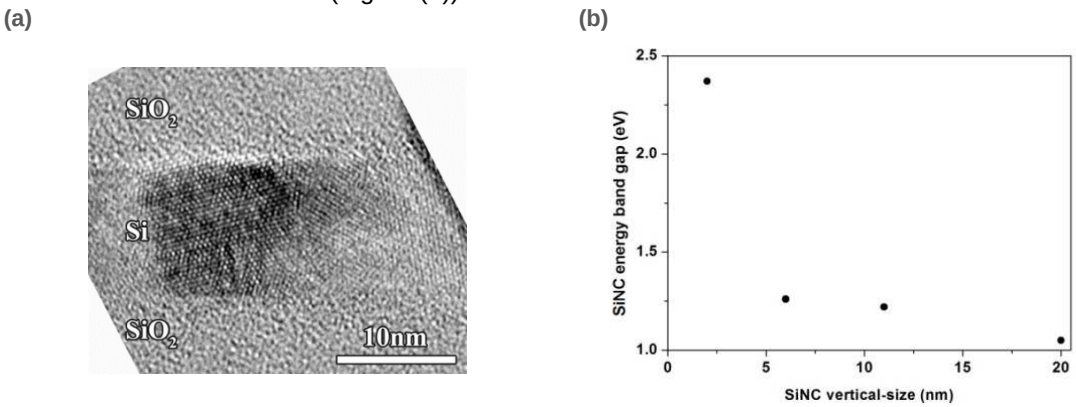

Fig. F1. *(a) Cross-section HRTEM image showing a SiNC. (b) Estimated energy band gap of the SiNCs within the different films*

The majority of the films had SiNCs touching each other without any observable oxidation at the grain boundaries. Only in the case of the thinnest film (SiNC vertical dimension ~ 2 nm) the SiNCs were well separated by silicon dioxide barriers. Absorption and energy band gaps of the SiNCs within the different films were deduced from suitable analysis of the optical transmission and reflection measurements. A shift of the energy band gap with decreasing SiNC was observed, which was consistent with quantum size effects in the SiNCs (Fig. F1(b)). The film containing the smallest SiNCs (with vertical dimension ~ 2 nm), besides a significant shift of the absorption edge to higher energies, showed light emission at room temperature which was due to the radiative recombination of photo-generated excitons in the localized SiNCs separated by SiO_2 tunnel barriers (Fig. F2(a)). Spectral dependence of the photocurrent coincided with the spectral dependence of the absorption (Fig. F2(b)). Specifically, photocurrent showed similar shift to higher energies as the size of the SiNCs decreased, confirming quantum size effects in the constituent SiNCs.

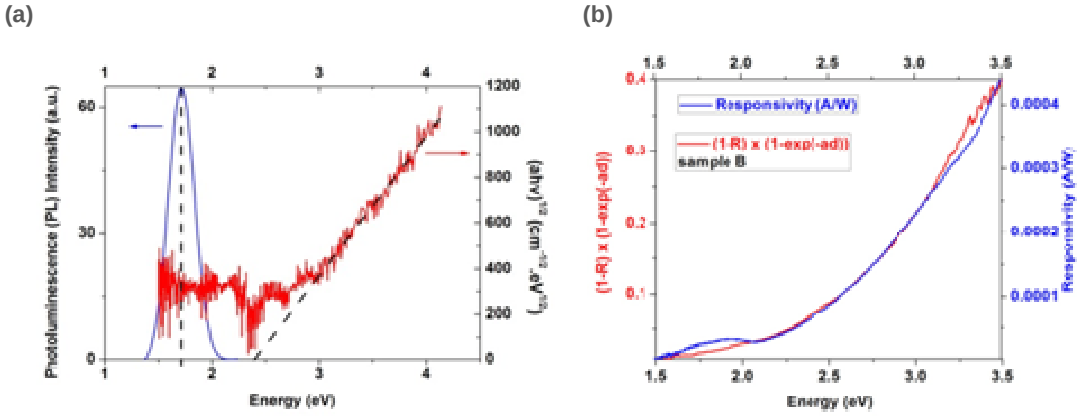

Fig. F2. *(a) Photoluminescence and absorption edge of 2nm SiNCs embedded in SiO_2. (b) Spectral dependence of responsivity (photocurrent normalized to the power of incident light) compared with the spectral dependence of the absorbed light.*

[F1] S. Gardelis, A.G. Nassiopoulou, P. Manousiadis, S. Milita, A. Gkanatsiou, N, Frangis, and Ch. B. Lioutas, "Structural and optical characterization of two-dimensional arrays of Si nanocrystals embedded in SiO_2 for photovoltaic applications", J. Appl. Phys. 111 (8), 0835346 (2012)

[F2] P. Manousiadis, S. Gardelis, and A.G. Nassiopoulou, "Lateral electrical transport and photocurrent in single and multilayers of two-dimensional arrays of Si nanocrystals", J. Appl. Phys. 112 (4), 043704 (2012)

PROJECT OUTPUT in 2012

Publications in International Refereed Journals

1. *High performance MIM capacitor using anodic alumina dielectric,*
   Hourdakis, E. and Nassiopoulou, A.G.
   Microelectronic Engineering, vol. 90, pp. 12-14 (2012)
2. *Novel Air Flow Meter for an Automobile Engine Using a Si Sensor with Porous Si Thermal Isolation,*
   E. Hourdakis, P. Sarafis and A. G. Nassiopoulou
   Sensors vol. 12 (11), pp. 14838-14850 (2012)
3. *Two-Terminal Charge-Trapping WORM Memory Device Using Anodic Aluminum Oxide"*
   Hourdakis, E. and Nassiopoulou, A.G.
   J. Nanosci. Nanotechnol. vol. 12 (10), pp. 7968-7974 (2012)
4. *Structural and optical characterization of two-dimensional arrays of Si nanocrystals embedded in SiO_2 for photovoltaic applications,*
   S. Gardelis, A. G. Nassiopoulou, P. Manousiadis, S. Milita, A. Gkanatsiou, N. Frangis, Ch. B. Lioutas, Journal of Applied Physics 111 (8), 083536 (2012)
5. *Lateral electrical transport and photocurrent in single and multilayers of two- dimensional arrays of Si nanocrystals,*
   P. Manousiadis, S. Gardelis, and A. G. Nassiopoulou
   Journal of Applied Physics 112 (4), 043704 (2012)

Published Conference Proceedings

1. *Arsenic Redistribution After Solid Phase Epitaxial Regrowth Of Shallow Pre-Amorphized Silicon Layers,*
   E. Demenev, D. Giubertoni, S. Gennaro, M. Bersani, E. Hourdakis, A. G. Nassiopoulou, M. A. Reading and J. A. van den Berg
   AIP Conf. Proc. 1496, 272 (2012)

Conference Presentations – Invited Talks

1. *Two terminal WORM device based on charge-trapping in porous anodic alumina,*
   E. Hourdakis and A.G. Nassiopoulou
   Micro&Nano 2012, Heraklion, Crete, Greece
2. *Arsenic redistribution after solid phase epitaxial regrowth of ultra-thin pre-amorphized silicon layers,*
   E. Demenev, D. Giubertoni, S. Gennaro, M. Bersani, E. Hourdakis, A. G. Nassiopoulou, M. A. Reading, and J. A. van den Berg
   International conference on Implantation Technology 2012, Valladolid, Spain
3. *Two-terminal charge-trapping WORM memory device using porous anodic alumina,*
   E. Hourdakis and A. G. Nassiopoulou
   E-MRS 2012, Strasbourg, France (poster)
4. *Role of surface chemical treatment on the optical properties of SiNWs fabricated by single step metal assisted chemical etching,*
   I. Leontis, A. G. Nassiopoulou and A. Othonos
   XXVIII Panhellenic Conference on Solid State Physics and Materials Science 2012, Patra, Greece
5. *Room and low-temperature thermal conductivity measurements of highly porous Si with nanostructured morphology,*
   K. Valalaki and A. G. Nassiopoulou
   Micro&Nano 2012, Heraklion, Crete, Greece
6. *Porous Si substrate technology for RF passives integration,*
   A. G. Nassiopoulou
   Workshop on Nanoelectronic Materials and Devices, organized by Micro&Nano, Athens, 17 December 2012 (invited)
7. *High performance RF passive devices in CMOS technology on a local porous Si substrate,*
   A. G. Nassiopoulou
   Workshop on Recent Developments in Nanoelectronics, Thessaloniki, 3 June, 2012 (invited)
8. *Nanostructured Si in the "More than Moore" Nanoelectronics field,*
   A. G. Nassiopoulou
   XI International Conference on Nanostructured Materials, 26-31 August 2012, Rhodes Greece (invited)

9. *Nanostructured porous Si as a local on-chip RF microplate for high performance RF device integration,*
   A. G. Nassiopoulou
   Workshop on Novel Materials, Devices and technologies for High performance RF applications, organized within the ESSDERC/ESCIRC Conference, Bordeaux France, 21 September 2012
10. *ECOSYSTEMS TECHNOLOGY & DESIGN for NANOELECTRONICS: a European Coordination Action: NANOTEC,*
    A. G. Nassiopoulou
    Tutorial, organized within the ESSDERC/ESCIRC Conference, Bordeaux France, 21 September 2012
11. *Optical properties, electrical transport and photocurrent in single and multilayered Silicon nanocrystal films,*
    S. Gardelis, P. Manousiadis, and A.G. Nassiopoulou
    EMRS 2012, Spring Meeting, Strasbourg, France
12. *Single and multilayers of two-dimensional arrays of Si nanocrystals for photovoltaics: Structural and optical characterization,*
    S. Gardelis, A. G. Nassiopoulou, P. Manousiadis, A. Gkanatsiou, N. Frangis, Ch. B. Lioutas
    XXVIII Panhellenic Conference on Solid State Physics and Materials Science 2012, Patra, Greece
13. *Electrical transport and photocurrent in two-dimensional arrays of silicon nanocrystals for photovoltaic applications,*
    S. Gardelis, P. Manousiadis, and A. G. Nassiopoulou
    Micro & Nano 2012, Heraklion, Grete, Greece

Teaching and Training Activities

1. Lectures on “Silicon processing for Nanoelectronics” by A. G. Nassiopoulou and E. Hourdakis within:
   a) the MSc program on Microelectronics organized by the Department of Informatics of the University of Athens, in cooperation with the Department of Microelectronics of NCSR Demokritos and
   b) the MSc program on “Microsystems and Nanoelectronics” organized by the National Technical University of Athens with the participation of the Department of Microelectronics of NCSR Demokritos
2. Lectures on “Micromechanics and Sensors”, by the S. Gardelis within the MSc program organized by the: Department of Informatics, University of Athens, in cooperation with the Department of Microelectronics of NCSR Demokritos

PROJECT II.2
MATERIALS AND DEVICES FOR MEMORY AND EMERGING ELECTRONICS

Project Leader: P. Normand

Permanent Researchers: V. Ioannou-Sougleridis, P. Dimitrakis

Collaborating Researchers: P. Argitis, N. Glezos, E. Gogolides, A.M. Douvas, K. Giannakopoulos

PhD Students: P. Goupidenis, N. Nikolaou

Graduate Students: D. Simatos, V. Poulakis

OBJECTIVES

- Development of dielectrics and nanostructured materials for inorganic/organic memory and advanced electronic applications.
- Study of the structural and electrical properties of the generated materials and demonstration of material functionality enabling the development of emerging electronic devices.
- Realization and testing of electronic devices with emphasis on non-volatile memory cells.

Activities

Our research activities in materials and structures for memory applications started in 1996 with the development of the low-energy ion-beam-synthesis (LE-IBS) technique in collaboration with Salford University (UK). Two-dimensional arrays of Si nanocrystals in thin gate dielectrics were demonstrated and further exploited in the fabrication of nanocrystal memories (NCMs). This activity was first supported by the EU project, FASEM (1997-2000). LE-IBS development with target the realization of non-volatile NCMs in an industrial environment has been conducted further within the framework of the EU project, NEON (2001-2004), in collaboration with the US implanter manufacturer, Axcelis.
In addition to our LE-IBS-NCM activities, major efforts have been devoted the last few years (see previous IMEL's annual reports) to the development of materials and devices for memory and emerging electronics including: (a) Memory devices by Si^+ irradiation through poly-Si/SiO_2 gate stack, (b) Memory devices using Ge-NCs produced by MBE, (c) hybrid silicon-organic and SiGe-organic memories, (d) Formation of Si NCs in thin SiO_2 layers by plasma Immersion, (e) Wet oxidation of LE Si-implanted Si_3N_4 for ONO memory stacks, (f) MOS structures with LE Ge-implanted thin gate oxides, (g) Proton radiation tolerance of NCMs, (h) Fabrication and characterization of SiO_2 films with Si NCs obtained by stencil-masked LE-IBS, (i) Hybrid organic thin film transistor by laser-induced-forward-transfer, (j) Fluorene-based cross-bar organic memory devices, (k) III-Nitrides quantum dots-resonant tunneling diodes as tunable wavelength UV-VIS phototodetectors, (l) Organic proton memories, (m) Proton transport in acid doped polymer matrices, (n) GaN quantum dots for NCMs, and (o) High-k dielectrics stacks for charge trapping memories

The above activities were conducted in collaboration with CEMES/CNRS (FR), FZR Dresden and ZMD AG (DE), STMicroelectronics (IT), Aarhus University (DK), Durham University (UK), Ion-Beam-Services (IBS, FR), MDM-INFM (IT), LETI/CEA (FR), NTUA (GR), INSA Toulouse (FR), Cambridge NanoTech (USA), TEI Crete (GR), Ioannina University (GR), University of Helsinki (FI), MRG/FORTH (GR) and Patras University (GR).

In 2012, our main activities described hereafter were focused on the following tasks: (A) Space charge polarization in acid doped polymer matrices using time-domain dielectric spectroscopy, (B)

High-k dielectrics stacks for advanced non-volatile memory devices, (C) Nanofloating gate memory devices using III-N quantum dots, (D) Front-end processing for Ge MOS technology, (E) Si nanocrystals in thin SiO_2 layers by plasma-immersion ion-implantation.

FUNDING

(1) “Organic electronic devices for radiation sensing”, Archimedes III project OEDDIR, TEI-Crete, Ministry of Education (2012-2015)
(2) "Charge trapping devices (memories) based on novel high-k dielectrics" GSRT-Herakleitos project, MIS: 346791 University of Patras (1/4/2011-31/10/2014)
(3) "Front-End Processes for Germanium MOS applications" Karatheodory, Project C906, University of Patras (1/2/2010-30/9/2013)
(4) “Spontaneous growth, properties and devices of III-V semiconductor nanowires”, NanoWire THALES project, University of Crete, Ministry of Education (2012-2015).

MAIN RESULTS in 2012

A. Space charge polarization in acid doped polymer matrices using time-domain dielectric spectroscopy

P. Goupidenis, P. Normand, A.M. Douvas, P. Dimitrakis, P. Argitis, E. Kapetanakis[1], V. Saltas[1], K. Beltsios[2], C. Pandis[3], A. Kyritsis[3], P. Pissis[3]
[1]*Department of Electronics, Technological Educational Institute of Crete*
[2]*Department of Materials Science Engineering, University of Ioannina*
[3]*Department of Physics, National Technical University of Athens*

We recently demonstrated gate dielectrics which insure the double function of super-capacitor and non-volatile information storage element using a stack made of a polymer layer doped with electrolytic molecules (ion conducting layer) and a polymer layer containing ion-trapping molecules (see Kapetanakis et al., Adv. Mater. 2008, and Org. Elec. 2009). The memory functionality of such devices depends on the macroscopic transport properties of the ion-conducting layer. This requires knowledge of the charge transport processes arising from the motion of the ions and their dependences on such controllable variables as temperature, film thickness and ionic concentration. In 2011, our efforts have been placed on the study of ion transport and polarization mechanisms in polymer blend electrolyte systems consisting of a poly methyl methacrylate (PMMA) matrix doped with polyoxometalate (POM, $H_3PW_{12}O_{40}$) molecules where the moving ions are in the form of protons. The properties of such dielectric systems were investigated by means of transient-current versus time response and capacitance-voltage measurements using MIM and MIS-type structures. Our investigations on MIM structures have shown that such materials are linear systems and therefore, the time dependent response function $I(t)$ can be Laplace or Fourier transformed for extracting the frequency-dependent electric susceptibility, $\chi(\omega)$. Frequency-dependent dielectric response measurements confirmed this result and thereby, the equivalence between the time and frequency domains.

In 2012, we performed additional time-dependent response investigations on the above dielectric systems for deeper understanding of proton kinetics and their dependence on parameters like humidity, electrolyte thickness and POM concentration. Particular emphasis has been also placed on the effect of the polarization time on the measured depolarization current, which can seriously affect the measurements in case the polarization process is not completed due to the superimposition of the continuing polarization on the depolarization current (see Fig. 1). For a 5%/5% HPW / PMMA (w/w ratio) system, $I(t)$ measurements at different temperatures and subsequent Fourier Transform calculations of $\chi''(\omega)$ revealed a depressed Debye-like behavior of the polarization/depolarization processes. The extracted loss peak frequency, ω_{peak}, follows an

Arrhenius behavior with activation energy around 0.93eV which can be understood as the barrier height of the proton migration process.

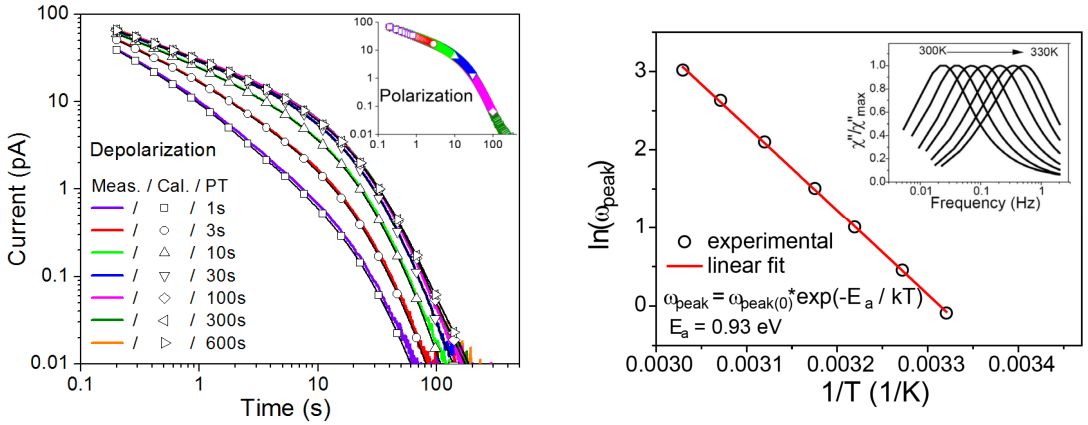

Fig. 1. *(Left) Measured and calculated (symbols) depolarization transient current responses at 23ºC after the application of different polarization times (PT); Inset: Corresponding polarization currents. (Right) Arrhenius plot obtained from the peak of the radial frequency (ω = 2π f) of χ" as a function of the measurement temperature. Inset: Normalized χ" (obtained from FT of the transient current response) as a function of the frequency (f) and temperature (300 to 330K).*

B. High-k dielectrics stacks for advanced non-volatile memory devices

N. Nikolaou, V. Ioannou-Sougleridis, P. Dimitrakis, P. Normand, K. Giannakopoulos, K. Mergia[2], D. Skarlatos[3],K. Kukli[4], J. Niinisto[4], M. Ritala[4], M. Leskela[4]
[1]*Institute of Nuclear Technology and Radiation Protection, IRTRP-NCSR 'Demokritos'*
[2]*Physics Department University of Patras*
[3]*Chemical Department of Helsinki University (FI)*

Replacement of one or more dielectric layers of the standard oxide-nitride-oxide (ONO) stack of SONOS memory leads to charge trapping devices with improved memory functionality and performance. Here, our objective is to examine the influence of advanced atomic layer deposition (ALD) precursor chemistry of high-k dielectrics, which are used as tunnel or blocking dielectrics of nitride-based memory structures. These activities are carried out in close collaboration with the University of Helsinki and the University of Patras through the GSRT-Herakleitos project "Charge trapping devices (memories) based on novel high-k dielectrics" (1/4/2011-31/10/2014).

In 2012, we conducted a systematic study of the structural and electrical properties of $Al_2O_3/Si_3N_4/SiO_2$ stacks for MANOS charge trapping memories using TMA/H_2O and TMA/O_3 chemistries for the deposition of the Al_2O_3 layer. Current density-applied electric field (J-E) measurements showed that above -10 MV/cm substantial differences appear in the characteristics of the two chemistries. In particular, at -14 MV/cm an order of magnitude higher leakage current flows through the TMA/H_2O samples. Our investigations on memory characteristics revealed that without high-temperature post-ALD annealing, the TMA/O_3 process deposits Al_2O_3 films with enhanced write/erase performance, while TMA/H_2O samples have limited ability to remove trapped electrons

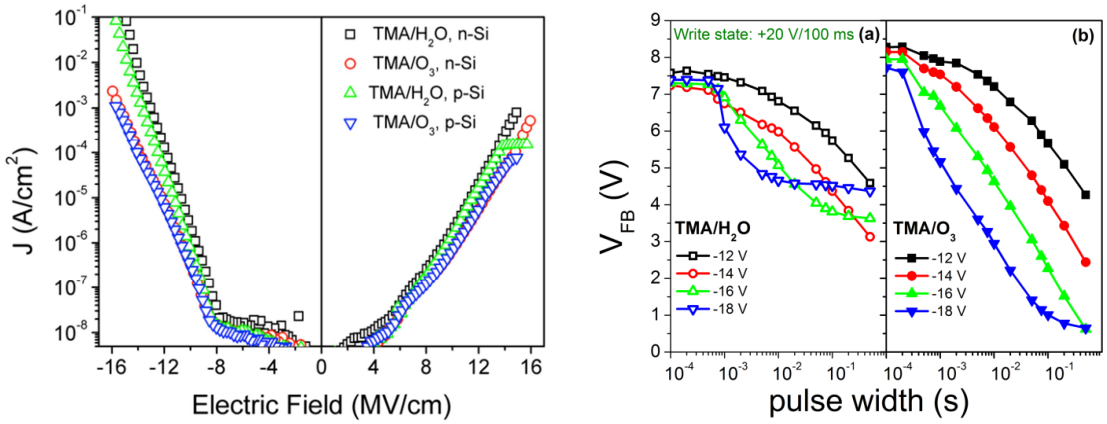

Fig. 2. *(a) J-E characteristics of the $SiO_2/Si_3N_4/Al_2O_3$ triple gate stacks, (b) Erase performance characteristics of the TMA/H_2O and TMA/O_3 MANOS capacitors.*

C. Nanofloating gate memory devices using III-N quantum dots

P. Dimitrakis, P. Normand, E. Papadomanolaki[1], E. Iliopoulos[1,2], C. Bonafos[3]
[1] *Department of Physics, University of Crete (GR)*
[2] *MRG/FORTH (GR)*
[3] *CEMES-CNRS, Université de Toulouse (FR)*

There has been a tremendous development in the flash memory technology over the past three decades. Nevertheless, there are very important issues for the scaling of conventional flash below 16 nm technology nodes. To address these shortcomings, a number of memory technologies based on alternative concepts have been developed and new devices with promising performance have been demonstrated. In that context, substantial effort has been directed towards the development of nanocrystal or quantum dot (QD) nonvolatile memories (NVM) because of their compatibility with CMOS technology and more recently, their potential for flexible electronics applications. The QDs act as discrete charge storage nodes allowing exploitation of quantum effects and device scaling for the realization of memory devices that operate at lower voltages and higher speeds compared to conventional flash without compromising the criterion of nonvolatility. However, both long charge retention and fast operation at low voltages have not been met at the moment. Various approaches have been proposed to successfully combine low-voltage fast operation with long data retention such as the work function engineering. This can be achieved by forming semiconductor QDs exhibiting negative conduction band offset with respect to the substrate such as III-N QDs. The last three years we have demonstrated GaN QD memory capacitors with true NVM retention characteristics at room temperature utilizing Molecular Beam Deposition (MBD). These results were accompanied by comprehensive transmission electron microscopy (TEM) studies.

This year we have focused our efforts on the evolution of GaN QDs formed by MBD on thin SiO_2 layers and performed systematic studies on the performance of memory capacitors using such QDs embedded in SiO_2. More specifically, GaN-QDs were prepared by exposure of the SiO_2 surface to the gallium beam, under simultaneous irradiation with an active nitrogen flux produced by the RF-plasma nitrogen source, and subsequent annealing (ripening) of the deposited layer. In all cases deposition took place under nitrogen-rich conditions (the active nitrogen species arrival rate was higher that the corresponding one for Ga atoms). The deposited GaN amount was controlled by the Ga flux and the deposition time. The GaN dose was measured in equivalent monolayers (MLs) of epitaxial GaN and samples with 5, 8, 10, 14 and 18 MLs were fabricated. TEM examinations revealed that the size of QDs is increased up 10 MLs while for 14 and 18 MLs a continuous polycrystalline GaN layer is formed. The memory windows obtained from C-V measurements (1 MHz) follow the QDs size (Fig.3L) while hole-injection and subsequent hole-trapping was not detected. Incremental step pulse programming operation of the above devices is presented in Fig.3

(right). The programming window of devices with the smallest QDs exhibits no saturation even after application of very high pulse height.

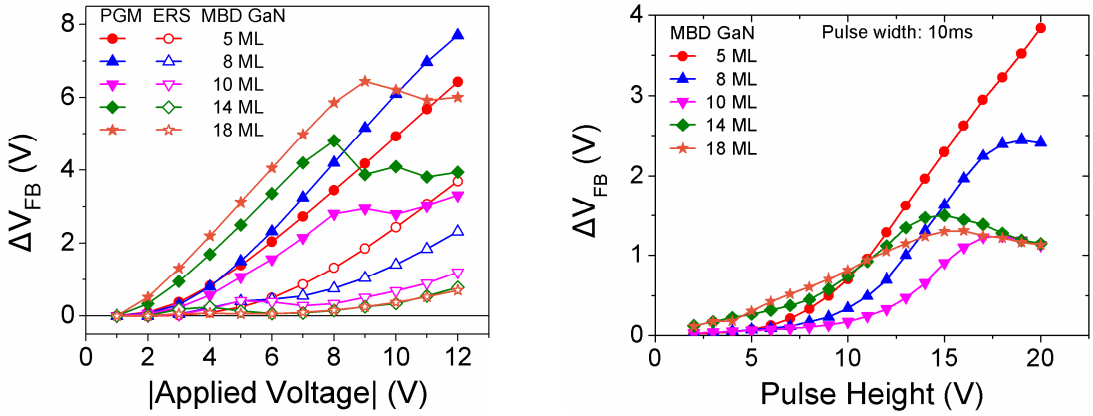

Fig. 3. *Flat-band voltage (ΔV_{FB}) shift obtained from the hysteresis of bi-directional C-V (1 MHz) measurement characteristics (Left) and under pulsed conditions (Right).*

D. Front-end processing for Ge MOS technology

N. Poulakis, V. Ioannou-Sougleridis, P. Normand, P. Dimitrakis, A. Dimoulas[1], E. Simoen[2], D. Skarlatos[3], M. Bersani[4], M. Barozzi[4], D. Giubertoni[4]
[1]*Department of Materials Science NCSR 'Demokritos'*
[2]*Physics department University of Patras*
[3]*IMEC, Kapeldreef 75, B-3001 Leuven, Belgium*
[4]*CMM-Irst, Fondazione Bruno Kessler, Trento, Italy*

High mobility substrates such as strained Si, SiGe and Ge are considered as an alternative to the severe limitations (especially in terms of drive current) in MOSFET performance scaling. Compared to Si, Ge substrates are particularly attractive because not only their higher carrier mobility but also the lower thermal budget required for processing. However, Ge front end technology faces two main problems: The surface passivation of n-channel MOSFET and the formation of n+/p junction diodes at low thermal budgets due to the fast diffusion of n-type dopants. Here, our research objectives are twofold: A) Fabrication of high-k dielectrics (HfO_2, ZrO_2 and $Al2O_3$) on Ge substrates and characterization of the Ge/dielectric interfaces. Significant part of this work is directed towards examining the influence of nitrogen incorporation on the electrical properties of the Ge-dielectric interface. For this purpose nitrogen is introduced into the Ge substrate by ion implantation and subsequently driven to the surface by annealing. Diffusion issues of nitrogen in Ge are of great importance since the control of the Ge-dielectric interface requires knowledge of the nitrogen concentration at the surface. B) The second objective of our activities is the development of junction diodes on Ge substrates at temperatures lower than 400 ^{o}C. Our approach for fabricating such n^{+}/p Ge diodes is based on platinum-assisted-dopant activation. A 50 nm-thick Pt layer is first deposited on top of phosphorus or boron-implanted selected Ge regions, followed by annealing within the range of 300-350^{o}C. The end result is the formation of a junction diode with high forward drive current and acceptable levels of reverse leakage currents. Part of these activities is supported by the University of Patras project "Karatheodory-2009, Project C906 "Front-End Processes for Germanium MOS applications" (1/2/2010-30/9/2013).

This year, we concentrated our efforts on: (a) Detailed study of the electrical properties of Al_2O_3–Ge interface using both n and p type Ge substrates, at room and low temperatures. (b) Study of the nitrogen diffusion in Ge. (c) Study the diodes reverse characteristics at room and low temperatures to separate the bulk and periphery contributions of the current and capacitance characteristics and thereby, to determine the diffusion current, the generation lifetime and the recombination lifetime as a function of temperature.

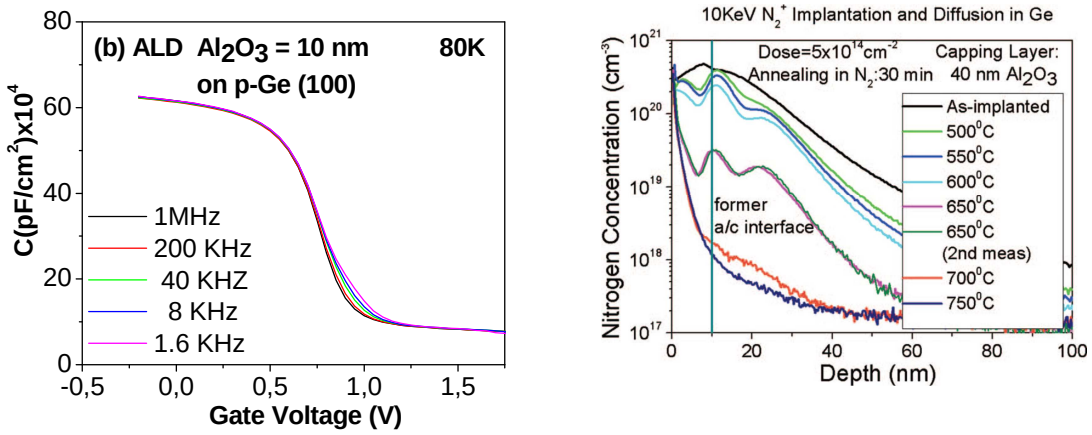

Fig. 4. *(a) C-V characteristics at 80K of Pt/Al_2O_3/p-Ge MOS capacitors with Al_2O_3 deposited at 300◦C within the frequency range 1 MHz-1.6 kHz showing limited frequency dispersion. (b) Nitrogen depth profiles after 10 keV - 5×10^{14} cm^{-2} N_2^+ implantation in Ge and subsequent furnace annealing.*

E. Si nanocrystals in thin SiO_2 layers by plasma-immersion ion-implantation

P. Normand, P. Dimitrakis, V. Ioannou-Sougleridis, E. Kapetanakis[1], F. Torregrosa[2], Y. Spiegel[2], C. Bonafos[3], G. Ben Assayag[3], A. Slaoui[4]

[1]*Department of Electronics, Technological Educational Institute of Crete (GR)*
[2]*Ion-Beam-Services, Peynier (FR)*
[3]*CEMES-CNRS, Toulouse (FR)*
[4]*InESS-CNRS, Strasbourg (FR)*

Six years ago, we initiated research activities aiming at the development of a new Si-nanocrystal (Si-NC) synthesis route based on the plasma-immersion ion-implantation (PIII) technique. These activities were conducted in collaboration with CEMES/CNRS and one French SME (Ion Beam Services, IBS) in the framework of a bilateral French-Greek Project (EPAN. M.4.3.6.1E). While more research work was needed to provide reliable fabrication processes, the basic conditions required for the PIII-assisted synthesis of Si-NCs in SiO_2 thin films were established. The last three years, the R&D PIII activities conducted at IBS and CNRS have recently conducted to the realization of Si-NCs 2D-arrays in SiO_2 matrices. Last year a new framework between IBS, three CNRS Institutes (CEMES, CIMAP, InESS) and IMEL/NCSRD has been established (Confidentiality Agreement June 30th 2011) to evaluate and optimize the PIII-produced-Si-NCs materials for the purpose of their exploitation in Flash-type memory devices or other emerging areas like NC solar cells. Our team is in charge of the production of Si wafers with ultra-thin thermally grown SiO_2 layers, is involved in the post-PIII processing steps and is responsible for the fabrication, electrical characterization and memory testing of the produced Si-NC dielectrics.

In 2002, the successful fabrication of two-dimensional Si-NCs arrays in thin SiO_2 films using PIII and subsequent rapid thermal annealing was announced at the IIT's conference. The effect of plasma and implantation conditions on the structural and electrical properties of the produced NC-SiO_2 layers was reported with emphasis on the advantages/disadvantages of the PIII technique compared to the conventional low-energy ion implantation technique. As in the case of the latter technique, we demonstrated that a fine tuning of the NCs characteristics (position, average size and surface density) is possible for the PIII route by optimizing the nominal oxide thickness and implantation energy and dose. Finally, electrical characterization of MOS devices revealed that the PIII-produced-Si NC structures were appealing for memory applications.

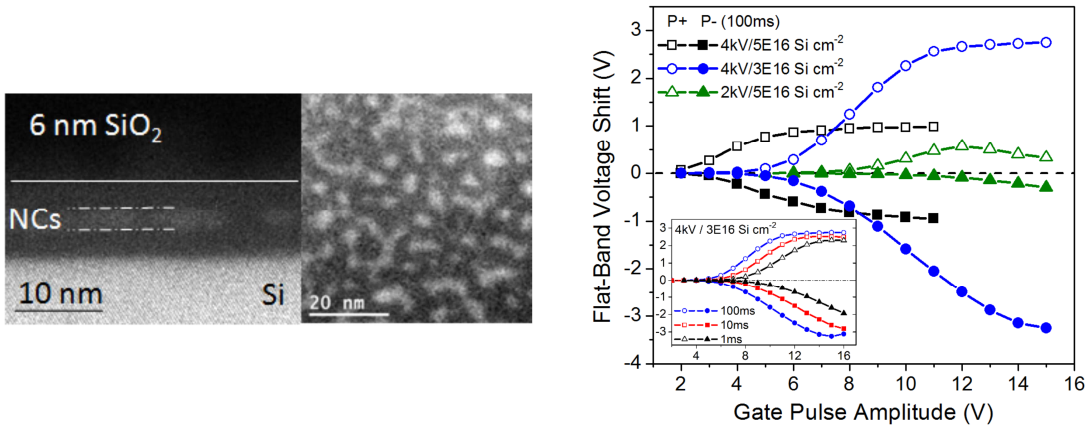

Fig. 5. *(Left) Cross-sectional and plan-view EFTEM observations (CEMES/CNRS) of 6nm-thick SiO_2 implanted at 4kV for $5x10^{16}$ cm^{-2} with $SiF_4/SiH_4/H_2$ based pulsed plasma and annealed at 1050°C for 1 minute. (Right) Flat-band voltage shift of PIII-processed samples as a function of the applied (positive and negative) gate pulse voltage of 100ms duration. Inset: Flat-band voltage shift of a 4kV / $3x10^{16}$ Si cm^{-2} sample as a function of the applied gate pulse voltage for pulse durations of 1, 10 and 100ms.*

PROJECT OUTPUT in 2012

Publications in International Refereed Journals

1. *Influence of atomic layer deposition chemistry on high-k dielectrics for charge trapping memories,*
   N. Nikolaou, P. Dimitrakis, P. Normand, V Ioannou-Sougleridis, K. Giannakopoulos, K. Mergia, K. Kukli, J. Niinistö, M. Ritala, M. Leskelä
   Solid-State Electronics 68, 38-47 (2012)
2. *Extraction of the characteristics of Si nanocrystals by the charge pumping technique,*
   R. Diaz, J. Grisolia, G. BenAssayag, S. Schamm-Chardon, C. Castro, B. Pecassou, P. Dimitrakis, P. Normand
   Nanotechnology 23 (8), Issue 8, AN 085206 (2012).
3. *Si and Ge nanocrystals for future memory devices (Review),*
   C. Bonafos, M. Carrada, G. Benassayag, S. Schamm-Chardon, J. Groenen, V. Paillard, B. Pecassou, A. Claverie, P. Dimitrakis, E. Kapetanakis, V. Ioannou-Sougleridis, P. Normand, B. Sahu, A. Slaoui
   Materials Science in Semiconductor Processing 15, 615-626 (2012)
4. *Implantation energy effect on photoluminescence spectroscopy of Si nanocrystals locally fabricated by stencil-masked ultra-low-energy ion-beam-synthesis in silica,*
   R. Diaz, C. Suarez, A. Arbouet, R. Marty, V. Paillard, F. Gloux, C. Bonafos, S. Schamm-Chardon, J. Grisolia, P. Normand, P. Dimitrakis, G. Benassayag
   Nuclear Instruments and Methods in Physics Research, Section B: Beam Interactions with Materials and Atoms 272, 53-56 (2012).
5. *Interfacial properties of ALD-deposited Al_2O_3/p-type germanium MOS structures: Influence of oxidized Ge interfacial layer dependent on Al_2O_3 thickness,*
   M. Botzakaki, A. Kerasidou, L. Sygellou, V. Ioannou-Sougleridis, N. Xanthopoulos, S. Kennou, S. Ladas, N.Z. Vouroutzis, Th. Speliotis, D. Skarlatos
   ECS Solid State Letters 1, P32-P34 (2012).
6. *Conduction mechanisms in tungsten-polyoxometalate self-assembled molecular junctions,*
   D. Velessiotis, A.M. Douvas, P. Dimitrakis, P. Argitis, N. Glezos
   Microelectronic Engineering 97, 150-153 (2012)
7. *Nitrogen implantation and diffusion in crystalline Ge: Implantation energy, temperature and Ge surface protection dependence,*
   D. Skarlatos, M. Bersani, M. Barozzi, D. Giubertoni, N. Z. Vouroutzis and V. Ioannou-Sougleridis
   ECS J. Solid State Science and Technology 1, P315-P319 (2012)

Published Conference Proceedings

1. *GaN quantum dots as charge storage elements for memory devices,*
   P. Dimitrakis, P. Normand, C. Bonafos, E. Papadomanolaki, E. Iliopoulos
   Materials Research Society Symposium Proceedings Vol. 1430, 29-34 (2012).
2. *SONOS memory devices with ion beam modified nitride layers,*
   D. Simatos, P. Dimitrakis, V. Ioannou-Sougleridis, P. Normand, K. Giannakopoulos, B. Pecassou, G. BenAssayag
   Materials Research Society Symposium Proceedings Vol. 1430, 35-40 (2012)
3. *Resistive switching memory using titanium-oxide nanoparticle films,*
   E. Verrelli, D. Tsoukalas, P. Normand, N. Boukos, A.H. Kean
   Proceedings of the European Solid-State Device Research Conference 2012, Article number 6343382, 258-261 (2012).

International Conference Presentations – Invited Talks

1. *GaN quantum dots as charge storage elements for memory devices,*
   P. Dimitrakis, P. Normand, C. Bonafos, E. Papadomanolaki, E. Iliopoulos
   MRS 2012 Spring Meeting, Symposium E, April 9-13, San Francisco, CA, USA
2. *SONOS memory devices with ion beam modified nitride layers,*
   D. Simatos, P. Dimitrakis, V. Ioannou-Sougleridis, P. Normand, K. Giannakopoulos, B. Pecassou, G. BenAssayag
   MRS 2012 Spring Meeting, Symposium E, April 9-13, San Francisco, CA, USA
3. *The effect of oxygen source in atomic layer deposited Al_2O_3 as blocking oxide in MANOS memory capacitors,*
   N. Nikolaou, V. Ioannou-Sougleridis, P. Dimitrakis, P. Normand, D. Skarlatos, Th. Speliotis, K. Kukli, J. Niinistö, M. Ritala, M. Leskelä
   E-MRS 2012 Spring Meeting, Symposium L, May 14-18, Strasbourg, France
4. *GaN quantum dots for nano-floating memory devices,*
   P. Dimitrakis, P. Normand, C. Bonafos, E. Papadomanolaki, E. Iliopoulos
   E-MRS 2012 Spring Meeting, Symposium L, May 14-18, Strasbourg, France
5. *Atomic layer deposition of high-k dielectrics for flash memories,*
   N. Nikolaou, P. Dimitrakis, P. Normand, V. Ioannou-Sougleridis, K. Giannakopoulos, K. Mergia, K. Kukli, J. Niinistö, M. Ritala, M. Leskelä
   12th International Conference on Atomic Layer Deposition, ALD 2012, June 17-20, Dresden, Germany
6. *Fabrication of Si nanocrystals in thin SiO_2 layers by Plasma Immersion Ion Implantation followed by RTA; Application to flash memories,*
   Y. Spiegel, C. Bonafos, A. Slaoui, F. Torregrosa, J. Groenen, S. Bhabani, G. Ben-Assayag, P. Normand
   19th International Conference on Ion Implantation Technology, ITT 2012, June 25-29, Valladolid, Spain
7. *Study of the ALD-deposited Al_2O_3/Germanium interface,*
   S. Ladas, M. Botzakaki, A. Kerasidou, N.Z. Vouroutzis, N. Xanthopoulos, L. Sygellou, S. Kennou, V. Ioannou-Sougleridis, Th. Speliotis, S.N. Georga, C.A. Krontiras, D. Skarlatos
   EDS 2012, June 24-29, Thessaloniki, Macedonia, Greece
8. *Diffusion of implanted oxygen in germanium,*
   D. Skarlatos, M. Bersani, M. Barozzi, D. Giubertoni, N. Z. Vouroutzis, V. Ioannou-Sougleridis
   EDS 2012, June 24-29, Thessaloniki, Macedonia, Greece.
9. *Quantum-dots for memory applications* (Invited Talk),
   P. Dimitrakis, P. Normand, V. Ioannou-Sougleridis, C. Bonafos, G. BenAssayag, E. Iliopoulos
   E-MRS 2012 Fall Meeting, Symposium H, September 17-21, Warsaw, Poland
10. *A combination of stencil-masked and low-energy ion implantation for a local synthesis of silicon nanocrystals in ultrathin SiO_2,*
    R. Diaz, J. Grisolia, B. Pecassou, P. Dimitrakis, P. Normand, L. Ressier, , C. Constancias, J. Brugger, G. Benassayag
    38th International Conference on Micro and Nano Engineering (MNE 2012), September 16-20, Toulouse, France
11. *Current-transport studies of metal/organic/metal diodes based on triphenylsulfonium salts addition in a semi-conducting polymer matrix,*
    S. Kazazis, D. G. Georgiadou, P. Dimitrakis, P. Normand, P. Argitis
    5th International Conference on Micro - Nanoelectronics, Nanotechnologies and MEMS, October 7-10, 2012, Heraklion, Crete, Greece
12. *Photoluminescence study of Si nanocrystals embedded in SiO_2 matrixes,*
    E. Verrelli, A. Kontos, I. Raptis, P. Dimitrakis, P. Normand, D. Tsoukalas

5th International Conference on Micro - Nanoelectronics, Nanotechnologies and MEMS, October 7-10, 2012, Heraklion, Crete, Greece

13. *GaN QDs embedded in silicon oxide for charge-storage applications,*
P. Dimitrakis, P. Normand, C. Bonafos, E. Papadomanolaki, E. Iliopoulos
5th International Conference on Micro - Nanoelectronics, Nanotechnologies and MEMS, October 7-10, 2012, Heraklion, Crete, Greece
14. *Top electrode protrusions for the forming free operation of resistive memories based on metal-oxide nanoparticles,*
E. Verrelli, D. Tsoukalas, P. Normand, N. Boukos, A.H Kean
5th International Conference on Micro - Nanoelectronics, Nanotechnologies and MEMS, October 7-10, 2012, Heraklion, Crete, Greece
15. *Group IV Semiconductor Quantum-dot Non-volatile Memories (Invited Talk),*
P. Dimitrakis, P. Normand, V. Ioannou-Sougleridis, G. BenAssayag, C.Bonafos
MRS 2012 Fall Meeting, Symposium DD, November 25-30, Boston, USA.
16. *Electrical Properties of Axially Modulated p-n Si Nanowires,*
A. Smyrnakis, A. Zeniou, E. Gogolides, P. Normand, P. Dimitrakis
MRS 2012 Fall Meeting, Symposium DD, November 25-30, Boston, USA.

National Conference Presentations

$SiO_2/Si_3N_4/Al_2O_3$ memory capacitors: effect of oxygen source in ALD chemistry,
N. Nikolaou, V. Ioannou-Sougleridis, P. Dimitrakis, P. Normand, D. Skarlatos, K. Kukli, J. Niinistö, M. Ritala, M. Leskelä
XXVIII Greek conference of Solid State Physics, 23-26 September 2012, Patras, Greece

Edition of Conference Proceedings

Materials and Physics of Emerging Nonvolatile Memories,
Y. Fujisaki, P. Dimitrakis, E. Tokumitsu, M.N. Kozicki
Mater. Res. Soc. Symp. Proc. Vol. 1440, Cambridge, 2012

Conference and Workshop Organization

Materials and Physics of Emerging Nonvolatile Memories,
Y. Fujisaki, P. Dimitrakis, E. Tokumitsu, M.N. Kozicki
Symposium E, MRS Spring Meeting 2012, 9-13 April, San Francisco, CA, USA

PROJECT II.3
MOLECULAR MATERIALS AS COMPONENTS OF ELECTRONIC DEVICES

Project Leader: N.Glezos

Permanent Researchers: P.Argitis, P.Normand

Permanent Scientific Staff: A. Douvas

Post Doctorals Scientists: D.Velessiotis

PhD Students: A.Balliou

External Collaborators: Jiri Pfleger, Stan .Nespourek, Samrana Kazim, David Rais (Czech Academy of Sciences), Ulf Soderval, Bengt Nilsson (Chalmers University)

OBJECTIVES

Our research field focuses mainly on the investigation of functional molecules as core components of hybrid molecular-semiconductor and molecular-metal devices. Dealing with molecular electronic devices requires understanding of the electrical properties from atomistic to mesoscopic scale, precise control of the morphology of the molecular structures and the involved interfaces, as well as stability and device variability reduction. Hybrid devices on semiconducting and/or metal surfaces are a test bed for molecular layers, while they can be directly exploited for fast switching, diode and memory applications as well as for chemical or bio-sensors. By selecting the device topology it is possible to highlight electronic and electrical properties of the molecular components, realize devices (exploiting self-assembly and bottom-up fabrication techniques) that will function as non-volatile memories, switches or electrically gated q-bit devices and realize more complex structures such as hybrid networks that could function via bootstrapping heuristics. Specific objectives are:

- To investigate the potential of molecular materials to be used as active components in molecular devices e.g. as switching or memory elements.
- to develop consistent evaluation methods based on the electronic transport properties at the nano- level for the characterization of molecular few layered systems as part of hybrid devices.
- to produce physical parameters (film thickness, surface molecular density, contact potential) that could be cross-checked with other surface characterization methods
- To develop techniques for thin film deposition and characterization of molecular materials.

FUNDING

- Greek-Czech Cooperation Project, 2011-2013
- Greek-Sloval Cooperation Project, 2012-2014

MAIN RESULTS in 2012

The main results obtained in 2012 within the different tasks of the project are given below.

1. Study of conduction mechanisms in molecular junctions made of tungsten-polyoxometalate self-assembled monolayers and bilayers

D. Velessiotis, A.M. Douvas, P. Dimitrakis, P. Argitis, N. Glezos

Polyoxometalates are inorganic salts or acids in which the anion is a complex oxide of transition metals. The anion is organized in a well-defined, closed-pack form, with a certain number of metal-oxygen polyedra surrounding one or more heteroanions. They are highly reactive -yet stable- substances, thus having a plethora of diverse applications. It is exactly this combination of wealthy chemistry/photochemistry, in other words the ability of polyoxometalate anions to exchange electrons with their environment, with their structural stability and well-defined dimensions that has led the research community to consider polyoxometalates as potential candidates for use in molecular electronic and photoelectronic applications.

The next step with the study of 12-phosphotungstic acid (POM) self-assembled materials, taken by our team in 2012, was the comparison between the 3-Aminopropyl triethoxysilane (APTES)/POM monolayer (1L) material junctions and the APTES/POM/12-diaminodoecane (DD)/POM bilayer (2L) material junctions for different temperature conditions (Fig 1). In general, it was found that the conduction mechanisms which apply for the 1L material junctions, were applying for the 2L material junctions too. This means that for lower applied fields (~1.5MV/cm or less) or below a certain temperature (T_t), tunneling was the dominant conduction mechanism, while for higher applied fields and high temperatures a simple (Arrhenius) hopping mechanism was followed by our system (Fig 2).

While qualitatively the two materials behaved in the same way, there were significant differences in the quantitative parameters of the conduction mechanisms concerned. In the hopping regime, the activation energy (E_a) of the 1L junctions was confirmed to be in the neighborhood of 80meV, more specifically 85meV for the 50nm-distant and 76meV for the 75nm-distant junctions. The 2L junctions presented much lower values of E_a in these two distances, namely 55meV and 41meV, respectively. Moreover, the values of T_t were different for the two materials; more specifically T_t was 150K for the 1L and 120K for the 2L junctions. In the tunneling regime, the value of the mean tunneling barrier (φ) obtained (by the Fowler-Nordheim representation of the current-voltage characteristics – see Fig. 3), was significantly lower in the case of 2L material (330meV) than that already obtained for the 1L material (500meV – more or less equal to the expected difference between the Au Fermi level and the POM LUMO).

The above results expressed quantitatively the general idea (already presented before) that POM anions can be considered as a group of regularly arranged semiconducting islands that were placed between the two Au electrodes. It is clear that increased presence of POM anions favored conductivity of the studied device; this was clearly revealed in the lower values of E_a, T_t and φ obtained in the 2L junctions.

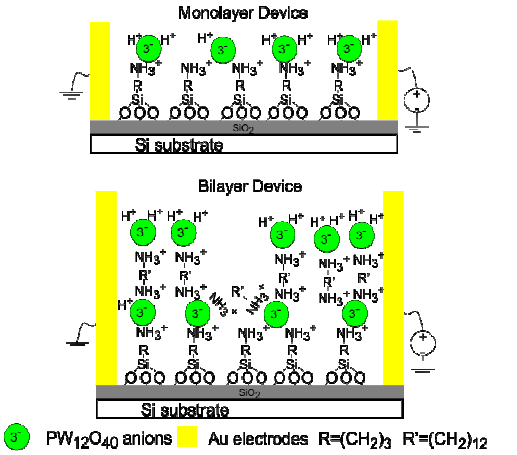

Fig. 1. *Single and double layer junctions' schematics (not in scale)*

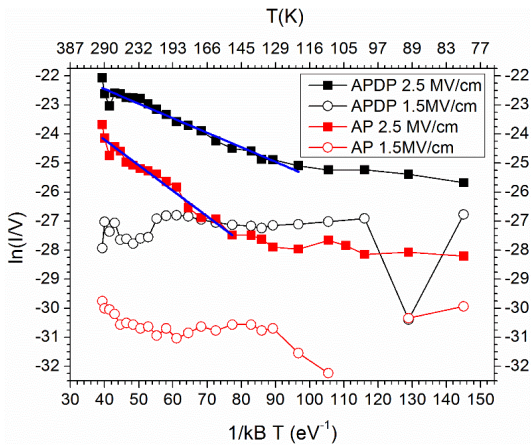

Fig. 1. *Arrhenius plots of single (AP) and double layer (APDP) junctions for two different values of applied field. The blue linear fitting lines produce the E_a values provided in text.*

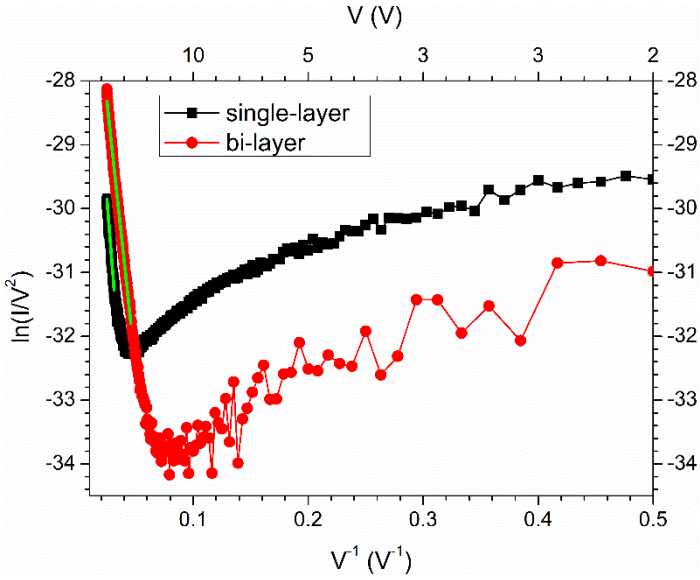

Fig. 2. *Fowler-Nordheim representation of th100nm-distant junctions for the single and bilayer materials. The solid green fitting lines are used to produce the tunneling barrier values referenced in text*

2. Utilization of tungsten polyoxometalate molecules (POMs) as active nodes for dynamic carrier exchange in hybrid MIS structures

A. Balliou, A. M. Douvas, P. Normand, P. Argitis, N. Glezos

In this work we study the utilization of tungsten-polyoxometalate molecules (POM) as active nodes for potential switching and/or fast writing memory applications. The active molecules are being integrated in hybrid-layer MIS structures, which serve as an investigation/optimization precursor towards the design of more sophisticated devices.

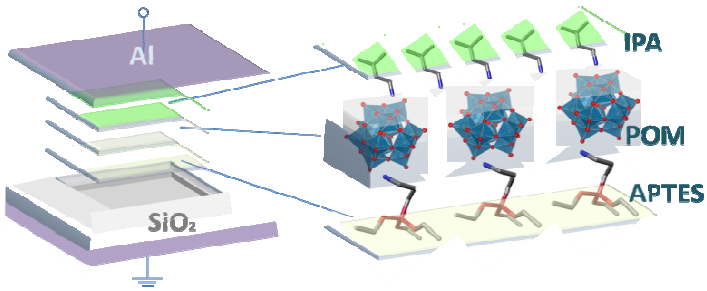

Fig.4. *Planar MIS structure and incorporated molecular layers in the active region. From bottom to top: APTES (3-aminopropyl triethoxysilane) , forming an ordered molecular template on SiO2, POM anion cage molecules self-arranged on top via electrostatic interactions in aqueous environment and IPA (iso-pentylamine) oligolayer serving as passivation coating, gate dielectric and oxidation prohibitor from the metal gate.*

The charging ability as well as the electronic structure of the molecular layer is probed by means of electrical characterization, namely: capacitance-voltage characteristics, quasi-static and dynamic current-voltage measurements, as well as transient capacitance measurements under step voltage polarization. The measurements are performed in a wide range of temperatures (80K-300K) in order to discriminate between the different transport mechanisms.

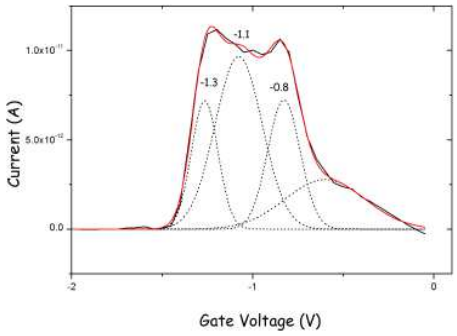

Fig. 5. *Peak analysis of a typical peak of the POM islands' charging current at T=240 K resulting in a state triplet. The measurements were performed in dark faraday cage under ramp rate voltage excitation (dynamic type excitation) and forward sweep. The ramp rate was set at 0.25 V/s.*

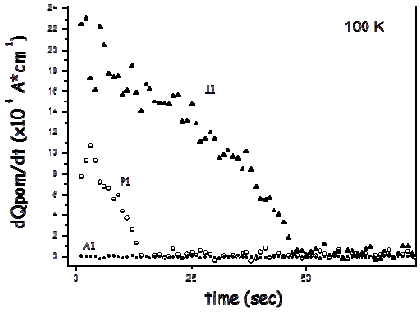

Fig. 6. *Rate of change of the space-charge region generated charge versus time, for the molecular layer incorporating MIS devices in all fabrication steps in T=100K. The Qpom quantity in the y axis is the charge that is being trapped and de-trapped within the molecular epilayers. Curve A1 concerns only APTES functionalization, P1 is the device after POM incorporation and I1 is the final device after passivation of the functional POM layer with the IPA molecular oligolayer.*

It is argued that the transient current peaks observed are manifestations of dynamic carrier exchange between the gate and the POM nano-islands, while the transient C(t) curves under conditions of molecular charging can supply information, via a modified Zerbst equation, for the rate of change of the charge that is being trapped and de-trapped within the molecular epilayer.

The presence of the charged POM epilayer is expected to reduce the minority-carrier lifetime (τ_{geff}) due to the net increase of the recombination rate that is introduced from the POM-controlled displacement current. This effect can be advantageous in high-speed applications when a short lifetime to achieve fast charge storage time is a desirable feature.
Structural characterization via surface and cross sectional SEM topographies as well as AFM, SE, UV and FTIR spectroscopies facilitate the extraction of accurate electronic structure characteristics and open the path for the design of new devices with on-demand- tuning of their interfacial properties via controlled modification of the POM layer.

3. Formation of Au nano-particle/CuPcSu ligands complex networks

A. Balliou, S. Kazim, N.Glezos, J.Pfleger

We fabricated planar devices based on nano-dimensional components, namely semiconducting conjugated oligomers and metal nanoparticles (NPs) and studied their electronic transport properties. Spherical gold (Au) NPs were linked by means of copper 3-diethylamino-1-propylsulphonamide sulfonic acid substituted phthalocyanine (CuPcSu) molecules to form a network confined between Au nanodistant electrodes. The fabrication of the network was realized via three different approaches: (a) liquid phase approach: Au NPs (av. diameter ~17 nm) prepared as hydrosol via chemical reduction were functionalized with CuPcSu and drop cast on the substrate, (b) self-assembling technique: The SiO2 surface was chemically modified with a stable, positively charged template molecule (3-aminopropyl triethoxysilane, APTES) and the CuPcSu surface-functionalized Au NPs were subsequently adsorbed on the surface driven by electrostatic-type forces and (c) solid state approach: Ultra-fine (av. diam. ~ 1.5 nm) Au NPs were prepared by thermal evaporation and inter-particle gaps were filled with CuPcSu ligands in a subsequent step. The above systems were confined between Au nano-electrodes with inter-electrode distances of 25, 50 and 75 nm fabricated on n-Si/SiO_2 substrate via e-beam lithography.

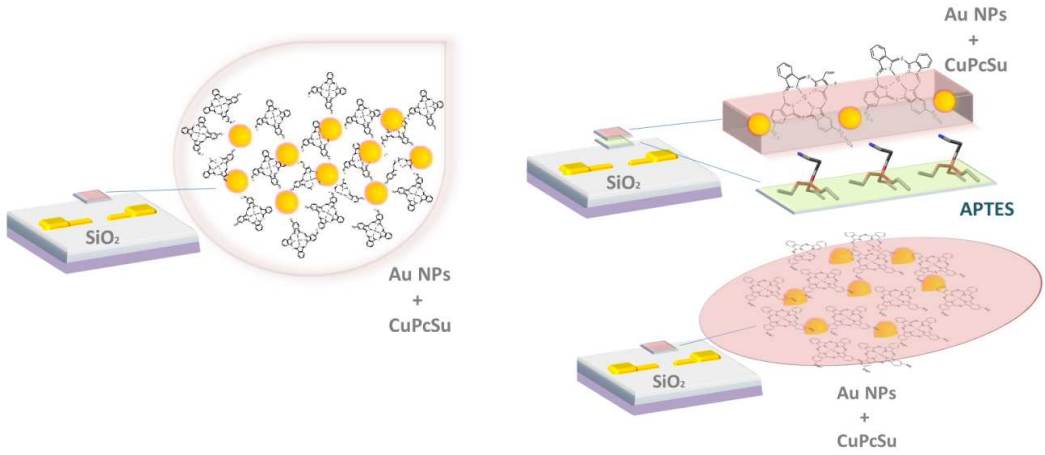

Fig. 7. *Schematics of the realized composite networks. Au/CuPcSu complexes fabricated via: (a) liquid phase approach, (b) self-assembling technique and (c) solid state approach.*

The conduction mechanisms of these 2D systems were studied using quasi-static and dynamic voltage-current measurements in the 78K-300K temperature range. It was possible to discriminate between various transport mechanisms typical for such structures (i.e. tunnelling and hopping), to evaluate conduction thresholds and to reveal charging effects involving few electrons, at lower temperatures. The interpretation was assisted by AFM, FE-SEM and TEM imaging techniques. The system of evaporated NPs (case c) resulted in formation of closely-packed linked NP networks and yielded the best stability and results' reproducibility.

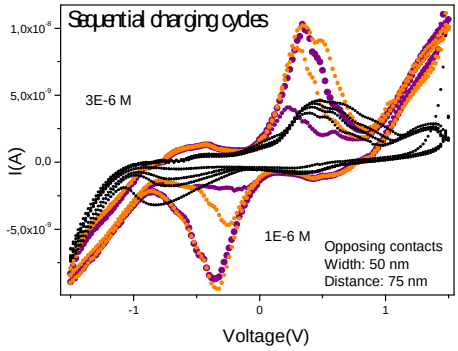

Fig. 8. *Left: Liquid phase approach -- Few electron charging effects under sequential voltage cycles for 75 nm distant junctions of opposing electrodes. The color curves were performed at low CuPcSu concentration (1E-6 M), while the black ones at higher concentration (3E-6 M). The intensity of the current peaks increases upon repetition of measurement cycles for both cases. All voltage cycles are performed from -2 to 2 V and back under quasi-static double staircase excitation.*

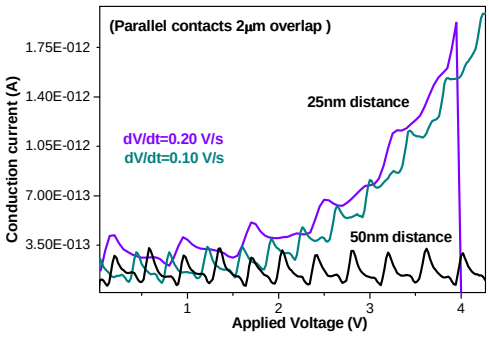

Fig. 9. *Solid state approach -- Resonant charge transport through the molecule-NP chains during dynamic I-V measurements in the form of ramp rate excitation. Two contact distances, namely 25 and 50 nm are presented. The measurements were held out at 78 Kelvin.*

PROJECT OUTPUT in 2012

Conference Presentations

1. *On the Electrical Behavior of Planar Tungsten Polyoxometalate Self-Assembled Mono- and Bi-Layer Junctions,*
   D. Velessiotis, A. M. Douvas, P. Dimitrakis, P. Argitis, N. Glezos
   Frontiers in Electronic Materials (FEM 2012), June 17 to 20, Aachen, Germany
2. *Charging Effects and Electron Transport Phenomena associated with the redox properties of self-assembled Polyoxometalate Molecules*,
   A.Balliou, A.Douvas , D.Velessiotis, V.Ioannou-Sougleridis, P.Normand, P.Argitis, N.Glezos,
   Frontiers in Electronic Materials (FEM 2012), June 17 to 20, Aachen, Germany
3. *Study of the transport mechanisms and charging effects in nanodevices based on inorganic polyoxometalate molecules,*
   38th International Conference on Micro and Nano Engineering (MNE 2012), September 16 to 20, Toulouse, France
4. *Electronic Conduction Mechanisms in Polyoxometalate Seld-Assembled Planar Molecular Junctions,*
   D. Velessiotis, A. M. Douvas, P. Dimitrakis, P. Argitis, N. Glezos
   Materials Today Virtual Conference: Nanotechnology, December 11-13, http://www.materialstoday.com/virtualconference/materials-today-virtual-conference-nanotechnology

PROJECT II.4

COMPUTATIONAL NANOTECHNOLOGY

Project Leader: N. Papanikolaou

PhD Students: E. Almpanis

External Collaborators: N. Stefanou, (University of Athens), Ch. Tserkezis, A. Christofi (PhD students University of Athens), G. Gantzounis, (California Institute of Technology), B. Auguie (Victoria University of Wellington, New Zealand)

OBJECTIVES

Our research is focused on photonics and plasmonics, as well as elastic wave propagation in periodic media. We use multiple scattering methods and in-house-developed simulation software to study optical, elastic and acoustooptic properties in the nanoscale.

MAIN RESULTS in 2012

Chiral plasmonic nanostructres

Artificial plasmonic architectures consisting of either chiral metallic building units or nonchiral metallic nanoparticles arranged in chiral geometries such as pyramids, tetrahedra, helices as shown in Fig. 1, provide unique opportunities to achieve extraordinary optical activity effects, which can be tuned within a wide range from near-infrared to ultraviolet frequencies and offer impressive possibilities, among others, in the design of subwavelength components for polarization-control applications in miniaturized optical devices. Research on chiral plasmonic architectures is at the frontier of nanophotonics also because of potential applications in biology, chemistry, and optics of novel metamaterials. These structures can be realized in the laboratory using modern nanofabrication methods like lithography, or even molecular self-assembly.

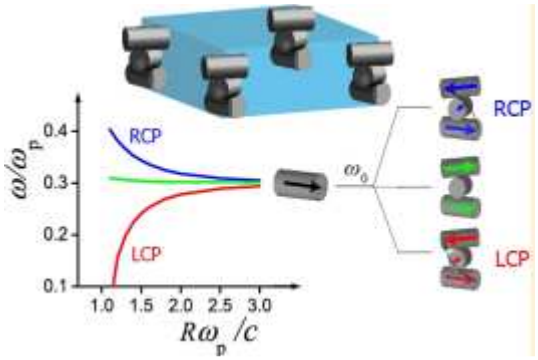

***Fig. 1**: Unit cell of a tetragonal structure with a basis of three mutually twisted metallic nanorods and a schematic view of the formation of hybrid plasmon modes in the three-nanorod helical metamolecule. The bottom left diagram shows the variation of the eigenfrequencies of these modes as a function of the interparticle distance, as obtained by a point-dipole model.*

Plasmonic nanolenses

Plasmonic nanoantennas and nanolenses, consisting of two or more metallic nanoparticles in proximity, have recently attracted much interest due to their ability to produce highly confined electromagnetic fields in the interparticle region, thus leading to enhanced Raman scattering, fluorescence, absorption, and nonlinear effects. Of particular interest are nanolenses consisting of self-similar chains of metallic nanospheres with decreasing radii and separations, as depicted in Fig. 2. When such a nanolens is optically excited, a hot-spot, where the local EM field is enhanced by orders of magnitude, is formed in the region between the two smallest spheres.

Our study shows that the interaction between the hot-spot modes of an isolated nanolens with the Rayleigh–Wood anomalies of the periodic lattice leads to a further enhancement of the local field intensity, which can be controlled by an appropriate choice of the geometrical parameters involved.

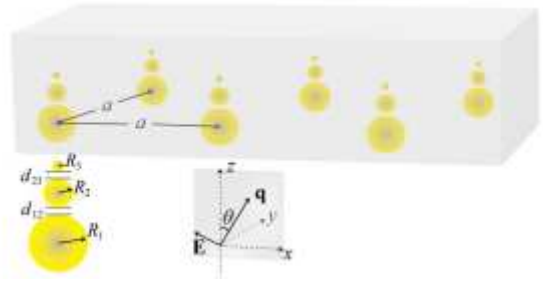

***Fig. 2**: Schematic view of a square lattice of nanolenses in a glass matrix. Each nanolens consists of three silver spheres with decreasing radii R_1 33.8 nm, R_2 13 nm, and R_3 5 nm, and separations d_{12} 7.8 nm and d_{23} 3 nm. The nanolense achieves strong concentration of the electromagnetic field in the region between the two smaller spheres.*

Spontaneous light emission in simultaneous photonic-phononic cavities

It has long been recognized that the spontaneous emission of an excited atom is not an inherent property of the atom but also depends on its environment, since the latter can drastically alter the vacuum fields that drive the excited atom to its ground state. In this respect, enhanced spontaneous emission has been demonstrated inside dielectric multilayer microcavities, slabs, dielectric particles, and waveguides. Recently, there is a growing interest on dynamic photonic structures, controlled by elastic waves, and consequent phenomena. Elastic waves can change the geometry and refractive index of a photonic cavity, and thus modify its optical properties. The interplay between optical and elastic waves is exploited in the emerging field of cavity optomechanics, where the optical pressure of localized light in a cavity produces an elastic wave through mechanical deformation. Additionally, it has been shown that appropriately designed cavities (Fig. 3) that support simultaneously photonic and phononic localized resonant modes, so-called phoxonic cavities, allow for strong nonlinear acousto-optic (AO) interactions. We have theoretically studied the modulation of spontaneous light emission of active centers through elastic waves in multilayer phoxonic structures that support dual photonic-phononic localized modes, in the bulk or at the surface. Our results show that strong dynamic modulation of the spontaneous emission can be achieved through an enhanced acousto-optic interaction when light and elastic energy are simultaneously localized in the same region.

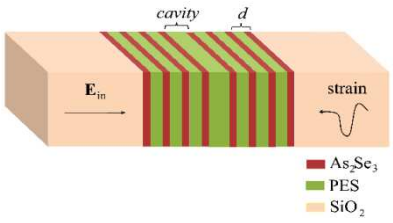

***Fig. 3:** A multilayer dual photonic-phononic cavity structure between two Bragg mirrors. Both electromagnetic and elastic waves (of different frequencies) can be localized inside the cavity to achieve enhanced acoustooptic interaction. Several materials can be used for the multilayers.*

PROJECT OUTPUT in 2012

Publications in International Refereed Journals

1. *Diffractive chains of plasmonic nanolenses: combining near-field focusing and collective enhancement mechanisms,*
   E. Almpanis, N. Papanikolaou, B. Auguié, C. Tserkezis, and N. Stefanou
   Opt. Lett. 37, 4624 (2012)
2. *Tuning the spontaneous light emission in phoxonic cavities,*
   Almpanis, E., Papanikolaou N., Gantzounis, G. and Stefanou N.
   J. Opt. Soc. Am. B, 29, pp. 2567-2574 (2012)
3. *Giant Optical Activity of Helical Architectures of Plasmonic Nanorods,*
   Christofi, A., Stefanou, N., Gantzounis, G., and Papanikolaou, N.
   J. Phys. Chem. C, 116 (31), 16674−16679 (2012)

Published Conference Proceedings

1. *Helical assemblies of plasmonic nanorods as chiral metamaterials,*
   Christofi, A., Stefanou, N., Gantzounis, G., and Papanikolaou, N.
   Proc. of SPIE Vol. 8423, 84230A (2012)
2. *Acousto-optic interaction enhancement in dual photonic-phononic cavities,*
   Papanikolaou, N., Gantzounis, G., Almpanis, E., Stefanou N.
   (2012) Proc. of SPIE Vol. 8425, 84250M

Conference Presentations

1. *Helical assemblies of plasmonic nanorods as chiral metamaterials,*
   Christofi, A., Stefanou, N., Gantzounis, G., and Papanikolaou
   SPIE Photonics Europe, Brussels April (2012)
2. *Acousto-optic interaction enhancement in dual photonic-phononic cavities,*
   Papanikolaou, N., Gantzounis, G., Almpanis, E., Stefanou N.
   SPIE Photonics Europe, Brussels April (2012)
3. *Efficient control of spontaneous light emission by elastic waves,*
   E. Almpanis, G. Gantzounis, I.E. Psarobas, N. Papanikolaou, C. Tserkezis, N. Stefanou, B. Djafari-Rouhani, Y. Pennec, V. Laude, A. Martinez
   E-MRS Strasburg, 14-18 May (2012)
4. *Tuning the spontaneous light emission in phoxonic cavities,*
   E. Almpanis, G. Gantzounis, N. Stefanou, N. Papanikolaou,
   "Son et Lumiere: phononics and photonics at the nanoscale", Les Houches, France, 17-28 September (2012)
5. *Tuning the spontaneous light emission in phoxonic cavities,*
   E. Almpanis, G. Gantzounis, N. Stefanou, N. Papanikolaou
   5th International Conference on Micro-nanotechnologies and MEMS, Crete, Greece, 7-10 October (2012)

PROGRAM III

SENSORS and MEMs

PROGRAM III

SENSORS and MEMs

PROJECTS

- MECHANICAL AND CHEMICAL SENSORS
- ENERGY HARVESTING MATERIALS AND DEVICES
- BIO-MICROSYSTEMS
- THIN FILM DEVICES FOR LARGE AREA ELECTRONICS
- CIRCUITS & DEVICES FOR SENSOR NETWORKS & SYSTEMS
- PHOTONIC CRYSTALS, METAMORPHIC MATERIALS AND NOVEL RF SYSTEMS

PERSONNEL

RESEARCHERS

S. Chatzandroulis, I. Raptis, C. Tsamis, K. Misiakos, D.N. Kouvatsos, H.Contopanagos, E. Gogolides, A. Tserepi, E. Makarona

POST DOCTORAL SCIENTISTS

P. Oikonomou, A. Olzierski, D.C. Moschou

OTHER STAFF UNDER CONTRACT (TECHNICAL PERSONNEL)

A. Botsialas, A. Salapatas

PhD STUDENTS

P. Broutas, G. Niarchos

MSc STUDENTS

M.-I. Georgaki, S. Katsaridis, S. Voulazeris

STUDENTS

T. Kyrasta

PROJECT III.1A
MECHANICAL AND CHEMICAL SENSORS

Permanent Researchers: S. Chatzandroulis, I. Raptis

Post Doctoral Scientists: P. Oikonomou, A. Olzierski

MSc Students: M.-I. Georgaki

Other staff under contract (technical personnel): A. Botsialas

External Collaborators: M. Sanopoulou (Physical Chemistry Depart./IAMPPNM/NCSR Demokritos), D. Goustouridis (TEI of Piraeus), M. Chatzichristidi (Univ. Athens), D. Dimou, S. Katsikas (Prisma Electronics S.A.)

OBJECTIVES

- Development of micromachining processes for the realization of novel chemical and mechanical sensors
- Development of low power silicon sensors based on new materials and new processes
- Design, fabrication and testing of microsystems using silicon based sensors
- Realization of sensors for specific industrial applications with emphasis on medical, food and automotive fields

FUNDING

ALEPOU “Autonomous and integrated system for in-situ and continuous contaminant gases monitoring in industrial environments” Funded by General Secretariat for Research & Technology – 19SMEs2010

MAIN ACTIVITIES in 2012

In 2012 our main activities were focused on the following tasks:

A. Polymer based chemocapacitor arrays
B. Zero-Power colorimetric humidity sensors
C. Capacitive Type Sensors

A. Polymer based chemocapacitor arrays

P. Oikonomou[1], A, Botsialas[1], I. Raptis[1], M. Sanopoulou[2]
[1]Department of Microelectronics, IAMPPNM, NCSR ‘Demokritos’
[2]Department of Physical Chemistry, IAMPPNM, NCSR ‘Demokritos’

In the research field of gas sensors there is an increasing need for low cost and low power consumption devices that are capable of measuring the temperature, the humidity and the gaseous composition of the ambient atmosphere. For this purpose, complete systems are needed where the sensor array, the read-out electronics and the power supply are integrated in the same miniaturized module. A hybrid gas sensing module consisting of (a) 8-polymer coated capacitive sensor array and (b) low power control and read-out electronics was developed, fig 1 and fig 2, aiming at the detection of volatile organic compounds in air.

In chemocapacitors, the swelling of the polymeric film that is induced by sorption of analyte molecules causes a change of the effective dielectric constant of the polymeric layer and thus an increase of the capacitance of the device. In order to improve the sensing performance of the device a software tool aiming at the prediction of chemocapacitor response was introduced.

It is based on experimental determination of the swelling ability of polymeric sensing materials due to the sorption of analytes-extracted data by swelling measurements based on White Light Reflectance Spectroscopy (WLRS)-in conjunction with finite element electromagnetic modeling for the InterDigitated Electrode (IDE) capacitor. The methodology was tested against experimental capacitance measurements in different polymer–vapor analyte systems with very promising results. A typical example of the responses of several polymer coated sensors of the sensor array upon exposure to tetrahydrofuran (THF) vapors in conjunction with the simulated responses according to the applied proposed methodology is illustrated in fig. 3, implying a feasible calculation of the capacitance value of any IDE layout when it is coated with the polymer of interest and also when this polymer-coated IDE is exposed to different vapor concentrations of the target-analyte.

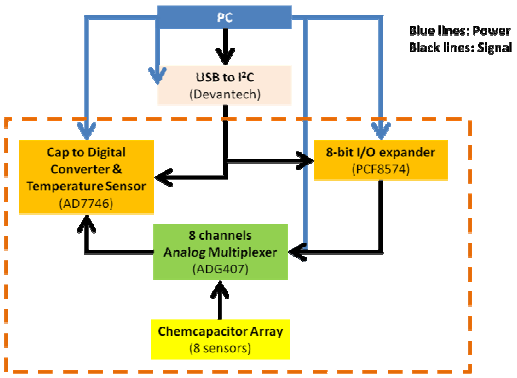

Fig. 1. *Block diagram of the gas sensing module and electronic interface with the PC for the data acquisition and data processing. For wireless data transmission, the USB to I^2C chip will be replaced by a wireless module.*

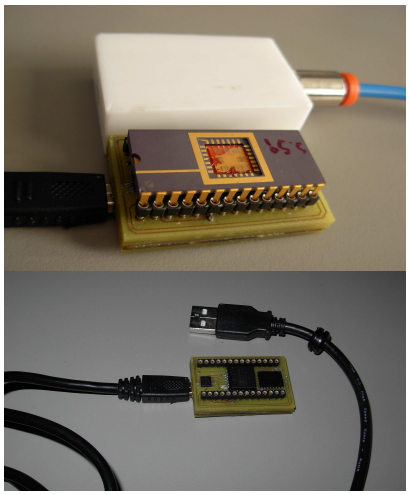

Fig. 2. *Photos from the gas sensing module: (top image) 8-sensor array and electronics and chamber, (bottom image) the read-out and control electronics sub-module.*

Furthermore, temperature effects has been recently evaluated as of critical importance for accurate measurement in real environments and several approaches have been suggested in order to either remove this effect by operating the device at constant temperature or by accurate recording of the temperature during operation of the sensor and compensating for temperature variations. Accurate recording of temperature concurrently to the capacitance signal of the sensors enabled the construction of a temperature (ΔT)-capacitance (ΔC) calibration curve for each sensor. The linear ΔC–ΔT relations were found to depend on the specific polymeric sensing layer, and were then used to demonstrate the importance of the said correction, in Volatile Organic Compounds (VOCs) sensing in humid environment and under relatively unstable temperature conditions. By subtracting the interfering signal of temperature change we can ensuree that the sensors capacitance response upon exposure to certain analyte or mixture of analytes is a result of the sorption capacity of the polymer-coated sensor and not due to temperature variations, fig. 4. This way the sensor array can be used for applications in real environments where the operation temperature is unstable.

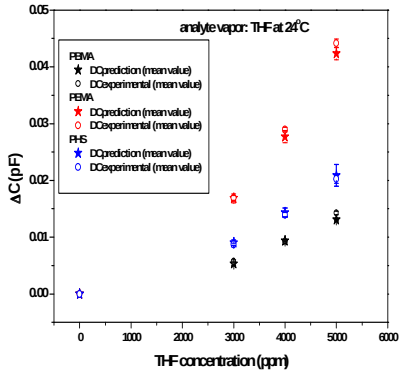

Fig. 3. *Capacitance change of chemocapacitors coated with PBMA, PEMA and PHS layers upon sorption of THF as measured (open points) and as calculated from the modelling approach based on polymer swelling (filled points). The error bars represent standard deviation derived from at least three samples. The agreement between the modelling and the experimental results is very good.*

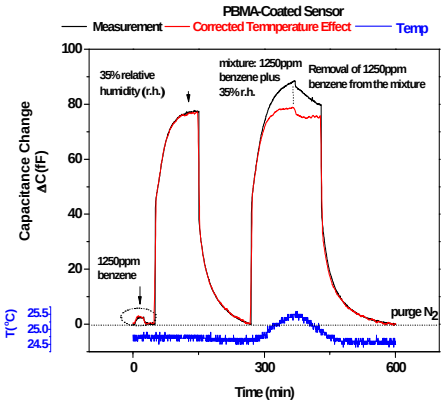

Fig. 4. *Dynamic response of a PBMA-coated sensor to controlled concentrations of water, benzene vapor and their mixture. The temperature is measured with the embedded to the capacitance converter temperature sensor.*

B. Zero-Power colorimetric humidity sensors

M.-I. Georgaki, P. Argitis, N. Papanicolaou[1], I. Raptis[1], M. Chatzichristidi[2]

[1]Department of Microelectronics, IAMPPNM, NCSR 'Demokritos'
[2]Department of Chemistry, University of Athens

One-Dimension Photonic Crystals (1-D PC) is a multilayer stack of two alternating transparent materials with different refractive indices. Such 1-D PC acts as Bragg mirror, fig. 5, and upon illumination with broad-band light a particular reflectance spectrum with narrow-band and high reflectance spectral region is observed whereas all other wavelengths are highly transmitted through the multilayer stack. The optical properties of the 1-D PC depend on film thicknesses, layers' refractive indices etc.

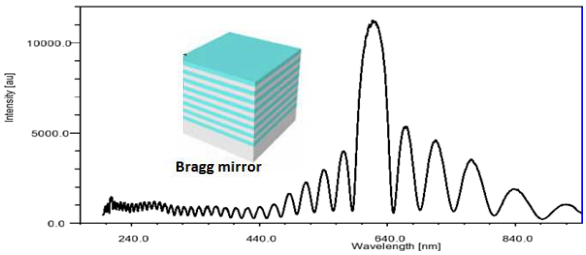

Fig. 5. *Theoretical reflectance spectrum from a Bragg mirror. On the left side a schematically representation of an eight bilayer stack is depicted.*

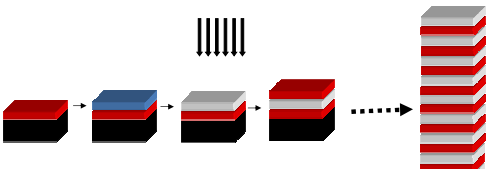

Fig. 6. *Process flow chart for the fabrication of the 1-D polymeric photonic crystal. The PHEMA layers are spin coated and Post Apply Baked while the EPR layers are processed as chemically amplified resists: spin coated, Post Apply Baked, uniformly exposed at DUV and Post Exposure Baked*

A novel 1-D polymeric photonic crystal was designed, fabricated and evaluated as a humidity sensor. The polymeric photonic crystal is consisted of a multilayer stack of sequential hydrophilic (PHEMA: Poly Hydroxy Ethyl MethAcrylate) and hydrophobic (EPR: epoxy based negative tone resist) layers applied using conventional photolithographic steps: spin-coating and DUV exposure, fig. 6. These two polymeric materials are dissolved at different casting solvents which is a prerequisite for the successful deposition of the related layers. The polymeric PCs

were evaluated through dissolution experiments and SIMS measurements revealing very well defined interfaces between the hydrophilic and hydrophobic layers.

During exposure in a humidity environment, the hydrophilic layers of the sensor swell, hence growing its optical path and giving a red-shift of the reflectance peak and consequently a different colour of the device. The colorimetric humidity sensor does not require external power since its sensing ability is based on the reflectance peak shift of the photonic crystal in the visible spectrum (colour change of the sensor).

The reflectance spectra at equilibrium from 0 to 90%RH are illustrated in fig. 7 showing a linear red-shift of the reflectance peak by 62nm. In order to enhance the spectral shift due to humidity the PHEMA film thickness should increase whereas the EPR decrease in order to keep the reflectance peak shift in the visible range. By considering 40nm as the lower thickness limit for reliable and reproducible application through spin-coating of high quality polymeric film, PHEMA film thickness should be 140nm. In fig. 8 the reflectance peak shift for various combinations of PHEMA-Cross-EPR film thickness is illustrated. Film thicknesses have been carefully selected in order that the reflectance peak at nitrogen to be nearly the same for all cases. Clearly the increase of PHEMA film thickness provide of larger reflectance peak shift for the same humidity change.

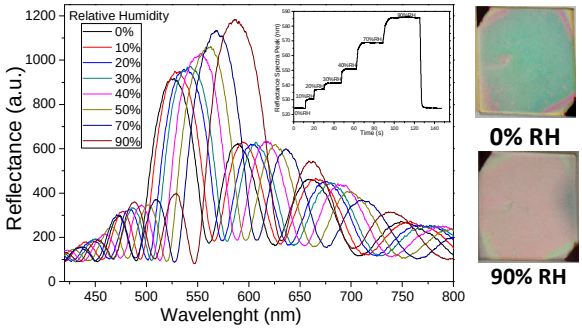

Fig. 7 *Reflectance spectra (raw data) for various humidity concentrations. Increase of humidity level in the environment causes swelling of hydrophilic PHEMA and thus red-shift of the reflectance peak.*

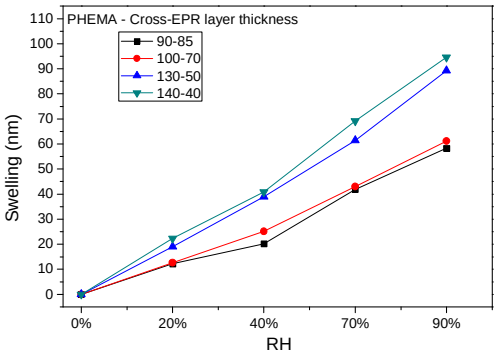

Fig. 8. *Effect of layer thickness of both PHEMA and cross-EPR for various combinations aiming at similar wavelength of the reflectance peak (λo) at dry environment. The increased layer thickness of the hydrophilic material causes enhanced responses in terms of shift per humidity change. In all cases the spectral shift is linear in respect to the humidity level revealing a linear swelling of PHEMA layers.*

C. Capacitive Type Sensors*

S. Chatzandroulis, V. Tsouti, I. Ramfos, P. Broutas, I. Zergioti[1], D. Tsoukalas[1], G.Tsekenis[2], P. Normand
[1]National Technical University of Athens,
[2]Foundation of Biomedical Research, Academy of Athens, Greece

Micromechanical Capacitive DNA Sensor Arrays

A micromechanical capacitive biosensor array has been developed using a novel fabrication process. Each biosensor in the array consists of a flexible membrane and a fixed electrode implemented on the substrate. Probe molecules are immobilized on the membrane surface and the surface stress variations during biological interactions force the membrane to deflect and effectively change the capacitance between the flexible membrane and the fixed substrate. The array consists of 60 sensors and thus is suitable for parallel sensing. The process is characterized by the self-alignment of the sensitive flexible membranes and the use of silicon fusion bonding to fabricate the complete device.

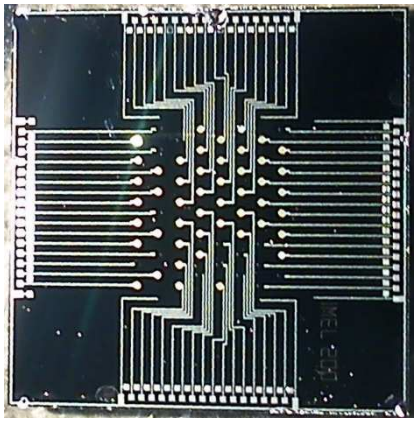
(a)

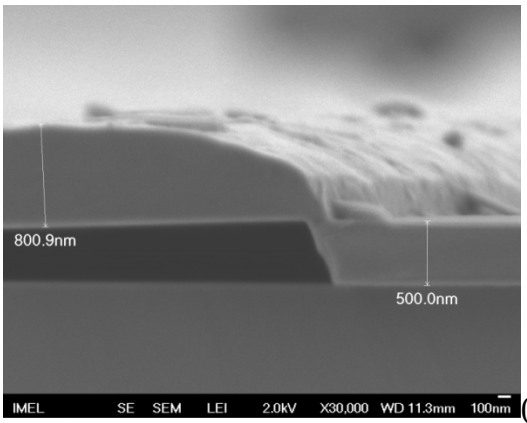

(b)

Fig. 9. *(a) Microphotograph of a fully processed biosensor array and (b) SEM view of the circular membranes.*

The array performance was tested using the K-ras gene which is linked to colon cancer. In these tests, alleles of the gene (Wild Type και Mutant) were printed and immobilized on sensor array membranes using Laser Induced Forward Transfer (LIFT) at NTUA (Figure 2). The tests were performed in a flow cell into which a test sample of mutated K-ras is inserted after a first wash with a buffer solution. To enable the concurrent measurement of multiple biosensors in the array a switch relay matrix is used to select the sensing element to be read using an HP4278A capacitance meter. Control of the whole system is performed via a Labview program running on a PC. First experimental results indicate that the sensors were able to detect the interaction between the mutant probes and the mutated part of the K-ras gene (red line in Figure 3). In the same graph, the response of a sensor on which the wild type probe was immobilized and subsequently did not interact with the mutated part of the K-ras gene is depicted (blue line), as well as the response of a simple Al capacitor (with no deflectable electrode) on which mutated probes were immobilized (magenta line in Figure 3 3).

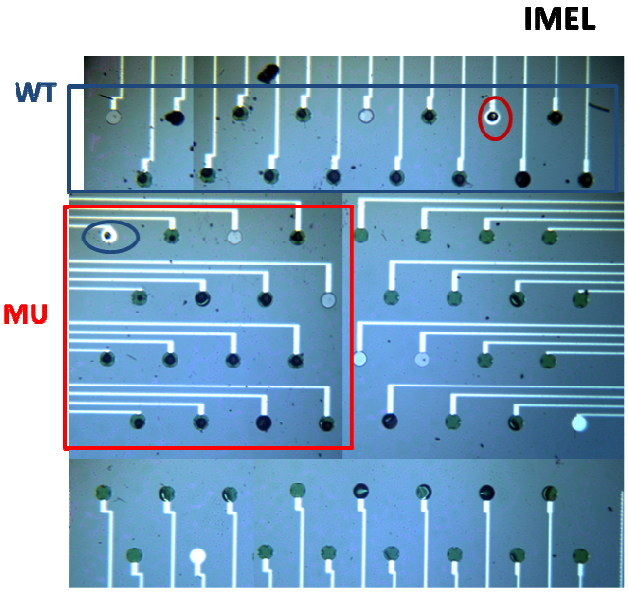

Fig. 10. *Capacitive biosensor array onto which K-ras probes (20 μM) were printed and immobilized. The array hosts Si membranes 1.34μm thick with 200μm diameter.*

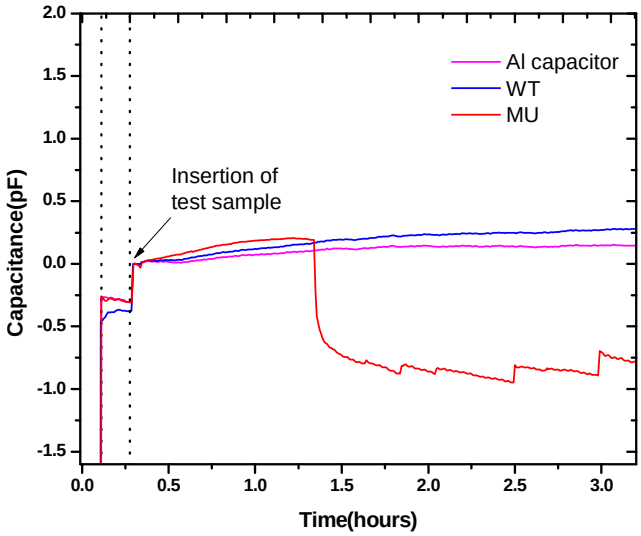

Fig. 11. *Response of sensing elements in the sensor array to mutated (MU) K-ras genes (100 ng/μl). The test sample is inserted at around 18 min (~0.3h). Only the biosensor with the immobilized mutant probes changes its capacitance (~ 1pF) whereas the biosensor with the immobilized WT probes as well as the Al capacitor remain stable after the sample insertion.*

PROJECT OUTPUT in 2012

Publications in International Refereed Journals

1. *Microfabricated disposable lab-on-a-chip sensors with integrated bismuth microelectrode arrays for voltammetric determination of trace metals,*
   Ch.Kokkinos, A.Economou, I.Raptis
   Anal. Chem. Acta 710 1(2012)
2. *Polymer-BaTiO3 Composites: Dielectric constant and vapour sensing properties in chemcapacitor applications,*
   K.Manoli, P.Oikonomou, E.Valamontes, I.Raptis, M.Sanopoulou
   J. Appl. Polym. Sci. 125 2577(2012)
3. *Compensation of Temperature Variations in Chemcapacitive Gas Sensing Systems,*
   P.Oikonomou, A.Botsialas, D.Goustouridis, E.Valamontes, M.Sanopoulou, I.Raptis
   Sensor Lett. 10 736(2012)
4. *Chemocapacitor performance modeling by means of polymer swelling optical measurements,*
   P.Oikonomou, A.Botsialas, K.Manoli, D.Goustouridis, E.Valamontes, M.Sanopoulou, I.Raptis, G.P.Patsis
   Sens. Act. B 171-172 409(2012)
5. *Sensitivity Study of Surface Stress Biosensors Based on Ultra-thin Si Membranes,*
   V.Tsouti & S.Chatzandroulis
   Microelectronic Engineering, vol. 90, pp. 29-32 (2012)
6. *Evaluation of Capacitive Surface Stress BioSensors,*
   V.Tsouti, C.Boutopoulos, M.Ioannou, D.Goustouridis, D.Kafetzopoulos, I.Zergioti, D.Tsoukalas, P.Normand, S.Chatzandroulis
   Microelectronic Engineering, vol. 90, pp. 37-39 (2012)
7. *Capacitive Microsystems for Biological Sensing,*
   V. Tsouti, C. Boutopoulos, I. Zergioti, S. Chatzandroulis
   Biosensors and Bioelectronics, vol. 27 (1), pp. 1-11 (2011)
8. *A 16-channel capacitance-to-period converter for capacitive sensor applications,*
   Ramfos, S. Chatzandroulis
   Analog Integrated Circuits & Signal Processing Analog Integrated Circuits and Signal Processing, June 2012, Vol. 71, issue 3, pp 383-389, DOI: 10.1007/s10470-011-9738-y
9. *Self-Aligned Process for the Development of Surface Stress Capacitive Biosensor Arrays,*
   V. Tsouti, M.K. Filippidou, C. Boutopoulos, P. Broutas, I. Zergioti, S. Chatzandroulis
   Sens. Act. B , Vol. 166–167, pp. 815-818 (2012)
10. *Surface functionalization studies and direct laser printing of oligonucleotides towards the fabrication of a micromembrane DNA capacitive biosensor,*
    G. Tsekenis, M. Chatzipetrou, J. Tanner, S. Chatzandroulis, D. Thanos, D. Tsoukalas, I. Zergioti
    Sens. Act. B, vol. 175, pp. 123–131 (2012)

Published Conference Proceedings

1. *Real time detection of volatile organic compounds through a chemocapacitor system,*
   E.Valamontes, G.Patsis, D.Goustouridis, P.Oikonomou, A.Botsialas, I.Raptis, M. Sanopoulou
   IMCS 2012 (Nuremberg, Germany, 05/2012)
2. *Zero-Power humidity sensor based on 1-D photonic crystal colour change,*
   M.-I.Georgaki, A.Botsialas, P.Argitis, M.Chatzichristidi, J.Rysz, A.Budkowski, I.Raptis
   EuroPtrode 2012 (Barcelona, Spain, 04/2012)

Conference Presentations

Fabrication of a capacitive micro-mechanical biosensor array with self-alignment of the ultrathin Si diaphragm and laser printing of bioreceptors,
S. Chatzandroulis, V. Tsouti, G. Tsekenis, M. Chatzipetrou, D. Thanos, I. Zergioti
2012 MRS Spring Meeting & Exhibit, April 9 - April 13, 2012, San Francisco, California

Masters Dissertations completed in 2012

Realization of photonic polymeric multilayers as humidity sensors,
Maria-Isidora Georgaki
MSc Thesis held at IMEL/NCSR Demokritos (Supervisor: I. Raptis)
Defended at the National and Kapodistrian University of Athens, Dept. of Chemistry

PROJECT III.1B
ENERGY HARVESTING MATERIALS AND DEVICES

Project Leader: C. Tsamis

Post Doctoral Scientists: E. Makarona

PhD Students: G. Niarchos

MSc Students: S. Katsaridis, S. Voulazeris

Students: T. Kyrasta

External Collaborators: Z. L. Wang (Georgia Institute of Technology), Z. Georgoussi (Institute of Biosciences & Applications, NCSR-D), C.A. Krontiras (Univ. of Patras), S.N. Georga (Univ. of Patras), N. Xanthopoulos (Univ. of Patras), S. Kennou (Univ. of Patras), S. Ladas (Univ. of Patras)

OBJECTIVES

- Design and optimization of Energy Scavengers for autonomous Microsystems
- Novel materials for high efficiency energy conversion (mechanical, thermal, etc)
- Development of MEMS-based vibrational harvesters with improved power characteristics
- Development of Flexible Energy Harvesters with Nanotextured Films
- Multifunctional ZnO Nanostructures for Smart Textiles & Biomedical Applications

FUNDING

- "*Development of Innovative sensor systems offering distributed intelligence – MEMSENSE*", National Funds and European Regional Development Funds, NSRF 2007–2013, contract no. 45 (5/2009 - 2/2013)
- "*Nanostructured ThermoElectric Systems for Green Transport & Energy Efficient Applications*", NanoTEG, EU ENIAC (7/2011-6/2014)
- *"Self-assembled ZnO Nanostructures for Engineered Neuronal Networks",* European Regional Development Fund (ERDF) under the Hellenic National Strategic Reference Framework (NSRF) 2007-2013, Hungarian-Greek Intergovernmental S&T Cooperation Programme, Contract No HUN53 (9/2012-8/2015)

MAIN RESULTS in 2012

Energy Scavenging from the ambient has been actively explored using several methods such as solar power, electromagnetic fields, thermal gradients, fluid flow, energy produced by the human body, and the action of gravitational fields. Mechanical vibration is a potential power source, which is easily accessible through Microelectromechanical Systems (MEMS) technology for conversion to electrical energy. The reported examples use a mass–spring system that resonates when the frame of the device is vibrated. The motion of the mass relative to the frame is damped by one of several energy conversion mechanisms, namely electromagnetic force, electrostatic force, or piezoelectric force.

From these scavenger types, the ones based on piezoelectric principle appear to be very promising and has been the main target of our activities. MEMS-based as well as microgenerators based on flexible substrate has been fabricated and characterized. Arrays of ZnO nanowires as well as nanostructured ZnO films have been exploited as the energy converting material. This is due to the unique properties of ZnO as well as the potentiality to growth ZnO at low temperatures using low cost, large area hydrothermal techniques.

In addition, new applications for ZnO technologies have been identified and pursued ranging from pyroelectric energy harvesters, smart textiles to control of surface wettability and biomedical applications.

SOI-based Vibrational Energy Harvesting Microgenerators

G. Niarchos, E. Makarona, G. Voulazeris, Th. Speliotis, A. Arapoyanni*, C. Tsamis

**Department of Informatics and Telecommunications, National Kapodistrian University of Athens, Athens, Greece*

The miniaturization of MEMS devices and the corresponding decrease of their consumption solves only partially the requirement for autonomous wireless sensor devices. Rendering a device completely autonomous and battery-free has as a prerequisite the development of equally miniaturized power micro/nanogenerators that can become an integral part of the sensor chips. ZnO-nanowire nanogenerators have successfully converted nanoscale mechanical energy into electricity, but the production of a viable, cost-efficient micro-nanogenerator that can be readily integrated on-chip along with the devices to be powered-up is still elusive. Towards this goal, we have successfully fabricated a cantilevered microgenerator based on SOI technology employing as its functional core a novel nanotextured ZnO film as the piezoelectric material.

As starting material, SOI wafers were used with a silicon overlayer thickness –and hence a cantilever thickness- of 5μm. The piezoelectric nanotextured layers, sandwiched between aluminum electrodes, were developed via the hydrothermal technique on seeding layers that were either deposited by sputtering or by spin-coating of solutions (sol-gels and zero-gels). During the growth the wafers were placed face down on the surface of aqueous equimolar solutions of zinc nitrate hexahydrate [$Zn(NO_3)_2.6H_2O$] and hexamine (HMTA). Depending on the growth conditions (solution concentration, temperature, duration) the properties of the piezoelectric material could be tuned according to the required specifications. Fig. 1 is a photograph of a single die containing 4 microgenerators. We can distinguish the proof mass as well as the electrodes of the device. Fig. 2 shows that the hydrothermal technique can produce in a controlled and repeatable way highly textured columnar ZnO films with a thickness of up to several μm.

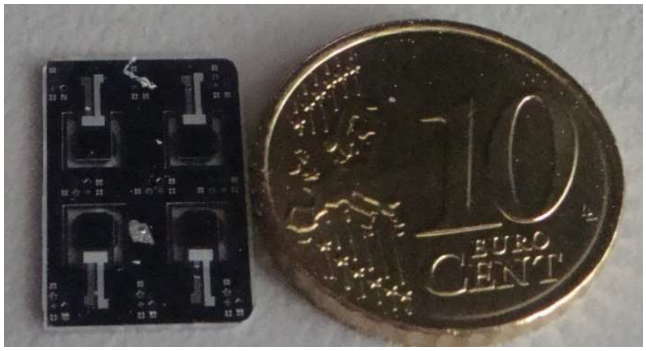

Fig. 1. *Photograph showing the actual size of single die containing 4 microgenerators.*

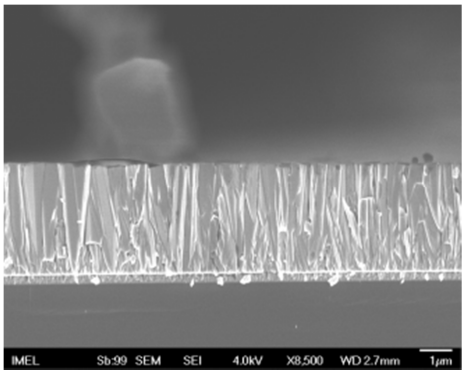

Fig 2. *ZnO nanotextured film on Al electrodes.*

The microgenerators containing the ZnO nantoextured films even when imposed to random impulses were able to provide output voltages up to hundreds of mV for open circuit (Figs.3, 4). Detailed measurements and a systematic analysis are performed for various mechanical excitations and external loads showing the feasibility of the proposed methodology for on-chip power generation. It is important to note that the measurements are performed in air. The presence or air has a significant impact of device performance due to damping phenomena and results in significant reduction (more than 2 orders of magnitude) of voltage and thus power output.

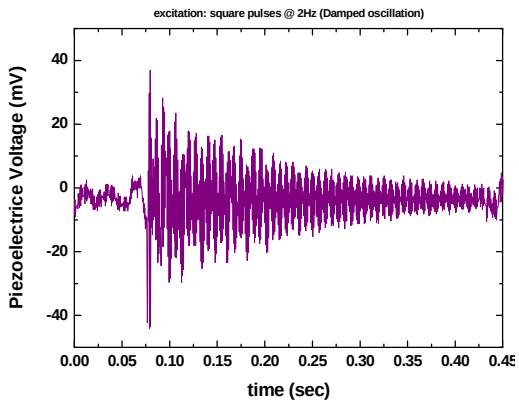

Fig. 3. *Microgenerator voltage as a function of time upon excitation by square pulses. The measurements are performed in air.*

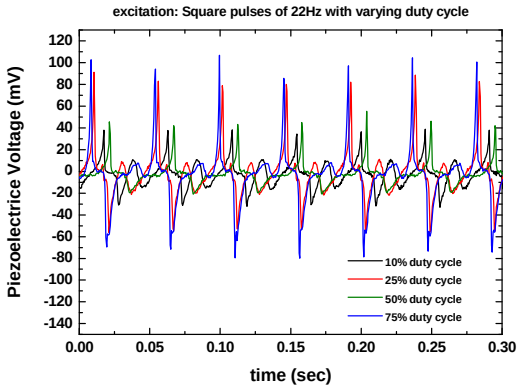

Fig. 4. *Microgenerator response upon excitation of square pulses of various duty cycles :10%(black), 25% (red), 50% (green) και 75% (blue).*

Flexible piezoelectric microgenerators based on nanotextured ZnO films

G. Niarchos, E. Makarona, Th. Kyrasta, G. Voulazeris, Th. Speliotis, C. Tsamis, L. Lin*, Y. Hu*, Z. L. Wang*

*School of Material Science and Engineering, Georgia Institute of Technology, Atlanta, Georgia 30332, USA

Piezoelectric microgenerators were developed onto flexible substrates employing novel nanotextured ZnO grown on Kapton/PET substrates. It is known that the growth of ZnO nanowire arrays as well as nanostructured ZnO films requires the presence of a ZnO seeding layer onto the substrate. This layer provides the necessary nucleation sites upon which the ZnO nanostructures can grow and develop. Traditionally, fine (50-200nm) ZnO films deposited by sputtering have been used to facilitate the hydrothermal growth. However, in order to further reduce cost alternative methodologies are required. In our approach we have used two alternative chemical techniques based on zero-gels with the scope to further reduce the fabrication cost and complexity and to optimize the fabrication time.

All devices are employing either high-density vertical-ZnO nanorod arrays or nanotextured ZnO films grown via a facile, low-cost hydrothermal method on Kapton and Polyethylene terephthalate (PET) substrates (Fig. 1). The first method exploits ZnO seeding layers formed by sputtering, and the other two purely chemically developed seeding layers by spin-coating of HMTA-based sol-gel and zinc-acetate ethanol solution. Typical output voltages achieved under instantaneous and sinusoidal external excitation reached up to 4V (Figs. 2,3). The alternative fabrication techniques are compared in order to assess their performance in terms of output power versus cost and ease-of-fabrication and to optimize a rapid and cost-efficient method for driving small and low-power devices (Fig. 4).

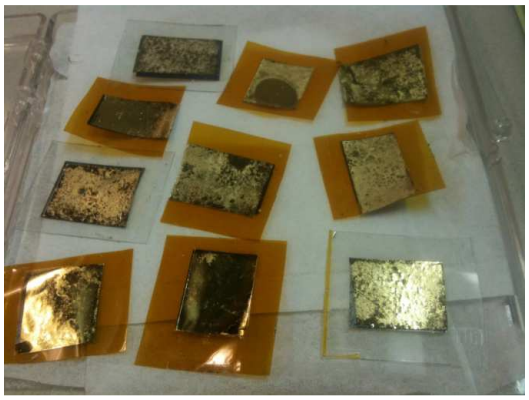

Fig 1: Photograph of microgenerators on kapton and PET.

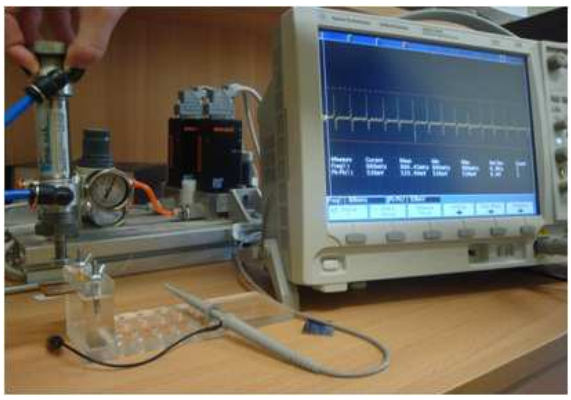

Fig. 2: Photograph of the measurement setup.

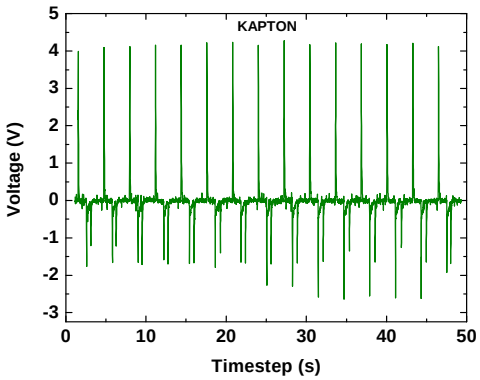

Fig. 3. *Output voltage as a function of time for a flexible microgenerator on a Kapton substrate.*

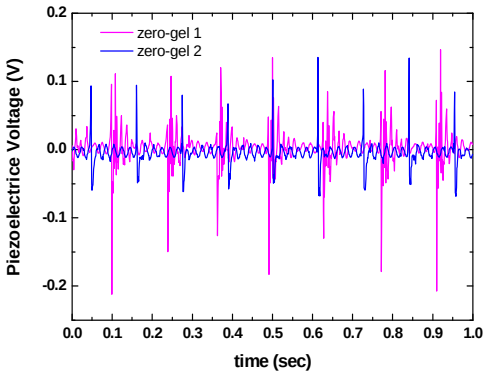

Fig. 4. *Comparison of microgenerators on Kapton using the two alternative seeding layer techniques.*

Multifunctional ZnO Nanostructures for Biomedical Applications & Smart Textiles

E. Makarona, Th. Kyrasta, Z. Georgoussi, A. Kritharidou and C. Tsamis

The human brain contains more than 100 billion neurons and at least nine more times glial cells. These cells connect among themselves through synapses building a network of immense complexity. In order to comprehend how the brain function, it is important to elucidate how synapse form and how the biochemical signals relate information to one another. So far neuroscientists and neurophysiologists employ tow different approaches: (i) either the use of thin brain slices –which even though they maintain the inner structuring of the brain intact, contain a very large number of cells rendering single-cell observation impossible, and (ii) neuronal cultures –which allow single-cell or cell-to-cell observation and the recording of biochemical events in cells, but in general are not easy to organize on predefined patterns or control the connectivity of the cells. One of the open issues is to fabricate templates where the cells will selectively adhere on predefined patterns while they will be guided to form connections on preselected pathways**.** Of course, such templates should maintain the viability and functionality of the cells over the course of several days, necessary for the full development of the networks.

Towards this goal a new methodology for the production of patterned templates suitable for the development of neuronal networks is currently being developed. The templates are designed to control through nanotopographical features the selective adhesion of neuronal cells on predefined locations of the pattern while preserving the viability of the cells and guiding the formation of synapses along preselected pathways. The methodology explored has at its core the hydrothermal growth of ZnO nanostructures which is a very versatile method allowing the control of the morphological characteristics of the nanostructures through tuning of simple key parameters. The methodology is mainly focusing on the development of ZnO nanostructures on Si wafers with standard microfabrication techniques in order to establish its potential for mass production and integration with other types of microelectronic devices.

The biocompatibility and cell viability studies were performed in parallel with the template fabrication optimization studies. HEK (Human Embryonic Kidney) and Neuro2A (mouse neuroblastoma cells) were cultured onto the patterned templates and it was confirmed that the ZnO nanostructures are indeed biocompatible and can maintain cell viability and proliferation (Fig. 5).

A very important finding was that the cells tended to adhere onto the nanorods, and a minimum amount, less than 15%, was attached to the flat surfaces, even though these surfaces are topographically more relevant to the conventional glass slides used for culturing. In addition, the cells tended to adapt to the shape of the lithographic patterns rather than migrate to the flat areas (Fig. 6a). The cells proliferated and neurite outgrowth was also observed (Fig. 6b)

suggesting that networking should be feasible upon activation of the neurons. In other words, selective adhesion of cells guided through nanotopographical features was achieved.

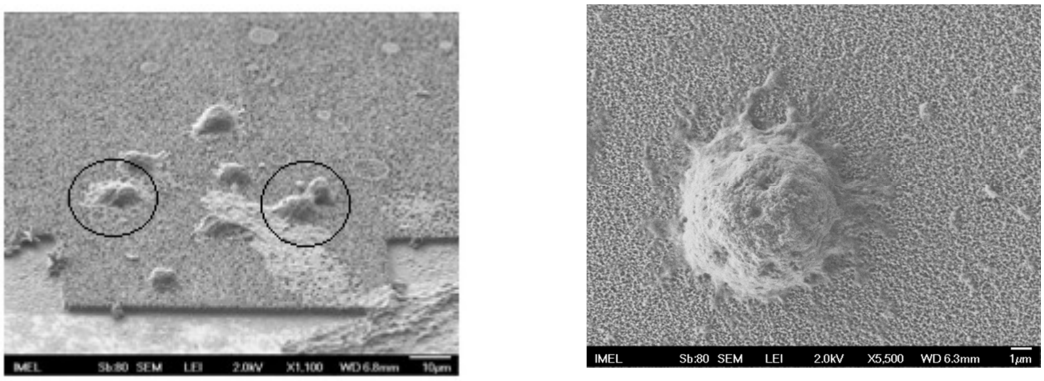

(a) **(b)**

Fig. 5. SEM images of Neuro2A cells after 72hrs of culturing on patterned Si wafers with ZnO nanorods where it is evident that the cells maintain their viability, their shape and functionality, and they can proliferate (encircled regions) and extend philopodia (magnification to the right)

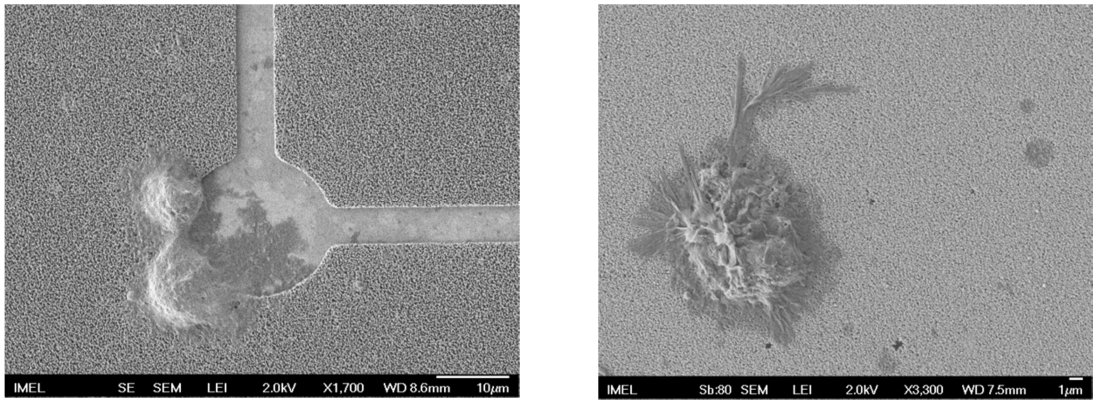

(a) **(b)**

Fig. 6. Characteristic SEM images of Neuro2A cells after 48hrs in culture over the templates with ZnO nanorods where (a) a clear preference of the cells to adhere onto the nanorods and conform to the borderlines of the patterns, and (b) neurite outgrowth were observed.

In parallel, a new activity has begun focusing onto the integration of ZnO on fabrics for the creation of smart textiles that can be employed in a plethora of applications such as antimicrobial coatings, energy harvesting fabrics and athletic garments. E-textiles, also known as electronic textiles or smart textiles, are fabrics that enable digital components and electronics to be embedded in them. Many intelligent clothing, smart clothing, wearable technology, and wearable computing projects involve the use of e-textiles. Electronic textiles are distinct from wearable computing because emphasis is placed on the seamless integration of textiles with electronic elements like microcontrollers, sensors, and actuators. Furthermore, e-textiles need not be wearable; for instance, e-textiles are also found in interior design.

Initial results where the hydrothermal growth of ZnO nanorods has been applied to several types of natural (cotton, silk and linen) and synthetic fabrics (polyester and acrylic) are very promising and already show a great potential for the production of smart textiles with an emphasis in energy harvesting applications (Fig. 7).

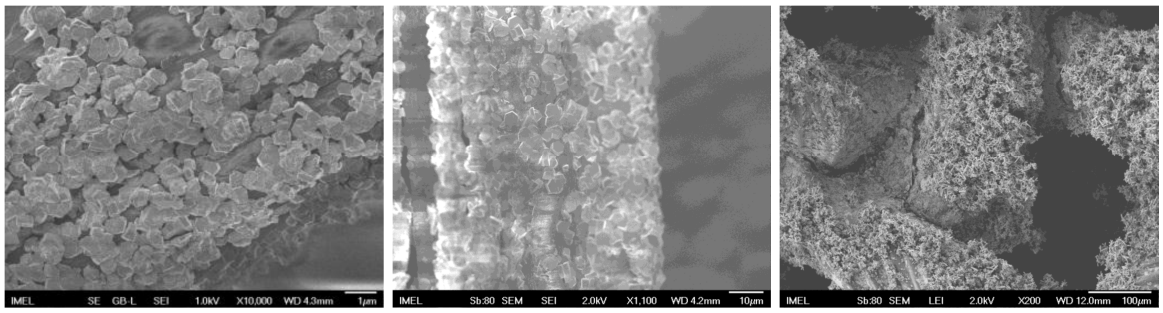

(a) **(b)** **(c)**

Fig. 7. Successful implementation of ZnO nanorods on (a) silk, (b) cotton and (c) polyester fabrics for the development of smart textiles for energy harvesting applications

PROJECT OUTPUT in 2012

Conference Presentations

1. *Comparison of ZnO-based Piezoelectric Nanogenerators on flexible substrates,*
   G. Niarchos, E. Makarona, Th. Kyrasta, G. Voulazeris, Th. Speliotis, C. Tsamis, L. Lin, Y. Hu, Z. L. Wang
   CIMTEC 2012, Symposium E: Next Generation Micro/Nano Systems, June 10-14, 2012, Montecatini Terme, Italy
2. *SOI-based Vibrational Energy Harvesting Microgenerators,*
   G. Niarchos, E. Makarona, G. Voulazeris, Th. Speliotis, A. Arapoyanni, C. Tsamis
   EUROSENSORS XXVI, 9-12 September 2012, Kraków, Poland
3. *ALD deposited ZrO_2 ultrathin films on Si substrates: morphology and electrical evaluation,*
   M. Botzakaki, G. Skoulatakis, N. Xanthopoulos, C.Tsamis, E. Makarona, S. Kennou, S. Ladas, S.N. Georga and C.A. Krontiras
   XXVIII Panhellenic Conference on Solid State Physics and Material Science
4. *ALD deposited ZrO_2 ultrathin layers on Si and Ge substrates: A multiple technique characterization*¸
   M. Botzakaki, G. Skoulatakis, N. Xanthopoulos, C.Tsamis, E. Makarona, S. Kennou, S. Ladas, S.N. Georga and C.A. Krontiras
   5th International Conference on Micro&Nanoelectronics, Nanotechnology and MEMs
5. *Flexible piezoelectric microgenerators based on nanotextured ZnO films,*
   E. Makarona, G. Niarchos, G. Voulazeris, C. Tsamis,
   To appear in SPIE Microtechnologies, 24 - 26 April 2013, Grenoble, France

Published Conference Proceedings

1. Special Issue: 25th Anniversary Eurosensors XXV, Sensors & Actuators: Physical, Eds.: C. Tsamis & G. Kaltsas (2012)
2. Special Issue: 25th Anniversary Eurosensors XXV, Sensors & Actuators: Chemical, Eds.: C. Tsamis & G. Kaltsas (2012)

Masters Dissertations completed in 2012

1. *Vibrational energy harvester for Wireless Sensor Networks,*
   S. Katsaridis,
   Dept. of Informatics and Telecommunications, Univ. of Athens, April 2012
2. *Modeling and Fabrication of a Piezoelectric Energy Harvester Collecting the Ambient Mechanical Energy From Environmental Vibrations,*
   G. Voulazeris
   Dept. of Informatics and Telecommunications, Univ. of Athens, October 2012

PROJECT III.2
BIO-MICROSYSTEMS

Project Leader: K. Misiakos

Permanent Researchers: I. Raptis, E. Gogolides, A. Tserepi

Post Doctoral Scientists: E. Makarona

Other staff under contract (technical personnel): A. Botsialas, A. Salapatas

External Collaborators: S.E. Kakabakos, P.Petrou (IRRP/NCSR-D)

OBJECTIVES

- Development of bioanalytical lab-on-a-chip devices based on monolithic optoelectronic transducers (bioactivated optocouplers).
- Development of white light interferometric setup for label free monitoring of biomolecular reactions.
- Develop highly sensitive and/or label free assays suitable for Point of Care and Point of Need applications

FUNDING

- EU, FP7-ICT, STREP, "FOODSNIFFER", Monolithically integrated interferometric biochips for label-free early detection of human diseases (start 01-09-2012, duration 36months), www.foodsniffer.eu

MAIN RESULTS in 2012

A: Monolithically integrated interferometric biochips for label-free biosensing

The progress of integrated optical structures, such as waveguides and gratings, has allowed the implementation of various evanescent wave sensors which found wide application in real-time monitoring of biomolecular interactions offering high sensitivity, and fast response time. Among the evanescent field sensors, the Mach–Zehnder Interferometric (MZI), fig. 1a biosensor is one of the most promising devices due to its high sensitivity and accuracy. In the framework of the European funded FOODSNIFFER the **Broad-Band Mach-Zehnder Interferometry (BB-MZI) approach** that has been patented[1] by our group is combined with an on-chip spectrum analyzer and miniaturized and self-aligned LEDs all **monolithically integrated on the same Si chip and manufactured by mainstream silicon technology.** This radical concept is going to be applied at the Point of Need detection of harmful substances in food and in particular of certain pesticides, allergens and mycotoxins.

[1] *a) K. Misiakos, S. Kakabakos "Integrated optoelectronic silicon biosensor for the detection of biomolecules labeled with chromophore groups or nanoparticles", PCT WO2007/074348, US7319046 b) K. Misiakos, S. Kakabakos, I. Raptis, E. Makarona, "Integrated optoelectronic silicon biosensor for the detection of biomolecules labeled with chromophore groups or nanoparticles", OBI, 1006509 2008 c) I. Raptis, K. Misiakos, S. Kakabakos, P. Petrou, E. Makarona, M. Kitsara, "Monolithically Integrated Physical Chemical and Biological Sensor Arrays based on Broad-band Mach-Zehnder Interferometry", PCT WO2009/115847 A1 (2009)*

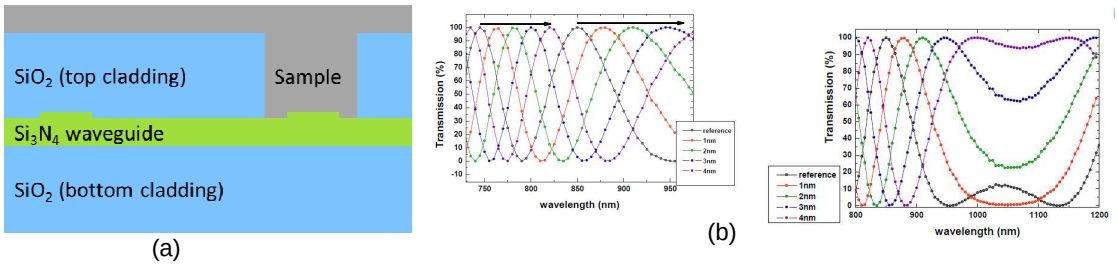

(a) (b)

Fig. 1. *a) MZI structure. The cladding layer over the sensing arm is removed and is appropriately functionalized. The core of the waveguide is appropriately structured to be monomodal. b) Simulation of transmission spectra for BB-MZI device upon binding of target molecules with an equivalent thickness in the 0-4nm range. The thickness of the silicon nitride layer is 150nm.*

The FOODSNIFFER optoelectronic transducer is based on the monolithic optocoupler platform that has been developed at the Institute of Microelectronics. The optocoupler consists of a waveguide self-aligned to a VIS-NIR light source (avalanche photodiode) and a common photodetector, fig. 2a. By dicing off the photodetector part, fig. 2b the transmission spectrum could be monitored by an external spectrometer coupled to an optical fiber aligned in front of the chip facet, fig. 2c.

In the course of the FOODSNIFFER project, the monomodal waveguide is patterned to a Mach-Zehnder interferometer and its principle of operation is the spectroscopic interference due to the optical path difference originating by biochemical events. The output of the BB-MZI photonic structure is coupled to a miniaturized spectrum analyzer and an array of photodetectors. This way all necessary active and passive optical components are integrated on the same chip resulting in a miniaturized optoelectronic lab-on-a-chip. The particular chip will be the only one integrating such optical and electronic devices offering that way a unique miniaturized optoelectronic platform for sensing applications without any compromise in sensitivity. The integrated nature of the basic biosensor scheme allows for the development of arrays tailored to specific diagnostic applications. Each biosensor array will be comprised of individually functionalized light source/optical waveguide series coupled to a single spectrum analyzer and a photodetector array.

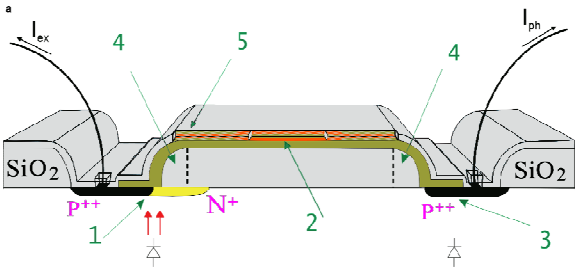

(a)

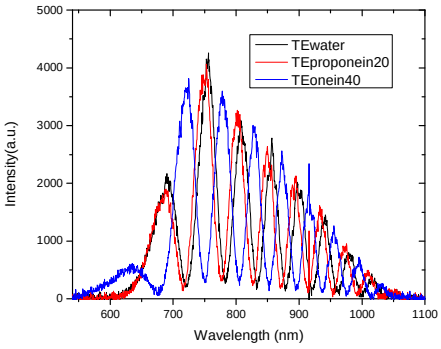

(c)

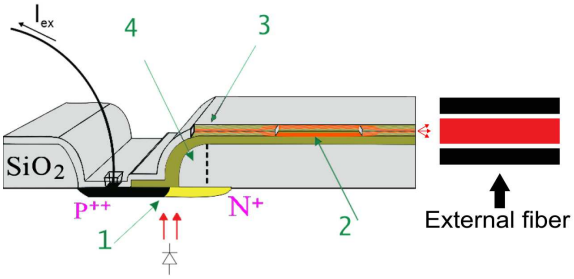

(b)

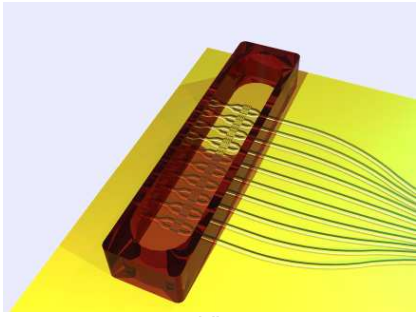

(d)

Fig. 2. *a) Schematic of the monolithic optocoupler. Light emitting diodes (1) and detectors (3) are optically coupled through a self-aligned silicon nitride layer (2) while the spacers (4) provide for the smooth waveguide bending. The nitride layer is shaped as Mach-Zehnder interferometer (5) and the top cladding layer over the sensing arm is removed and functionlized for the targeted analytes. b) Semi-integrated version of the chip showing the cleaved emitting edge of the integrated waveguide optically coupled to an external fiber connected to a USB powered portable spectrometer. c) Spectral shifts as a result of a cover medium change. The waveguides are photonically engineered so that an increase in the effective refractive index of the sensing waveguide will cause a blue shift. The black curve correspond to water, the red one to a propanol/water mixture of 1/20 (R.I. change 3.6X10^{-3}) and the blue one to a propanol/water mixture of 1/40 (R.I. change 1.8X10^{-3}). Sensitivities in excess of 15 μm/RIU are obtained and Limits of Detection (LOD) of 1.510^{-6} RIU. Here, the exposed arm length is 2 mm. d) Schematic detail of the FOODSNIFFER chip showing the BB-MZI array and the microfluidic channel on top for the supply of the sample to be analyzed.*

B. Microfluidics and LOC (see detailed description in Project I.2, section D2)

Significant work has been carried out for both microfluidics and microarrays for bioanalytical applications and is described in detail in Project I.2, section D2.
In the area of microfluidics, the following 3 topics were pursued:

I. Phosphopeptide Enrichment and Separation in an Affinity Microcolumn on a Silicon Microchip: Comparison of Sputtered and Wet-Deposited TiO_2 Stationary-Phase (see Fig. 3a,b,c). This work is a continuation of our previous work in polymeric microchips.
II. Continuous-flow microfluidic device for DNA amplification (μPCR) on flexible polyimide substrate and integration in a Lab-On-Chip platform (see Fig. 3d,e). Improvements over previous design were implemented and device efficiency for PCR was demonstrated.
III. Comparison of pressure drop and flow field in Superhydrophobic and superhydrophilic, hierarchical, plasma-nanotextured polymeric microchannels.

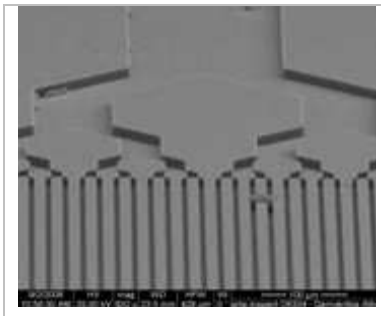

(a)

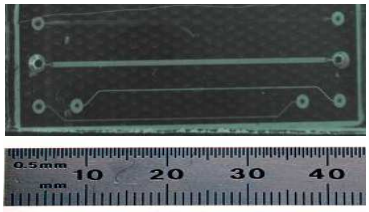

(b)

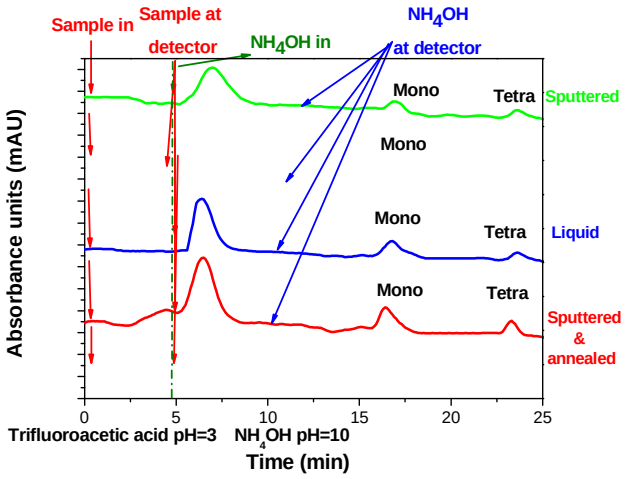

(c)

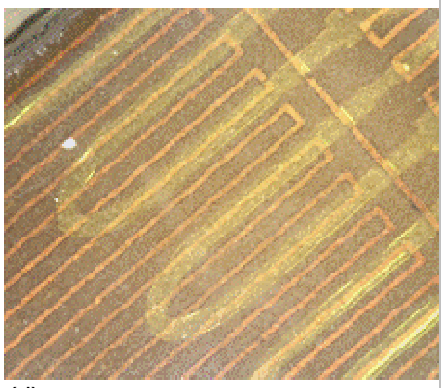

(d)

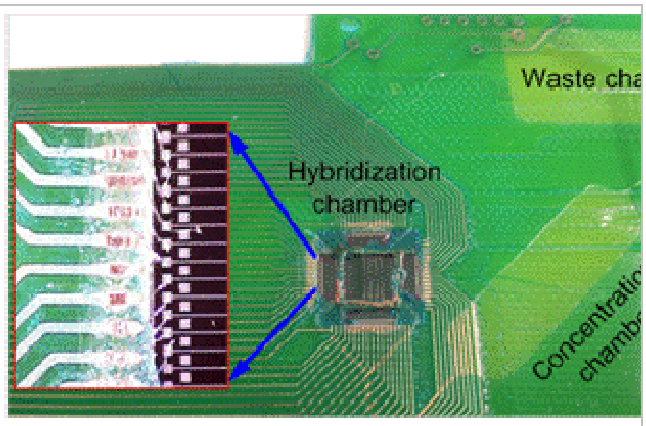

(e)

Fig. 3. *(a), (b) Silicon microcolumn consisting of 32 parallel microchannels. (c) Affinity chromatography on chip is demonstrated, with retention, elution and separation of the peptide mixtures using the three different microcolumns. Some baseline shifts are due to shifting of the intensity of the Deuterium lamp. The sample quantity is 0.1nmol for each peptide. (d) Fabricated μPCR chip with integrated microheaters. (e) Prototype of a Lab-On-a-Chip on PCB integrating a μPCR device and an array of Si-based biosensors*

In the area of microarrays, a new method for nanoscale protein patterning was developed and demonstrated for very high density microarrays based on colloidal lithography and plasma processing (see Fig. 4).

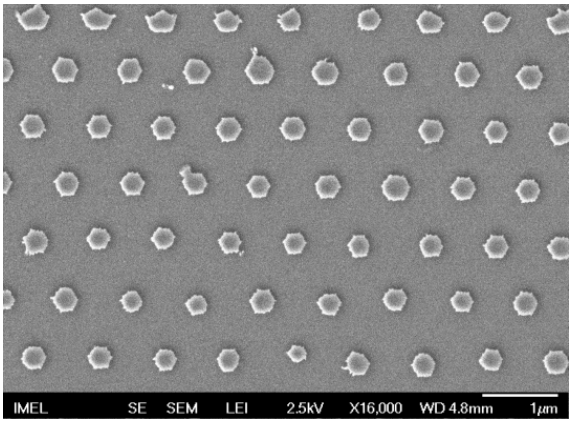

(a)

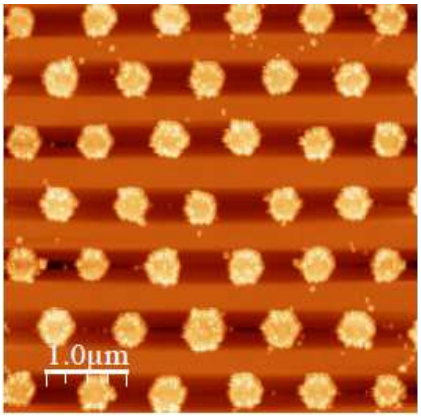

(b)

Fig. 4. *(a) SEM image of 300 nm SiO_2 nanoislands patterned on Si using colloidal lithography and plasma etching. (b) Atomic Force Microscopy image of SiO_2 nanoislands after selective immobilization of BSA on the plasma modified nanoislands only versus the Si surface.*

Detailed description of the above can be found in Project I.2 (Section D2)

PROJECT OUTPUT in 2012

Publications in International Refereed Journals

1. *Spectroscopic and microscopic characterization of biosensor surfaces with protein/amino-organosilane/silicon structure,*
   K.Awsiuk, A.Bernasik, M.Kitsara, A.Budkowski, P.Petrou, S.Kakabakos, S.Prauzner-Bechcicki, J.Rysz, I.Raptis
   Colloids Surf. B 90 159 (2012)

Published Conference Proceedings

1. *All-Si optoelectronic lab-on-a-chip for label-free multi-analyte biosensing*,
   I.Raptis, P.Petrou, E.Makarona, A.Botsialas, A.Psarouli, S. Kakabakos, G.Jobst, R.Stoffer, M.Hoekman, M.Sopanen, K.Tukkiniemi, K.Misiakos
   EuroPtrode 2012 (Barcelona, Spain, 04/2012)
2. *Label free biochemical determinations based on the contrast monitoring of periodic patterns*,
   I. Archontas, A. Salapatas, K. Misiakos
   IMCS 2012 , p.1359-1361, The 14th International Meeting on Chemical Sensors, May 20 - 23, 2012, Nuremberg, Germany
3. *Real-time Label-free Monitoring of Biomolecular Reactions by Monolithically Integrated Mach-Zehnder Biosensors,*
   I. Raptis, P. Petrou, E. Makarona, A. Botsialas, A. Psarouli, S. Kakabakos, G. Jobst, R. Stoffer, M. Hoekman, M. Sopanen, K. Tukkiniemi, K. Misiakos 8th Aegean Analytical Chemistry Days Conference, p. 38, September 16-20, 2012, IZTECH, Izmir, Turkey

Invited Talks

All-Silicon Optoelectronic Lab-On-a-Chip For Label-Free Multi-Analyte Biosensing: The PYTHIA Aproach,
I. Raptis, E.Makarona, A.Botsialas, K.Misiakos, P.Petrou, A.Psarouli, S.Kakabakos, G.Jobst, M.Hoekman, R.Heideman, H.Leewuis, R.Stoffer, M.Sopanen, K.Tukkiniemi
IC-MAST 2012, Budapest, Hungary, May 2012

PROJECT III.3

THIN FILM DEVICES for LARGE AREA ELECTRONICS

Project Leader: D.N. Kouvatsos

Post Doctoral Scientists: D.C. Moschou

External Collaborators: C.A. Dimitriadis (University of Thessaloniki), G.J. Papaioannou (University of Athens), N. Stojadinovic (University of Nis), A.T. Voutsas (Sharp Laboratories of America)

OBJECTIVES

The project general research objective is the development and characterization of new technologies for thin film transistors and other thin film based devices. The principal particular objective for the past decade has been the optimization of the active layer of polysilicon films obtained using advanced excimer laser crystallization methods and of the resulting performance parameters of thin film transistors (TFTs) fabricated in such films. Such advanced TFTs are necessary for next generation large area electronics systems. Specifically, the targets of the TFT and poly-Si thin film investigation are:

- Evaluation of device parameter hot carrier and irradiation stress-induced degradation and identification of ageing mechanisms in TFTs fabricated in advanced excimer laser annealed (ELA) polysilicon films with sequential lateral solidification (SLS).
- Investigation of the influence of the crystallization technique and the film thickness on TFT performance, defect densities and degradation for technology optimization.
- Investigation of effects of variations in the transistor structure and in the fabrication process on device performance and reliability.
- Investigation of polysilicon active layer defects using transient drain current and noise analysis in ELA TFTs.
- Assessment of material properties of poly-Si thin films using optical measurements.

On the application level, the project aims at the utilization of these advanced TFTs in the development of novel TFT-addressed displays and microsystems, in collaboration with various research and development partners. Such systems would incorporate thin film sensors and other elements, or possibly thin film polysilicon photovoltaics. Polysilicon film characterization would determine the efficiency of silicon photovoltaic elements as a function of the grain size and geometry. Another possibility being pursued is support for the development of thin film photoelectric sensor – ZnO TFT microsystem modules. Detailed proposals on these subjects with European consortia have been formulated.

FUNDING

- Sharp Labs of America grant, 2003–2005.
- Two GSRT bilateral Greece-Serbia projects, 2003–2007.
- PENED contract, project code 03ED550, 2005–2009.
- Two postdoctoral fellowships (Dr. Exarchos 2008–2010, Dr. Moschou 2010–2012).
- Currently, participation in IMEL cooperation project with Heliosphera (project leader Dr. D. Tsoukalas).

MAIN RESULTS in 2012

Our work during 2012, following the earlier electrical characterization of various technologies of single gate TFTs and the material / optical investigation of polysilicon films, focused in the characterization, degradation and noise investigation of double gate TFTs, fabricated using sequential lateral solidification excimer laser annealing (SLS ELA) techniques. Also, it included characterization work in polysilicon thin film photovoltaic elements. Work on thin film integrated microsystems is still in the form of funding proposals and is not discussed here.

Task 1: Characterization and degradation study of double gate SLS ELA TFTs

Advanced polysilicon TFTs, fabricated at very low temperatures using SLS ELA techniques, are essential for large area electronics and high performance flat panel displays. This task aims at the characterization and reliability investigation of poly-Si TFTs having various device structures and film microstructures (derived from different SLS ELA conditions), with determination of process parameters that affect device performance. During 2012 we continued the investigation of double gate TFTs. The second gate allows for additional possibilities, such as the control of TFT electrical characteristics and parameters by appropriately biasing the bottom gate; thus, DG TFTs are considered very important for future large area electronics. The dimensions of both gates affect TFT characteristics, in ways like giving rise to short channel effects, as well as affecting the degradation behavior of the devices. Such effects were extensively studied during 2011, as previously reported. In 2012 there was further work at confirming these findings. In particular, it has been evident that a significant V_{th} increase with increasing top gate length occurs in double gate TFTs due to the larger number of grain boundaries and relevant traps included in larger channels. Moreover, trap generation during DC bias stress, as probed through the $V_{g,max} – V_{th}$ parameter, which we have previously shown to be directly proportional to the grain boundary trap density, was clearly shown to significantly increase for larger top gate lengths.

In degradation investigations, we have applied equivalent DC stress in DG TFTs of different top gate lengths, with a constant channel width and bottom gate length. Also, to ensure that we only see effects from the top gate operation, the bottom gate bias was kept constant at -3 V, pushing the carriers towards the top interface. The channel length significantly affects the degradation characteristics; degradation was much more intense in longer devices, despite the scaling of the stress field. This is attributed to the larger number of sub-boundaries and grain boundaries as the channel length increases, causing more pronounced scattering of the free carriers towards the top interface and larger grain-boundary trap generation. Two V_{th} degradation mechanisms are observed: hole injection only for large channels and electron injection common for all devices. From the S stress evolution we inferred that these mechanisms mainly refer to trap generation at the interface and not to oxide injection. $G_{m,max}$ shows a similar behavior for all TFTs, featuring a monotonous decrease. This was attributed to grain boundary and sub-boundary trap generation, as also indicated by the $V_{g,max}$ - V_{th} stress time evolution.

In addition, the transconductance variation against the bottom gate bias for various top gate or bottom gate lengths was also investigated for TFTs with a channel width W of 16 μm. The increase of the bottom gate bias forces the current carriers deeper in the poly-Si active layer, thus “seeing” more traps; more traps are expected to be present as we go deeper, since the top interfaces are superior to the bottom ones as we have shown in previous work. This is the reason both for the observed increase of $V_{g,max}$-V_{th} with increasing V_{gb} and for the decreasing $G_{m,max}\times L_{top}$ with increasing bottom gate bias (Fig. 1). The values of $G_{m,max}$ have been multiplied by the top gate length so as to normalize them and be able to compare them. However, in this plot we do not see clear short channel effects, as we did for V_{th} and $V_{g,max}$-V_{th}. This could be attributed to the fact that this parameter is known to be affected not only by trap densities but also by scattering of the carriers at the interfaces. This factor could be very different in these devices and thus “mask” any short channel effects. In Fig. 1 we also see the behavior of $G_{m,max}$. Since the top length is the same in all of these devices and the parameters are extracted from top operation characteristics (I_{ds}-V_{gt}), no $G_{m,max}$ normalization is necessary like before. However, again we do not see any clear trend of $G_{m,max}$ with L_{top}/L_{bottom}. Therefore, we conclude that short channel effects are less intense on the $G_{m,max}$ parameter than on V_{th} for double gate polysilicon TFTs.

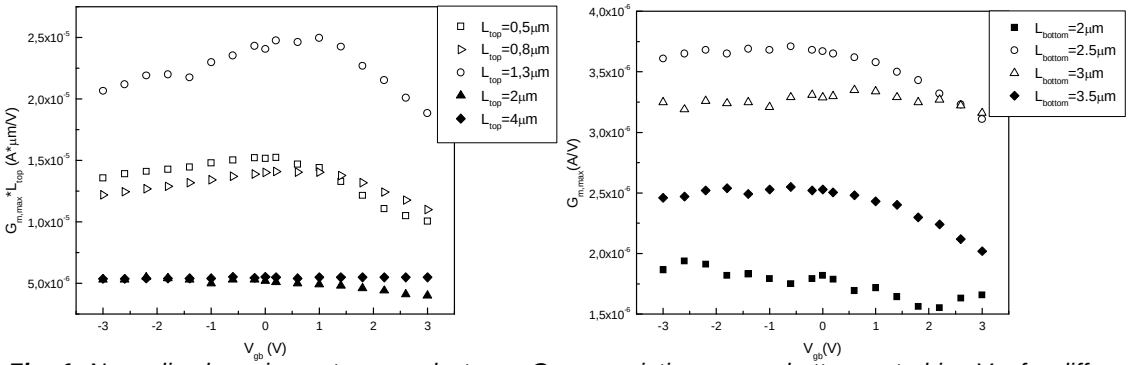

Fig. 1. *Normalized maximum transconductance $G_{m,max}$ variation versus bottom gate bias V_{gb} for different top gate lengths, with W = 16 μm and L_{bottom} = 4 μm (left). Maximum transconductance $G_{m,max}$ variation versus bottom gate bias V_{gb} for different bottom gate lengths, with W = 8 μm and L_{top} = 2 μm (right).*

Task 2: Low frequency noise investigation

Emphasis in recent work was placed in concluding the investigation of noise in SLS ELA TFTs. Those devices had bottom gate lengths L_{bottom} of 2,5 μm or 4 μm and a channel width W = 16 μm. The top gate length L_{top} varied from 0.5 μm to 1.3 μm.The drain current noise power spectral density S_I versus frequency was investigated; these measurements were carried out at the Aristotle University of Thessaloniki, in a project collaboration.

For sub-micron devices (L_{top} = 0.5 μm) the drain current noise spectra, before stress, exhibit 1/f noise behaviour (flicker noise) in the regions from weak to strong inversion. After stress, they consist of two distinct components: a flicker noise and a Lorentzian noise characterized by a plateau at low frequencies and a fall-off according to $1/f^2$, related to trapping / detrapping processes of carriers at discrete traps, with the corner frequency f_c directly related to the trap time constant τ characterizing the capture and emission processes of electrons in the traps. This corner frequency f_c does not change with top gate voltage V_{gt}, as shown in Fig. 2, which suggests that the trap centers responsible for the observed Lorentzian noise are located in a semiconductor region at some distance from the top gate oxide/polysilicon interface. The physical mechanism of the flicker noise is the variation of the interfacial oxide charge after dynamic trapping and detrapping of free carriers into slow oxide traps at/or near the interface, through tunneling, which leads to surface potential fluctuation and in turn to fluctuations in the inversion charge density. The observed increase of the normalized noise, also shown in Fig. 2, indicates an increase of the interface trap density from 1.2×10^{12} to 2×10^{12} cm^{-2} eV^{-1} after stress for time t = 10^4 s.

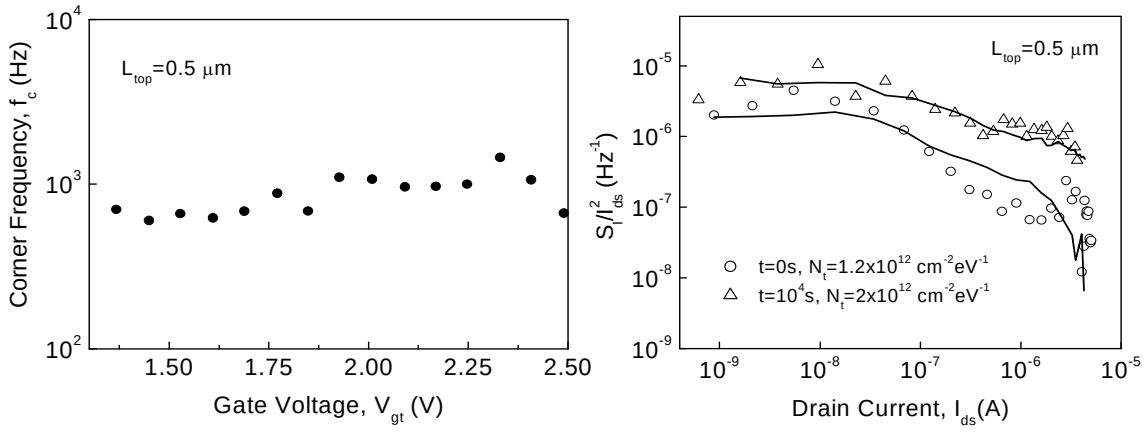

Fig. 2. *Drain current dependence of the time constant τ for the Lorentzian components in DG polySi TFT with L_{top} = 0.5 μm and L_{bottom} = 4 μm (left). Normalized drain current spectral density S_I / I_{ds}^2 as a function of drain current I_{ds} measured at f = 50 Hz for a DG polySi TFT with W = 16 μm, L_{top} = 0.5 μm and L_{bottom} = 4 μm before and after stressing. The solid lines correspond to $S_{Vfb}\times(g_m/I_{ds})^2$ and the symbols to experimental data.*

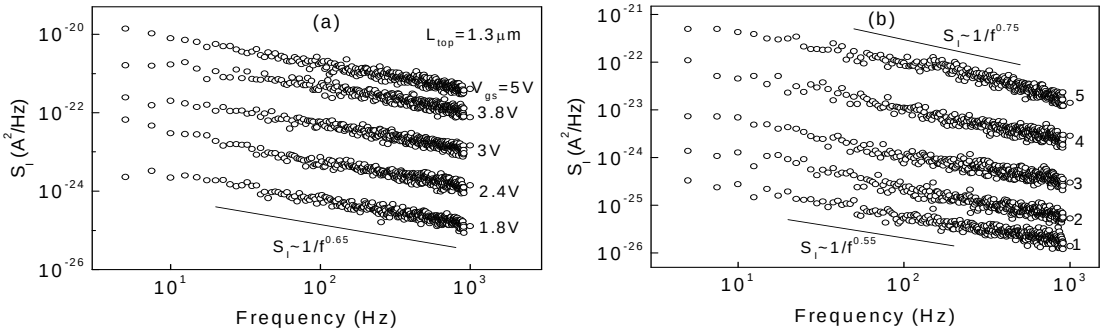

Fig. 3. *Typical noise spectra, measured at drain voltage V_{ds} = 0.1 V and different drain currents in a DG polysilicon TFT with W = 8 μm, L_{top} = 1.3 μm and L_{bottom} = 2.5μm before (a) and after stressing (b).*

In the case of longer DG TFT (L_{top} = 1.3 μm), the drain current noise spectra show $1/f^{\gamma}$ behavior, with $\gamma < 1$, both before and after stress, as shown in Fig. 3. This fact indicates a non-uniform trap distribution with increasing density towards the interface, with a greater number of high-frequency traps. As shown in Fig. 4 (left), the $1/f^{\gamma}$ noise in the 1.3 μm unstressed TFT exhibits a γ value of 0.65, independent of gate bias. The normalized drain current spectral density S_I / I_{ds}^2 versus I_{ds} plot, in Fig. 4 (right) shows that the flicker noise is due to the carrier number with correlated mobility fluctuation model; the density of the interface traps calculated from the obtained value of S_{Vfb} is 2.7×10^{12} cm^{-2} eV^{-1}. It is noticed that in unstressed devices N_t is lower when the top gate length is reduced, which can be explained as a short channel effect. After stress the exponent γ increases with increasing gate bias; this means that the trap concentration becomes higher towards the band edges and thus the channel carriers tunneling into the gate oxide encounter an increasing trap density due to band-bending caused by the gate bias. This indicates a hot-carrier stress-induced generation of band tail states (spatially located at the grain boundaries and sub-boundaries), which explains the pronounced stress-induced on-state current decrease in long channel DG polysilicon TFTs, in which a large number of grain boundaries and sub-boundaries are present in the channel. Thus, these low frequency noise measurement results support the degradation mechanisms of DG ELA polysilicon TFTs inferred from electrical bias stress measurements.

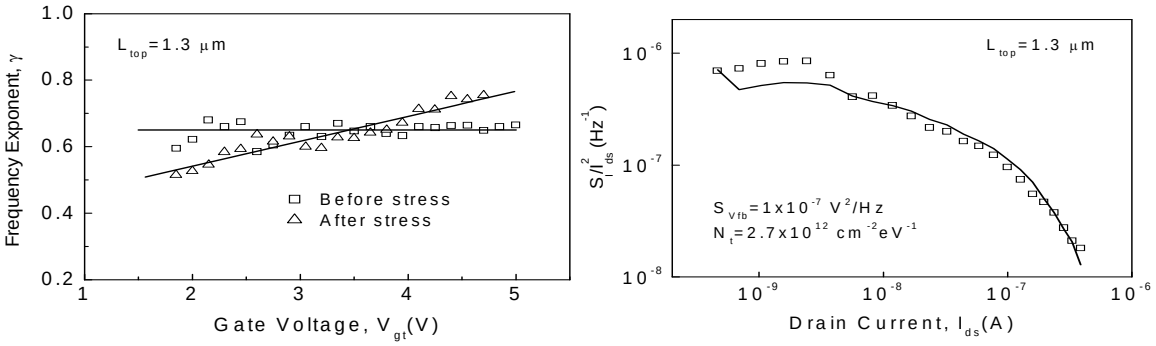

Fig. 4. *Frequency noise exponent vs. gate voltage for a DG polySi TFT with W = 8 μm, L_{top} = 1.3 μm and L_{bottom} = 2.5 μm before stress and after stress (left). Normalized drain current spectral density S_I / I_{ds}^2 as a function of drain current I_{ds} measured at f = 50 Hz for a DG polySi TFT with W = 8 μm, L_{top} = 1.3 μm and L_{bottom} = 2.5 μm before stress; the solid line corresponds to $S_{Vfb}\times(g_m/I_{ds})^2$ and the symbols to experimental data (right).*

Task 3: Characterization of thin film polysilicon photovoltaic elements

This investigation is being performed by Dr. Moschou in a cooperation relevant to the project's aims, as it concerns a thin film technology, in this case for photovoltaic applications. In this work, a Sun Simulator instrument was used for the controlled illumination of tandem thin film devices, fabricated with different polysilicon thin film deposition technologies. Three different

photovoltaic elements, fabricated by Heliosphera, were measured under illumination of controlled intensity to extract their operating parameters and elucidate their dependence on illumination. The light source had a spectrum set to very closely approach that of the Sun; it supplied incident energy density of 127 W/m^2 to 1114 W/m^2 (A.M 1.5), as measured with a photometer. As expected, for all samples a rise in the electric current with increasing incident light intensity was observed, with differences in their efficiency corresponding to the differing fabrication technique. The open circuit voltage seemed to increase with incident power for all samples in an almost logarithmic fashion. We also observed a nearly linear increase of derived power with incident illumination. Finally, the dependence of the efficiency factor on light intensity in the radiation range under investigation was evident. In the case of amorphous silicon films an initial increase of the efficiency factor with subsequent stabilization is observed. For the tandem devices a maximum in efficiency is observed at an intermediate optical power value; the efficiency is certainly higher than that of amorphous silicon samples.

PROJECT OUTPUT in 2012

Publications in International Refereed Journals

1. *Short channel effects on LTPS TFT degradation,*
   Moschou, D.C., C.G. Theodorou, N.A. Hastas, A. Tsormpatzoglou, D.N. Kouvatsos, A.T. Voutsas and C.A. Dimitriadis, , in press
   Journal of Display Technology
2. *Vg,max - Vth: A new electrical characterization parameter reflecting the polysilicon film quality of LTPS TFTs,*
   Moschou, D.C., F.V. Farmakis, D.N. Kouvatsos and A.T. Voutsas,
   Microelectronic Engineering 90, 76, February 2012
3. *Hydrogen passivation on sequential lateral solidified poly-Si TFTs,*
   Michalas, L., M. Koutsoureli, G.J. Papaioannou, D.N. Kouvatsos and A.T. Voutsas
   Microelectronic Engineering 90, 72, February 2012
4. *On the optical properties of SLS ELA polycrystalline silicon films,*
   Moschou, D.C., N. Vourdas, D. Davazoglou, D.N. Kouvatsos, V.E. Vamvakas and A.T. Voutsas
   Microelectronic Engineering 90, 69, February 2012

Conference Presentations

1. *Short channel effects in double gate polycrystalline silicon SLS ELA TFTs,*
   D.C. Moschou, D.N. Kouvatsos and A.T.Voutsas
   Proceedings of the 28th International IEEE Conference on Microelectronics (MIEL 2012), Nis, Serbia, May 2012 (to appear)
2. *Trap properties of asymmetrical double gate polysilicon thin-film transistors with low frequency noise in terms of the grain boundaries direction,*
   N. Hastas, A. Tsormpatzoglou, D.N. Kouvatsos, D.C. Moschou, A.T. Voutsas and C.A. Dimitriadis
   Proceedings of the 28th International IEEE Conference on Microelectronics (MIEL 2012), Nis, Serbia, May 2012 (to appear)
3. *Short channel effects on LTPS TFT degradation,*
   D.C. Moschou, N.A. Hastas, A. Tsormpatzoglou, D.N. Kouvatsos, C.A. Dimitriadis, and A.T. Voutsas
   Proceedings of the 8th International TFT Conference (ITC 2012), Lisbon, Portugal, January 2012.

PROJECT III.4
CIRCUITS & DEVICES FOR SENSOR NETWORKS & SYSTEMS

Project Leaders: S.Chatzandroulis, H.Contopanagos

PhD Students: P. Broutas

External Collaborators: E.D. Kyriakis-Bitzaros (TEI of Piraeus)

OBJECTIVES

The main objective of the activity is the development of the necessary technologies for future sensor networks and systems. In the context of this objective the research targets of sensor readout, wireless telemetry, RF remote powering in the near as well as the far field are pursued. Special consideration is given in operation in special environments such as large engineering structures (e.g. buildings, bridges, naval ships etc).

MAIN RESULTS in 2012

Wireless telemetry and RF remote powering of sensor tags

RF power-harvesting systems are of particular interest in autonomous sensor tag design because of their ability to draw power from electromagnetic fields generated by controlled and stable RF power sources. RF sensor tags are based on the technology of RF identification systems which are widely used in product chain applications. A variety of real-time monitoring applications such as structural health monitoring in large structures, often require the deployment of such remotely powered sensor tags. In this case the tags are often installed in inaccessible places or integrated in the monitored structure during construction.

In this work, a power-harvester with an embedded antenna operating at the 430 MHz band capable of operating near ground or metal planes has been developed. The tag uses discrete components including an onboard microcontroller for supervision of system functions and interfacing with different types of low power sensors, thus resulting to a flexible passive sensor platform. Furthermore, the system comprises a low-profile optimized multi-slotted PIFA (Planar Inverted F Antenna) integrated within the system volume, which enables operation near metal and ground surfaces, and results in a slim packaged system. A power harvesting strategy that allows tag operation over cycles has been implemented in order to allow operation at an incident power level that is lower than the power required when the tag is fully active. Tag operation is divided in two cycles; a standby mode during which only the energy-accumulation supervising circuit is active, as well as a fully operational mode.

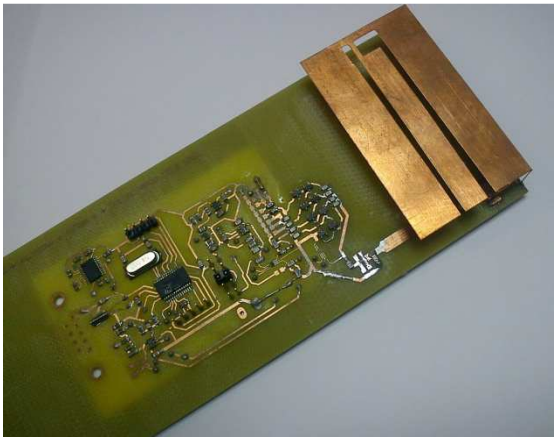

Fig. 1. *System implementation on FR4 PCB with the PIFA antenna.*

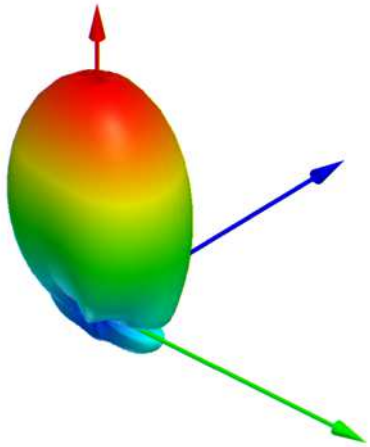

Fig. 2. *Simulated radiated gain of the antenna with the backplane 1cm apart.*

In order to compare the performance of the selected PIFA antenna to a half-wavelength dipole antenna, measurements with a Vector Network Analyzer (VNA) in free space as well as near a metal plate have been performed in order to compare the two antennas. In addition, a wireless link established between a low power base station emitting 200 mW of power at 430 MHz and the tag placed at 1cm distance from a metal plane has been demonstrated.

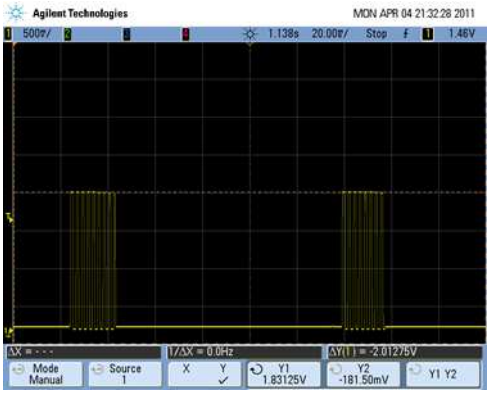

Fig. 3. *Output pulse train of the microcontroller, with the system placed 1cm apart from the metal plane.*

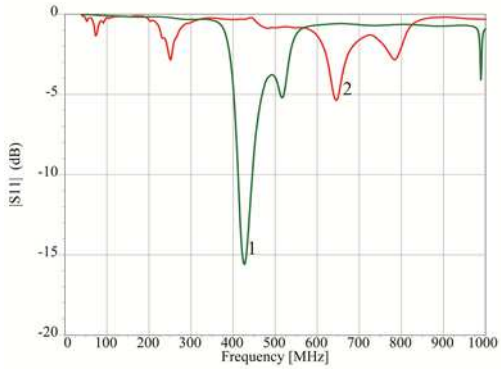

Fig. 4. *Comparison of the PIFA antenna performance (curve 1) to the dipole antenna (curve 2) at a distance of 1cm above a metal plate*

PROJECT OUTPUT in 2012

Publications in International Refereed Journals

1. *Embedded multi-slotted PIFAs for remotely powered passive UHF RFID tags,*
   H. Contopanagos, P. Broutas and S. Chatzandroulis
   Microwave and Opt. Tech. Lett., Vol. 54, No. 10 (October 2012), pp. 2379-2383
2. *A RF power harvester with integrated antenna capable of operating near ground planes,*
   P. Broutas, H. Contopanagos, D. Tsoukalas and S. Chatzandroulis
   Sensors and Actuators A, Vol. 186, (October 2012), pp. 284-288
3. *A low-power RF harvester for a smart passive sensor tag with integrated antenna,*
   P. Broutas, H. Contopanagos, E. Kyriakis-Bitzaros, D. Tsoukalas and S. Chatzandroulis
   Sensors and Actuators A, Vol. 176 (April 2012), pp. 34-45

PROJECT III.5

PHOTONIC CRYSTALS, METAMORPHIC MATERIALS AND NOVEL RF SYSTEMS

Project Leader: H. Contopanagos

External Collaborators: C. Kyriazidou, N. Alexopoulos (Broadcom Corporation, Irvine, USA); F. De Flaviis (University of California, Irvine, USA)

OBJECTIVES

To design, optimize and fabricate photonic crystals and frequency-agile metamaterials (metamorphic materials) for electromagnetically active filters, substrates and radomes for applications in novel embedded antenna architectures, filters, waveguides and resonators operating in the microwave/mm-wave region, for applications in novel RF transceivers.

MAIN RESULTS in 2012

Design, Fabrication and Measurement of Spiral Artificial Magnetic Conductors and Dipole Antennas integrated on-package for single-chip 60 GHz Radio Transceivers

The new generation of integrated radio transceivers operating at 60-GHz offer unsurpassed communication band width up to 9 GHz and data transmission speeds unmatched by current devices. These transceivers require antenna elements and arrays optimally designed and integrated close to transceiver dies, preferably embedded on-package. Artificial Magnetic Conductors (AMCs) are promising artificial materials for antenna integration. We develop the theory and extract the design rules of novel package-integrated dipole antennas on a spiral AMcs. Design and fabrication are subject to the essential package technology constraints and performance requirements crucial to 60GHz radios: Large bandwidths (≥15%) covering the 57-66 GHz spectrum plus extra band-edge to allow for parasitic detuning; Directional broadside radiation with minimal back radiation on the die side, necessary for realizing highly directional and steerable arrays; Small areas and thin profiles fitting on-package integration and layout rules. In this work we present novel designs of package-integrated antennas and arrays on spiral AMCs, satisfying all the above technology and performance requirements. Further, we present prototype fabrication details and measurements of a novel package-integrated dipole antenna on a spiral AMC. The design principles used, have been presented quite generally in [1]. The measured results presented here [2] show an impedance matching bandwidth far exceeding the required spectrum and 5 dBi broadside gain for a single-element AMC- antenna system occupying a package area of 1.65×2.75 mm^2.

Fabrication and measurement of On-Package Spiral AMC Dipole Antenna

The package-integrated AMC/dipole system containing 3×5 spiral AMC Unit Cells (UC), is shown as fabricated in Fig. 1a. The dipole is 1.42 mm long and 100um wide and is fed through vertical vias that traverse the whole package and end up in a Ground-Signal-Ground (GSG) pad configuration directly probed in our measurements. When connected to the underlying die, it will be fed by a coplanar-waveguide of the same characteristic impedance. Fig. 1a shows our GSG to dipole transition that has been implemented in the design for impedance matching. The AMC UC contains a square spiral leaving a margin of 15 um from the UC edges, and a metal trace width of 100um. The spiral contains 1.25 turns and the long and short spiral metal gaps are 30 um.

The spiral AMC has been designed to project tuned AMC behavior at the package metal layer where the dipole is printed, according to the design rules of [1]. Fig. 1b shows HFSS simulations of the reflection coefficient for normal plane-wave incidence on the transversely infinite packaged AMC of Fig. 1a, de-embedded up to the antenna metallization layer. We observe a broadband AMC behavior, quantified by $\mathrm{Re}\{S_{11}(f)\}\geq 0$, ranging from 46-58 GHz. According to the design rules in [1], an appropriately designed dipole antenna printed on this material will radiate and can have excellent matching in the frequency band starting from the AMC peak (~52 GHz) and up to at least the frequency where $\mathrm{Re}\{S_{11}(f_0)\}=\mathrm{Im}\{S_{11}(f_0)\}$(~66 GHz). This on-package spiral AMC has a total thickness of λ/20, where λ is the wavelength in air at the AMC peak of 52 GHz. Hence it is appropriately thin for package integration.

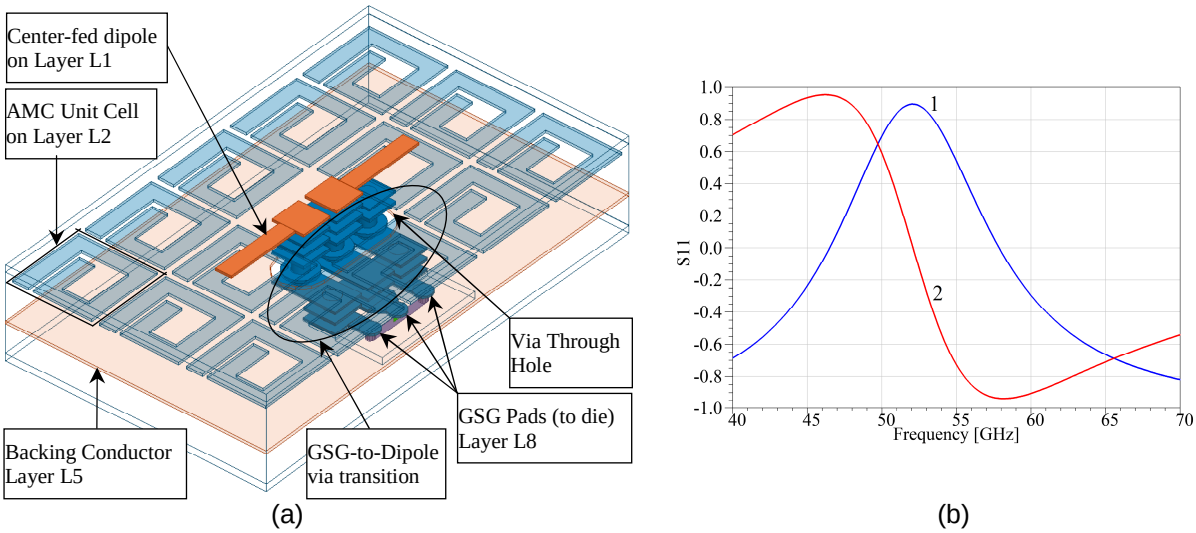

***Fig.1**. (a) 3D view of on-package spiral AMC dipole antenna. AMC UC size: 0.55×0.55 mm^2. System size: 1.65×2.75 mm^2. (b) AMC complex reflection coefficient* $S_{11}=[1]+j[2]$.

Let us now briefly describe our measurement set-up. Since the antenna operates at V band and has a coplanar differential feed we used a contact GSG 50-Ohm probe to feed it on the opposite side from where radiation occurs. To land the probe we clearly cannot use a traditional probe station set up where the sample is normally placed on a metal chuck for the measurement as that would block its radiation and corrupt the antenna return loss as well. To overcome these difficulties a dedicated system was designed. The system consists of a probe positioner mounted on a large plexiglass plate where a square hole in the center of the plate is used to support the antenna leaving free its radiating side. Probing is done on the back side (with respect to the radiation), therefore the antenna is free to radiate downward during probing. The system is mounted on an optically isolated table for easy probing, equipped with a digital microscope. A computer-controlled rotating arm with a V band receiver moves around the antenna to collect its radiation. Antenna, probe and receiver antenna can be rotated by 90° individually, to allow collecting four radiation patterns at each frequency (E-plane, H-plane, Co-pol and Cross-pol). A conical horn having 21dB gain is used to calibrate the system and extract the absolute gain information of our antenna.

In Fig. 2a we show the measured return loss of the system of Fig. 1a. The antenna is quite broadband, with excellent matching and a -10 dB matching band extending from 57 GHz up to well above 67 GHz (maximum frequency of our analyzer), by far exceeding the 60-GHz radio application range (57-66 GHz). Fig. 2b shows the maximum antenna gain above the dipole center, versus frequency. Simulations and measurements are in good agreement and the maximum measured gain averages to 5dBi, showing a directive compact antenna.

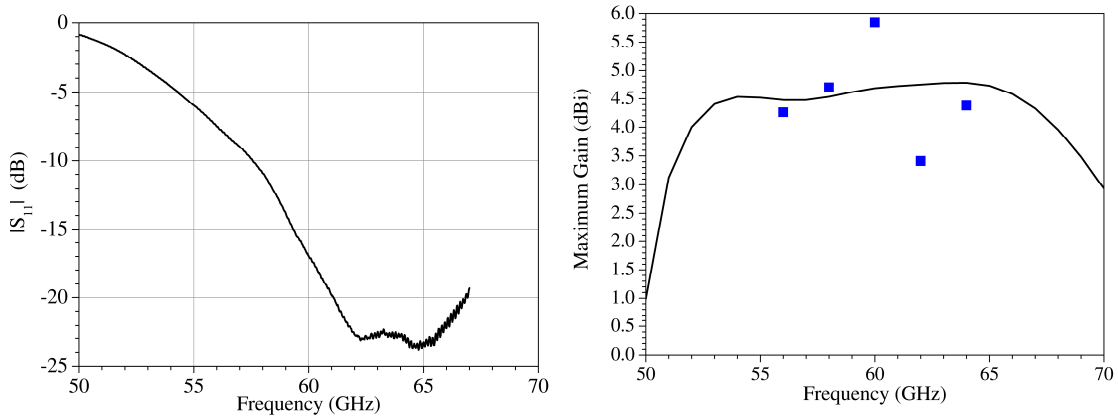

(a) (b)

***Fig.2**. (a) Measured return loss of the system of Fig. 1a. (b) HFSS simulations (solid curve) and measurements (discrete points) of the maximum gain.*

In conclusion, we presented the design and measurements of a novel antenna and spiral AMC system integrated on-package appropriate for on-chip 60 GHz radio transceivers. A single-element shows measured gain of about 5 dBi and impedance bandwidth far greater than needed for these applications. The overall on-package system size is quite small, at 1.65×2.75 mm^2, making this system very promising for on-package array implementations, for 60 GHz radio applications.

PROJECT OUTPUT in 2012

Publications in International Refereed Journals

1. *Space-Frequency projection of Planar AMCs on integrated antennas for 60 GHz radios,*
   C. Kyriazidou, H. Contopanagos and N. Alexopoulos, IEEE Transactions on Antennas and Propagation, Vol. 60, No. 4 (April 2012), pp. 1899-1909.

Published Conference Proceedings

1. *Planar Spiral AMCs integrated on 60 GHz Antennas,*
   H. Contopanagos, C. Kyriazidou, F. De Flaviis and N. Alexopoulos, IEEE Antennas and Propagation Society Intl. Symposium Digest, Chicago, IL, USA, 8-14 July 2012, pp.1-2.

ANNEXES

ANNEX I: PERSONNEL

RESEARCHERS

1. Argitis P.
2. Chatzandroulis S.
3. Contopanagos H.
4. Davazoglou D.
5. Gardelis S.
6. Glezos N.
7. Gogolides E.
8. Ioannou-Sougleridis V.
9. Kouvatsos D.
10. Misiakos K.
11. Nassiopoulou A. G.
12. Normand P.
13. Papanikolaou N.
14. Raptis I.
15. Tsamis C.
16. Tserepi A.
17. Tsoukalas D.

TECHNICAL AND ADMINISTRATIVE PERSONNEL

1. Bolomiti E. (Contract)
2. Boukouras K. (Contract)
3. Fillipidou M. (Contract)
4. Georgiou Ch.
5. Kalpouzou M. (Contract)
6. Karmpadaki M. (Contract)
7. Lagouvardou M.
8. Matziaris G. (Contract)
9. Mavropoulis I.
10. Mpotsialas A. (Contract)
11. Sergis E.
12. Skoulikidou Ch. (Contr.)
13. Tokpasidou E.
14. Zeniou A. (Contract)

POST DOCTORAL SCIENTISTS

1. Chronis N. (Contract)
2. Gianneta V. (Contract)
3. Giannakopoulos K. (Contr.)
4. Hourdakis E.
5. Kokkoris G.
6. Makarona E. (Contract)
7. Moschou D. (Contract)
8. Olziersky A. (Contract)
9. Papadakis G. (Contract)
10. Papadimitropoulos G. (Contr.)
11. Sotiropoulos A. (Contract)
12. Tsipas P. (Contract)
13. Tsougeni K. (Contract)
14. Tsouti V.
15. Velessiotis D.
16. Vourdas N. (Contract)

OTHER SCIENTIFIC STAFF

1. Constandoudis V.
2. Dimitrakis P.
3. Douvas A.
4. Vasilopoulou M.

PhD STUDENTS

1. Almpanis E.
2. Aksenov G. (Contract)
3. Broutas P.
4. Ellinas K. (Contract)
5. Georgiadou D.
6. Kuppuaswamy V. (Contr.)
7. Leontis I. (Contract)
8. Manouras T.
9. Manousiadis P.
10. Mpalliou A.
11. Niarchos G.
12. Oikonomou P.
13. Ramfos I. (Contract)
14. Salapatas A. (Contract)
15. Sarafis P. (Contract)
16. Skoro N. (Contract)
17. Smyrnakis A.
18. Valalaki K. (Contract)

ANNEX II : INFRUSTRUCTURE

PROCESSING

Equipment	Techniques/competences
Silicon processing laboratory in a clean room area of 300 m^2, equipped with the following: ■ 4 laminar flow benches for acids and solvents ■ 7 horizontal hot-wall atmospheric pressure diffusion furnaces ■ 2 horizontal LPCVD tubes for nitride & oxide (TEOS) and polysilicon ■ 1 horizontal LPCVD tube for LTO ■ Ion Implanter (EATON medium current, 200 KeV) ■ Optical lithography (i-line) Mask Aligners (resolution down to 0.6 μm) ■ E-beam lithography 100keV (Vistec EBPG5000+) ■ Reactive Ion Etching tool ■ Metallization equipment (Thermal & e-gun evaporation) ■ Optical microscope for wafers inspection ■ Rapid thermal Processing tool **Processing equipment not in clean room:** ■ High Density Plasma Etcher ■ Thin film deposition systems ■ Anisotropic Si etching bench	■ Nanopatterning technologies ■ Advanced Plasma etching, processing and simulation ■ Deposition of high quality dielectrics ■ Deposition of polycrystalline and nanocrystalline Si ■ Fabrication of Si nanostructures embedded in a dielectric matrix, ordering of nanostructures ■ Fabrication of CMOS devices ■ Fabrication of nanoscaled CMOS devices (FinFET, NWFETs) ■ Nanocrystal non-volatile memories ■ Micromachining, sensor fabrication, microfluidics ■ Molecular materials and devices ■ Thin film devices 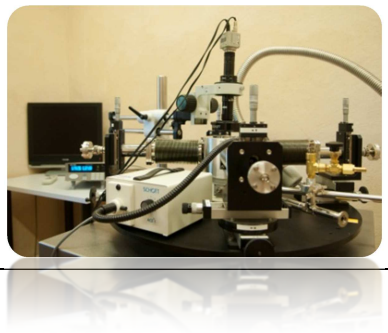

CHARACTERIZATION & MODELLING

Equipment	Techniques/competences
DC Electrical measurements ■ 3 probe stations for wafer level measurements ■ HP measuring systems (4142B, 4084B, 8110A, 4140B, 4284, 4192A, 34401, 16500A) ■ Keithley measuring equipment (230, 220, 617, 195A, 6517A) ■ Oxford cryostat for temperatures in the range LN-320K ■ Janis low temperature wafer prober(4 probes) ■ Semiconductor Parameter Analyzer **RF measurements** ■ Anritsu 37269D Vector Network Analyzer 40MHz-	**Characterization of Dielectrics** ■ Admittance/Impedance measurements (10Hz-1MHz, LN-400K) ■ -V measurements (2 up to 4-terminal devices, LN-400K) ■ Dielectric strength and charge-to-breakdown measurements (ISO/IEC 17025) ■ Bias-Temperature-Stress measurements **Characterization of MIS Devices** ■ Admittance/Impedance measurements (10Hz up to 1MHz, LN-400K) ■ I-V measurements (2 up to 4-terminal devices, LN-400K)

40GHz

- Cascade Microtech Summit 9101 Analytical Probe Station for 150mm wafers

Optical

- Jobin Yvon spectrometer, 300-1600nm
- Ar+ laser
- HeCd 325 nm laser
- UV-Vis spectrometer
- Oxford optistat cryostat, 4.2-320K
- FTIR: Bruker, Tensor 27

Morphology, structural characterization

- JEOL JSM-7401F FEG SEM, Point-to-point resolution below ~1nm
- Leo 440 SEM with Elphy/Raith e-beam lithography attachment
- AFM (Veeco CP-II)
- KLA-Tencor XP-2 Stylus profilometer
- STM (NT-MDT)

Testing equipment

- Systems for testing of gas flow, gas pressure, acceleration, humidity sensors, biosensors and systems, microfluidics testing etc.

Modeling and simulation software

- Synopsys TCAD for process and device modeling
- Floops and Floods
- Synopsis – Coventorware
- Mentor graphics
- BeamPROP, FemSIM (RSoft suite)
- COMSOL
- RF modeling

- Hot-carrier stress measurements
- Bias-Temperature-Stress measurements

EEPROM device characterization and reliability measurements
Characterization of RF components

Optical characterization

- Absorption measurements in UV-VIS-IR wavelength range
- Photoluminescence (PL)
- Laser excitation: 325 nm, 457.8nm, 488nm, 514.5nm
- Spectrometer: 350nm-1600nm
- Electroluminescence (EL): 350nm-1600nm
- Photocurrent-photovoltage (UV-VIS)
- FTIR

Characterterization of sensors

- Gas sensors
- Microflow sensors
- Accelerometers
- Optical devices
- Biosensors
- Microfluidics

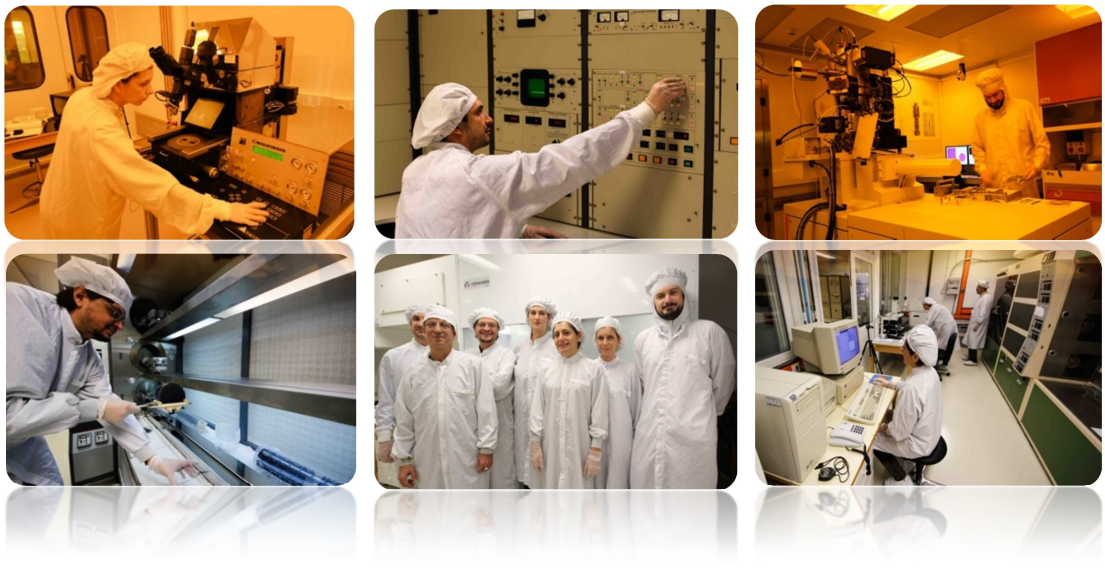

ANNEX III: RESEARCH AND EDUCATION OUTPUT

Publications in International Refereed Journals and Published Conference Proceedings

1. M. Vasilopoulou, A.M. Douvas, D.G. Georgiadou, L.C. Palilis, S. Kennou, L. Sygellou, A. Soultati, I. Kostis, G. Papadimitropoulos, D. Davazoglou P. Argitis
   The influence of hydrogenation and oxygen vacancies on molybdenum oxides work function and gap states for application in organic optoelectronics
   Journal of the American Chemical Society, 134, 16178-16187 (2012)
2. M. Vasilopoulou, L.C. Palilis, D. G. Georgiadou, S. Kennou, I. Kostis, D. Davazoglou, P. Argitis
   Barrierless hole injection through sub-bandgap occupied states in OLEDs using substoichiomeric MoOx anode interfacial layer
   Applied Physics Letters, 100, 013311 (2012)
3. M. Vasilopoulou, D.G. Georgiadou, L.C. Palilis, P. Argitis, S. Kennou, L. Sygellou, N. Konofaos, A. Iliadis, I. Kostis, G. Papadimitropoulos, D. Davazoglou
   Reduced Transition Metal Oxides as Electron Injection Layers in Hybrid-PLEDs
   Microelectronic Engineering, 90, 59-61, (2012)
4. M. Vasilopoulou, G. Papadimitropoulos, L.C. Palilis, D. G. Georgiadou, P. Argitis, S. Kennou, I. Kostis, N. Vourdas, N.A. Stathopoulos, D. Davazoglou
   High performance organic light emitting diodes using substoichiometric tungsten oxide as efficient hole injection layer
   Organic Electronics, 13, 796-806 (2012)
5. M. Vasilopoulou, A.M. Douvas, P. Argitis
   Patternable Fluorinate Polyhedral Oligomeric Silsequioxane-Functionalized polymer materials with ultra low dielectric constants
   Materials Chemistry and Physics, 135, 880-83 (2012)
6. D. Velessiotis, A.M. Douvas, P. Dimitrakis, P. Argitis, N. Glezos
   Conduction mechanisms in tungsten-polyoxometalate self-assembled molecular junctions
   Microelectronic Engineering, 97, 150-53 (2012)
7. D. G. Georgiadou, L. C. Palilis, M. Vasilopoulou , G. Pistolis , D. Dimotikali and P. Argitis
   Effect of triphenylsulfonium triflate addition in wide band-gap polymer light-emitting diodes: improved charge injection, transport and electroplex-induced emission tuning
   RSC Advances, 2, 11786-11792 (2012)
8. N.Vourdas, G. Papadimitropoulos, I. Kostis, M. Vasilopoulou, D. Davazoglou
   Substoichiometric hot-wire WO_x films deposited in reducing environment
   Thin Solid Films, 520, 3614 (2012)
9. N. Vourdas, K. Dalamagkidis, I. Kostis, M. Vasilopoulou, D. Davazoglou
   Omnidirectional antireflective properties of porous tungsten oxide films with in-depth variation of void fraction and stoichiometry
   Optics Communications, 285, 5229-5234, (2012)
10. D. Kontziampasis, V. Constantoudis, E. Gogolides
    Plasma directed organization of nanodots on polymers: Effects of polymer type and etching time on morphology and order
    Plasma Processes and Polymers, 9, 866-872 (2012)
11. M.K., Vijaya-Kumar, V. Constantoudis, E. Gogolides, A.V. Pret, R. Gronheid
    Contact edge roughness metrology in nanostructures: Frequency analysis and variations
    Microelectronic Engineering, 90, 126-130 (2012)
12. V. Constantoudis, G. P. Patsis, E. Gogolides
    Fractals and device performance variability: The key role of roughness in micro and nanofabrication
    Microelectronic Engineering, 90, 121-125 (2012)
13. G. Kokkoris, E. Gogolides
    The potential of ion-driven etching with simultaneous deposition of impurities for inducing periodic dots on surfaces
    Journal of Physics D: Applied Physics, 45, 165204 (2012)
14. N. Cheimarios, G. Kokkoris and A. G. Boudouvis
    Multiscale computational analysis of the interaction between the wafer micro-topography and the film growth regimes in chemical vapor deposition processes
    ECS Journal of Solid State Science and Technology, 1, 197-203 (2012)
15. A. K. Karlis,F. K. Diakonos, V. Constantoudis
    A consistent approach for the treatment of Fermi acceleration in time-dependent billiards
    Chaos, 22, 026120 (2012)
16. P. K. Papachristou, E. Katifori, F. K. Diakonos, V. Constantoudis, E. Mavrommatis

Quantum versus classical dynamics in a driven barrier: The role of kinematic effects
Physical Review E - Statistical, Nonlinear, and Soft Matter Physics, 86, 036213 (2012)

17. M. Kalimeri, V. Constantoudis, C. Papadimitriou, K. Karamanos, F. K. Diakonos, H. Papageorgiou
Entropy analysis of word-length series of natural language texts: Effects of text language and genre
International Journal of Bifurcation and Chaos, 22, 1250223 (2012)
18. A. Skarmoutsou, C. A., Charitidis, A. K. Gnanappa, A. Tserepi, E. Gogolides
Nanomechanical and nanotribological properties of plasma nanotexturedsuperhydrophilic and superhydrophobic polymeric surfaces
Nanotechnology, 23, 505711 (2012)
19. A.K. Gnanappa, D.P. Papageorgiou, E. Gogolides, A. Tserepi, A. G. Papathanasiou, A.G. Boudouvis
Hierarchical, plasma nanotextured, robust superamphiphobic polymeric surfaces structurally stabilized through a wetting-drying cycle
Plasma Processes and Polymers, 9, 304-315 (2012)
20. D. P. Papageorgiou, A. Tserepi, A.G. Boudouvis, A.G. Papathanasiou
Superior performance of multilayered fluoropolymer films in low voltage electrowetting
Journal of Colloid and Interface Science, 368, 592-598 (2012)
21. T. Rudin, K. Tsougeni, E. Gogolides, S. E. Pratsinis
Flame aerosol deposition of TiO2 nanoparticle films on polymers and polymeric microfluidic devices for on-chip phosphopeptide enrichment
Microelectronic Engineering, 97, 341-344 (2012)
22. K. Tsougeni, G. Koukouvinos, P.S. Petrou, A. Tserepi, S. E. Kakabakos, E. Gogolides
High-capacity and high-intensity DNA microarray spots using oxygen-plasma nanotextured polystyrene slides
Analytical and Bioanalytical Chemistry, 403, 2757-2764 (2012)
23. A. Malainou, P. S. Petrou, S. E. Kakabakos, E. Gogolides, A. Tserepi
Creating highly dense and uniform protein and DNA microarrays through photolithography and plasma modification of glass substrates
Biosensors and Bioelectronics, 34, 273-281 (2012)
24. K. Tsougeni, P. S. Petrou, D. P. Papageorgiou, S. E. Kakabakos, A. Tserepi, E. Gogolides
Controlled protein adsorption on microfluidic channels with engineered roughness and wettability
Sensors and Actuators, B: Chemical, 161, 216-222 (2012)
25. D. C. Moschou, N. Vourdas, D. Davazoglou, D.N. Kouvatsos, V.E., Vamvakas, A.T. Voutsas
On the optical properties of SLS ELA polycrystalline silicon films
Microelectronic Engineering, 90, 69 (2012)
26. G. Papadimitropoulos, I. Kostis, R. Triantafyllopoulou, V. Tsouti, M. Vasilopoulou, D. Davazoglou
Investigation of porous hot-wire WO_3 thin films for gas sensing application
Microelectronic Engineering, 90, 51 (2012)
27. I. Kostis, L. Michalas, M. Vasilopoulou, N. Konofaos, G. Papaioannou, A. A. Iliadis, S. Kennou, K. Giannakopoulos, G. Papadimitropoulos, D. Davazoglou
Hot-wire substoichiometric tungsten oxide films deposited in hydrogen environment with n-type conductivity
Journal of Physics D: Applied Physics, 45, 445101 (2012)
28. E. Hourdakis and A. G. Nassiopoulou
High performance MIM capacitor using anodic alumina dielectric
Microelectronic Engineering, 90, 12-14 (2012)
29. E. Hourdakis, P. Sarafis and A. G. Nassiopoulou
Novel Air Flow Meter for an Automobile Engine Using a Si Sensor with Porous Si Thermal Isolation
Sensors 12, 14838-14850 (2012)
30. E. Hourdakis, A. G. Nassiopoulou
Two-Terminal Charge-Trapping WORM Memory Device Using Anodic Aluminum Oxide
Journal of Nanoscience and Nanotechnology, 12, 7968-7974 (2012)
31. S. Gardelis, A. G. Nassiopoulou, P. Manousiadis, S. Milita, A. Gkanatsiou, N. Frangis, Ch. B. Lioutas
Structural and optical characterization of two-dimensional arrays of Si nanocrystals embedded in SiO_2 for photovoltaic applications
Journal of Applied Physics, 111, 083536 (2012)
32. P. Manousiadis, S. Gardelis, and A. G. Nassiopoulou
Lateral electrical transport and photocurrent in single and multilayers of two-dimensional arrays of Si nanocrystals
Journal of Applied Physics 112, 043704 (2012)
33. N. Nikolaou, P. Dimitrakis, P. Normand, V Ioannou-Sougleridis, K. Giannakopoulos, K. Mergia, K. Kukli, J. Niinistö, M. Ritala, M. Leskelä
Influence of atomic layer deposition chemistry on high-k dielectrics for charge trapping memories
Solid-State Electronics 68, 38-47 (2012)
34. R. Diaz, J. Grisolia, G. BenAssayag, S. Schamm-Chardon, C. Castro, B. Pecassou, P. Dimitrakis, P. Normand
Extraction of the characteristics of Si nanocrystals by the charge pumping technique
Nanotechnology 23, 085206 (2012)

35. C. Bonafos, M. Carrada, G. Benassayag, S. Schamm-Chardon, J. Groenen, V. Paillard, B. Pecassou, A. Claverie, P. Dimitrakis, E. Kapetanakis, V. Ioannou-Sougleridis, P. Normand, B. Sahu, A. Slaoui
Si and Ge nanocrystals for future memory devices (Review)
Materials Science in Semiconductor Processing 15, 615-626 (2012)
36. R. Diaz, C. Suarez, A. Arbouet, R. Marty, V. Paillard, F. Gloux, C. Bonafos, S. Schamm-Chardon, J. Grisolia, P. Normand, P. Dimitrakis, G. Benassayag
Implantation energy effect on photoluminescence spectroscopy of Si nanocrystals locally fabricated by stencil-masked ultra-low-energy ion-beam-synthesis in silica
Nuclear Instruments and Methods in Physics Research, Section B: Beam Interactions with Materials and Atoms 272, 53-56 (2012)
37. M. Botzakaki, A. Kerasidou, L. Sygellou, V. Ioannou-Sougleridis, N. Xanthopoulos, S. Kennou, S. Ladas, N.Z. Vouroutzis, Th. Speliotis, D. Skarlatos
Interfacial properties of ALD-deposited Al_2O_3/p-type germanium MOS structures: Influence of oxidized Ge interfacial layer dependent on Al_2O_3 thickness
ECS Solid State Letters 1, 32-34 (2012)
38. E. Almpanis, N. Papanikolaou, B. Auguié, C. Tserkezis, and N. Stefanou
Diffractive chains of plasmonic nanolenses: combining near-field focusing and collective enhancement mechanisms
Optics Letters, 37, 4624 (2012)
39. E. Almpanis, N. Papanikolaou, G. Gantzounis, N. Stefanou
Tuning the spontaneous light emission in phoxonic cavities
Journal of the Optical Society of America B, 29, 2567-2574 (2012)
40. A. Christofi, N. Stefanou, G. Gantzounis, N. Papanikolaou
Giant Optical Activity of Helical Architectures of Plasmonic Nanorods
Journal of Physical Chemistry C, 116, 16674−16679 (2012)
41. Ch.Kokkinos, A.Economou, I.Raptis
Microfabricated disposable lab-on-a-chip sensors with integrated bismuth microelectrode arrays for voltammetric determination of trace metals
Analytica Chimica Acta, 710, 1 (2012)
42. K.Manoli, P.Oikonomou, E.Valamontes, I.Raptis, M.Sanopoulou
Polymer-BaTiO3 Composites: Dielectric constant and vapour sensing properties in chemcapacitor applications
Journal of Applied Polymer Science, 125, 2577 (2012)
43. P.Oikonomou, A.Botsialas, D.Goustouridis, E.Valamontes, M.Sanopoulou, I.Raptis
Compensation of Temperature Variations in Chemcapacitive Gas Sensing Systems
Sensor Letters, 10, 736 (2012)
44. P.Oikonomou, A.Botsialas, K.Manoli, D.Goustouridis, E.Valamontes, M.Sanopoulou, I.Raptis, G.P.Patsis
Chemocapacitor performance modeling by means of polymer swelling optical measurements
Sensors and Actuators B, 409, 171-172 (2012)
45. V.Tsouti & S.Chatzandroulis
Sensitivity Study of Surface Stress Biosensors Based on Ultra-thin Si Membranes
Microelectronic Engineering, 90, 29-32 (2012)
46. V.Tsouti, C.Boutopoulos, M.Ioannou, D.Goustouridis, D.Kafetzopoulos, I.Zergioti, D.Tsoukalas, P.Normand, S.Chatzandroulis
Evaluation of Capacitive Surface Stress BioSensors
Microelectronic Engineering, 90, 37-39 (2012)
47. V. Tsouti, C. Boutopoulos, I. Zergioti, S. Chatzandroulis
Capacitive Microsystems for Biological Sensing,
Biosensors and Bioelectronics, 27, 1-11 (2012)
48. Ramfos, S. Chatzandroulis
A 16-channel capacitance-to-period converter for capacitive sensor applications
Analog Integrated Circuits & Signal Processing Analog Integrated Circuits and Signal Processing, 71, 383-389 (2012)
49. V. Tsouti, M.K. Filippidou, C. Boutopoulos, P. Broutas, I. Zergioti, S. Chatzandroulis
Self-Aligned Process for the Development of Surface Stress Capacitive Biosensor Arrays
Sensors and Actuators B, 166–167, 815-818 (2012)
50. G. Tsekenis, M. Chatzipetrou, J. Tanner, S. Chatzandroulis, D. Thanos, D. Tsoukalas, I. Zergioti
Surface functionalization studies and direct laser printing of oligonucleotides towards the fabrication of a micromembrane DNA capacitive biosensor
Sensors and Actuators B, 175, 123–131 (2012)
51. K.Awsiuk, A.Bernasik, M.Kitsara, A.Budkowski, P.Petrou, S.Kakabakos, S.Prauzner-Bechcicki, J.Rysz, I.Raptis
Spectroscopic and microscopic characterization of biosensor surfaces with protein/amino-organosilane/silicon structure
Colloids and Surfaces B, 90, 159 (2012)
52. D.C. Moschou, F.V. Farmakis, D.N. Kouvatsos and A.T. Voutsas

Vg,max - Vth: A new electrical characterization parameter reflecting the polysilicon film quality of LTPS TFTs
Microelectronic Engineering, 90, 76 (2012)
53. L. Michalas, M. Koutsoureli, G.J. Papaioannou, D.N. Kouvatsos and A.T. Voutsas
Hydrogen passivation on sequential lateral solidified poly-Si TFTs
Microelectronic Engineering, 90, 72 (2012)
54. H. Contopanagos, P. Broutas and S. Chatzandroulis
Embedded multi-slotted PIFAs for remotely powered passive UHF RFID tags
Microwave and Optical Technology Letters, 54, 2379-2383 (2012)
55. P. Broutas, H. Contopanagos, D. Tsoukalas and S. Chatzandroulis
A RF power harvester with integrated antenna capable of operating near ground planes
Sensors and Actuators A, 186, 284-288 (2012)
56. P. Broutas, H. Contopanagos, E. Kyriakis-Bitzaros, D. Tsoukalas and S. Chatzandroulis
A low-power RF harvester for a smart passive sensor tag with integrated antenna
Sensors and Actuators A, 176, 34-45 (2012)
57. C. Kyriazidou, H. Contopanagos and N. Alexopoulos
Space-Frequency projection of Planar AMCs on integrated antennas for 60 GHz radios
IEEE Transactions on Antennas and Propagation, 60, 1899-1909 (2012)
58. L. E. P. Kyllönen, V. Chinuswamy, D. Maffeo, E. T. Kefalas, Z. Pikramenou, I. M. Mavridis, K. Yannakopoulou, N. Glezos
Electronic transport between Au surface and STM tip via a multipodal cyclodextrin host - metallo-guest supramolecular system
Journal of Physical Organic Chemistry, 25, 198-206 (2012)
59. A. Kaloudi-Chantzea, N. Karakostas, F. Pitterl, C.P. Raptopoulou, N. Glezos, G. Pistolis
Efficient supramolecular synthesis of a robust circular light-harvesting Bodipy-dye based array
Chemical Communications, 48, 12213-12215 (2012)
60. N. Papanikolaou, Psarobas, I.E., Stefanou, N., Djafari-Rouhani, B., Bonello, B., Laude, V.
Light modulation in phoxonic nanocavities
Microelectronic Engineering, 90, 155-158 (2012)
61. A.C.Cefalas, E.Sarantopoulou, S.Kolia, M.Kitsara, I.Raptis, E.Bakalis
Entropic nanothermodynamic potential from molecular trapping within photon induced nano-voids in photon processed PDMS layer
Soft Matter, 8, 5561 (2012)
62. S. C. Boyatzis, A. M. Douvas, V. Argyropoulos, A. Siatou, M. Vlachopoulou
Characterization of a water-dispersible metal protective coating with fourier transform infrared spectroscopy, modulated scanning calorimetry, and ellipsometry
Applied Spectroscopy, 66, 580-590 (2012)
63. N. Škoro, E. Gogolides
Characterization of hydrogen based RF plasmas suitable for removal of carbon layers
Proceedings of 26thSPIG, Zrenjanin, Serbia, 231 (August 27-31, 2012)
64. G. Kokkoris, V. Constantoudis, E. Gogolides
3d modeling of LER transfer from the resist to the underlying substrate: The effect of the resist roughness
Proceedings of SPIE - The International Society for Optical Engineering, 8328, 83280V (2012)
65. V.-K.M. Kuppuswamy, V. Constantoudis, E. Gogolides, A. VaglioPret, R. Gronhei
Contact edge roughness and CD uniformity in EUV: Effect of photo acid generator and sensitizer
Proceedings of SPIE - The International Society for Optical Engineering, 8322, art. no. 832207 (2012)
66. V. Constantoudis, V.K. MurugesanKuppuswamy, E. Gogolides
Noise effects on contact edge roughness and CD uniformity measurement
Proceedings of SPIE - The International Society for Optical Engineering, 8324, art. no. 83240K. (2012)
67. K. Ellinas, K. Tsougeni, M. Vlachopoulou A. Tserepi, E. Gogolides
Hierarchical, Plasma Nanotextured, Superamphiphobic Polymeric Surfaces
Proceedings of 13th International Conference on Plasma Surface Engineering (2012)
68. V. Stathopoulos, A. Papandreou, N. Vourdas, A. Tserepi, E. Gogolides
Development and characterisation of superhydrophobic α-alumina ceramic membranes with plasma surface nanotexturing
Proceedings of Spring EMRS 2012 Meeting, Strasbourg, France (May 14-18, 2012)
69. N. Vourdas, D. Moschou, G. Kokkoris, G. Papadakis, S. Chatzandroulis, A. Tserepi
Development of a continuous-flow μPCR device with microheatingelementsintegrated with biosensors towards a LoC system for disease diagnosis
Proceedings of 3rd European Microfluidics Conference, paper no. 128 (2012)
70. K. Tsougeni, K. Ellinas, A. Glynou, T. Christoforidis, D.S. Mathioulakis, A. Tserepi, E. Gogolides
Flow study in randomly-rough superhydrophilic and superhydrophobic plasma nanotexturedmicrochannels using micro-PIV
Proceedings of 3rd European Microfluidics Conference, paper no. 132 (2012)
71. K. Ellinas, K. Tsougeni, P.S. Petrou, D.P. Papageorgiou, S.E. Kakabakos, A. Tserepi, E. Gogolides
Control of flow and protein adsorption on plasma nanotextured microfluidics

Proceedings of 3rd European Microfluidics Conference, paper no. 133 (2012)
72. E. Demenev, D. Giubertoni, S. Gennaro, M. Bersani, E. Hourdakis, A. G. Nassiopoulou, M. A. Reading and J. A. van den Berg
Arsenic Redistribution After Solid Phase Epitaxial Regrowth Of Shallow Pre-Amorphized Silicon Layers
AIP Conference Proceedings 1496, 272 (2012)
73. P. Dimitrakis, P. Normand, C. Bonafos, E. Papadomanolaki, E. Iliopoulos
GaN quantum dots as charge storage elements for memory devices
Materials Research Society Symposium Proceedings 1430, 29-34 (2012)
74. D. Simatos, P. Dimitrakis, V. Ioannou-Sougleridis, P. Normand, K. Giannakopoulos, B. Pecassou, G. BenAssayag
SONOS memory devices with ion beam modified nitride layers
Materials Research Society Symposium Proceedings, 1430, 35-40 (2012)
75. E. Verrelli, D. Tsoukalas, P. Normand, N. Boukos, A.H. Kean
Resistive switching memory using titanium-oxide nanoparticle films
Proceedings of the European Solid-State Device Research Conference 2012, Article number 6343382, 258-261 (2012)
76. A. Christofi, N. Stefanou, G. Gantzounis, N. and Papanikolaou
Helical assemblies of plasmonic nanorods as chiral metamaterials
Proceedings of SPIE, 8423, 84230A (2012)
77. N. Papanikolaou, G. Gantzounis, E. Almpanis, N. Stefanou
Acousto-optic interaction enhancement in dual photonic-phononic cavities
Proceedings of SPIE, 8425, 84250M (2012)
78. E.Valamontes, G.Patsis, D.Goustouridis, P.Oikonomou, A.Botsialas, I.Raptis, M. Sanopoulou
Real time detection of volatile organic compounds through a chemocapacitor system
IMCS 2012 (Nuremberg, Germany, 05/2012)
79. M.-I.Georgaki, A.Botsialas, P.Argitis, M.Chatzichristidi, J.Rysz, A.Budkowski, I.Raptis
Zero-Power humidity sensor based on 1-D photonic crystal colour change
EuroPtrode 2012 (Barcelona, Spain, 04/2012)
80. D.C. Moschou, N.A. Hastas, A. Tsormpatzoglou, D.N. Kouvatsos, C.A. Dimitriadis, and A.T. Voutsas
Short channel effects on LTPS TFT degradation
Proceedings of the 8th International TFT Conference (ITC 2012), Lisbon, Portugal, (January 2012)
81. H. Contopanagos, C. Kyriazidou, F. De Flaviis and N. Alexopoulos
Planar Spiral AMCs integrated on 60 GHz Antennas
IEEE Antennas and Propagation Society Intl. Symposium Digest, Chicago, IL, USA, pp.1-2 (8-14 July 2012)
82. D. Velessiotis, A. M. Douvas, P. Dimitrakis, P. Argitis, N. Glezos
On the Electrical Behavior of Planar Tungsten Polyoxometalate Self-Assembled Mono- and Bi-Layer Junctions
Frontiers in Electronic Materials (FEM 2012), June 17 to 20, Aachen, Germany (2012)
83. A.Balliou, A.Douvas , D.Velessiotis, V.Ioannou-Sougleridis, P.Normand, P.Argitis, N.Glezos,
Charging Effects and Electron Transport Phenomena associated with the redox properties of self-assembled Polyoxometalate Molecules
Frontiers in Electronic Materials (FEM 2012), June 17 to 20, Aachen, Germany (2012)
84. A.Balliou, N.Glezos
Study of the transport mechanisms and charging effects in nanodevices based on inorganic polyoxometalate molecules,
38th International Conference on Micro and Nano Engineering (MNE 2012), September 16 to 20, Toulouse, France (2012)
85. D. Velessiotis, A. M. Douvas, P. Dimitrakis, P. Argitis, N. Glezos
Electronic Conduction Mechanisms in Polyoxometalate Seld-Assembled Planar Molecular Junctions
Materials Today Virtual Conference: Nanotechnology, December 11-13, http://www.materialstoday.com/virtualconference/materials-today-virtual-conference-nanotechnology (2012)
86. D.C. Moschou, D.N. Kouvatsos and A.T.Voutsas
Short channel effects in double gate polycrystalline silicon SLS ELA TFTs
Proceedings of the 28th International IEEE Conference on Microelectronics (MIEL 2012), Nis, Serbia, (May 2012)
87. N. Hastas, A. Tsormpatzoglou, D.N. Kouvatsos, D.C. Moschou, A.T. Voutsas and C.A. Dimitriadis
Trap properties of asymmetrical double gate polysilicon thin-film transistors with low frequency noise in terms of the grain boundaries direction
Proceedings of the 28th International IEEE Conference on Microelectronics (MIEL 2012), Nis, Serbia (May 2012)
88. I.Raptis, P.Petrou, E.Makarona, A.Botsialas, A.Psarouli, S. Kakabakos, G.Jobst, R.Stoffer, M.Hoekman, M.Sopanen, K.Tukkiniemi, K.Misiakos
All-Si optoelectronic lab-on-a-chip for label-free multi-analyte biosensing
EuroPtrode 2012 (Barcelona, Spain, 04/2012)
89. P.Petrou, A.Gerardino, I.Raptis, Th.Speliotis, S.Kakabakos, N.Papanikolaou
Nano-patterned gold sirfaces for fluorescence enhancement in biosensing

EuroPtrode 2012 (Barcelona, Spain, 04/2012)

90. E. Agocs, P. Petrik, M. Fried, A. G. Nassiopoulou
Optical characterization using ellipsometry of Si nanocrystal thin layers embedded in silicon oxide
Materials Research Society Symposium Proceedings 1321, 367-372 (2012)
91. D. Moschou, N. Vourdas, G. Kokkoris, G. Tsekenis, V. Tsouti, I. Zergioti, A. Tserepi, S. Chatzandroulis
Fabrication of a label-free micromechanical capacitive biosensor and integration with μPCR towards a LoC for disease diagnosis
Proceedings of the 16th Int. Conference on Miniaturized Systems for Chemistry and Life Sciences (μTAS) (2012)
92. X. Zianni
The effect of the modulation shape in the ballistic thermal conductance of modulated nanowires
Journal of Solid State Chemistry, 193, 53 (2012)
93. K.Termentzidis, T. Barreteau, Y. Ni, H Huedro, A-L Delaye, X. Zianni, Y. Chalopin, P. Chantrenne and S. Volz
Thermal conductivity and Kapitza resistance of diameter modulated SiC nanowires, a molecular dynamics study
Journal f Physics: Conference Series 395, 012107 (2012)
94. X.Zianni and P.Chantrenne
Thermal conductivity of diameter-modulated nanowires within a frequency-dependent model for the phonon boundary scattering
Journal of Electronic Materials, DOI: 10.1007/s11664-012-2304-2 (2012)
95. N. Neophytou, X. Zianni, M. Ferri, A. Roncaglia, G.F. Cerofolini, and D. Narducci
Nanograin effects on the thermoelectric properties of poly-Si nanowires
Journal of Electronic Materials, DOI: 10.1007/s11664-012-2424-8 (2012)
96. K. Termentzidis,T. Barreteau, Y. Ni, H Huedro, A-L Delaye, X. Zianni, Y. Chalopin, P. Chantrenne and S. Volz
Thermal conductivity and Kapitza resistance of diameter modulated SiC nanowires, a molecular dynamics study
Journal of Physics: Conference Series 395, 012107 (2012)

Invited Talks

1. P. Argitis, M. Vasilopoulou, A.M. Douvas, D.G. Georgiadou, A. Soultati, I. Kostis, G. Papadimitropoulos, D. Davazoglou, S. Kennou, L. Sygellou, L.C. Palilis
Control of Charge Injection/Extraction Barriers in Organic Optoelectronic Devices
28th Panhellenic Conference on Solid State Physics & Materials Science, Patras, Greece (Sept. 2012)
2. P. Argitis
Electron/Hole Extraction Layers in Organic Photovoltaics
Workshop on Biomimetic Utilization of Solar Energy, University of Crete, Department of Chemistry, Iraklion, Crete, Greece (October 2012)
3. P. Argitis
RTD Activities in the field of Organic Electronics at NCSR Demokritos
Organic Electronics Meeting, Thessaloniki, Greece (19 November 2012)
4. P. Argitis
Approaches for improved charge injection/extraction in organic optoelectronic devices
Workshop on Molecular/Organic Electronics, Technical University of Cyprus, Limassol, Cyprus (December 2012)
5. V. Constantoudis, V.K. Murugesan Kuppuswamy, N. Karasmani, G. Giannakopoulos, E. Gogolides
Morphological characterization of nanostructures through the analysis of SEM images
9th International Conference on Nanosciences & Nanotechnologies (NN) Thessaloniki, Greece (July 3-6, 2012)
6. A. Smyrnakis, A. Zeniou, E. Almpanis, N. Papanikolaou, P. Dimitrakis, E. Gogolides
High aspect ratio, plasma etched silicon nanowires for photovoltaic application: Fabrication and characterization
XI International Conference on Nanostructured Materials (NANO 2012) Rhodes, Greece (August 26-31, 2012)
7. V. Constantoudis, V.K. Murugesan Kuppuswamy, N. Karasmani, G. Giannakopoulos, E. Gogolides
Morphological characterization of nanostructures through the analysis of SEM and AFM images
38th International Micro & Nano Engineering Conference (MNE), Toulouse, France (Sept. 16-20, 2012)
8. E. Gogolides, K. Tsougeni, K. Ellinas, A. Tserepi, P. Petrou, S. Kakabakos
Autonomous, plasma Nanotextured smart microfluidics, and Lab on a Chip systems for chemical and biological analysis

5th International Conference on Micro-Nanoelectronics, Nanotechnologies and MEMS, Kokkini Hani, Heraklion, Greece (7-10 October 2012)

9. A. G. Nassiopoulou
Porous Si substrate technology for RF passives integration
Workshop on Nanoelectronic Materials and Devices, organized by Micro&Nano, Athens (17 Dec. 2012)
10. A. G. Nassiopoulou
High performance RF passive devices in CMOS technology on a local porous Si substrate
Workshop on Recent Developments in Nanoelectronics, Thessaloniki (3 June, 2012)
11. A. G. Nassiopoulou
Nanostructured Si in the "More than Moore" Nanoelectronics field
XI International Conference on Nanostructured Materials, Rhodes Greece (26-31 August 2012)
12. P. Dimitrakis, P. Normand, V. Ioannou-Sougleridis, C. Bonafos, G. BenAssayag, E. Iliopoulos
Quantum-dots for memory applications
E-MRS 2012 Fall Meeting, Symposium H, Warsaw, Poland (September 17-21, 2012)
13. P. Dimitrakis, P. Normand, V. Ioannou-Sougleridis, G. BenAssayag, C.Bonafos
Group IV Semiconductor Quantum-dot Non-volatile Memories
MRS 2012 Fall Meeting, Symposium DD, Boston, USA (November 25-30, 2012)
14. I. Raptis, E.Makarona, A.Botsialas, K.Misiakos, P.Petrou, A.Psarouli, S.Kakabakos, G.Jobst, M.Hoekman, R.Heideman, H.Leewuis, R.Stoffer, M.Sopanen, K.Tukkiniemi
All-Silicon Optoelectronic Lab-On-a-Chip For Label-Free Multi-Analyte Biosensing: The PYTHIA Aproach
IC-MAST 2012, Budapest, Hungary (May 2012)

Book Chapters

1. I. Raptis, G.P. Patsis
Simulation of Electron Beam Exposure and Resist Processing for Nano-Patterning (Chapter)
Nanofabrication Techniques and Principles Editors: M, Stepanova, S. Dew Springer (2012)
2. X.Zianni
The effect of the modulation shape in the ballistic thermal conductance of modulated nanowires
Journal of Solid State Chemistry, 193, 53 (2012)

Edition of Conference Proceedings

1. Y. Fujisaki, P. Dimitrakis, E. Tokumitsu, M.N. Kozicki
Materials and Physics of Emerging Nonvolatile Memories,
Materials Research Society Symposium Proceedings, 1440, Cambridge (2012)
2. C. Tsamis, G. Kaltsas
Special Issue: 25th Anniversary Eurosensors XXV, Sensors & Actuators: Physical, Eds. (2012)

Conference and Workshop Organization

1. Y. Fujisaki, P. Dimitrakis, E. Tokumitsu, M.N. Kozicki (Symposium Chairpersons and Proceedings Editors)
Materials and Physics of Emerging Nonvolatile Memories
Symposium E, MRS Spring Meeting 2012, San Francisco, CA, USA (9-13 April 2012)
2. A. G. Nassiopoulou and F. Balestra (Workshop Chairpersons)
Novel materials, devices and technologies for high performance on-chip RF applications
organized within ESSDERC/ESCIRC 2012, Bordeaux, France (September 2012)
3. A. G. Nassiopoulou and V. Grabinski (Chairpersons)
Tutorial on "EU project NANOTEC on Ecosystems Technology & Design for Nanoelectronics: an experience in Europe"
organized within ESSDERC/ESCIRC 2012, Bordeaux, France (September 2012)

Teaching and Training Activities

1. E. Gogolides, D. Davazoglou, A. Nassiopoulou
Microelectronics and Microsystems fabrication processes
Postgraduate Programs on Microsystems and Nanodevices of the National Technical University of Athens and Micro and Nano Electronics of the National and Kapodistrian Univ. of Athens
2. E. Gogolides, G. Kokkoris, V. Constantoudis, A. Tserepi

Plasma Processing for Micro and Nano Fabrication
Postgraduate Program on Microelectronics of the National and Kapodistrian Univ. of Athens

3. D. Mathioulakis, I. Anagnostopoulos, A. Tserepi, G. Kokkoris
   Microfluidic systems
   Postgraduate Program on Microsystems and Nanodevices of the National Technical University of Athens
4. *E. Gogolides, G. Kokkoris, V. Constantoudis, A. Tserepi*
   SimulationofMicroandNano-Patterning
   Postgraduate Program on Mathematical Modelling in Modern Technologies and Financial Engineering of the NationalTechnical University of Athens
5. V. Constantoudis
   Measurement and characterization of nanostructure morphology: Fractal and stochastic aspects
   Demokritos Summer School, 09-20 July 2012
6. G. Kokkoris
   Process and device simulation
   Postgraduate Program on Microelectronics of the National and Kapodistrian University of Athens
7. A. Tserepi
   Microfluidic devices: technology and applications
   Demokritos Summer School, 09-20 July 2012
8. A. G. Nassiopoulou and E. Hourdakis
   Lectures on "*Silicon processing for Nanoelectronics*" within:
   a) the MSc program on Microelectronics organized by the Department of Informatics of the University of Athens, in cooperation with the Department of Microelectronics of NCSR Demokritos and
   b) the MSc program on "Microsystems and Nanoelectronics" organized by the National Technical University of Athens with the participation of the Department of Microelectronics of NCSR Demokritos
9. S. Gardelis
   Lectures on "*Micromechanics and Sensors*", by the within the MSc program organized by the: Department of Informatics, University of Athens, in cooperation with the Department of Microelectronics of NCSR Demokritos

Doctoral Dissertations completed in 2012

1. Theodoros Manouras
   Lithographic Materials Based on Photoinduced Cleavage of Polyacetals Backbone
   University of Athens, Department of Chemistry (June 2012)
2. Pagona Pavli
   Photochemical Modifications of Thin Polymeric Films for Nanobiotechnology Applications
   National Technical University of Athens, Department of Chemical Engineering (October 2012)
3. Dimitra G. Georgiadou
   Modification of Optoelectronic Characteristics in Organic Light Emitting Devices by Using Sulfonium Salts
   National Technical University of Athens, Department of Chemical Engineering (December 2012)
4. Vijayakumar Murugesan Kuppuswamy
   Contact edge roughness in EUV lithography: Metrology and process evaluation
   National Technical University of Athens, School of Chemical Engineering, Athens, Thesis Research Supervisor at NCSR Demokritos: Dr. E. Gogolides, Dr V. Constantoudis, Thesis Supervisor at NTUA: Prof. A. Boudouvis (2012)

Masters Dissertations completed in 2012

1. A. Soultati
   High performance organic photovoltaic devices using transition metal oxides as hole injection/extraction layers
   University of Athens, Department of Informatics and Telecomunications
   Supervisors: M. Vasilopoulou, P. Argitis
   (February 2012)
2. S. Tzanni
   Binding of photodegradable polymers on surfaces
   University of Athens, Department of Chemistry
   Supervisors: M. Chatzichristidi, P. Argitis
   (October 2012)
3. E. Kouris

Mathematical modeling of a continuous flow microfluidic device for DNA amplification by Polymerase Chain Reaction
MSc Thesis held at IMEL/NCSR Demokritos
Defended at the National and Kapodistrian University of Athens, Physics Department
Supervisors: G. Kokkoris, A. Tserepi
(2012)

4. A. Zeniou
Nanopillars and vertical silicon nanowires fabrication using silicon plasma etching processes in room temperature
MSc Thesis held at IMEL/NCSR Demokritos
Defended at the National and Kapodistrian University of Athens, Dept. of Informatics and Telecommunications
Supervisor: E. Gogolides
(2012)
5. N. Karasmani
Analysis of Rough Surfaces with Network Theory
MSc Thesis held at IMEL/NCSR Demokritos, Defended at National Technical University of Athens, School of Applied Mathematical and Physical Sciences
Supervisor: V. Constantoudis
(2012)
6. M.-I. Georgaki
Realization of photonic polymeric multilayers as humidity sensors
MSc Thesis held at IMEL/NCSR Demokritos
Defended at the National and Kapodistrian University of Athens, Dept. of Chemistry
Supervisor: I. Raptis
(2012)
7. S. Katsaridis
Vibrational energy harvester for Wireless Sensor Networks
Department of Informatics and Telecommunications, Univ. of Athens
Supervisor: C. Tsamis
(April 2012)
8. G. Voulazeris
Modeling and Fabrication of a Piezoelectric Energy Harvester Collecting the Ambient Mechanical Energy From Environmental Vibrations
Department of Informatics and Telecommunications, Univ. of Athens
Supervisor: C. Tsamis
(October 2012)

ANNEX IV: FUNDED PROJECTS in 2012

A. EU Projects

- MiNaSys-CoE (Regpot-2009) Contract No 245040
  "Micro and Nano Systems Center of Excellence"
  Duration: 1/12/2009-31/7/2013
  Project leader: D. Tsoukalas – P. Argitis

- SPAM (FP7) - Contract No 215723 (Marie Curie)
  "A Supra-disciplinary approach to research and training in surface Physics for Advanced Manufacturing"
  Duration: 01/10/2008 – 30/09/2012
  Project leader: E. Gogolides

- LOVE-FOOD (FP7-ICT-2011-8) - Contract No 317742
  "Love wave fully integrated Lab-on-Chip platform for food pathogen detection"
  Duration: 01/09/2012 – 31/08/2015
  Project leader: A. Tserepi

- SE2A - ENIAC JU (FP7) - Contract No 120009
  "Nanoelectronics for Sale, Fuel Efficient and Environment Friendly Automotive Solutions"
  Duration: 1/1/2009-31/03/2012
  Project leader: A. Nassiopoulou

- Network of Excellence NANOFUNCTION (FP7) - Contract No 257375
  "Beyond CMOS Nanodevices for Adding Functionalities to CMOS"
  Duration: 1/9/2010-31/8/2013
  Project leader: A. Nassiopoulou

- Coordination and Support Action NANO-TEC - Contract No 257964
  "Beyond CMOS Nanodevices for Adding Functionalities to CMOS"
  Duration: 1/9/2010-28/2/2013
  Project leader: A. Nassiopoulou

- FOODSNIFFER - EU, FP7-ICT, STREP - Contract No 318319
  "Monolithically integrated interferometric biochips for label-free early detection of human diseases
  Duration: 01/09/2012 – 1/9/2015
  Project leader: I. Raptis

- IKYDA, IKY DAAD Collaborative Project with LM University of Munich (2012)
  Project leader: P. Argitis

B. Projects funded by GSRT

- DoW (GSRT) - Contract No. LS7(276)
  "DNA on waves: an integrated diagnostic system"
  Duration: 07/12/2011 – 06/12/2014
  Project leader: A. Tserepi

- DESIREDROP (GSRT) - Contract No. MIS 380835
  "Design and fabrication of robust superhydrophobic/philic surfaces and their application in the realization of "smart" microfluidic valves"
  Duration: 01/02/2012 – 30/09/2015
  Project leader: A. Tserepi

- CORSED (GSRT) - Contract No. PE8(844)
  "Control of Surface Roughness by Simultaneous to Plasma Etching Deposition"
  Duration: 21/06/2012 – 20/06/2015
  Project leader: A. Tserepi

- PlasmaNanoFactory (GSRT) - Contract No. 695
  "Plasma directed assembly of nanostructures and applications"
  Duration: 26/09/2012 – 25/09/2015
  Project leader: E. Gogolides

- SYNERGASIA "TFT Solar" - Contract No. 09ΣΥΝ-42-861
  Duration: 18/2/2011 – 17/2/2014
  Project leader: D. Tsoukalas – D. Davazoglou

- Greek-Czech Cooperation Project
  Duration: 2011-2013
  Project leader: N. Glezos

- Greek-Sloval Cooperation Project
  Duration: 2012-2014
  Project leader: N. Glezos

- "Development of Innovative sensor systems offering distributed intelligence – MEMSENSE", National Funds and European Regional Development Funds, NSRF 2007–2013, contract no. 45
  Duration: 5/2009 - 2/2013
  Project Leader: C. Tsamis

- "Nanostructured ThermoElectric Systems for Green Transport & Energy Efficient Applications", NanoTEG, EU ENIAC
  Duration: 7/2011-6/2014
  Project Leader: C. Tsamis

- "Self-assembled ZnO Nanostructures for Engineered Neuronal Networks", European Regional Development Fund (ERDF) under the Hellenic National Strategic Reference Framework (NSRF) 2007-2013, Hungarian-Greek Intergovernmental S&T Cooperation Programme, Contract No HUN53
  Duration: 9/2012-8/2015
  Project Leader: C. Tsamis

Institute members also participate in the following programs administered by other organizations

- ALEPOU “Autonomous and integrated system for in-situ and continuous contaminant gases monitoring in industrial environments” Funded by General Secretariat for Research & Technology – 19SMEs2010
  Duration: 1/9/2012 – 1/3/2015

- Thalis "Polymeric photonic systems for application in information technologies, Photopolys”
  Duration: 2012-2015

- Archimides III “Novel and highly efficient Hybrid organic photovoltaic, NHyOPV”
  Duration: 2012-2014

- Archimides III “Novel low power consumption Hybrid OLEDs with improved operational characteristics, NHyOLED”
  Duration: 2012-2014

- Archimides III “Organic Electronic Devices for Radiation Detection”
  Duration: 2012-2015

- Archimides III “Advanced Low Cost Electrochromic Windows”
  Duration: 2012-2015

- “Blu-Ray” Development of Optical Discs Technology
  Duration: 2011-2014

- “Organic electronic devices for radiation sensing”, Archimedes III project OEDDIR, TEI-Crete, Ministry of Education
  Duration: 2012-2015

- "Charge trapping devices (memories) based on novel high-k dielectrics" GSRT-Herakleitos project, MIS: 346791 University of Patras
  Duration: 1/4/2011-31/10/2014

- "Front-End Processes for Germanium MOS applications" Karatheodory, Project C906, University of Patras
  Duration: 1/2/2010-30/9/2013

- “Spontaneous growth, properties and devices of III-V semiconductor nanowires”, NanoWire THALES project, University of Crete, Ministry of Education
  Duration: 2012-2015